Ghent University
Faculty of Pharmaceutical Sciences

Non-viral Delivery Strategies to Guide Therapeutic Nucleic Acids through Cellular Barriers

Niet-virale afgifte strategieën voor transfer van therapeutische nucleïnezuren doorheen cellulaire barrières

Roosmarijn Vandenbroucke
MSc, Biotechnology

Thesis submitted to obtain the degree of
Doctor in Pharmaceutical Sciences

Proefschrift voorgedragen tot het bekomen van de graad van
Doctor in de Farmaceutische Wetenschappen

2008

Dean:
Prof. dr. apr. Jean Paul Remon

Promoters:
Prof. dr. apr. Niek N. Sanders
Prof. dr. apr. Jo Demeester

Co-promoter:
Prof. dr. apr. Stefaan C. De Smedt

Laboratory of General Biochemistry and Physical Pharmacy

Gent, 9 januari 2008

De promotoren:

Prof. dr. apr. Niek N. Sanders

Prof. dr. apr. Jo Demeester

De co-promotor:

Prof. dr. apr. Stefaan C. De Smedt

De auteur:

Roosmarijn E. Vandenbroucke

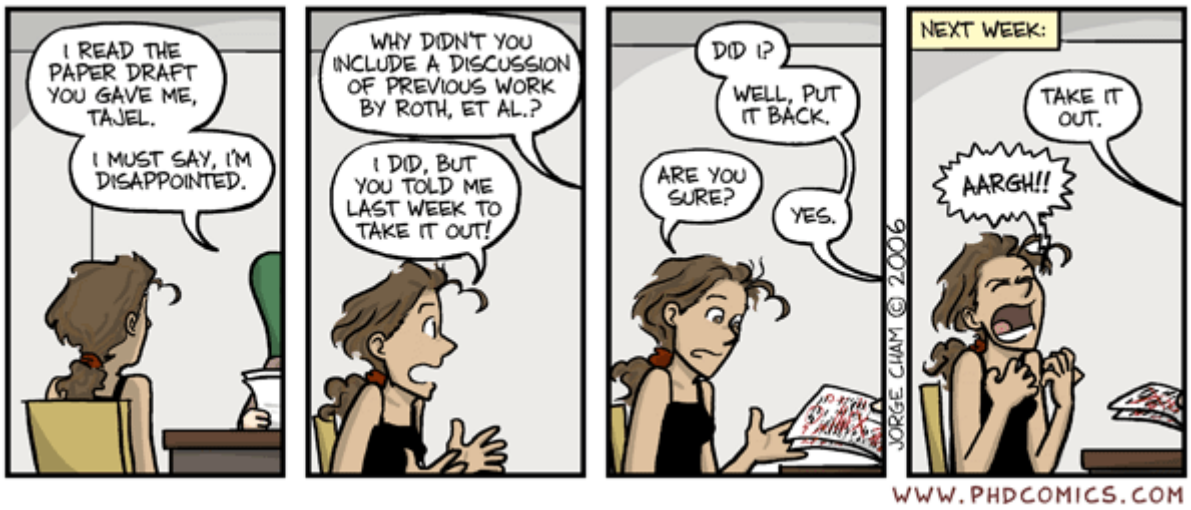

WWW.PHDCOMICS.COM

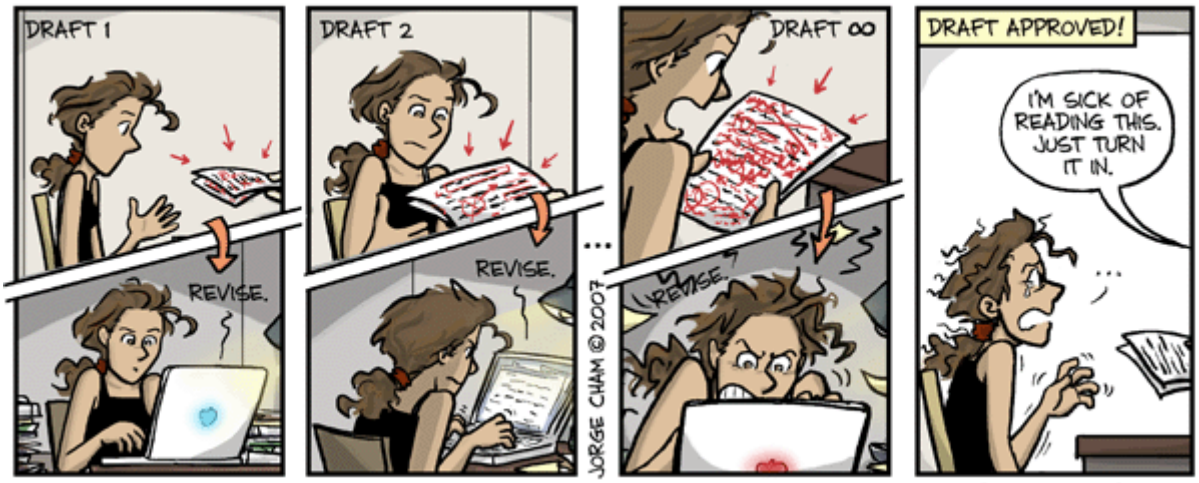

WWW.PHDCOMICS.COM

www.phdcomics.com

DANKWOORD

Vijf jaar geleden stapte ik nietsvermoedend het labo op het tweede verdieping van het FFW binnen, onwetend over wat mij allemaal nog te wachten stond, maar nu is het dan eindelijk zover: hier zit ik… te schrijven aan de allerlaatste pagina's van dit doctoraat, het eindresultaat van 5 jaar zweten en zwoegen. Goed beseffende dat dit hoogstwaarschijnlijk de eerst én meest gelezen pagina's van dit hele boekje zullen worden… Tijd dus om even terug te blikken en de nodige mensen te bedanken!

Eerst zeker en vast een woordje van dank voor mijn (co-)promotoren Prof. dr. apr. Jo Demeester and Prof. dr. apr. Stefaan De Smedt. Dank je voor de kans die ik gekregen heb om op jullie labo te doctoreren! Stefaan, jouw wetenschappelijk enthousiasme is bewonderenswaardig en hopelijk kan je nog veel studenten inspireren om zich voor de wetenschap in te zetten. Jo, dankzij jou is ons labo zo goed uitgerust en vooral bedankt voor de steun op enkele cruciale momenten! Mijn promotor Prof. (!?!) dr. apr. Niek N. Sanders verdient zeker een extra vermelding. Niek, als jouw eerste 'echte' doctoraatsstudent ben ik ervan overtuigd dat we samen een mooi parcours afgelegd hebben. Net zoals in mijn scriptie zijn we erin geslaagd om de aanwezige hindernissen te overbruggen en mag het eindresultaat er zeker wezen! Bedankt voor alles en heel veel succes met je nieuwe uitdaging!

Maar dit boekje zou er natuurlijk nooit gekomen zijn zonder de vele collega's. In de eerste plaats mijn bureaugenootjes Lies, Ine & Bruno. Lies, we zijn er ongeveer samen aan begonnen en binnenkort zit het er ook voor jou op, nog even volhouden dus, hé! Jouw opgewektheid en eeuwige glimlach waren steeds een oppepper tijdens de moeilijkere momenten. Ine, jij hebt nog een iets langere tijd voor de boeg, maar zoals je nu als een sneltrein vooruit gaat, komt dat zeker en vast dik in orde! Tussen haakjes, door jullie gezamenlijke afwezigheid die drie maanden heb ik eens te meer beseft hoezeer ik jullie gezelschap en babbels ga missen als ik hier weg ben. We houden zeker contact, hé! Bruno, de vreemde vogel in de bijt tussen die drie vrouwen, veel succes nog verder en zeker nu je een trapje hoger klimt ☺! Bart, jij verdient zeker en vast een speciale vermelding. De term 'manusje-van-alles' klinkt te negatief om te omvatten wat jij voor het labo en al je collega's betekent. Bedankt voor al je hulp en raad, enerzijds op wetenschappelijke vlak maar niet in het minst daarbuiten! Sofie, 'die van hiernaast', al behoor je officieel niet tot ons labo, je bent er de laatste jaren een onmisbaar deel van gaan uitmaken. Jaja, ik zal je pesterijen nog missen in de toekomst! Heel veel succes nog met jouw doctoraat, want nu je ventje er (bijna) is, is het jouw beurt, hé! Vervolgens zijn er natuurlijk nog de mannen van 'aan den overkant': Koen, Stefaan & Kevin. Koen, als er iets is dat we gemeen hebben dan is het toch wel het freaky muggenziften over figuren, maar laat ze er maar mee lachen, 't is het resultaat dat telt, hé! En ik ben er echt van overtuigd dat jouw doctoraat iets zal zijn om trots op te zijn! Stefaan, dank je voor de oppeppende babbels en ook voor jou veel succes dit jaar, zowel met je doctoraat als jullie eerste spruit! Kevin, begonnen als mijn stagiair waarbij het niet steeds van leien dakje liep door de verkeerde pDNAs, tegenstribbelden cellen en een oude fluorimeter, maar intussen ook al zowat halverwege: succes nog! Ook jij, Marie-Luce, heb ik enkele maandjes mogen begeleiden en intussen ben je zelf aan je doctoraat begonnen. Ik ben blij dat ik weet dat we het practicum in goeie handen kunnen achterlaten en ik wens je echt super veel succes de komende jaren! Farzaneh, I wish you all the best this year with the well deserved end of your PhD! I can't stress enough how much I admire your strength the last years, as it must have been very tough for you! I regret that I sometimes didn't had more time to help you, but if you need any help the coming months, just let me know! Dries, jouw enthousiasme en energie is echt iets om jaloers op te zijn. En ook jij zal over enkele jaren ongetwijfeld een prachtwerk afleveren! En dan nog onze postdocs Kevin & Katrien, twee vaste waarden op het labo en natuurlijk ook Tinneke & Barbara, die intussen het labo verlaten hebben. Bedankt voor alles! Daarnaast zijn er nog de meest recente labo aanwinsten: Broes, Nathalie & Chaobo, lang hebben we niet

samengewerkt, maar alle drie heel veel succes de volgende jaren en jullie zullen de toekomst van het labo moeten verzekeren! En last but not least, Trientje & Bruintje, ook jullie zijn onmisbaar op het labo! Zo hebben jullie mij geleerd eerst mijn postvak te bekijken alvorens mijn beklag te doen over niet uitbetaalde onkosten, hebben jullie er al die keren voor gezorgd dat de treintickets op de juiste plaats belandden, zorgden jullie ervoor dat de juiste hotels gereserveerd werden, dat de kopiemachine zijn werk deed, dat we een stift hadden in de juiste kleur, voor een grapje tussendoor, enzovoort. Teveel om op te sommen… bedankt!

Mijn eerste stapjes in de wetenschap heb ik natuurlijk al meer dan 5 jaar geleden gezet. Kristin, dank je om mij als eerste de kneepjes van het vak te leren en ik heb dan misschien een beetje gesleuteld aan het scenario, maar uiteindelijk ben ik dan toch ook aan de eindmeet geraakt! Koen, hoewel je nu eindelijk terug in het land bent, lukt het eigenlijk veel te weinig om eens bij te babbelen. Tijd om daar verandering in te brengen! Sven, merci om onze getuige te zijn, om er af en toe eens met 'mijne vent' op uit te trekken en veel succes met al je toekomstplannen!

Gelukkig is er ook nog leven buiten de wetenschap. An, onze eerste kennismaking die avond in de sjakosj is intussen al een kleine 10 jaar geleden en intussen zijn de herinneringen bijna niet meer bij te houden. Van nachtelijke achtervolgingen op de fiets door Gent na een dagje uit de hand gelopen shoppen, over het bijna verkocht worden aan 'nen hollander' voor een goed prijsje, tot het uitwisselen van babyadvies & -kleertjes. Dank je voor alles en dat 100% gemeend, zonder dat ik een glaasje op heb ☺! Petra, de komende maanden zullen voor ons verbazend gelijk verlopen… spannend, hé! Altijd leuk om nog eens af te spreken en bij te kletsen! Katrien, jij hebt die lang verhoopte eindmeet al bereikt. Ik duim voor een stralende toekomst! Heidi, Koen & Carl, ik beloof het, vanaf september ben ik weer van de partij! Als ik nog met jullie mee kan, tenminste…

Moe & va, waarschijnlijk hebben jullie niet steeds begrepen waar ik de laatste jaren allemaal mee bezig was, maar dank je om er steeds te zijn als ik jullie nodig had en ik weet dat ik altijd op jullie zal kunnen rekenen. Monique, Gwenn & Sara, Myriam & Marc dank je voor het vele babysitten de laatste weken. Lore heeft in elk geval met volle teugen genoten van al die aandacht!

Lieve Stefan, ik weet het, de laatste maanden zijn niet de makkelijkste geweest. Het extra werk dat ik je bezorgd heb, variërend van last minute verbeteringen tot het vele huishoudelijke werk dat eventjes niet mijn prioriteit was, heb je met glans tot een goed einde gebracht! Dank je voor zoveel zaken, te talrijk om op te sommen. Nu is het jouw beurt om je eens door mij te laten bedienen… alhoewel… met de nieuwe spruit op komst… ☺?

Mijn lieve, kleine Lore, je beseft waarschijnlijk amper wat je mama de laatste maanden al die tijd achter die 'papi' (lees: computer) zat uit te voeren. Goddelijk om te zien hoe je probeerde om toch maar mijn aandacht te krijgen door mij allerlei zelfgemaakt voedsel te voederen, door je bal te tonen nadrukkelijk aangevuld met het woord 'pewen' (lees: spelen) en zeker door smekend naar mij te kijken en 'mamaaaa?' te zeggen alsof je mij 1001 dingen zou willen vertellen. Jouw glimlach maakt elk dag de moeite waard!

Bedankt allemaal!

Tielt, 3 januari 2008

Roos

TABLE OF CONTENTS

LIST OF ABBREVIATIONS

AAV	Adeno-Associated Virus
AAVS1	AAV integration site-1
AdV	Adenovirus
AFM	Atomic Force Microscopy
Ago2	Argonaute 2
AP	Adaptor Protein
ARF6	Adenosine Diphosphate-Ribosylation Factor 6
ATP	Adenosine Triphosphate
ATTC	American Type Culture Collection
BCA	Bicinchoninic Acid
bp	Basepair
BSA	Bovine Serum Albumin
CCLR	Cell Culture Lysis Reagent
CDC42	Cell Division Cycle 42
CDE	Clathrin-Dependent Endocytosis
CFTR	Cystic Fibrosis Transmembrane Regulator
CIDIC	Confocal Image Assisted 3D Integrated Quantification
CIE	Clathrin-Independent Endocytosis
CLSM	Confocal Laser Scanning Microscopy
CMV	Cytomegalovirus
CPP	Cell Penetrating Peptide
CytoD	Cytochalasin D
DIC	Differential Interference Contrast
DLS	Dynamic Light Scattering
DMEM	Dulbecco's Modified Eagle's Medium
DN	Dominant Negative
DNA	Desoxyribonucleic Acid
DOPE	1,2-Dioleoyl-sn-Glycero-3-Phosphoethanolamine
DOTAP	N-(1-(2,3-Dioleoyloxy)propyl)-N,N,N-Trimethylammoniumchloride
DPPC	1,2-Dipalmitoyl-sn-Glycero-3-Phosphocholine
dsDNA	Double Stranded DNA
dsRNA	Double Stranded RNA
DSPE-PEG	1,2-Distearoyl-sn-Phosphatidylethanolamine PEG
DSPE-PEG$_{2000}$-biotin	DSPE-[biotinyl PEG$_{2000}$]
DSPE-PEG$_{2000}$-MAL	DSPE-[maleimide PEG$_{2000}$]
DTT	Dithiothreitol
ECM	Extracellular Matrix
EDTA	Ethylenediaminetetraacetic Acid

eGFP	Enhanced Green Fluorescent Protein
ER	Endoplasmatic Reticulum
ERC	Endocytic Recycling Compartment
EtBr	Ethidium Bromide
F	Phenylalanine
FBS	Fetal Bovine Serum
FCS	Fluorescence Correlation Spectroscopy
FG repeats	Phenylalanine-Glycine repeats
FITC	Fluorescein Isothiocyanate
gDNA	Genomic DNA
GDP	Guanosine Diphosphate
GFP	Green Fluorescent Protein
GlcNAc	N-Acetylglucosamine
GPI	Glycosylphosphatidylinositol
GST	Glutathione S-Transferase
GTP	Guanosine Triphosphate
GTPase	Guanosine Triphosphatase
HA	Hemagglutinin
HBV	Hepatitis B Virus
HCV	Hepatitis C Virus
HCC	Hepatocellular Carcinoma
Hepes	4-(2-Hydroxyethyl)-1-Piperazineethanesulfonic Acid
HIV-1	Human Immunodeficiency Virus-1
HIV-1 Tat	HIV-1 Transactivator of Transcription
HSRRB	Health Science Research Resource Bank
HSV	Herpes Simplex Virus
hTF	Human Transferrin-AlexaFluor633
HuH-7	Human Hepatoma-7
IFN	Interferon
INM	Inner Nuclear Membrane
kb	Kilobase
kDa	Kilodalton
KO	RNAi Knock Out
LacCer	BODIPY FL C_5-Lactosylceramide
LB	Luria–Bertani Medium
LBGT	Laser Beam Gene Transduction
L-Gln	L-Glutamine
LPS	Liposome
LPX	Lipoplex

MAA	Methacrylic Acid
mBCD	Methyl-β-Cyclodextrin
MDa	Megadalton
MEND	Multifunctional Envelope-type Nano Device
MP	Macropinocytosis
mRNA	Messenger RNA
MTT	3-(4,5-Dimethylthiazol-2-yl)-2,5-Diphenyltetrazolium Bromide
ND	Not Determined
NE	Nuclear Envelope
NES	Nuclear Export Signal
NLS	Nuclear Localization Signal
NMR	Nuclear Magnetic Resonance
NPC	Nuclear Pore Complex
N:P ratio	Nitrogen to Phosphate Ratio
NTR	Nuclear Transport Receptor
Nups	Nucleoporins
ONM	Outer Nuclear Membrane
ORF	Open Reading Frame
PAA	Poly(amidoamine)
PAGE	Polyacrylamide Gel Electrophoresis
PbAE	Poly(β-amino ester)
PBS	Phosphate Buffered Saline
PCI	Photochemical Internalization
PCS	Photon Correlation Spectroscopy
pDMAEMA	Poly(2-Dimethylaminoethyl Methacrylate)
pDNA	Plasmid DNA
PEG	Poly(ethylene Glycol)
PEG-siPlexes	PEGylated SiRNA-Liposome Complexes
PEI	Poly(ethyleneimine)
PLB	Passive Lysis Buffer
pLL	Poly-(L-lysine)
PM	Plasmamembrane
PMSF	Phenylmethylsulfonyl Fluoride
PNA	Peptide Nucleic Acid
PS	Photosensitizer
P/S	Penicilline-Streptomycine
PTD	Protein Transduction Domain
R8	Octaarginine
RISC	RNA Induced Silencing Complex
RLU	Relative Light Units

RNA	Ribonucleic Acid
RNAi	RNA interference
RNase	Ribonuclease
RPE	Retinal Pigment Epithelium
S	Serine
SD	Standard Deviation
SDS	Sodiumdodecylsulfate
SEAP	Secreted Alkaline Phosphatase
SG-LBGT	Femtosecond Laser Beam Gene Transduction
shRNA	Short Hairpin RNA
siRNA	Short Interfering RNA
siPlexes	SiRNA-Liposome Complexes
ssDNA	Single Stranded RNA
ssRNA	Single Stranded DNA
SV40	Simian Virus 40
Tat	Transactivator of Transcription Protein
TBE	Tris, Boric acid and EDTA buffer
TCEP	Tris-2(Carboxyethyl)Phosphine
TCHD	*Trans*-Cyclohexane-1,2-Diol
THF	Tetrahydrofurane
TNF-α	Tumor Necrosis Factor-α
TRITC	Tetramethylrhodamineisothiocyanate
UV	Ultraviolet
WGA	Wheat Germ Agglutinin
w/v	Weight/Volume

LIST OF SYMBOLS

λ_{em}	Emission Wavelenght
λ_{ex}	Excitation Wavelenght
ζ	Zeta Potential

General Introduction

Aim and Outline of this Thesis

General Introduction

Aim and Outline of this Thesis

Recent advances in biotechnology research have led to a boost of targets in a variety of diseases that can be treated by gene therapy approaches. Different types of nucleic acids, such as DNA, messenger RNA (mRNA) and short interfering RNA (siRNA), have shown potential to treat viral infections and inherited or acquired genetic disorders like cancer. To be effective, these nucleic acids should be delivered to a well defined compartment of the target cells. However, they encounter several major barriers before the target site is reached. Therefore, advanced delivery systems, either viral or non-viral carriers, are needed. Although recombinant viruses are the most efficient vehicles to deliver therapeutic nucleic acids into the cells, the genetic material they can carry is limited, they can induce insertional oncogenesis and severe immunogenic responses. As a consequence, several non-viral gene delivery systems have been developed for safe delivery of therapeutic nucleic acids into target cells. Unfortunately, in general these non-viral systems exhibit a low delivery efficiency due to their limited ability to cross the encountered cellular barriers before reaching their intracellular target site.

In brief, as clinical applications of gene therapy are largely dependent on the development of non-toxic and efficient delivery systems, the primary aim of this thesis was to improve the intracellular delivery of functional nucleic acids by addressing several cellular hurdles encountered by non-viral delivery vehicles.

Chapter 1 gives an overview of the main gene therapy strategies, the different available nucleic acid delivery systems and the intracellular barriers that have detrimental effects on the nucleic acid delivery efficiency of non-viral delivery systems. Although the endocytosis-mediated uptake of non-viral nucleic acid containing nanoparticles is a very efficient cellular uptake pathway, internalized molecules suffer from poor availability at the target sites such as the cytoplasm or nucleus. Therefore, it would be advantageous to bypass the endocytic pathway and somehow achieve cytosolic delivery of nucleic acids by other pathways, e.g. through coupling of the cell penetrating peptide HIV-1 Tat to the vehicle surface (**Chapter 2**) or through ultrasound combined with microbubbles (**Chapter 3**). As several problems were encountered studying the endocytic

pathways of non-viral delivery vectors, we had a closer look at the use of endocytosis inhibitors to study the endocytic uptake of gene complexes in **Chapter 4**. Since most non-viral delivery vectors are taken up by endocytosis, strategies to escape from the endosomes have been developed. In **Chapter 5**, we studied the use of biodegradable polymers for siRNA delivery and their ability to induce endosomal release of the siRNA into the cytoplasm. Once in the cytoplasm, siRNA has reached its intracellular target region. In contrast, pDNA still needs to cross a final and major barrier: the nuclear envelope (NE). In **Chapter 6** we tried to overcome this barrier by using a nuclear localization signal (NLS) containing peptide and in **Chapter 7** by using a small amphiphilic molecule called *trans*-cyclohexane-1,2-diol (TCHD).

Chapter 1

Introduction

ABSTRACT

While safer than viral strategies, the clinical applicability of non-viral nucleic acid delivery systems is still limited due to their poor *in vivo* efficacy. Indeed, upon administration, e.g. by intravenous injection, several extra- and intracellular barriers need to be overcome before the nucleic acids reach their intracellular target region, i.e. the cytoplasm for siRNA and the nucleus for pDNA. This chapter gives a short introduction to gene therapy and the delivery systems for nucleic acids and focuses mainly on the intracellular barriers encountered by non-viral nucleic acid containing nanoparticles.

It is well known that serum proteins can adsorb onto the nucleic acid vehicle surface resulting in the subsequent uptake of opsonized particles by macrophages and other immune cells. To avoid rapid clearance from the blood and thus prolong the circulation time of the vehicles, covering their surface with inert polymers such as PEG can be beneficial.

Once the target cell is reached, most particles are taken up through endocytic mechanisms, such as clathrin-dependent or -independent endocytosis or macropinocytosis. Upon endocytosis, these particles end-up in vesicles that are processed from early to late endosomes with lysosomes as their final destination. The harsh environment of the lysosomes, with low pH and destructive enzymes, will cause degradation and inactivation of most particles together with their cargo. Therefore, several strategies aimed to either avoid endosomal uptake, e.g. by using cell penetrating peptides or ultrasound, or to escape from endosomes, e.g. by using fusogenic peptides or pH-responsive polymers, have been developed.

When released in the cytoplasm and once dissociated from its carrier, siRNA molecules have reached their intracellular target region, but pDNA needs to be transported into the cell's nucleus to exert its function. When cells undergo mitosis, the nuclear envelope (NE) transiently breaks down and the permeability barrier to the nucleus is lost, opening the opportunity for the pDNA to enter the nucleus. Unfortunately, many target cells in gene therapy do not divide or divide very slowly, which makes the entry of plasmids into the nucleus a major limiting step in non-viral gene transfer. As it was shown that plasmids can be transported into the nuclei of non-dividing cells via the nuclear pore complex (NPC), non-viral pDNA delivery research has focused mainly on the enhancement of the pDNA NPC transport.

Chapter 1

Introduction

INTRODUCTION

Gene therapy is a promising approach to correct many genetic-based human diseases. Several strategies are followed to correct faulty genes: (i) addition of the normal gene, either transient or by inserting it into a non-specific place in the genome, to correct for the non-functional gene, (ii) replacement of the non-functional gene by the corresponding normal gene through homologous recombination, (iii) correction of the abnormal gene through selective reverse mutation, which returns the gene to its normal function and (iv) alteration of the gene regulation or gene expression level of a deregulated gene [1].

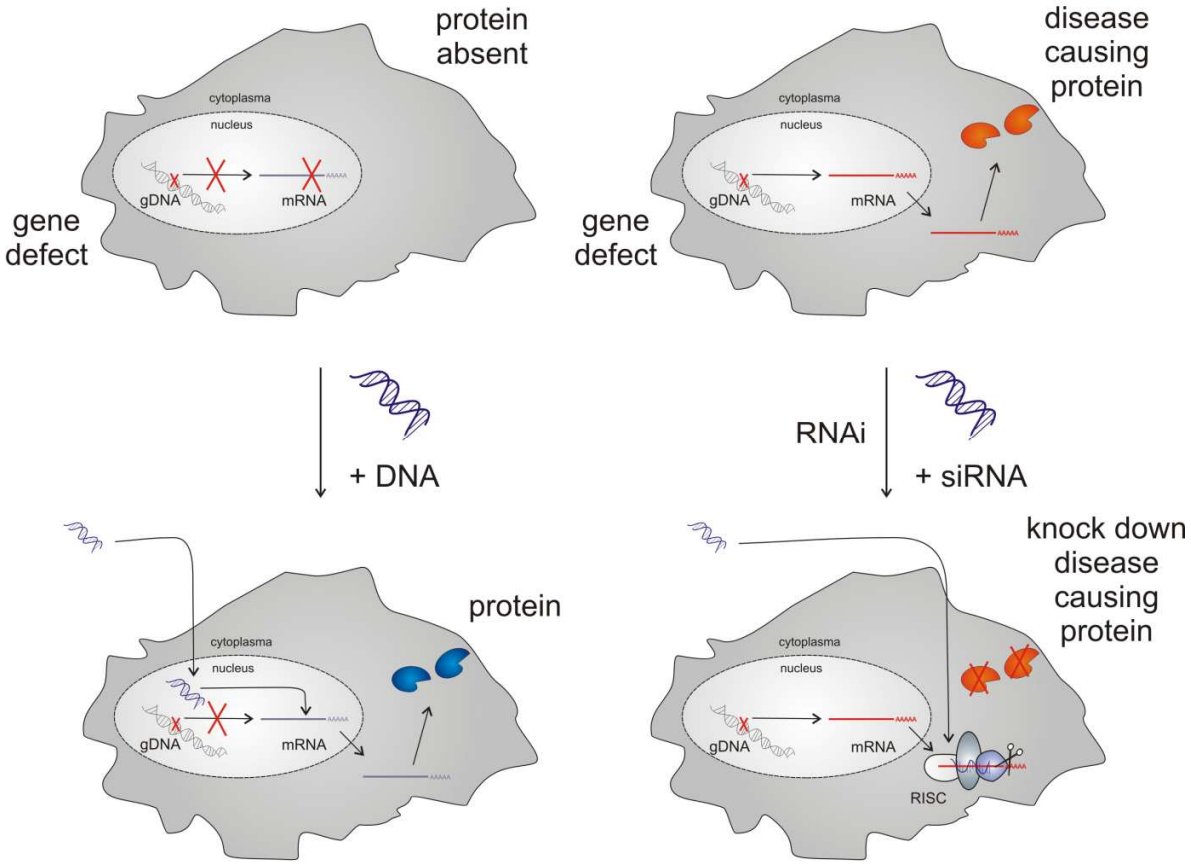

Figure 1. Genetic-based diseases, caused by a genomic mutation/deletion resulting in either an absent or a disease causing protein, can be treated by adding DNA encoding a therapeutic protein or by using the RNAi mechanism to knock down the disease causing protein, respectively.

In general, two types of genetic-based diseases can be distinguished (Fig. 1). A gene mutation or deletion can result on the one hand in the absence of a specific protein and on the other hand in the presence of a disease causing protein, e.g. by mutated activity or altered expression levels. The first type can be treated by adding the DNA that encodes the absent protein. The latter by using the RNA interference (RNAi) mechanism, resulting in specific protein expression knock down of unwanted or deregulated proteins (Fig. 2).

DNA can be introduced by viral expression cassettes (in case of viral vectors) or recombinant plasmids (in case of non-viral vectors), engineered to encode specific proteins. Plasmid DNA (pDNA) and viral vectors can be considered as pro-drugs that upon cellular internalization make use of the cellular transcription and translation apparatus to synthesize the protein of interest.

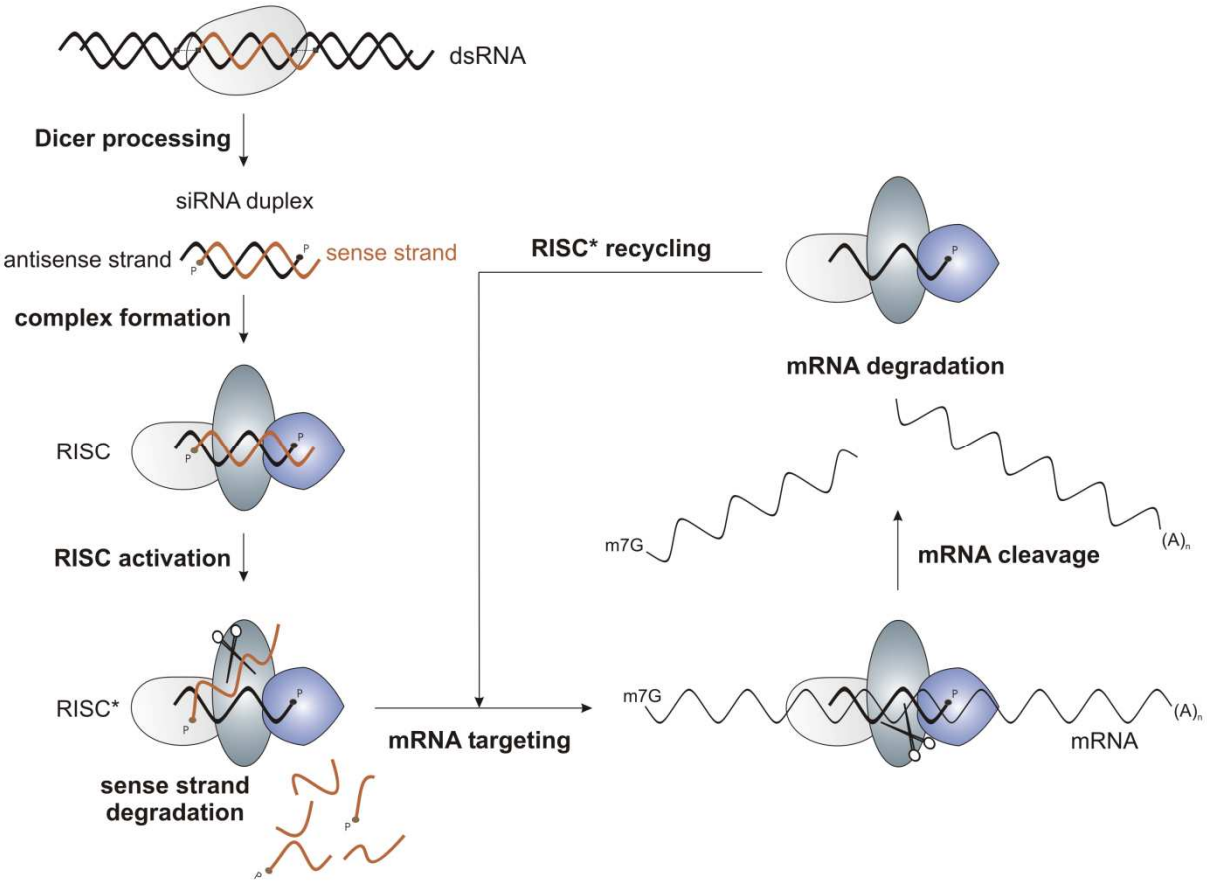

Figure 2. Overview of the RNAi mechanism (adapted from Raemdonck et al., *submitted*).

RNAi (Fig. 2) is a naturally occurring gene silencing mechanism initiated by double stranded RNA (dsRNA) that triggers sequence-specific cleavage of mRNA transcripts. In succession of pioneering research in plants [2] and nematodes [3], RNAi was evidenced in mammalian cells in 2001 by Tuschl and colleagues [4]. When long dsRNA enters the cell, it is immediately recognized and processed by Dicer, an RNase III type enzyme, resulting in short interfering RNAs (siRNAs), i.e. RNA duplexes

about ~21 to 25 nucleotides in length [5]. These siRNA molecules are subsequently incorporated into a protein complex called RNA induced silencing complex (RISC) that contains the Argonaute 2 (Ago2) endonuclease. Only one strand of the RNA duplex is retained inside the RISC, called the antisense or guide strand. It is suggested that the sense or passenger strand is initially cleaved by Ago2, thereby triggering its dissociation from the complex [6-8]. Finally, the activated RISC (RISC*) scans the messenger mRNA (mRNA) and binds to its complementary region, followed by Ago2 directed transcript cleavage between bases 10 and 11 with respect to the 5' end of the guide strand, leading to mRNA degradation [9]. As long dsRNA can induce severe interferon (IFN) responses in mammalian cells [10], inducing RNAi is mostly accomplished by the addition of chemically synthesized 21mer siRNAs, mimicking Dicer cleavage products, or by the intracellular production of siRNAs from short hairpin RNA (shRNA) precursors that can be continuously expressed from RNA polymerase III driven expression cassettes.

DELIVERY SYSTEMS FOR THERAPEUTIC NUCLEIC ACIDS

The use of nucleic acids as a drug faces major challenges. For instance, nucleic acids are prone to degradation by nucleases that are widely distributed in the body. Additionally, their size and high negative charge prevents them to cross the negatively charged cellular membrane. Subsequently, several delivery systems that protect the nucleic acids and/or facilitate their cellular uptake have been developed. Ideally, a nucleic acid delivery method needs to meet three major criteria: (1) it should protect the nucleic acids against degradation by nucleases, (2) it should bring the nucleic acids across the plasma membrane to the desired intracellular region of the target cells, and (3) it should have no detrimental effects on the cell [11]. In general, two types of delivery vehicles can be distinguished, i.e. viral and non-viral.

VIRAL DELIVERY SYSTEMS

Beyond any doubt, viruses such as retroviruses, adenoviruses, adeno-associated viruses and herpes simplex viruses, are currently the most efficient vehicles to deliver therapeutic DNA into the cell nucleus, as viruses hijack a variety of cellular mechanisms to bypass all cellular barriers and ferry their genomic material into the nucleus [12,13].

Retroviruses

Retroviruses are RNA containing infectious particles surrounded by a protein capsid and a lipid bilayer. They are variable in shape and size, but their average diameter is ~100 nm. After reverse transcription, the newly synthesized DNA is integrated into the genome of the host cell at which point the retroviral DNA is referred to as a provirus. They can carry up to 8 kb of foreign DNA and transduce dividing cells only [14]. The life cycle of retroviruses, involving integration of proviral DNA into the host cell genome and stable transmission to subsequent cell generations, offers the potential for long-term cure of inherited monogenic diseases. Lentiviruses, e.g. HIV-1, are a subclass of the retroviruses and are able to transduce both dividing and non-dividing cells.

Adenoviruses

Adenoviruses (AdV) were first isolated and cultured from tonsils and adenoid tissue [15] and now already 51 human AdV serotypes have been identified, grouped in six species (A–F), which mostly cause mild infection of the upper respiratory tract, gastrointestinal tract, and the eye [16]. AdV are icosahedral, non-enveloped, dsDNA viruses of ~70 nm diameter that transduce both diving and non-dividing cells [17]. The capsid is built up from 252 capsomers of which 240 are hexavalent and 12 (situated at the apices) are pentavalent. Wild type (wt) AdV is a lytic virus, killing infected cells and not integrating into chromosomes of permissive cells. However, wt AdV occasionally integrates into chromosomes of non-permissive cells [18]. They can carry about 8 kb foreign DNA and, as they mostly do not integrate into the host genome, the gene expression is rather limited in time (reviewed by [19]).

Adeno-associated viruses

Adeno-associated viruses (AAV) are non-enveloped single stranded DNA (ssDNA) viruses that belong to the parvoviruses. They are icosahedral, ~20-25 nm diameter, contain a capsid protein and transduce both dividing and non-dividing cells. AAV have the ability to stably integrate into the host cell genome at a specific site (designated AAV integration site-1 or AAVS1) in human chromosome 19 [20]. The cloning capacity of the vector is relatively limited and most therapeutic genes require the complete replacement of the viral 4,8 kb genome.

Herpes simplex viruses

Herpes simplex virus (HSV) is a dsDNA virus that can infect both dividing and non-dividing cells. Amplicons are defective, helper-dependent HSV type 1 (HSV-1) based vectors with a large transgenic capacity, allowing the delivery of up to 100 kb of foreign DNA. Both features make these vectors one of the most powerful, interesting and versatile gene delivery platforms (reviewed by [21]), although their utility in gene therapy has been impeded to some degree by their inability to achieve stable transgene expression. Introduction of the integrating elements of AAV into HSV-1 amplicon vectors has shown to significantly improve stable gene transduction by conferring the AAV-like capability of site-specific genomic integration [22].

NON-VIRAL GENE DELIVERY SYSTEMS

The above described viral gene delivery systems have important disadvantages, such as risk of insertional mutagenesis, immunogenicity and cytotoxicity [23,24]. Besides these clinically dangerous virus-mediated gene delivery systems, several non-viral gene delivery systems have been proposed for safe delivery of therapeutic nucleic acids into target cells. Basically, non-viral gene delivery methods are either physical, i.e. carrier-free, or chemical, i.e. carrier-based. Physical methods, including electroporation, hydrodynamic injection, sonoporation, laser assisted delivery, magnetofection and ballistic delivery employ a physical force that permeates the cell membrane and facilitates intracellular nucleic acid transfer. The chemical approaches use synthetic or naturally occurring compounds as carriers to deliver the nucleic acids into the target cells.

Physical methods

ELECTROPORATION. Electroporation, also referred to as electropermeabilization or electrotransfer, consists of the local application of electric pulses and has proven to be the most simple and efficient non-viral delivery method (reviewed by [25-27]). Until now, the exact mechanism by which electroporation enhances nucleic acid delivery into cells is not clear, though it is known that membranes become effectively permeable once a critical electrical potential has been achieved. Beside permeabilization, the appliance of electrical pulses was shown to facilitate the electrophoretic movement of pDNA into the nucleus and to exert some protection against cytosolic degradation [28-30]. A wide range of target tissues have been studied including skin, kidney, lung, liver, skeletal and cardiac muscles, joints, spinal cord, brain, retina, cornea, the vasculature and a variety of tumours [31-40]. Nevertheless, *in vivo* clinical applications are still limited due to the small effective

range of ~1 cm between the electrodes, the necessity of surgical procedure and the high voltage applied to tissues possibly resulting in irreversible tissue damage [41] or even affecting the stability of the gDNA.

HYDRODYNAMIC DELIVERY. Hydrodynamic delivery (reviewed by [42]), the first systemic delivery method for naked nucleic acids, is performed by a rapid injection of a large volume of naked nucleic acids solution via the tail vein of mice, inducing potent gene transfer predominantly in the liver [43,44]. Alternatively, rapid injection of naked DNA via the inferior vena cava resulted in gene expression mainly localized in the proximal tubular epithelial cells of the corticomedullary region of the kidney [45]. Of course, translating this simple and effective procedure to one that is applicable in humans is quite challenging.

SONOPORATION. Sonoporation is a technique that makes use of ultrasound for the intracellular delivery of nucleic acids. In contrast to e.g. electroporation and pressure-mediated delivery, ultrasound is a non-invasive and locally applicable technique. High-intensity focused ultrasound is already clinically used for therapeutic purposes (e.g. thermal destruction of tumours and treatment of kidney stones) and low level ultrasound is used for diagnostic purposes, making it an attractive technique for *in vivo* gene delivery. The application of ultrasound results in acoustic cavitation and is believed to produce transient membrane permeabilization, thus enhancing the delivery of nucleic acids to the cytoplasm. Addition of nucleation agents (reviewed by [46]), such as ultrasound contrast agents (also called gas-filled bubbles or (micro)bubbles), has shown to enhance cavitation and/or transfection efficiency [47-50] and to induce transient pores in the cell membrane immediately following treatment, as evidenced by electron microscopy images [51]. In contrast, other researchers suggest that ultrasound combined with microbubbles facilitate the uptake of macromolecules through endocytosis and macropinocytosis [52]. Both hypotheses are displayed in Fig. 3. Combining both electroporation and ultrasound (electro-sonoporation) has shown to be superior to either electroporation or ultrasound alone [53].

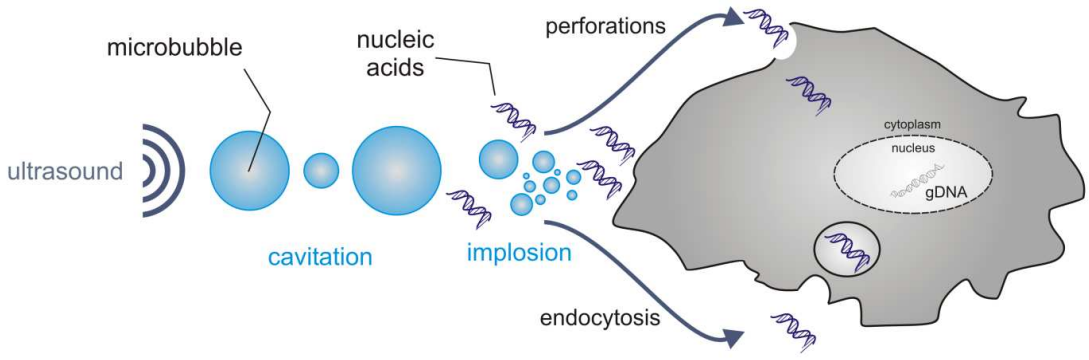

Figure 3. Principle of sonoporation in the presence of microbubbles and nucleic acids.

LASER BEAM GENE TRANSDUCTION, MAGNETOFECTION AND BALLISTIC DELIVERY. The use of a focused laser to enhance gene delivery, called laser beam gene transduction (LBGT), provides an energy source, possibly resulting in a local disruption of the cell membrane [54]. It remains to be seen if LBGT can be significantly scaled up in studies of larger muscles or other tissues, although Zeira et al. recently showed that by using femtosecond laser pulses (SG-LBGT) long term intradermal gene expression and genetic immunization could be obtained [55]. Also magnetofection, i.e. the use of strong magnetic fields providing an energy source to assist transfer of nucleic acids coupled to paramagnetic nanoparticles, can be used to enhance nucleic acid delivery (reviewed by [56-58]). Finally, particle bombardment through a gene gun is an ideal method for gene transfer to skin, mucosa, or surgically exposed tissues within a confined area [59-61].

Chemical methods

LIPOSOMES. Cationic liposomes are spherical, nano-sized artificial vesicles, composed of cationic and other (helper) lipids that form one or more (phospho)lipid bilayers enclosing aqueous compartments. Based on the strong negative charge of the nucleic acids, cationic liposomes (LPSs) were shown to be very efficient in binding nucleic acids, forming lipoplexes (LPXs) and transferring them into cells [62]. They are widely used because of their advantages over viral gene transfer: they are non-immunogenic, easy to produce and non-oncogenic (reviewed by [63,64]). The cationic LPX structure is still under discussion and depends on the composition of the LPS: an 'external' model, in which the nucleic acids are adsorbed onto the surface of cationic liposomes, or an 'internal' model, in which the nucleic acids are surrounded or 'coated' by a lipid envelope [65]. The commonly used cationic lipid N-(1-(2,3-dioleoyloxy)propyl)-N,N,N-trimethylammoniumchloride (DOTAP; Fig. 4A) and the neutral lipid 1,2-dioleoyl-sn-glycero-3-phosphoethanolamine (DOPE; Fig. 4B) are depicted in Fig. 4, together with the general structure of LPXs (Fig. 4C).

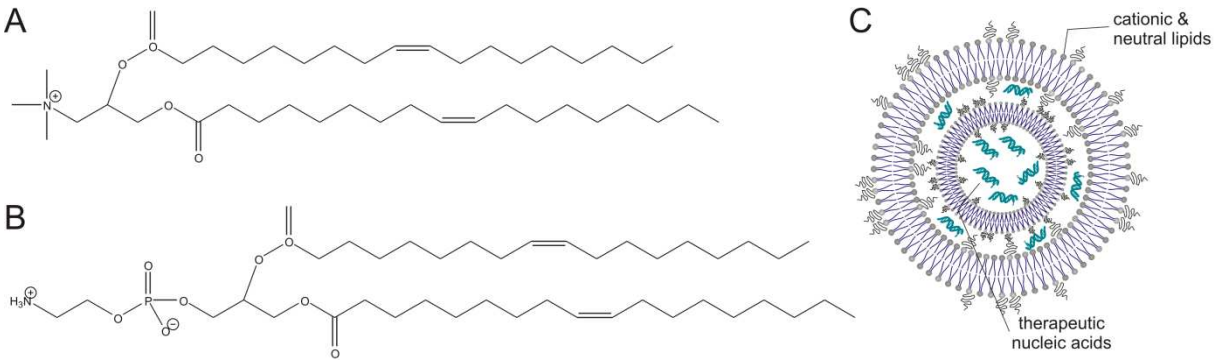

Figure 4. Representation of (A) DOTAP and (B) DOPE (C) LPXs

POLYMERS. Like cationic lipids, cationic polymers (reviewed by [66-72]) self-assemble with the negatively charged nucleic acids into so-called polyplexes due to electrostatic interactions. Different types of non-degradable and degradable polymers have been evaluated as nucleic acid delivery vehicles, e.g. poly(ethyleneimine) (PEI), poly(2-dimethylaminoethyl methacrylate) (pDMAEMA), poly-(L-lysine) (pLL), poly(ester)s and poly(urethane)s (Fig. 5).

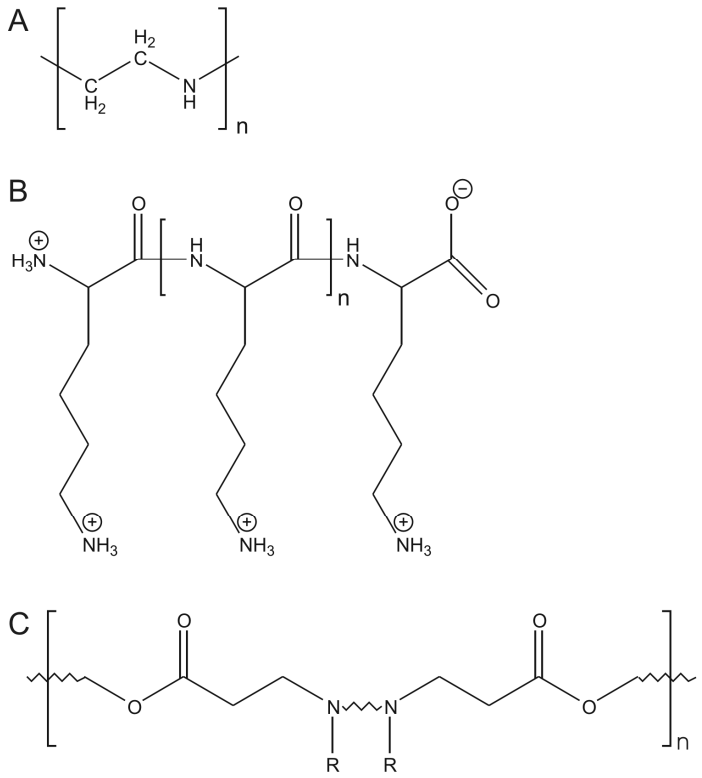

Figure 5. Structure of some commonly used cationic polymers: (A) linear PEI, (B) pLL and (C) poly(β-amino ester)

NON-VIRAL DELIVERY BARRIERS

Until now, the use of non-viral delivery systems for clinical gene therapy applications is limited by overall poor transfection efficiency [73,74]. Several extra- and intracellular barriers have been shown to dramatically affect the success of non-viral gene therapy (Fig. 6). Upon administration (e.g. by intravenous injection) the extracellular barriers include limited stability in the blood, adhesion to non-target tissues such as the endothelial cells lining the blood vessels, phagocytosis by macrophages, degradation of the nucleic acids, etc. Furthermore, once the target cell is reached, an additional series of barriers need to be crossed before the nucleic acids reach their intracellular target 'region': the cellular and/or endosomal membrane, the cytoplasm and in case of pDNA also the nuclear envelope (NE).

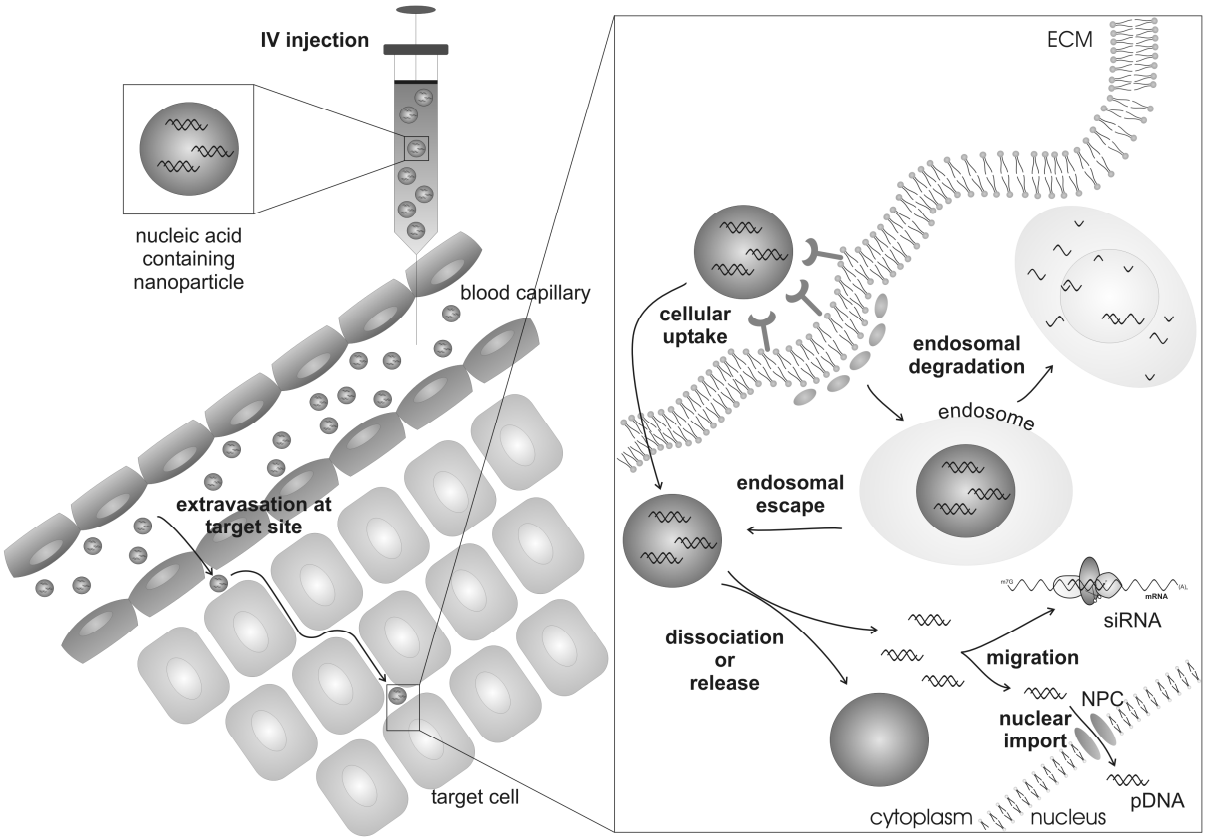

Figure 6. Overview of non-viral gene delivery barriers (adapted from Raemdonck et al., *submitted*).

EXTRACELLULAR BARRIERS

Naked nucleic acids, as well as nucleic acids complexed with polycations or LPSs, undergo major first-pass clearance by the liver upon intravenous administration [75-77]. Additionally, the presence of plasma nucleases reduces the half-life of DNA, and results in urinary excretion of degraded DNA [77]. Systemic administration of polybasic carriers, with or without simultaneous addition of nucleic acids, has been shown to activate the complement system, and the continued presence of administered carriers is likely to evoke an immune response [78]. Furthermore, these carriers accumulate in organs with very fine capillary structures such as the skin, lung, and the intestine, possibly due to the formation of aggregates with serum proteins, as suggested by Pouton and Seymour [79]. LPXs commonly exceed 100 nm in diameter, and are also expected to self-aggregate in the blood stream, resulting in limited passage through the wall of the blood vessel [79]. Accordingly, cells in areas with supernormal vessel permeability are easily transfected using LPXs [80-82] and techniques to enhance transfection efficiency *in vivo*, such as hydrodynamic injection, are based on the mechanical disruption of the structural integrity of the blood vessel wall barrier [83].

To avoid the adsorption of serum proteins onto the nanoparticle surface and the subsequent aggregation and uptake of opsonized particles by macrophages and other immune cells, various

strategies have been considered. For example, covering the surface with inert polymers could, in principle, reduce protein adsorption and their affinity to immune cells thereby minimizing the toxic responses. Toward this end, poly(ethylene glycol) lipid (PEG-lipid) conjugates have been incorporated into the LPXs to minimize the non-specific interactions with blood components [84-87]. It is believed that PEG, being hydrophilic and unable to interact with either nucleic acids or cationic lipids, results in longer circulation times of LPXs in the blood by minimizing the binding between LPXs and blood components.

CELLULAR UPTAKE

Once the target cell is reached, the cellular microenvironment may play a critical role in mediating the cellular response to the presented nucleic acids, especially as many diseases disrupt normal extracellular matrix (ECM) architecture, cell adhesion to the ECM and subsequent cellular activity (reviewed by [88]). After passage through the ECM, the nucleic acids must be taken up by the target cell. As the cell membrane is naturally impermeable to molecules larger than 1 kDa, cells posses a variety of active internalization mechanisms to accommodate cellular entry of larger molecules or complexes. It has been shown that several forms of endocytosis are involved in the cellular uptake of nucleic acid containing nanoparticles [89,90]. The internalization mechanism varies widely according to cell type [91], type of nanoparticle [92], presence of targeting ligand and particle size [93,94]. The majority of the reports suggests that endocytosis is the preferred route of cell entry for non-viral carriers [95]. Additionally, some reports deal with the involvement of endocytosis-independent uptake mechanisms active in some specific cases [96].

In general, endocytosis can be classified in two broad categories: phagocytosis and pinocytosis [97] (Fig. 7). Phagocytosis is typically restricted to specialized cells whereas pinocytosis occurs in all cell types. The different pinocytotic pathways can primarily be divided in macropinocytosis, clathrin-dependent (CDE) and clathrin-independent (CIE) endocytosis. Additionally, under CIE, one can make the discrepancy between dynamin-dependent and -independent endocytosis [91].

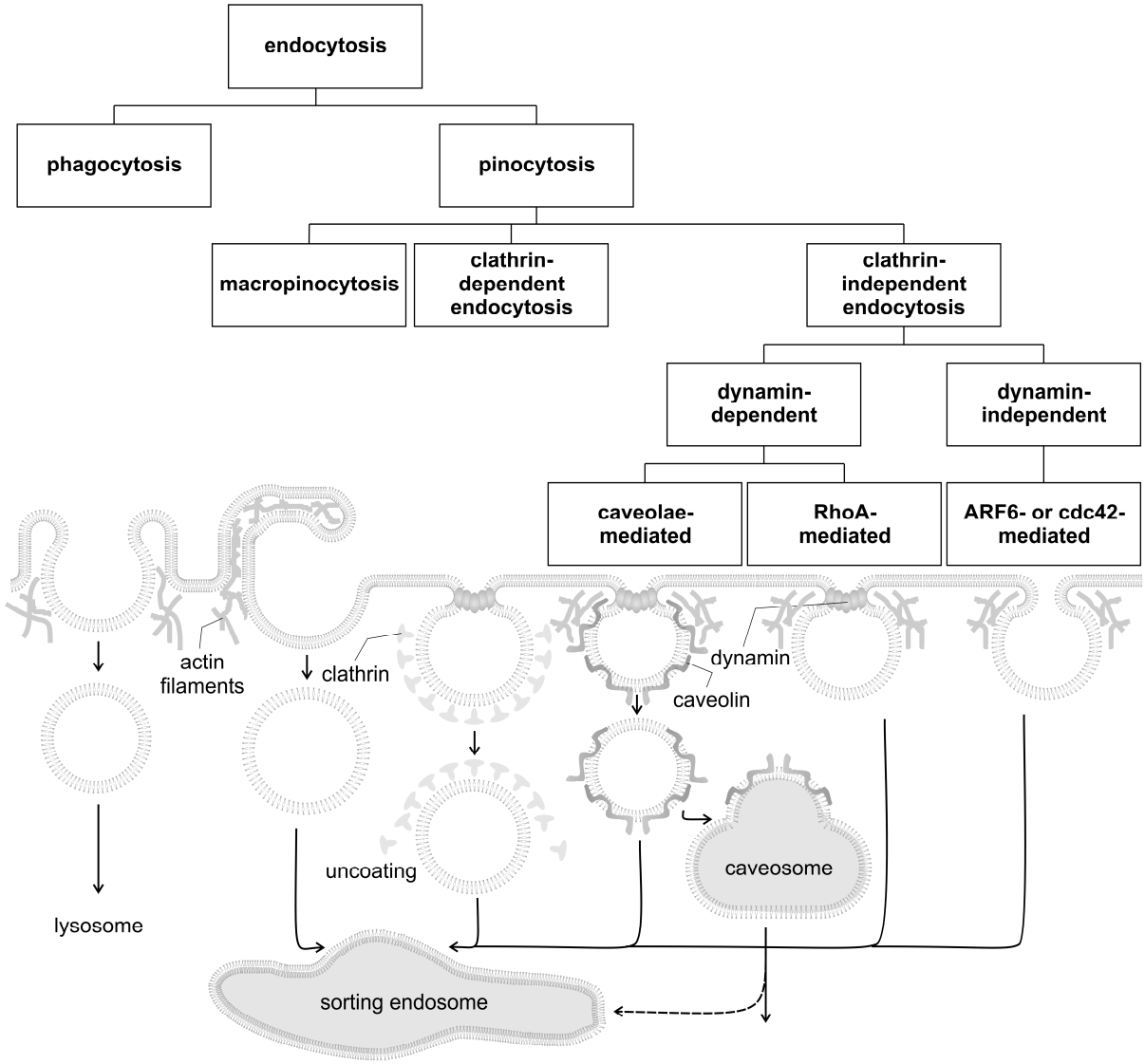

Figure 7. Endocytic internalization pathways (adapted from [91]).

Clathrin-dependent endocytosis (CDE)

CDE is the most important and best characterized endocytic pathway and is claimed to be the preferred pathway for particles ~200 nm in size [94]. During CDE, a local, clathrin-associated invagination of the plasmamembrane (PM), a coated pit, pinches off to form a membrane-derived coated vesicle. This is followed by GTPase dynamin-dependent fission of the mature vesicle [98] and the immediate release of the clathrin coat, resulting in 60-200 nm sized vesicles [99]. By fusion with the sorting (early) endosomes, CDE typically ends up in the acidifying and degrading endolysosomal pathway resulting in hydrolytic and enzymatic destruction of the endocytosed molecules.

Clathrin-independent endocytosis (CIE)

The current CIE classification is based on the role of dynamin and several small GTPases [91]. Dynamin-independent CIE is subdivided in ADP-ribosylation factor 6 (ARF6) and cell division cycle 42 (CDC42) regulated endocytosis. Dynamin-dependent CIE is subdivided in caveolae-mediated and RhoA-regulated endocytosis. All CIE endocytic pathways are related by the fact that the endocytic vesicles bud from a liquid, ordered membrane environment, called lipid rafts, enriched in unsaturated phospholipids, cholesterol, glycosphingolipids and certain proteins [100]. Additionally, all CIE processes strongly depend on the integrity of actin microfilaments [91]. Caveolae-mediated endocytosis is probably the best characterized CIE pathway. Caveolae are small (50-80 nm), smooth, flask-shaped invaginations of the PM that are characterized by the presence of caveolin [101]. The post-endocytic trafficking of CIE is quite diverse and mostly dependent on the cargo: from ending up in the early endosomes [91] to fusing with caveosomes [102]. Caveosomes are neutral endosomes which do not acidify [103] nor do they fuse with lysosomes [104]. Additionally, they have a longer life time compared to other endosomes [102].

Macropinocytosis (MP)

MP is a non-selective endocytic mechanism of suspended macromolecules that gives rise to vesicles with sizes up to 5 µm [105]. MP is based on the formation of membrane protrusions, often called ruffles, which can subsequently fuse with each other or with the PM to enclose large volumes [106]. Once taken up, the intracellular itinerary differs from cell to cell. In macrophages, the formed macropinosomes shrink, acidify and fuse with lysosomes. In contrast, in epithelial cell lines these vesicles do only partially acidify, do not fuse with lysosomes and are finally mostly exocytosed [107].

Phagocytosis

Phagocytosis shares many features with MP, but instead of membrane ruffles that form a macropinosome, the fagosome is formed by actin-driven pseudopodia that ingest micron-sized particles. This is no fluid-phase but adsorptive endocytosis and is exclusive for specialized cells such as macrophages and dendritic cells that engulf large structures, i.e. > 500 nm, such as bacteria, dead cells or yeast [108].

Endocytosis-independent uptake mechanisms

CELL PENETRATING PEPTIDES (CPPs). So called CPPs, e.g. the HIV-1 Tat peptide, have been reported to accomplish direct cytosolic delivery when attached to various cargoes, such as fluorochromes [109], proteins [110,111], oligonucleotides [112] and even magnetic nanoparticles [113] and liposomes [114,115]. Initially, analysis of fixed samples after incubation at low temperature and in the presence of metabolic inhibitors suggested that the uptake mechanism was energy-independent, excluding the involvement of endocytosis. The proposed uptake mechanism was called translocation or transduction and seemed to be non-saturable, very fast (i.e. within minutes), and independent of cell type. However, based on different observations, such as the redistribution of CPPs after cell fixation and the fact that endocytosis inhibitors such as cytochalasin D (cytoD) and low temperature did abolish the CPP uptake in living cells, serious issues were raised concerning the general nature of the translocation mechanism [116-118]. Subsequently, re-evaluation of the uptake of these peptides and their cargoes lead to the conclusion that endocytosis is the major uptake pathway [119,120]. The possibility of the energy-independent uptake of these peptides and their cargoes, however, cannot be excluded [121], and it may be possible that certain factors, which may affect the uptake mechanism, should be optimized to achieve a successful endocytosis-independent delivery.

MICROINJECTION, PERMEABILIZATION, ELECTRO- & SONOPORATION. Microinjection is a technique that permits the rapid delivery of nucleic acids into the cytosol or nucleus [122,123] In the case of permeabilization, pore-forming agents such as streptolysin O or anionic peptides similar to the N-terminal segment of the Hemagglutinin 2 (HA2) subunit of the influenza virus hemagglutinin that have the ability to fuse with the plasmamembrane, are used to induce transmembrane channels or large apertures in the cell membrane, which then allow the entry of large molecules [124,125]. However, both techniques are highly invasive and cannot be used for *in vivo* gene delivery. Finally, also electro- and sonoporation are alternative approaches to avoid endosomal uptake and are described above.

ENDOSOMAL ESCAPE

When the nanoparticle is taken up by endocytosis, it mostly ends up being degraded inside the lysosomes, unless it succeeds in escaping from the endosome before acidification takes place. A number of mechanisms have been proposed to facilitate the escape of particles from the endosomes.

Membrane-destabilizing and fusogenic lipids

The use of membrane-destabilizing lipids is widely studied and a variety of lipids have been used for this purpose. Several researchers have shown that lipid contact occurs between cationic lipids from the LPX and anionic lipids from the inner face of the endosomal membrane, resulting in flip-flop of anionic lipids from the cytoplasmic face of the endosomal membrane [126-128] (Fig. 8). These anionic lipids laterally diffuse into the LPX and form a charge neutralized ion-pair with the cationic lipids from the LPXs, resulting in destabilization of the LPXs, displacement of the negatively charged nucleic acids and their subsequent release into the cytoplasm of the cells.

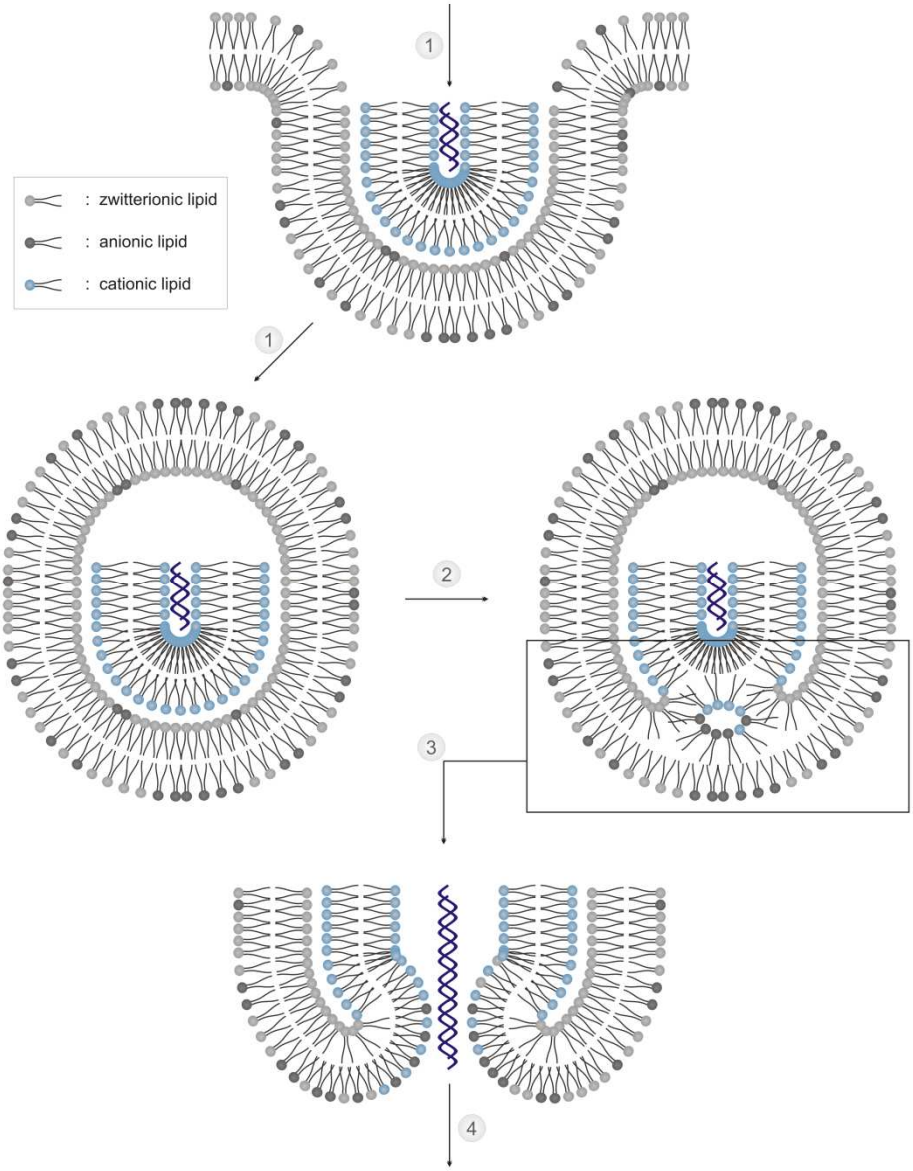

Figure 8. Schematic representation of the cationic lipid mechanism of endosomal release: (1) internalization, (2) initiation of endosomal membrane destabilization resulting in a flip-flop of anionic lipids, (3) lateral diffusion of the anionic lipids and formation of a charged neutralized ion-pair with the cationic lipid and (4) displacement of nucleic acids and diffusion into the cytoplasm (adapted from [127]).

Additionally, liposomes often contain lipids with pH-dependent fusogenic properties, i.e. lipids that undergo a phase transition in the low pH environment of the endo-/lysosomes, thereby promoting fusion with and/or destabilization of the endosomal membrane (reviewed by [129]). Cone-like lipids, such as the neutral lipid DOPE, can change at low pH from the lamellar phase into the inverted hexagonal phase, disturbing the endosomal membrane thereby provoking endosomal escape.

Osmotic pressure and swelling

Another strategy to obtain endosomal release is to use a carrier that can create an osmotic pressure inside the endosomes. Highly cationic polymers such as PEI and poly(amidoamine) (PAA) dendrimers contain several secondary amines that are easily protonated in the acidic environment of the late endosome and lysosome. These polymers are efficient transfection agents that are thought to act by a proton sponge effect. The high buffering capacity of these polymers prevents acidification of the endosomal compartment, and induces ion influx in endosomes, causing osmotic swelling, vesicle destabilization and finally endosomal rupture [130-132]. Additional work on these polymers has demonstrated that chain flexibility is a key feature for this effect, since polymer expansion appears to be an important parameter leading to endosomal swelling and subsequent disruption [130,133]. Increasing osmotic concentration within the endosome can also be obtained by using a biodegradable polymer, resulting in an increase of the osmotic pressure in the endosome, as proposed by Koping-Hoggard [134]. This increase in osmotic pressure after degradation was also proposed for poly(β-amino ester)s (PbAEs) by our group (Vandenbroucke et al., *in revision*). Alternatively, polymers can also have a `hydrogel effect´, i.e. 'swelling' polymer, resulting in endosomal rupture [135].

Endosomolytic peptides and polymers

The acidic environment of the endosome has led to the design of several gene delivery peptides that become endosomolytic at lower pH. Once inside the endosome, these peptides can either buffer against the pH drop and hence build up an osmotic pressure in the endosomes or fuse with the endosomal membrane leading to pore formation (reviewed by [136]). In an effort to translate the above described proton sponge activity to peptide based nucleic acid carriers, histidine has been added. Histidine-rich peptides contain an imidazole group with a pK of ~6.0, thereby allowing it to become protonated in the acidic environment of the endosome, with similar effects as e.g. PEI. On the other hand, fusogenic peptides have been used to promote endosomal escape and delivery of nucleic acids to the cytosol and/or nucleus. These peptides adopt an α-helical structure at endosomal

pH leading to hydrophobic and hydrophilic faces that can interact with the endosomal membrane to cause disruption and/or pore formation [137,138]. In an effort to mimic viral mechanisms of endosomal escape, Wagner et al. designed short peptides derived from the N terminus of the influenza virus hemagglutinin HA-2 [139,140]. Additionally the conjugation of melittin, a strong amphipathic, 26 amino acid peptide whose sequence is derived from the venom *Apis mellifera* (honey bee), to polycations resulted in a strong increase in gene expression in a variety of cell lines [141,142].

Similarly, pH-sensitive synthetic polymers, consisting of anionic carboxylated polymers such as acrylic and methacrylic acid (MAA) copolymers, were shown to permeabilize cell membranes at acidic pH and low concentrations. These characteristics are due to the neutralization of carboxyl groups, which gives the polymer a higher hydrophobicity and affinity for lipid membranes. When used at high concentrations, these polymers can even completely solubilize phospholipid bilayers [130,143].

Photochemical internalization

Photochemical internalization (PCI) was first presented in 1999 as a novel technology for the delivery of a variety of therapeutic molecules into the cytosol [130]. PCI technology employs specific, preferably amphiphilic [144], photosensitizing compounds, called photosensitizers (PS), which accumulate in the membranes of the endocytic vesicles. Examples of PS are mesotatraphenylporphine containing two sulfonate groups on adjacent phenyl rings ($TPPS_{2a}$) and aluminium phtalocyanine with two sulphonate groups on adjacent phthalate rings ($AlPcS_{2a}$). Upon illumination, PS become excited and induce the formation of reactive oxygen species, primarily singlet oxygen. This highly reactive intermediate can damage cellular components, but the short range of action and short life-time confine the damaging effect to the production site. This localized effect induces the disruption of the endocytic vesicles, thereby releasing the entrapped therapeutic molecules into the cytosol. Since its discovery, several studies have been published (reviewed by [145]), demonstrating that this technique can be used to enhance drug delivery, both *in vitro* and *in vivo* [146-148] for site-specific delivery of proteins [130], peptides [130], peptide nucleic acids [149,150], and pDNA carried by non-viral [130,151-153] and viral carrier systems [154].

NUCLEAR IMPORT

One of the crucial steps in non-viral pDNA delivery is the nuclear import, as the DNA must enter the nucleus to be transcribed, replicated, and/or integrated. The NE encloses the chromosomes as a selective barrier not allowing the passage of molecules larger than 40 kDa [155].

Therefore, the NE needs to be degraded during mitosis to assure that the chromosomes gain access to the microtubules of the cytoplasmic mitotic spindle [156]. This occurs by disassembly of the major structural elements of the NE during the mitotic prophase. In late anaphase, the dispersed NE components are reused in the assembly of two new NEs around the segregated chromatids [157] with help of several proteins such as POM121 [158] and MEL-28 [159,160]. During reassembly of the NE, nucleic acids present in the cytoplasm can reach the nucleus 'by accident'. In contrast, postmitotic and quiescent cells have no breakdown of the NE. In addition, the transport channels in quiescent cells show a lower rate of nuclear uptake and smaller functional size compared to proliferating cells [161,162]. Therefore, as many cells that are targeted in gene therapy do not divide or divide very slowly, the entry of therapeutic genes into the nucleus is a major limiting step in non-viral gene transfer (reviewed by [163-165]).

Obstacles encountered during pDNA nucleocytoplasmic trafficking

It is estimated that at least 10^5–10^6 plasmids per cell are required in the extracellular compartment to ensure nuclear uptake and transcription in non-mitotic cells [166]. Additionally, determination of the nucleocytoplasmic pDNA transport efficiency revealed that only 0.1-0.001 % of the cytoplasmic DNA was eventually transcribed in the nucleus in the absence of cell division [167-171]. The limited nuclear localization after cytosolic pDNA delivery can be attributed to three aspects during nucleocytoplasmic transport: (1) restricted diffusional mobility, (2) metabolic instability and (3) limited nuclear transport.

The size-dependent restricted mobility of DNA inside the cytoplasm [172] is mainly caused by the mesh-like structure of the cytoskeleton, as disrupting or reorganizating the actin cytoskeleton significantly increases the diffusion rate [173,174]. Subsequently, this restricted diffusion leads to an increased residence time of the pDNA inside the cytoplasm, favoring metabolic degradation by nucleases that transiently appear in the cytoplasm before nuclear translocation [175]. Finally, once the pDNA reaches the NE, the nucleocytoplasmic trafficking is controlled by the nuclear pore complex (NPC) that forms a channel across the NE [176].

Nuclear pore complex (NPC)

The NE forms the boundary between the nucleus and the cytoplasm, and consists of an inner nuclear membrane (INM) and an outer nuclear membrane (ONM). Both membranes are separated by a lumen, called the periplasmic space, which is contiguous with the endoplasmatic reticulum (ER) lumen. Increasing evidence shows that the NE also links the inside of the nucleus to the cytoskeleton

through complexes of lamins on the inner aspect of the INM, through transmembrane proteins of the INM called SUNs and through large nesprin isoforms localized specifically to the ONM [177].

The presence of the nuclear barrier requires a system to efficiently transport diverse sets of macromolecules across the double-membraned NE. The mediators of this exchange are large assemblies termed NPCs that span pores in the NE connecting the nuclear and cytoplasmic compartments [178]. The general architecture of NPCs is shared in all eukaryotes, and many of the NPC proteins are conserved across phyla. The vertebrate NPC (Fig 8) has a mass of ~125 megadalton (MDa) [179], containing 30-50 proteins [180] known as nucleoporins or Nups [178,181]. The NPC exhibits an 8-fold rotational symmetry core structure, the so-called spoke complex, that forms a ~40 nm-diameter translocation channel, and contains ring structures at both the cytoplasmic and the nuclear sides of the NE [182-185]. In addition, eight fibrils of distinctive shape are attached to both ring structures. The cytoplasmic fibrils have free distal ends, while the thin fibrils emanating from the nuclear ring are laterally interconnected at their ends, called the terminal ring. The nuclear fibrils and terminal ring are believed to represent a structural and functional entity, called the nuclear basket [186,187]. Additionally, three-dimensional reconstructions of electron microscopic data indicate the existence of eight small, peripheral channels that are supposed to penetrate the individual NPC subunits around the large central channel [188]. The peripheral channels in the NPC rim structures most probably function like ion channels with small electrical conductivity and specific gating characteristics [189], while the central channel functions like a nanomachine that transports macromolecules of different sizes and thus undergoes dramatic changes in conformation [190-192].

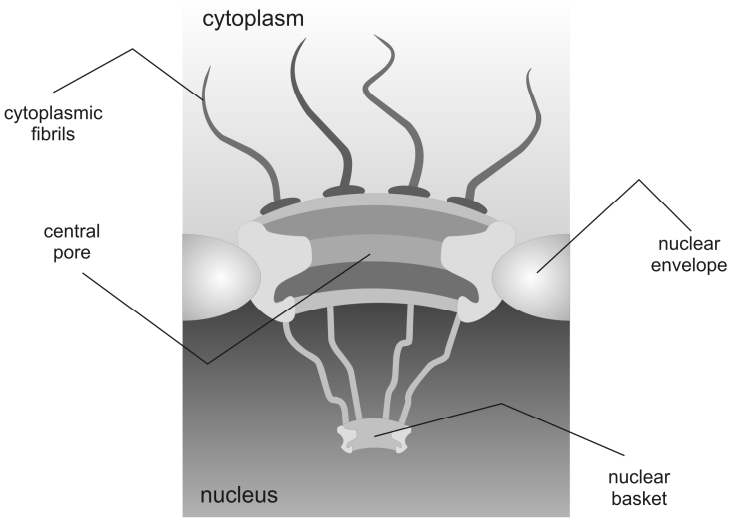

Figure 8. General structure of the NPC.

Water, ions, small macromolecules (< 20-40 kDa) [193] and small neutral particles (< 5 nm ∅) can diffuse freely across the NPC [194], while larger macromolecules generally need a particular

transport signal sequence, such as a nuclear localization signal (NLS) or nuclear export signal (NES) to be transported efficiently. NPCs can pass cargoes up to 30 nm diameter, at rates as high as several 100 macromolecules per sec; each transport factor-cargo complex dwelling in the NPC for a time at the order of 10 msec [195,196].

Nucleocytoplasmic transport components

NUCLEAR TRANSPORT RECEPTORS. Proteins that contain a NLS or NES are recognized by nuclear transport receptors (NTRs) that mediate their translocation through the nuclear envelope. The majority of NTRs belong to the family of karyopherin β proteins, also called importin β-like proteins (reviewed by [197,198]). According to their transport direction two subtypes can be distinguished, i.e. importins and exportins. As shown in Fig. 9, importins associate with their macromolecular cargo in the cytoplasm, either directly or indirectly via adaptor proteins. Subsequently, they dock to the Nups of the NPC, translocate through the central channel of the NPC and release their cargo. Most of the transport receptors use the GTPase Ran to control cargo association. The asymmetric distribution of RanGDP (mainly present in the cytoplasm) and RanGTP (mainly in the nucleus) ensures the directionality of nuclear transport [199,200]. Indeed, importins bind their cargoes in the cytoplasm in the absence of RanGTP and unload them upon binding to RanGTP in the nucleus. The export process, mediated by exportins, is essentially the reciprocal process, also regulated by the GTPase Ran.

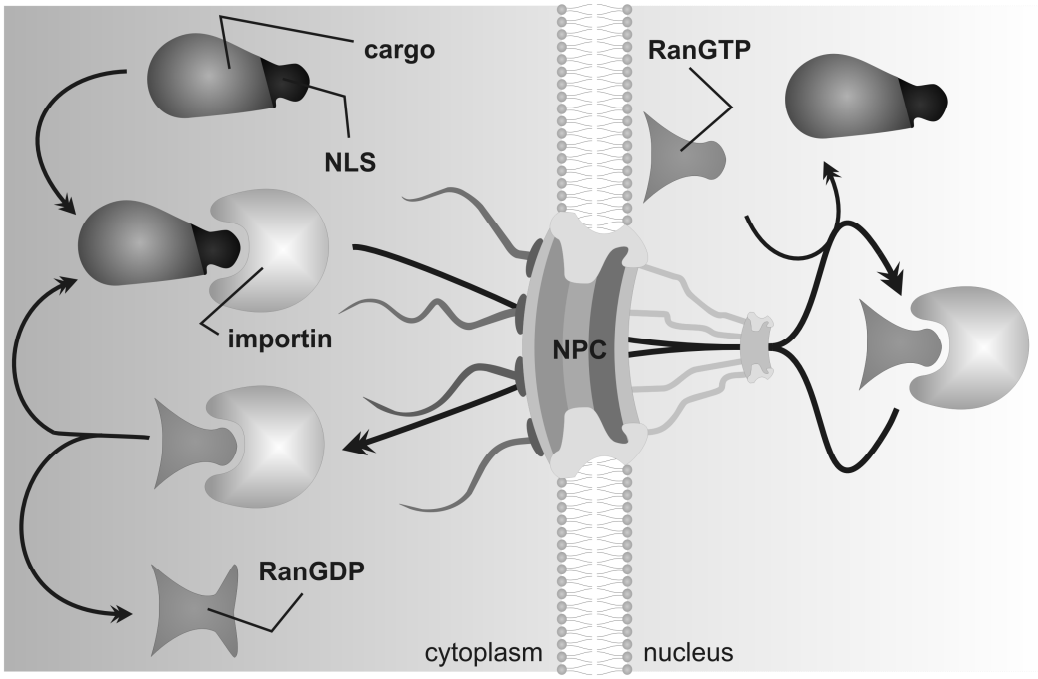

Figure 9. Overview of the active, NLS-dependent nuclear import mechanism.

CLASSICAL AND NON-CLASSICAL NLSS. Obtaining active protein transport into the nucleus requires the presence of NLSs which can interact with the NTRs. In general, NLSs can be subdivided into classical and non-classical sequences [201]. The classical NLS sequences are characterized by a stretch of basic, charged amino acids and interact with the importin α/importin β heterodimer [202] or are recognized by importin β alone [203] to facilitate nuclear import of their protein cargo. In contrast, non-classical NLS sequences lack this basic amino acid stretch and bind to transportin instead of importin [204].

NLS INDEPENDENT NUCLEAR TRANSPORT. In recent decades, the function of sugar molecules as nuclear transport signals has been clarified [205-207]. According to these reports, sugar-dependent nuclear transport is mediated by its receptor (i.e. lectin) and occurs in an energy-dependent manner via the NPCs. Moreover, since this pathway is not inhibited by an excess of NLS peptides, this sugar-mediated pathway appears to be quite different from the NLS-mediated pathway. The same reports also revealed sugar-specificity in nuclear delivery. Nuclear delivery of bovine serum albumin (BSA) modified with glucose, mannose, N-acetylglucosamine (GlcNAc), and fucose was clearly observed; in contrast, modification with galactose, lactose, and 6-phospomannose did not enhance nuclear delivery. Additionally, the sugar-dependent transport of BSA into the nucleus was shown to be cell cycle dependent as it was more efficient during the G_1/S transition and S phases, in contrast to NLS-mediated transport that did not sustain any difference during any stage cycle except a slight decrease for the G_2 phase [208]. Alternatively, proteins without NLS may be co-transported with another protein that do contain an NLS [209]. This 'piggy back mechanism' has been described in particular for some protein kinases [210].

Gateway models

The exact mechanism of the nucleocytoplasmic transport through the NPCs is still not completely elucidated. Different models have been proposed to explain how the nuclear permeability barrier is created, such as the 'Brownian affinity gate' [211,212], the 'oily spaghetti' [213], the 'affinity gradient' [214], the 'dimensionality reduction' [215], the 'polymer brush' [216], a 'two-gate' [217] and the 'selective phase' model [218-221]. Most models consider the NPC as a 'virtual gate' [222,223] (Fig. 9A), where the phenylalanine-glycine (FG) repeats of the Nups create a barrier for entrance into the NPC and transport through the NPC involves facilitated diffusion controlled by association and disassociation of transport receptors with FG Nups. They differ only in specific assumptions, such as the conformation and spatial deployment of the FG Nups, their physicochemical state, or the distribution of affinities of binding sites (reviewed by [224]). In contrast, an alternative model to the

'virtual gate' was proposed by Ribbeck and Görlich, called the 'selective phase' model (Fig. 9B), in which FG domains within the central channel of the NPC interact with each other to form a protein meshwork, forming a separate hydrophobic phase. Subsequently, the 'selective phase' model assumes that the central channel of the NPC has a sieve-like structure. NTR and NTR-cargo complexes can partition into this phase because of their capacity to bind to the FG repeats, thereby locally perturbing FG domain interactions. The capacity of Nups to form a three-dimensional meshwork with hydrogel-like properties was confirmed by Frey et al. who demonstrated that recombinant nucleoporins (Nsp1p) could form a free-standing hydrogel *in vitro* with an elasticity comparable to 0.4 % agarose (Fig. 9C) [225]. Additionally, mutation of the 55 phenylalanines (F) within the FG context of the essential yeast Nup Nsp1p to serines (S), resulted in the absence of gel formation and the mutated protein failed to bind to NTRs.

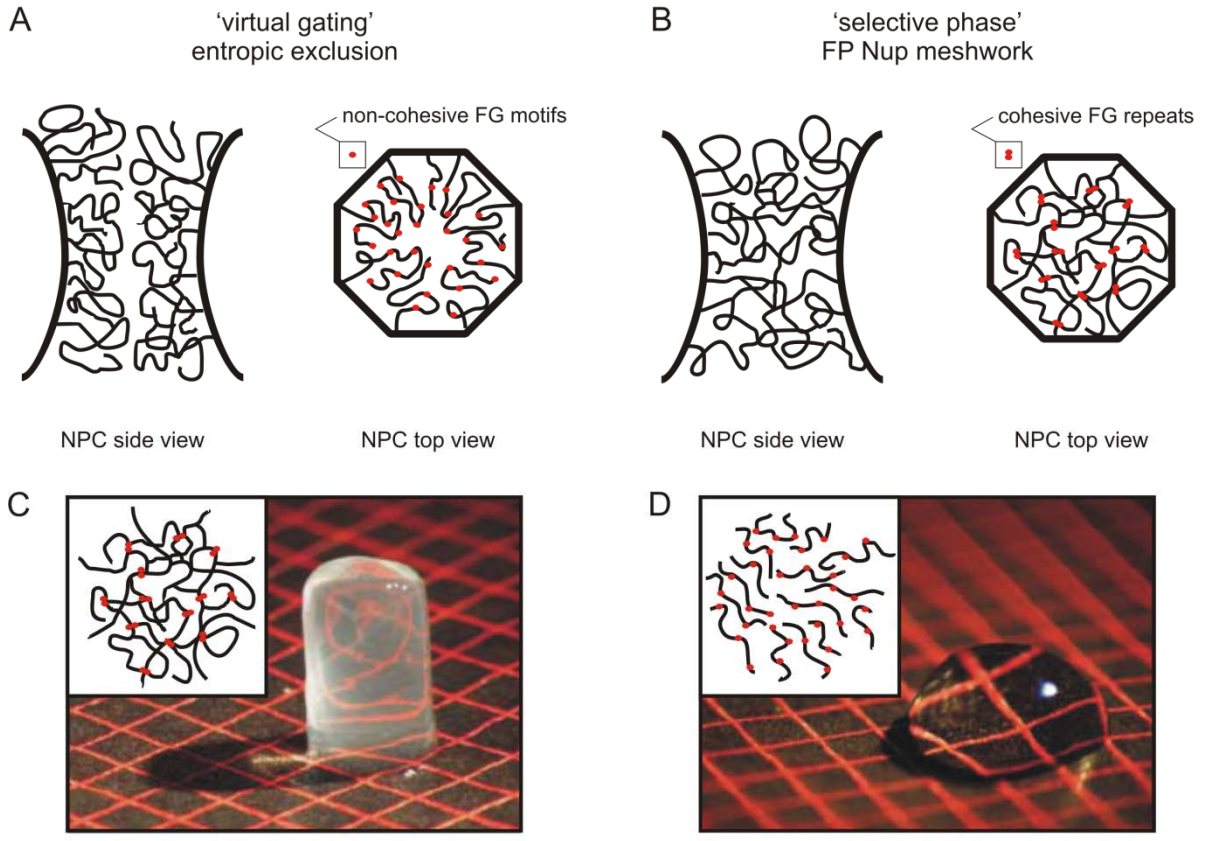

Figure 9. Two main models of the NPC permeability barrier. (A) The 'virtual-gate' model proposes that FG domains are non-cohesive, entropic bristles that repel the entry of non-karyophilic proteins into the NPC through Brownian motion. (B) The 'selective phase' model proposes that FG domains interact with each other via hydrophobic attraction between FG motifs to create a filamentous meshwork that sieves particles by size exclusion (adapted from [226]). (C) Formation of a hydrogel by the wt FG repeat domain from Nsp1p. Insert illustrates how interactions between the hydrophobic clusters (shown in red) crosslink the repeat domains. (D) Nsp1p with F→S mutated repeat domain was unable to form a hydrogel (adapted from [227]).

Opening the gateway

The molecular mass of pDNA can be estimated between 2 and 10 MDa. Subsequently, it is unlikely that pDNA can enter the nucleus via passive diffusion. Additionally, there are several reports indicating that the transport mechanisms for pDNA and molecules larger than 60 kDa share some characteristics, such as wheat germ agglutinin (WGA) sensitivity and temperature- and energy-dependent translocation [228], supporting the hypothesis that plasmid molecule accumulation proceeds by active transport via the NPC [229].

To promote the nuclear import of pDNA, different strategies are currently used: (i) hijacking the nuclear import machinery by attaching NLS peptides, NLS containing proteins or even importin β to the pDNA, (ii) compacting the pDNA in small nanosized particles to fit the NPC as a complex, (iii) mimicking the sophisticated viral mechanisms, and (iv) physical or chemical disruption of the nuclear barrier.

HIJACKING THE NUCLEAR IMPORT MACHINERY. Recruiting components from the nuclear import machinery to augment pDNA transport into the nucleus, requires the direct or indirect attachment of e.g. NLSs to pDNA, which can be achieved by different approaches (reviewed by [230-233]): (i) electrostatic interaction [234-243], (ii) covalent binding [244-250], (iii) via protein-DNA interaction [251,252], (iv) via peptide nucleic acid (PNA) clamps [253-256], (v) coupling to polymers [257-259], (vi) coupling to lipids [260-266] and (vii) coupling to recombinant lambda phage [267]. As an alternative to NLSs or NLS containing proteins, also importin and histones were used to enhance the nuclear pDNA delivery [268,269]. Although all these results support the fact that recruiting the nuclear import machinery can have some benefits for non-viral gene delivery, all these attempts have achieved only limited success compared to viral gene delivery. Probably, when condensing pDNA with NLSs or NLS-modified polycations, controlling the NLS surface display and density is difficult. Indeed, NLSs contain cationic amino acids which can interact with pDNA via strong electrostatic forces probably masking the NLS and hence preventing nuclear import enhancement.

COMPACTING THE PDNA. Although it was previously believed that complex dissociation precedes the nuclear uptake of pDNA [270], several researchers recently questioned this and showed that dissociation may not be a prerequisite for nuclear translocation. Furthermore, considering (1) the problems related to cytoplasmic mobility, (2) the limited pDNA stability and (3) the 25-30 nm cutoff of the NPC [271-273], it is reasonable to assume that compacting pDNA into cytoplasmic released nanoparticles can enhance transfection efficiency compared to naked cytoplasmic DNA release, particularly in slowly dividing and non-dividing cells [274]. Additionally, in case of LPXs, pDNA could be

detected in the nucleus in time intervals as low as 1 hr after LPX-mediated transfection, implying the involvement of dissociation independent mechanisms in this early nuclear delivery [275], such as LPX fusion with the nuclear membrane and subsequent pDNA release into the nucleus [276]. Furthermore, several nanoparticles were shown to end up inside the nucleus as a complex, i.e. without dissociation between DNA and carrier, e.g. DNA–PEI complexes [277,278] and multifunctional envelope-type nano device (MEND) nanoparticles [279].

MIMICKING VIRAL MECHANISMS. In general, sugars have been used as a tool in gene delivery to enhance the efficiency of cellular uptake. For example, galactose and mannose are specifically recognized by lectins expressed on the cell membrane surface, i.e. the asialoglycoprotein receptor and mannose receptor, respectively [280-282]. But in contrast to the influence on cellular uptake, different types of sugars, such as β-GlcNAc, α-mannose, and β-galactose, can also be used as nuclear targeting ligands, as already discussed above [283-285]. Nuclear lectin-mediated gene delivery by means of glycosylated polymers such as lactosylated pLL and lactosylated PEI, has been recently reported [286-291]. Additionally, Masuda et al. [292] developed a nuclear gene delivery system based on the novel concept of a 'degradable lipid envelope on the NPC', mimicking the mechanism of adenoviral nuclear entry. Once in the cytoplasm, the AdV capsid targets the NPC, allowing binding between capsid protein hexon and histone H1. Subsequently this leads to hexon–histone H1 complex transport into the nucleus by histone H1 import factors (i.e. importin 7 and importin β), triggering nuclear transfer of AdV gDNA in conjunction with disruption of the viral capsid [293]. In the study of Masuda et al. an octaarginine modified MEND (R8-MEND) was used, i.e. polycation-condensed pDNA followed by encapsulation with a stearylated R8 modified lipid envelope [279,294]. The presence of the R8 induces cellular uptake via macropinocytosis and uptake via this pathway is advantageous as it avoids a lysosomal degradation and releases its cargo into the cytoplasm [295,296]. Additionally, nuclear targeting was achieved through the addition of sugars on the MEND surface via anchorage of the cholesterol moiety of a sugar–cholesterol conjugate in the lipid envelope.

DISRUPTING THE BARRIER. Several studies showed that permeability is not 'fixed' but, in contrast, seems to be highly variable. Apparently, NPCs can undergo dramatic conformational changes, which subsequently strongly affect the electrical conductivity and macromolecule permeability of the central channel [297]. Different data stress the importance of combining both atomic force microscopy (AFM) and functional data, as it is not clear if the AFM derived terms 'NPC contraction, dilation or collapse' can be correlated to NPC ion and macromolecule permeability, although it is hypothesized that contracted NPCs are active pores while collapsed NPCs are inactive [298]. AFM images have shown that NPCs are calcium sensitive supramolecular structures that contract when the calcium

concentration is high [298], indicated by a sharp increase in NPC height and a narrowed NPC lumen. Additionally, after depletion of nuclear store calcium by inositol 1,4,5-trisphosphate or calcium chelators, fluorescent molecules conjugated to 10 kDa dextran were unable to enter the nucleus, while diffusion of molecules < 500 Da and ions was not affected [299,300]. In the presence of ATP, nucleoplasmic NPC rings were clearly contracted. Also CO_2 was shown to have an effect: cytosolic acidification by exposing the nuclear envelope to CO_2 induced NPC collapsing [301]. More recently, Enss et al. (2003) examined the effect of Ca^{2+}, pH and addition of an antibody against gp62, a glycoprotein located at the central channel entrance, on the NPC permeability for 10 kDa dextran, which is too large to penetrate the small peripheral channels but freely diffuses through open NPC central channels [302]. Neither Ca^{2+} nor pH influenced the NE permeability for 10 kDa, while the gp62 antibody reduced macromolecule diffusion. As it was previously shown that the peripheral channels could be activated by Ca^{2+} and ATP [303], these observations indicate that there are separate routes for macromolecules and ions to cross the NE, regulated by different mechanisms. Also different steroid hormones were tested on their functional and structural effect on nuclear pores of *Xenopus laevis* oocytes [304-306]. E.g. aldosteron was shown to influence the nuclear barrier integrity: ten minutes after aldosterone exposure a sharp increase in both electrical conductivity [305] and dextran permeability [307] was observed. These effects are possibly caused by the opening (or unplugging) of the central channels of a small 'aldosteronesensitive' population of NPCs, allowing both inorganic ions and macromolecules to travel through the central channel pathway. Shulga and Goldfarb demonstrated that aliphatic alcohols, such as methanol, ethanol, isopropanol, n-butanol, cyclohexanol, and 1,6-hexanediol, could increase the NPC permeability in wild-type yeast cells at high alcohol concentrations (1 to 5 %) [308]. In conjunction with increases in permeability, aliphatic alcohols, deoxyglucose, and chilling triggered the reversible dissociation of several Nups from the NPCs, consistent with the hypothesis that NPC gating occurs when molecular latches composed of FG repeats and structural nucleoporins dissociate. In contrast, it was also found that exposure of cell nuclei isolated from *Xenopus* oocytes to clinically relevant ethanol concentrations, i.e. concentrations between 0.05 and 0.2 %, decreased NE permeability within hours together with nucleus swelling and clustering of the nuclear pores in the NE [309]. In contrast to the above described aliphatic alcohol effects, this effect was not attributed to disruption of the hydrophobic interactions inside the central NPC channel, but to transcriptional processes, as blocking the transcriptional activity also prevented the permeability changes. The effect of the amphiphilic alcohol *trans*-cyclohexane-1,2-diol (TCHD) was studied more in detail by Ribbeck and Görlich to verify their NPC gateway model. They demonstrated that TCHD enhanced the rate of nuclear entry of the 40 kDa maltose binding protein [310]. Subsequently, our group studied whether non-selective gating of nuclear pores by an amphipathic alcohol like TCHD could also be used as an alternative method to facilitate nuclear entry

of plasmid DNA [311]. Indeed, addition of TCHD to the cellular medium resulted in reversible and enhanced nuclear membrane permeability for both high molecular weight dextrans and pDNA at non-toxic concentrations. Furthermore, TCHD enhanced the transfection efficiency of both naked pDNA and DOTAP:DOPE-based LPXs.

REFERENCES

(1) Karthikeyan B.V. & Pradeep A.R. Gene therapy in periodontics: a review and future implications. *J. Contemp. Dent. Pract.* **2006** 7(3) 83-91.

(2) Hamilton A.J. & Baulcombe D.C. A species of small antisense RNA in posttranscriptional gene silencing in plants. *Science* **1999** 286(5441) 950-952.

(3) Fire A., Xu S., Montgomery M.K., Kostas S.A., Driver S.E., & Mello C.C. Potent and specific genetic interference by double-stranded RNA in Caenorhabditis elegans. *Nature* **1998** 391(6669) 806-811.

(4) Elbashir S.M., Harborth J., Lendeckel W., Yalcin A., Weber K., & Tuschl T. Duplexes of 21-nucleotide RNAs mediate RNA interference in cultured mammalian cells. *Nature* **2001** 411(6836) 494-498.

(5) Lee Y.S., Nakahara K., Pham J.W. *et al.* Distinct roles for Drosophila Dicer-1 and Dicer-2 in the siRNA/miRNA silencing pathways. *Cell* **2004** 117(1) 69-81.

(6) Leuschner P.J., Ameres S.L., Kueng S., & Martinez J. Cleavage of the siRNA passenger strand during RISC assembly in human cells. *EMBO Rep.* **2006** 7(3) 314-320.

(7) Matranga C., Tomari Y., Shin C., Bartel D.P., & Zamore P.D. Passenger-strand cleavage facilitates assembly of siRNA into Ago2-containing RNAi enzyme complexes. *Cell* **2005** 123(4) 607-620.

(8) Rand T.A., Petersen S., Du F., & Wang X. Argonaute2 cleaves the anti-guide strand of siRNA during RISC activation. *Cell* **2005** 123(4) 621-629.

(9) Liu J., Carmell M.A., Rivas F.V. *et al.* Argonaute2 is the catalytic engine of mammalian RNAi. *Science* **2004** 305(5689) 1437-1441.

(10) Manche L., Green S.R., Schmedt C., & Mathews M.B. Interactions between double-stranded RNA regulators and the protein kinase DAI. *Mol. Cell Biol.* **1992** 12(11) 5238-5248.

(11) Gao X., Kim K.S., & Liu D. Nonviral gene delivery: what we know and what is next. *AAPS. J.* **2007** 9(1) E92-104.

(12) Anderson J.L. & Hope T.J. Intracellular trafficking of retroviral vectors: obstacles and advances. *Gene Ther.* **2005** 12(23) 1667-1678.

(13) Ding W., Zhang L., Yan Z., & Engelhardt J.F. Intracellular trafficking of adeno-associated viral vectors. *Gene Ther.* **2005** 12(11) 873-880.

(14) Jolly D. Viral vector systems for gene therapy. *Cancer Gene Ther.* **1994** 1(1) 51-64.

(15) Rowe W.P., Huebner R.J., Gilmore L.K., Parrott R.H., & Ward T.G. Isolation of a cytopathogenic agent from human adenoids undergoing spontaneous degeneration in tissue culture. *Proc. Soc. Exp. Biol. Med.* **1953** 84(3) 570-573.

(16) Horwitz M.S. Adenovirus immunoregulatory genes and their cellular targets. *Virology* **2001** 279(1) 1-8.

(17) Hitt M.M. & Graham F.L. Adenovirus vectors for human gene therapy. *Adv. Virus Res.* **2000** 55479-505.

(18) Mitani K. & Kubo S. Adenovirus as an integrating vector. *Curr. Gene Ther.* **2002** 2(2) 135-144.

(19) Douglas J.T. Adenoviral vectors for gene therapy. *Mol. Biotechnol.* **2007** 36(1) 71-80.

(20) Surosky R.T., Urabe M., Godwin S.G. *et al.* Adeno-associated virus Rep proteins target DNA sequences to a unique locus in the human genome. *J. Virol.* **1997** 71(10) 7951-7959.

(21) Cuchet D., Potel C., Thomas J., & Epstein A.L. HSV-1 amplicon vectors: a promising and versatile tool for gene delivery. *Expert. Opin. Biol. Ther.* **2007** 7(7) 975-995.

(22) Wang Y., Camp S.M., Niwano M. *et al.* Herpes simplex virus type 1/adeno-associated virus rep(+) hybrid amplicon vector improves the stability of transgene expression in human cells by site-specific integration. *J. Virol.* **2002** 76(14) 7150-7162.

(23) Zaiss A.K. & Muruve D.A. Immune responses to adeno-associated virus vectors. *Curr. Gene Ther.* **2005** 5(3) 323-331.

(24) Roberts D.M., Nanda A., Havenga M.J. *et al.* Hexon-chimaeric adenovirus serotype 5 vectors circumvent pre-existing anti-vector immunity. *Nature* **2006** 441(7090) 239-243.

(25) Isaka Y. & Imai E. Electroporation-mediated gene therapy. *Expert. Opin. Drug Deliv.* **2007** 4(5) 561-571.

(26) Heller L.C., Ugen K., & Heller R. Electroporation for targeted gene transfer. *Expert. Opin. Drug Deliv.* **2005** 2(2) 255-268.

(27) Favard C., Dean D.S., & Rols M.P. Electrotransfer as a non viral method of gene delivery. *Curr. Gene Ther.* **2007** 7(1) 67-77.

(28) Andre F. & Mir L.M. DNA electrotransfer: its principles and an updated review of its therapeutic applications. *Gene Ther.* **2004** 11 Suppl 1S33-S42.

(29) Satkauskas S., Bureau M.F., Puc M. *et al.* Mechanisms of in vivo DNA electrotransfer: respective contributions of cell electropermeabilization and DNA electrophoresis. *Mol. Ther.* **2002** 5(2) 133-140.

(30) Zaharoff D.A., Barr R.C., Li C.Y., & Yuan F. Electromobility of plasmid DNA in tumor tissues during electric field-mediated gene delivery. *Gene Ther.* **2002** 9(19) 1286-1290.

(31) Bigey P., Bureau M.F., & Scherman D. In vivo plasmid DNA electrotransfer. *Curr. Opin. Biotechnol.* **2002** 13(5) 443-447.

(32) Bloquel C., Fabre E., Bureau M.F., & Scherman D. Plasmid DNA electrotransfer for intracellular and secreted proteins expression: new methodological developments and applications. *J. Gene Med.* **2004** 6 Suppl 1S11-S23.

(33) Dezawa M., Takano M., Negishi H., Mo X., Oshitari T., & Sawada H. Gene transfer into retinal ganglion cells by in vivo electroporation: a new approach. *Micron.* **2002** 33(1) 1-6.

(34) Gehl J. Electroporation: theory and methods, perspectives for drug delivery, gene therapy and research. *Acta Physiol Scand.* **2003** 177(4) 437-447.

(35) Henshaw J.W., Zaharoff D.A., Mossop B.J., & Yuan F. Electric field-mediated transport of plasmid DNA in tumor interstitium in vivo. *Bioelectrochemistry.* **2007** 71(2) 233-242.

(36) Leblanc R., Vasquez Y., Hannaman D., & Kumar N. Markedly enhanced immunogenicity of a Pfs25 DNA-based malaria transmission-blocking vaccine by in vivo electroporation. *Vaccine* **2007**

(37) Lin C.R., Tai M.H., Cheng J.T. *et al.* Electroporation for direct spinal gene transfer in rats. *Neurosci. Lett.* **2002** 317(1) 1-4.

(38) McMahon J.M. & Wells D.J. Electroporation for gene transfer to skeletal muscles: current status. *BioDrugs.* **2004** 18(3) 155-165.

(39) Neumann E., Schaefer-Ridder M., Wang Y., & Hofschneider P.H. Gene transfer into mouse lyoma cells by electroporation in high electric fields. *EMBO J.* **1982** 1(7) 841-845.

(40) Ohashi S., Kubo T., Kishida T. *et al.* Successful genetic transduction in vivo into synovium by means of electroporation. *Biochem. Biophys. Res. Commun.* **2002** 293(5) 1530-1535.

(41) Durieux A.C., Bonnefoy R., Busso T., & Freyssenet D. In vivo gene electrotransfer into skeletal muscle: effects of plasmid DNA on the occurrence and extent of muscle damage. *J. Gene Med.* **2004** 6(7) 809-816.

(42) Herweijer H. & Wolff J.A. Gene therapy progress and prospects: hydrodynamic gene delivery. *Gene Ther.* **2007** 14(2) 99-107.

(43) Liu F., Song Y., & Liu D. Hydrodynamics-based transfection in animals by systemic administration of plasmid DNA. *Gene Ther.* **1999** 6(7) 1258-1266.

(44) Zhang G., Budker V., & Wolff J.A. High levels of foreign gene expression in hepatocytes after tail vein injections of naked plasmid DNA. *Hum. Gene Ther.* **1999** 10(10) 1735-1737.

(45) Wu X., Gao H., Pasupathy S., Tan P.H., Ooi L.L., & Hui K.M. Systemic administration of naked DNA with targeting specificity to mammalian kidneys. *Gene Ther.* **2005** 12(6) 477-486.

(46) Ferrara K., Pollard R., & Borden M. Ultrasound microbubble contrast agents: fundamentals and application to gene and drug delivery. *Annu. Rev. Biomed. Eng* **2007** 9415-447.

(47) Lawrie A., Brisken A.F., Francis S.E., Cumberland D.C., Crossman D.C., & Newman C.M. Microbubble-enhanced ultrasound for vascular gene delivery. *Gene Ther.* **2000** 7(23) 2023-2027.

(48) Lentacker I., De Geest B.G., Vandenbroucke R.E. *et al.* Ultrasound-responsive polymer-coated microbubbles that bind and protect DNA. *Langmuir* **2006** 22(17) 7273-7278.

(49) Li T., Tachibana K., Kuroki M., & Kuroki M. Gene transfer with echo-enhanced contrast agents: comparison between Albunex, Optison, and Levovist in mice--initial results. *Radiology* **2003** 229(2) 423-428.

(50) Pislaru S.V., Pislaru C., Kinnick R.R. *et al.* Optimization of ultrasound-mediated gene transfer: comparison of contrast agents and ultrasound modalities. *Eur. Heart J.* **2003** 24(18) 1690-1698.

(51) Taniyama Y., Tachibana K., Hiraoka K. *et al.* Development of safe and efficient novel nonviral gene transfer using ultrasound: enhancement of transfection efficiency of naked plasmid DNA in skeletal muscle. *Gene Ther.* **2002** 9(6) 372-380.

(52) Juffermans L.J., Kamp O., Dijkmans P.A., Visser C.A., & Musters R.J. Low-Intensity Ultrasound-Exposed Microbubbles Provoke Local Hyperpolarization of the Cell Membrane Via Activation of BK(Ca) CHANNELS. *Ultrasound Med. Biol.* **2007**

(53) Yamashita Y., Shimada M., Tachibana K. *et al.* In vivo gene transfer into muscle via electro-sonoporation. *Hum. Gene Ther.* **2002** 13(17) 2079-2084.

(54) Zeira E., Manevitch A., Khatchatouriants A. *et al.* Femtosecond infrared laser-an efficient and safe in vivo gene delivery system for prolonged expression. *Mol. Ther.* **2003** 8(2) 342-350.

(55) Zeira E., Manevitch A., Manevitch Z. *et al.* Femtosecond laser: a new intradermal DNA delivery method for efficient, long-term gene expression and genetic immunization. *FASEB J.* **2007** 21(13) 3522-3533.

(56) Plank C., Anton M., Rudolph C., Rosenecker J., & Krotz F. Enhancing and targeting nucleic acid delivery by magnetic force. *Expert. Opin. Biol. Ther.* **2003** 3(5) 745-758.

(57) Plank C., Schillinger U., Scherer F. *et al.* The magnetofection method: using magnetic force to enhance gene delivery. *Biol. Chem.* **2003** 384(5) 737-747.

(58) Plank C., Scherer F., Schillinger U., Bergemann C., & Anton M. Magnetofection: enhancing and targeting gene delivery with superparamagnetic nanoparticles and magnetic fields. *J. Liposome Res.* **2003** 13(1) 29-32.

(59) Yang C.H., Shen S.C., Lee J.C. *et al.* Seeing the gene therapy: application of gene gun technique to transfect and decolour pigmented rat skin with human agouti signalling protein cDNA. *Gene Ther.* **2004** 11(13) 1033-1039.

(60) Yang N.S., Burkholder J., Roberts B., Martinell B., & McCabe D. In vivo and in vitro gene transfer to mammalian somatic cells by particle bombardment. *Proc. Natl. Acad. Sci. U. S. A* **1990** 87(24) 9568-9572.

(61) Yang N.S. & Sun W.H. Gene gun and other non-viral approaches for cancer gene therapy. *Nat. Med.* **1995** 1(5) 481-483.

(62) Felgner P.L., Gadek T.R., Holm M. *et al.* Lipofection: a highly efficient, lipid-mediated DNA-transfection procedure. *Proc. Natl. Acad. Sci. U. S. A* **1987** 84(21) 7413-7417.

(63) Liu D., Ren T., & Gao X. Cationic transfection lipids. *Curr. Med. Chem.* **2003** 10(14) 1307-1315.

(64) Ma B., Zhang S., Jiang H., Zhao B., & Lv H. Lipoplex morphologies and their influences on transfection efficiency in gene delivery. *J. Control Release* **2007** 123(3) 184-194.

(65) Eastman S.J., Siegel C., Tousignant J., Smith A.E., Cheng S.H., & Scheule R.K. Biophysical characterization of cationic lipid: DNA complexes. *Biochim. Biophys. Acta* **1997** 1325(1) 41-62.

(66) Luten J., van Nostrum C.F., De Smedt S.C., & Henninck W.E. Biodegradable polymers as non-viral carriers for plasmid DNA delivery. *J. Control Release* **2007**

(67) Pietersz G.A., Tang C.K., & Apostolopoulos V. Structure and design of polycationic carriers for gene delivery. *Mini. Rev. Med. Chem.* **2006** 6(12) 1285-1298.

(68) Vasir J.K. & Labhasetwar V. Polymeric nanoparticles for gene delivery. *Expert. Opin. Drug Deliv.* **2006** 3(3) 325-344.

(69) Dubruel P. & Schacht E. Vinyl polymers as non-viral gene delivery carriers: current status and prospects. *Macromol. Biosci.* **2006** 6(10) 789-810.

(70) Brown M.D., Schatzlein A.G., & Uchegbu I.F. Gene delivery with synthetic (non viral) carriers. *Int. J. Pharm.* **2001** 229(1-2) 1-21.

(71) Merdan T., Kopecek J., & Kissel T. Prospects for cationic polymers in gene and oligonucleotide therapy against cancer. *Adv. Drug Deliv. Rev.* **2002** 54(5) 715-758.

(72) De Smedt S.C., Demeester J., & Hennink W.E. Cationic polymer based gene delivery systems. *Pharm. Res.* **2000** 17(2) 113-126.

(73) Wolff J.A. The "grand" problem of synthetic delivery. *Nat. Biotechnol.* **2002** 20(8) 768-769.

(74) Mastrobattista E., van der Aa M.A., Hennink W.E., & Crommelin D.J. Artificial viruses: a nanotechnological approach to gene delivery. *Nat. Rev. Drug Discov.* **2006** 5(2) 115-121.

(75) Kawabata K., Takakura Y., & Hashida M. The fate of plasmid DNA after intravenous injection in mice: involvement of scavenger receptors in its hepatic uptake. *Pharm. Res.* **1995** 12(6) 825-830.

(76) Yoshida M., Mahato R.I., Kawabata K., Takakura Y., & Hashida M. Disposition characteristics of plasmid DNA in the single-pass rat liver perfusion system. *Pharm. Res.* **1996** 13(4) 599-603.

(77) Hashida M., Takemura S., Nishikawa M., & Takakura Y. Targeted delivery of plasmid DNA complexed with galactosylated poly(L-lysine). *J. Control Release* **1998** 53(1-3) 301-310.

(78) Plank C., Mechtler K., Szoka F.C., Jr., & Wagner E. Activation of the complement system by synthetic DNA complexes: a potential barrier for intravenous gene delivery. *Hum. Gene Ther.* **1996** 7(12) 1437-1446.

(79) Pouton C.W. & Seymour L.W. Key issues in non-viral gene delivery. *Adv. Drug Deliv. Rev.* **2001** 46(1-3) 187-203.

(80) McLean J.W., Fox E.A., Baluk P. *et al.* Organ-specific endothelial cell uptake of cationic liposome-DNA complexes in mice. *Am. J. Physiol* **1997** 273(1 Pt 2) H387-H404.

(81) Thurston G., McLean J.W., Rizen M. *et al.* Cationic liposomes target angiogenic endothelial cells in tumors and chronic inflammation in mice. *J. Clin. Invest* **1998** 101(7) 1401-1413.

(82) Hashizume H., Baluk P., Morikawa S. *et al.* Openings between defective endothelial cells explain tumor vessel leakiness. *Am. J. Pathol.* **2000** 156(4) 1363-1380.

(83) Zhang G., Gao X., Song Y.K. *et al.* Hydroporation as the mechanism of hydrodynamic delivery. *Gene Ther.* **2004** 11(8) 675-682.

(84) Fenske D.B., MacLachlan I., & Cullis P.R. Stabilized plasmid-lipid particles: a systemic gene therapy vector. *Methods Enzymol.* **2002** 34636-71.

(85) Fenske D.B., MacLachlan I., & Cullis P.R. Long-circulating vectors for the systemic delivery of genes. *Curr. Opin. Mol. Ther.* **2001** 3(2) 153-158.

(86) Song L.Y., Ahkong Q.F., Rong Q. *et al.* Characterization of the inhibitory effect of PEG-lipid conjugates on the intracellular delivery of plasmid and antisense DNA mediated by cationic lipid liposomes. *Biochim. Biophys. Acta* **2002** 1558(1) 1-13.

(87) Ambegia E., Ansell S., Cullis P., Heyes J., Palmer L., & MacLachlan I. Stabilized plasmid-lipid particles containing PEG-diacylglycerols exhibit extended circulation lifetimes and tumor selective gene expression. *Biochim. Biophys. Acta* **2005** 1669(2) 155-163.

(88) Kong H.J. & Mooney D.J. Microenvironmental regulation of biomacromolecular therapies. *Nat. Rev. Drug Discov.* **2007** 6(6) 455-463.

(89) Khalil I.A., Kogure K., Akita H., & Harashima H. Uptake Pathways and Subsequent Intracellular Trafficking in Nonviral Gene Delivery. *Pharmacol Rev* **2006** 58(1) 32-45.

(90) Medina-Kauwe L.K., Xie J., & Hamm-Alvarez S. Intracellular trafficking of nonviral vectors. *Gene Ther* **2005** 12(24) 1734-1751.

(91) Mayor S. & Pagano R.E. Pathways of clathrin-independent endocytosis. *Nat Rev Mol Cell Biol* **2007** 8(8) 603-612.

(92) Wong A.W., Scales S.J., & Reilly D.E. DNA Internalized via Caveolae Requires Microtubule-dependent, Rab7-independent Transport to the Late Endocytic Pathway for Delivery to the Nucleus. *J. Biol. Chem.* **2007** 282(31) 22953-22963.

(93) Lai S.K., Hida K., Man S.T. *et al.* Privileged delivery of polymer nanoparticles to the perinuclear region of live cells via a non-clathrin, non-degradative pathway. *Biomaterials* **2007** 28(18) 2876-2884.

(94) Rejman J., Oberle V., Zuhorn I.S., & Hoekstra D. Size-dependent internalization of particles via the pathways of clathrin-and caveolae-mediated endocytosis. *Biochemical Journal* **2004** 377159-169.

(95) Wattiaux R., Laurent N., Wattiaux-De Coninck S., & Jadot M. Endosomes, lysosomes: their implication in gene transfer. *Advanced Drug Delivery Reviews* **2000** 41(2) 201-208.

(96) Kunisawa J., Masuda T., Katayama K. *et al.* Fusogenic liposome delivers encapsulated nanoparticles for cytosolic controlled gene release. *J. Control Release* **2005** 105(3) 344-353.

(97) Conner S.D. & Schmid S.L. Regulated portals of entry into the cell. *Nature* **2003** 422(6927) 37-44.

(98) Mousavi S.A., Malerod L., Berg T., & Kjeken R. Clathrin-dependent endocytosis. *Biochemical Journal* **2004** 3771-16.

(99) Kirchhausen T. Clathrin. *Annual Review of Biochemistry* **2000** 69(1) 699-727.

(100) Simons K. & Toomre D. Lipid rafts and signal transduction. *Nature Reviews Molecular Cell Biology* **2000** 1(1) 31-39.

(101) Smart E.J., Graf G.A., McNiven M.A. *et al.* Caveolins, liquid-ordered domains, and signal transduction. *Molecular and Cellular Biology* **1999** 19(11) 7289-7304.

(102) Pelkmans L., Kartenbeck J., & Helenius A. Caveolar endocytosis of simian virus 40 reveals a new two-step vesicular-transport pathway to the ER. *Nature Cell Biology* **2001** 3(5) 473-483.

(103) Parton R.G. & Richards A.A. Lipid rafts and caveolae as portals for endocytosis: New insights and common mechanisms. *Traffic* **2003** 4(11) 724-738.

(104) Pelkmans L. Secrets of caveolae- and lipid raft-mediated endocytosis revealed by mammalian viruses. *Biochimica et Biophysica Acta-Molecular Cell Research* **2005** 1746(3) 295-304.

(105) Grimmer S., van Deurs B., & Sandvig K. Membrane ruffling and macropinocytosis in A431 cells require cholesterol. *J Cell Sci* **2002** 115(14) 2953-2962.

(106) Jones A.T. Macropinocytosis: searching for an endocytic identity and role in the uptake of cell penetrating peptides. *Journal of Cellular and Molecular Medicine* **2007** 11(4) 670-684.

(107) Swanson J.A. & Watts C. Macropinocytosis. *Trends in Cell Biology* **1995** 5(11) 424-428.

(108) Allen L.A.H. & Aderem A. Molecular definition of distinct cytoskeletal structures involved in complement- and Fc receptor-mediated phagocytosis in macrophages. *Journal of Experimental Medicine* **1996** 184(2) 627-637.

(109) Vives E., Brodin P., & Lebleu B. A truncated HIV-1 Tat protein basic domain rapidly translocates through the plasma membrane and accumulates in the cell nucleus. *J. Biol. Chem.* **1997** 272(25) 16010-16017.

(110) Fawell S., Seery J., Daikh Y. *et al.* Tat-mediated delivery of heterologous proteins into cells. *Proc. Natl. Acad. Sci. U. S. A* **1994** 91(2) 664-668.

(111) Schwarze S.R., Ho A., Vocero-Akbani A., & Dowdy S.F. In vivo protein transduction: delivery of a biologically active protein into the mouse. *Science* **1999** 285(5433) 1569-1572.

(112) Astriab-Fisher A., Sergueev D., Fisher M., Shaw B.R., & Juliano R.L. Conjugates of antisense oligonucleotides with the Tat and antennapedia cell-penetrating peptides: effects on cellular uptake, binding to target sequences, and biologic actions. *Pharm. Res.* **2002** 19(6) 744-754.

(113) Lewin M., Carlesso N., Tung C.H. *et al.* Tat peptide-derivatized magnetic nanoparticles allow in vivo tracking and recovery of progenitor cells. *Nat. Biotechnol.* **2000** 18(4) 410-414.

(114) Torchilin V.P., Rammohan R., Weissig V., & Levchenko T.S. TAT peptide on the surface of liposomes affords their efficient intracellular delivery even at low temperature and in the presence of metabolic inhibitors. *Proc. Natl. Acad. Sci. U. S. A* **2001** 98(15) 8786-8791.

(115) Tseng Y.L., Liu J.J., & Hong R.L. Translocation of liposomes into cancer cells by cell-penetrating peptides penetratin and tat: a kinetic and efficacy study. *Mol. Pharmacol.* **2002** 62(4) 864-872.

(116) Futaki S. Oligoarginine vectors for intracellular delivery: design and cellular-uptake mechanisms. *Biopolymers* **2006** 84(3) 241-249.

(117) Lundberg M. & Johansson M. Positively charged DNA-binding proteins cause apparent cell membrane translocation. *Biochem. Biophys. Res. Commun.* **2002** 291(2) 367-371.

(118) Richard J.P., Melikov K., Vives E. *et al.* Cell-penetrating peptides. A reevaluation of the mechanism of cellular uptake. *J. Biol. Chem.* **2003** 278(1) 585-590.

(119) Lundberg M., Wikstrom S., & Johansson M. Cell surface adherence and endocytosis of protein transduction domains. *Mol. Ther.* **2003** 8(1) 143-150.

(120) Richard J.P., Melikov K., Vives E. *et al.* Cell-penetrating peptides. A reevaluation of the mechanism of cellular uptake. *J. Biol. Chem.* **2003** 278(1) 585-590.

(121) Thoren P.E., Persson D., Isakson P., Goksor M., Onfelt A., & Norden B. Uptake of analogs of penetratin, Tat(48-60) and oligoarginine in live cells. *Biochem. Biophys. Res. Commun.* **2003** 307(1) 100-107.

(122) Kleuss C., Hescheler J., Ewel C., Rosenthal W., Schultz G., & Wittig B. Assignment of G-protein subtypes to specific receptors inducing inhibition of calcium currents. *Nature* **1991** 353(6339) 43-48.

(123) Leonetti J.P., Mechti N., Degols G., Gagnor C., & Lebleu B. Intracellular distribution of microinjected antisense oligonucleotides. *Proc. Natl. Acad. Sci. U. S. A* **1991** 88(7) 2702-2706.

(124) Barry E.L., Gesek F.A., & Friedman P.A. Introduction of antisense oligonucleotides into cells by permeabilization with streptolysin O. *Biotechniques* **1993** 15(6) 1016-8, 1020.

(125) Midoux P., Mayer R., & Monsigny M. Membrane permeabilization by alpha-helical peptides: a flow cytometry study. *Biochim. Biophys. Acta* **1995** 1239(2) 249-256.

(126) Gordon S.P., Berezhna S., Scherfeld D., Kahya N., & Schwille P. Characterization of interaction between cationic lipid-oligonucleotide complexes and cellular membrane lipids using confocal imaging and fluorescence correlation spectroscopy. *Biophys. J.* **2005** 88(1) 305-316.

(127) Zelphati O. & Szoka F.C., Jr. Mechanism of oligonucleotide release from cationic liposomes. *Proc. Natl. Acad. Sci. U. S. A* **1996** 93(21) 11493-11498.

(128) Zelphati O. & Szoka F.C., Jr. Intracellular distribution and mechanism of delivery of oligonucleotides mediated by cationic lipids. *Pharm. Res.* **1996** 13(9) 1367-1372.

(129) Simoes S., Moreira J.N., Fonseca C., Duzgunes N., & de Lima M.C. On the formulation of pH-sensitive liposomes with long circulation times. *Adv. Drug Deliv. Rev.* **2004** 56(7) 947-965.

(130) Berg K., Selbo P.K., Prasmickaite L. *et al.* Photochemical internalization: a novel technology for delivery of macromolecules into cytosol. *Cancer Res.* **1999** 59(6) 1180-1183.

(131) Boussif O., Lezoualc'h F., Zanta M.A. *et al.* A versatile vector for gene and oligonucleotide transfer into cells in culture and in vivo: polyethylenimine. *Proc. Natl. Acad. Sci. U. S. A* **1995** 92(16) 7297-7301.

(132) Haensler J. & Szoka F.C., Jr. Polyamidoamine cascade polymers mediate efficient transfection of cells in culture. *Bioconjug. Chem.* **1993** 4(5) 372-379.

(133) Tang M.X., Redemann C.T., & Szoka F.C., Jr. In vitro gene delivery by degraded polyamidoamine dendrimers. *Bioconjug. Chem.* **1996** 7(6) 703-714.

(134) Koping-Hoggard M., Tubulekas I., Guan H. *et al.* Chitosan as a nonviral gene delivery system. Structure-property relationships and characteristics compared with polyethylenimine in vitro and after lung administration in vivo. *Gene Ther.* **2001** 8(14) 1108-1121.

(135) Ishii T., Okahata Y., & Sato T. Mechanism of cell transfection with plasmid/chitosan complexes. *Biochim. Biophys. Acta* **2001** 1514(1) 51-64.

(136) Martin M.E. & Rice K.G. Peptide-guided gene delivery. *AAPS. J.* **2007** 9(1) E18-E29.

(137) Deshayes S., Morris M.C., Divita G., & Heitz F. Cell-penetrating peptides: tools for intracellular delivery of therapeutics. *Cell Mol. Life Sci.* **2005** 62(16) 1839-1849.

(138) Mahat R.I., Monera O.D., Smith L.C., & Rolland A. Peptide-based gene delivery. *Curr. Opin. Mol. Ther.* **1999** 1(2) 226-243.

(139) Wagner E., Plank C., Zatloukal K., Cotten M., & Birnstiel M.L. Influenza virus hemagglutinin HA-2 N-terminal fusogenic peptides augment gene transfer by transferrin-polylysine-DNA complexes: toward a synthetic virus-like gene-transfer vehicle. *Proc. Natl. Acad. Sci. U. S. A* **1992** 89(17) 7934-7938.

(140) Plank C., Oberhauser B., Mechtler K., Koch C., & Wagner E. The influence of endosome-disruptive peptides on gene transfer using synthetic virus-like gene transfer systems. *J. Biol. Chem.* **1994** 269(17) 12918-12924.

(141) Boeckle S., Fahrmeir J., Roedl W., Ogris M., & Wagner E. Melittin analogs with high lytic activity at endosomal pH enhance transfection with purified targeted PEI polyplexes. *J. Control Release* **2006** 112(2) 240-248.

(142) Meyer M., Zintchenko A., Ogris M., & Wagner E. A dimethylmaleic acid-melittin-polylysine conjugate with reduced toxicity, pH-triggered endosomolytic activity and enhanced gene transfer potential. *J. Gene Med.* **2007** 9(9) 797-805.

(143) Thomas J.L., Barton S.W., & Tirrell D.A. Membrane solubilization by a hydrophobic polyelectrolyte: surface activity and membrane binding. *Biophys. J.* **1994** 67(3) 1101-1106.

(144) Prasmickaite L., Hogset A., & Berg K. Evaluation of different photosensitizers for use in photochemical gene transfection. *Photochem. Photobiol.* **2001** 73(4) 388-395.

(145) Hogset A., Prasmickaite L., Selbo P.K. *et al.* Photochemical internalisation in drug and gene delivery. *Adv. Drug Deliv. Rev.* **2004** 56(1) 95-115.

(146) Selbo P.K., Sivam G., Fodstad O., Sandvig K., & Berg K. In vivo documentation of photochemical internalization, a novel approach to site specific cancer therapy. *Int. J. Cancer* **2001** 92(5) 761-766.

(147) Dietze A., Peng Q., Selbo P.K. *et al.* Enhanced photodynamic destruction of a transplantable fibrosarcoma using photochemical internalisation of gelonin. *Br. J. Cancer* **2005** 92(11) 2004-2009.

(148) Ndoye A., Dolivet G., Hogset A. *et al.* Eradication of p53-mutated head and neck squamous cell carcinoma xenografts using nonviral p53 gene therapy and photochemical internalization. *Mol. Ther.* **2006** 13(6) 1156-1162.

(149) Folini M., Berg K., Millo E. *et al.* Photochemical internalization of a peptide nucleic acid targeting the catalytic subunit of human telomerase. *Cancer Res.* **2003** 63(13) 3490-3494.

(150) Shiraishi T. & Nielsen P.E. Photochemically enhanced cellular delivery of cell penetrating peptide-PNA conjugates. *FEBS Lett.* **2006** 580(5) 1451-1456.

(151) Prasmickaite L., Hogset A., Tjelle T.E., Olsen V.M., & Berg K. Role of endosomes in gene transfection mediated by photochemical internalisation (PCI). *J. Gene Med.* **2000** 2(6) 477-488.

(152) Kloeckner J., Prasmickaite L., Hogset A., Berg K., & Wagner E. Photochemically enhanced gene delivery of EGF receptor-targeted DNA polyplexes. *J. Drug Target* **2004** 12(4) 205-213.

(153) Oliveira S., Fretz M.M., Hogset A., Storm G., & Schiffelers R.M. Photochemical internalization enhances silencing of epidermal growth factor receptor through improved endosomal escape of siRNA. *Biochim. Biophys. Acta* **2007** 1768(5) 1211-1217.

(154) Engesaeter B.O., Bonsted A., Berg K. *et al.* PCI-enhanced adenoviral transduction employs the known uptake mechanism of adenoviral particles. *Cancer Gene Ther.* **2005** 12(5) 439-448.

(155) Macara I.G. Transport into and out of the nucleus. *Microbiol. Mol. Biol. Rev.* **2001** 65(4) 570-94, table.

(156) Roux K.J. & Burke B. From pore to kinetochore and back: regulating envelope assembly. *Dev. Cell* **2006** 11(3) 276-278.

(157) Hetzer M.W., Walther T.C., & Mattaj I.W. Pushing the envelope: structure, function, and dynamics of the nuclear periphery. *Annu. Rev. Cell Dev. Biol.* **2005** 21347-380.

(158) Antonin W., Franz C., Haselmann U., Antony C., & Mattaj I.W. The integral membrane nucleoporin pom121 functionally links nuclear pore complex assembly and nuclear envelope formation. *Mol. Cell* **2005** 17(1) 83-92.

(159) Fernandez A.G. & Piano F. MEL-28 is downstream of the Ran cycle and is required for nuclear-envelope function and chromatin maintenance. *Curr. Biol.* **2006** 16(17) 1757-1763.

(160) Galy V., Askjaer P., Franz C., Lopez-Iglesias C., & Mattaj I.W. MEL-28, a novel nuclear-envelope and kinetochore protein essential for zygotic nuclear-envelope assembly in C. elegans. *Curr. Biol.* **2006** 16(17) 1748-1756.

(161) Feldherr C.M. & Akin D. The permeability of the nuclear envelope in dividing and nondividing cell cultures. *J. Cell Biol.* **1990** 111(1) 1-8.

(162) Feldherr C.M. & Akin D. Regulation of nuclear transport in proliferating and quiescent cells. *Exp. Cell Res.* **1993** 205(1) 179-186.

(163) Lechardeur D. & Lukacs G.L. Nucleocytoplasmic transport of plasmid DNA: a perilous journey from the cytoplasm to the nucleus. *Hum. Gene Ther.* **2006** 17(9) 882-889.

(164) Wagstaff K.M. & Jans D.A. Nucleocytoplasmic transport of DNA: enhancing non-viral gene transfer. *Biochem. J.* **2007** 406(2) 185-202.

(165) van der Aa M.A., Mastrobattista E., Oosting R.S., Hennink W.E., Koning G.A., & Crommelin D.J. The nuclear pore complex: the gateway to successful nonviral gene delivery. *Pharm. Res.* **2006** 23(3) 447-459.

(166) Tseng W.C., Haselton F.R., & Giorgio T.D. Transfection by cationic liposomes using simultaneous single cell measurements of plasmid delivery and transgene expression. *J. Biol. Chem.* **1997** 272(41) 25641-25647.

(167) Capecchi M.R. High efficiency transformation by direct microinjection of DNA into cultured mammalian cells. *Cell* **1980** 22(2 Pt 2) 479-488.

(168) Dowty M.E., Williams P., Zhang G., Hagstrom J.E., & Wolff J.A. Plasmid DNA entry into postmitotic nuclei of primary rat myotubes. *Proc. Natl. Acad. Sci. U. S. A* **1995** 92(10) 4572-4576.

(169) Zabner J., Fasbender A.J., Moninger T., Poellinger K.A., & Welsh M.J. Cellular and molecular barriers to gene transfer by a cationic lipid. *J. Biol. Chem.* **1995** 270(32) 18997-19007.

(170) Pollard H., Toumaniantz G., Amos J.L. *et al.* Ca2+-sensitive cytosolic nucleases prevent efficient delivery to the nucleus of injected plasmids. *J. Gene Med.* **2001** 3(2) 153-164.

(171) Lechardeur D. & Lukacs G.L. Nucleocytoplasmic transport of plasmid DNA: a perilous journey from the cytoplasm to the nucleus. *Hum. Gene Ther.* **2006** 17(9) 882-889.

(172) Lukacs G.L., Haggie P., Seksek O., Lechardeur D., Freedman N., & Verkman A.S. Size-dependent DNA mobility in cytoplasm and nucleus. *J. Biol. Chem.* **2000** 275(3) 1625-1629.

(173) Dauty E. & Verkman A.S. Actin cytoskeleton as the principal determinant of size-dependent DNA mobility in cytoplasm: a new barrier for non-viral gene delivery. *J. Biol. Chem.* **2005** 280(9) 7823-7828.

(174) Geiger R.C., Taylor W., Glucksberg M.R., & Dean D.A. Cyclic stretch-induced reorganization of the cytoskeleton and its role in enhanced gene transfer. *Gene Ther.* **2006** 13(8) 725-731.

(175) Torriglia A., Chaudun E., Chany-Fournier F., Jeanny J.C., Courtois Y., & Counis M.F. Involvement of DNase II in nuclear degeneration during lens cell differentiation. *J. Biol. Chem.* **1995** 270(48) 28579-28585.

(176) Dingwall C. & Laskey R.A. Nuclear import: a tale of two sites. *Curr. Biol.* **1998** 8(25) R922-R924.

(177) Worman H.J. & Gundersen G.G. Here come the SUNs: a nucleocytoskeletal missing link. *Trends Cell Biol.* **2006** 16(2) 67-69.

(178) Davis L.I. The nuclear pore complex. *Annu. Rev. Biochem.* **1995** 64865-896.

(179) Reichelt R., Holzenburg A., Buhle E.L., Jr., Jarnik M., Engel A., & Aebi U. Correlation between structure and mass distribution of the nuclear pore complex and of distinct pore complex components. *J. Cell Biol.* **1990** 110(4) 883-894.

(180) Fontoura B.M., Blobel G., & Matunis M.J. A conserved biogenesis pathway for nucleoporins: proteolytic processing of a 186-kilodalton precursor generates Nup98 and the novel nucleoporin, Nup96. *J. Cell Biol.* **1999** 144(6) 1097-1112.

(181) Fabre E. & Hurt E. Yeast genetics to dissect the nuclear pore complex and nucleocytoplasmic trafficking. *Annu. Rev. Genet.* **1997** 31277-313.

(182) Allen T.D., Cronshaw J.M., Bagley S., Kiseleva E., & Goldberg M.W. The nuclear pore complex: mediator of translocation between nucleus and cytoplasm. *J. Cell Sci.* **2000** 113(Pt 10) 1651-1659.

(183) Fahrenkrog B. & Aebi U. The vertebrate nuclear pore complex: from structure to function. *Results Probl. Cell Differ.* **2002** 3525-48.

(184) Suntharalingam M. & Wente S.R. Peering through the pore: nuclear pore complex structure, assembly, and function. *Dev. Cell* **2003** 4(6) 775-789.

(185) Vasu S.K. & Forbes D.J. Nuclear pores and nuclear assembly. *Curr. Opin. Cell Biol.* **2001** 13(3) 363-375.

(186) Goldberg M.W. & Allen T.D. High resolution scanning electron microscopy of the nuclear envelope: demonstration of a new, regular, fibrous lattice attached to the baskets of the nucleoplasmic face of the nuclear pores. *J. Cell Biol.* **1992** 119(6) 1429-1440.

(187) Jarnik M. & Aebi U. Toward a more complete 3-D structure of the nuclear pore complex. *J. Struct. Biol.* **1991** 107(3) 291-308.

(188) Hinshaw J.E., Carragher B.O., & Milligan R.A. Architecture and design of the nuclear pore complex. *Cell* **1992** 69(7) 1133-1141.

(189) Mazzanti M., Bustamante J.O., & Oberleithner H. Electrical dimension of the nuclear envelope. *Physiol Rev.* **2001** 81(1) 1-19.

(190) Jaggi R.D., Franco-Obregon A., Muhlhausser P., Thomas F., Kutay U., & Ensslin K. Modulation of nuclear pore topology by transport modifiers. *Biophys. J.* **2003** 84(1) 665-670.

(191) Perez-Terzic C., Pyle J., Jaconi M., Stehno-Bittel L., & Clapham D.E. Conformational states of the nuclear pore complex induced by depletion of nuclear Ca2+ stores. *Science* **1996** 273(5283) 1875-1877.

(192) Shahin V., Danker T., Enss K., Ossig R., & Oberleithner H. Evidence for Ca2+- and ATP-sensitive peripheral channels in nuclear pore complexes. *FASEB J.* **2001** 15(11) 1895-1901.

(193) Macara I.G. Transport into and out of the nucleus. *Microbiol. Mol. Biol. Rev.* **2001** 65(4) 570-94, table.

(194) Feldherr C.M. & Akin D. The location of the transport gate in the nuclear pore complex. *J. Cell Sci.* **1997** 110 (Pt 24)3065-3070.

(195) Kubitscheck U., Grunwald D., Hoekstra A. *et al.* Nuclear transport of single molecules: dwell times at the nuclear pore complex. *J. Cell Biol.* **2005** 168(2) 233-243.

(196) Yang W., Gelles J., & Musser S.M. Imaging of single-molecule translocation through nuclear pore complexes. *Proc. Natl. Acad. Sci. U. S. A* **2004** 101(35) 12887-12892.

(197) Mosammaparast N. & Pemberton L.F. Karyopherins: from nuclear-transport mediators to nuclear-function regulators. *Trends Cell Biol.* **2004** 14(10) 547-556.

(198) Strom A.C. & Weis K. Importin-beta-like nuclear transport receptors. *Genome Biol.* **2001** 2(6) REVIEWS3008.

(199) Gorlich D. Transport into and out of the cell nucleus. *EMBO J.* **1998** 17(10) 2721-2727.

(200) Smith A.E., Slepchenko B.M., Schaff J.C., Loew L.M., & Macara I.G. Systems analysis of Ran transport. *Science* **2002** 295(5554) 488-491.

(201) Jans D.A., Chan C.K., & Huebner S. Signals mediating nuclear targeting and their regulation: application in drug delivery. *Med. Res. Rev.* **1998** 18(4) 189-223.

(202) Hodel M.R., Corbett A.H., & Hodel A.E. Dissection of a nuclear localization signal. *J. Biol. Chem.* **2001** 276(2) 1317-1325.

(203) Jans D.A., Chan C.K., & Huebner S. Signals mediating nuclear targeting and their regulation: application in drug delivery. *Med. Res. Rev.* **1998** 18(4) 189-223.

(204) Pollard V.W., Michael W.M., Nakielny S., Siomi M.C., Wang F., & Dreyfuss G. A novel receptor-mediated nuclear protein import pathway. *Cell* **1996** 86(6) 985-994.

(205) Duverger E., Pellerin-Mendes C., Mayer R., Roche A.C., & Monsigny M. Nuclear import of glycoconjugates is distinct from the classical NLS pathway. *J. Cell Sci.* **1995** 108(Pt 4) 1325-1332.

(206) Monsigny M., Rondanino C., Duverger E., Fajac I., & Roche A.C. Glyco-dependent nuclear import of glycoproteins, glycoplexes and glycosylated plasmids. *Biochim. Biophys. Acta* **2004** 1673(1-2) 94-103.

(207) Rondanino C., Bousser M.T., Monsigny M., & Roche A.C. Sugar-dependent nuclear import of glycosylated proteins in living cells. *Glycobiology* **2003** 13(7) 509-519.

(208) Rondanino C., Bousser M.T., Monsigny M., & Roche A.C. Sugar-dependent nuclear import of glycosylated proteins in living cells. *Glycobiology* **2003** 13(7) 509-519.

(209) Hicks G.R. & Raikhel N.V. Protein import into the nucleus: an integrated view. *Annu. Rev. Cell Dev. Biol.* **1995** 11155-188.

(210) Schmalz D., Hucho F., & Buchner K. Nuclear import of protein kinase C occurs by a mechanism distinct from the mechanism used by proteins with a classical nuclear localization signal. *J. Cell Sci.* **1998** 111 (Pt 13)1823-1830.

(211) Rout M.P., Aitchison J.D., Suprapto A., Hjertaas K., Zhao Y., & Chait B.T. The yeast nuclear pore complex: composition, architecture, and transport mechanism. *J. Cell Biol.* **2000** 148(4) 635-651.

(212) Rout M.P., Aitchison J.D., Magnasco M.O., & Chait B.T. Virtual gating and nuclear transport: the hole picture. *Trends Cell Biol.* **2003** 13(12) 622-628.

(213) Macara I.G. Transport into and out of the nucleus. *Microbiol. Mol. Biol. Rev.* **2001** 65(4) 570-94, table.

(214) Ben-Efraim I. & Gerace L. Gradient of increasing affinity of importin beta for nucleoporins along the pathway of nuclear import. *J. Cell Biol.* **2001** 152(2) 411-417.

(215) Peters R. Translocation through the nuclear pore complex: selectivity and speed by reduction-of-dimensionality. *Traffic.* **2005** 6(5) 421-427.

(216) Lim R.Y., Huang N.P., Koser J. *et al.* Flexible phenylalanine-glycine nucleoporins as entropic barriers to nucleocytoplasmic transport. *Proc. Natl. Acad. Sci. U. S. A* **2006** 103(25) 9512-9517.

(217) Patel S.S., Belmont B.J., Sante J.M., & Rexach M.F. Natively unfolded nucleoporins gate protein diffusion across the nuclear pore complex. *Cell* **2007** 129(1) 83-96.

(218) Ribbeck K. & Gorlich D. Kinetic analysis of translocation through nuclear pore complexes. *EMBO J.* **2001** 20(6) 1320-1330.

(219) Ribbeck K. & Gorlich D. The permeability barrier of nuclear pore complexes appears to operate via hydrophobic exclusion. *EMBO J.* **2002** 21(11) 2664-2671.

(220) Kustanovich T. & Rabin Y. Metastable network model of protein transport through nuclear pores. *Biophys. J.* **2004** 86(4) 2008-2016.

(221) Bickel T. & Bruinsma R. The nuclear pore complex mystery and anomalous diffusion in reversible gels. *Biophys. J.* **2002** 83(6) 3079-3087.

(222) Rout M.P., Aitchison J.D., Suprapto A., Hjertaas K., Zhao Y., & Chait B.T. The yeast nuclear pore complex: composition, architecture, and transport mechanism. *J. Cell Biol.* **2000** 148(4) 635-651.

(223) Rout M.P., Aitchison J.D., Magnasco M.O., & Chait B.T. Virtual gating and nuclear transport: the hole picture. *Trends Cell Biol.* **2003** 13(12) 622-628.

(224) Tran E.J. & Wente S.R. Dynamic nuclear pore complexes: life on the edge. *Cell* **2006** 125(6) 1041-1053.

(225) Frey S., Richter R.P., & Gorlich D. FG-rich repeats of nuclear pore proteins form a three-dimensional meshwork with hydrogel-like properties. *Science* **2006** 314(5800) 815-817.

(226) Patel S.S., Belmont B.J., Sante J.M., & Rexach M.F. Natively unfolded nucleoporins gate protein diffusion across the nuclear pore complex. *Cell* **2007** 129(1) 83-96.

(227) Frey S., Richter R.P., & Gorlich D. FG-rich repeats of nuclear pore proteins form a three-dimensional meshwork with hydrogel-like properties. *Science* **2006** 314(5800) 815-817.

(228) Dowty M.E., Williams P., Zhang G., Hagstrom J.E., & Wolff J.A. Plasmid DNA entry into postmitotic nuclei of primary rat myotubes. *Proc. Natl. Acad. Sci. U. S. A* **1995** 92(10) 4572-4576.

(229) Brisson M. & Huang L. Liposomes: conquering the nuclear barrier. *Curr. Opin. Mol. Ther.* **1999** 1(2) 140-146.

(230) Lechardeur D., Verkman A.S., & Lukacs G.L. Intracellular routing of plasmid DNA during non-viral gene transfer. *Adv. Drug Deliv. Rev.* **2005** 57(5) 755-767.

(231) Lechardeur D. & Lukacs G.L. Intracellular barriers to non-viral gene transfer. *Curr. Gene Ther.* **2002** 2(2) 183-194.

(232) Pouton C.W., Wagstaff K.M., Roth D.M., Moseley G.W., & Jans D.A. Targeted delivery to the nucleus. *Adv. Drug Deliv. Rev.* **2007** 59(8) 698-717.

(233) van der Aa M.A., Mastrobattista E., Oosting R.S., Hennink W.E., Koning G.A., & Crommelin D.J. The nuclear pore complex: the gateway to successful nonviral gene delivery. *Pharm. Res.* **2006** 23(3) 447-459.

(234) Collas P. & Alestrom P. Nuclear localization signals enhance germline transmission of a transgene in zebrafish. *Transgenic Res.* **1998** 7(4) 303-309.

(235) Subramanian A., Ranganathan P., & Diamond S.L. Nuclear targeting peptide scaffolds for lipofection of nondividing mammalian cells. *Nat. Biotechnol.* **1999** 17(9) 873-877.

(236) Liang M.R., Alestrom P., & Collas P. Glowing zebrafish: integration, transmission, and expression of a single luciferase transgene promoted by noncovalent DNA-nuclear transport peptide complexes. *Mol. Reprod. Dev.* **2000** 55(1) 8-13.

(237) Bremner K.H., Seymour L.W., Logan A., & Read M.L. Factors influencing the ability of nuclear localization sequence peptides to enhance nonviral gene delivery. *Bioconjug. Chem.* **2004** 15(1) 152-161.

(238) Mesika A., Kiss V., Brumfeld V., Ghosh G., & Reich Z. Enhanced intracellular mobility and nuclear accumulation of DNA plasmids associated with a karyophilic protein. *Hum. Gene Ther.* **2005** 16(2) 200-208.

(239) Arenal A., Pimentel R., Garcia C., Pimentel E., & Alestrom P. The SV40 T antigen nuclear localization sequence enhances nuclear import of vector DNA in embryos of a crustacean (Litopenaeus schmitti). *Gene* **2004** 33771-77.

(240) Akita H., Tanimoto M., Masuda T. *et al.* Evaluation of the nuclear delivery and intra-nuclear transcription of plasmid DNA condensed with micro (mu) and NLS-micro by cytoplasmic and

nuclear microinjection: a comparative study with poly-L-lysine. *J. Gene Med.* **2006** 8(2) 198-206.

(241) Masuda T., Akita H., & Harashima H. Evaluation of nuclear transfer and transcription of plasmid DNA condensed with protamine by microinjection: the use of a nuclear transfer score. *FEBS Lett.* **2005** 579(10) 2143-2148.

(242) Ritter W., Plank C., Lausier J. *et al.* A novel transfecting peptide comprising a tetrameric nuclear localization sequence. *J. Mol. Med.* **2003** 81(11) 708-717.

(243) Rudolph C., Plank C., Lausier J., Schillinger U., Muller R.H., & Rosenecker J. Oligomers of the arginine-rich motif of the HIV-1 TAT protein are capable of transferring plasmid DNA into cells. *J. Biol. Chem.* **2003** 278(13) 11411-11418.

(244) Ciolina C., Byk G., Blanche F., Thuillier V., Scherman D., & Wils P. Coupling of nuclear localization signals to plasmid DNA and specific interaction of the conjugates with importin alpha. *Bioconjug. Chem.* **1999** 10(1) 49-55.

(245) Nagasaki T., Myohoji T., Tachibana T., Futaki S., & Tamagaki S. Can nuclear localization signals enhance nuclear localization of plasmid DNA? *Bioconjug. Chem.* **2003** 14(2) 282-286.

(246) Neves C., Byk G., Scherman D., & Wils P. Coupling of a targeting peptide to plasmid DNA by covalent triple helix formation. *FEBS Lett.* **1999** 453(1-2) 41-45.

(247) Sebestyen M.G., Ludtke J.J., Bassik M.C. *et al.* DNA vector chemistry: the covalent attachment of signal peptides to plasmid DNA. *Nat. Biotechnol.* **1998** 16(1) 80-85.

(248) Tanimoto M., Kamiya H., Minakawa N., Matsuda A., & Harashima H. No enhancement of nuclear entry by direct conjugation of a nuclear localization signal peptide to linearized DNA. *Bioconjug. Chem.* **2003** 14(6) 1197-1202.

(249) van der Aa M., Koning G., van der Gugten J. *et al.* Covalent attachment of an NLS-peptide to linear dna does not enhance transfection efficiency of cationic polymer based gene delivery systems. *J. Control Release* **2005** 101(1-3) 395-397.

(250) Zanta M.A., Belguise-Valladier P., & Behr J.P. Gene delivery: a single nuclear localization signal peptide is sufficient to carry DNA to the cell nucleus. *Proc. Natl. Acad. Sci. U. S. A* **1999** 96(1) 91-96.

(251) Chan C.K., Hubner S., Hu W., & Jans D.A. Mutual exclusivity of DNA binding and nuclear localization signal recognition by the yeast transcription factor GAL4: implications for nonviral DNA delivery. *Gene Ther.* **1998** 5(9) 1204-1212.

(252) Vaysse L., Harbottle R., Bigger B., Bergau A., Tolmachov O., & Coutelle C. Development of a self-assembling nuclear targeting vector system based on the tetracycline repressor protein. *J. Biol. Chem.* **2004** 279(7) 5555-5564.

(253) Branden L.J., Mohamed A.J., & Smith C.I. A peptide nucleic acid-nuclear localization signal fusion that mediates nuclear transport of DNA. *Nat. Biotechnol.* **1999** 17(8) 784-787.

(254) Branden L.J., Christensson B., & Smith C.I. In vivo nuclear delivery of oligonucleotides via hybridizing bifunctional peptides. *Gene Ther.* **2001** 8(1) 84-87.

(255) Bremner K.H., Seymour L.W., Logan A., & Read M.L. Factors influencing the ability of nuclear localization sequence peptides to enhance nonviral gene delivery. *Bioconjug. Chem.* **2004** 15(1) 152-161.

(256) Ludtke J.J., Zhang G., Sebestyen M.G., & Wolff J.A. A nuclear localization signal can enhance both the nuclear transport and expression of 1 kb DNA. *J. Cell Sci.* **1999** 112(Pt 12) 2033-2041.

(257) Chan C.K. & Jans D.A. Enhancement of polylysine-mediated transferrinfection by nuclear localization sequences: polylysine does not function as a nuclear localization sequence. *Hum. Gene Ther.* **1999** 10(10) 1695-1702.

(258) Chan C.K., Senden T., & Jans D.A. Supramolecular structure and nuclear targeting efficiency determine the enhancement of transfection by modified polylysines. *Gene Ther.* **2000** 7(19) 1690-1697.

(259) Carlisle R.C., Bettinger T., Ogris M., Hale S., Mautner V., & Seymour L.W. Adenovirus hexon protein enhances nuclear delivery and increases transgene expression of polyethylenimine/plasmid DNA vectors. *Mol. Ther.* **2001** 4(5) 473-483.

(260) Aronsohn A.I. & Hughes J.A. Nuclear localization signal peptides enhance cationic liposome-mediated gene therapy. *J. Drug Target* **1998** 5(3) 163-169.

(261) Hagstrom J.E., Sebestyen M.G., Budker V., Ludtke J.J., Fritz J.D., & Wolff J.A. Complexes of non-cationic liposomes and histone H1 mediate efficient transfection of DNA without encapsulation. *Biochim. Biophys. Acta* **1996** 1284(1) 47-55.

(262) Keller M., Harbottle R.P., Perouzel E. *et al.* Nuclear localisation sequence templated nonviral gene delivery vectors: investigation of intracellular trafficking events of LMD and LD vector systems. *Chembiochem.* **2003** 4(4) 286-298.

(263) Murray K.D., Etheridge C.J., Shah S.I. *et al.* Enhanced cationic liposome-mediated transfection using the DNA-binding peptide mu (mu) from the adenovirus core. *Gene Ther.* **2001** 8(6) 453-460.

(264) Preuss M., Tecle M., Shah I., Matthews D.A., & Miller A.D. Comparison between the interactions of adenovirus-derived peptides with plasmid DNA and their role in gene delivery mediated by liposome-peptide-DNA virus-like nanoparticles. *Org. Biomol. Chem.* **2003** 1(14) 2430-2438.

(265) Wiseman J.W., Scott E.S., Shaw P.A., & Colledge W.H. Enhancement of gene delivery to human airway epithelial cells in vitro using a peptide from the polyoma virus protein VP1. *J. Gene Med.* **2005** 7(6) 759-770.

(266) Vandenbroucke R.E., De Smedt S.C., Demeester J., & Sanders N.N. Cellular entry pathway and gene transfer capacity of TAT-modified lipoplexes. *Biochim. Biophys. Acta* **2007** 1768(3) 571-579.

(267) Akuta T., Eguchi A., Okuyama H. *et al.* Enhancement of phage-mediated gene transfer by nuclear localization signal. *Biochem. Biophys. Res. Commun.* **2002** 297(4) 779-786.

(268) Wagstaff K.M., Glover D.J., Tremethick D.J., & Jans D.A. Histone-mediated transduction as an efficient means for gene delivery. *Mol. Ther.* **2007** 15(4) 721-731.

(269) Nagasaki T., Kawazu T., Tachibana T., Tamagaki S., & Shinkai S. Enhanced nuclear import and transfection efficiency of plasmid DNA using streptavidin-fused importin-beta. *J. Control Release* **2005** 103(1) 199-207.

(270) Zabner J., Fasbender A.J., Moninger T., Poellinger K.A., & Welsh M.J. Cellular and Molecular Barriers to Gene-Transfer by A Cationic Lipid. *J. Biol. Chem.* **1995** 270(32) 18997-19007.

(271) Liu G., Li D., Pasumarthy M.K. *et al.* Nanoparticles of compacted DNA transfect postmitotic cells. *J. Biol. Chem.* **2003** 278(35) 32578-32586.

(272) Fink T.L., Klepcyk P.J., Oette S.M. *et al.* Plasmid size up to 20 kbp does not limit effective in vivo lung gene transfer using compacted DNA nanoparticles. *Gene Ther.* **2006** 13(13) 1048-1051.

(273) Pante N. & Kann M. Nuclear pore complex is able to transport macromolecules with diameters of about 39 nm. *Mol. Biol. Cell* **2002** 13(2) 425-434.

(274) Mastrobattista E., van der Aa M.A., Hennink W.E., & Crommelin D.J. Artificial viruses: a nanotechnological approach to gene delivery. *Nat. Rev. Drug Discov.* **2006** 5(2) 115-121.

(275) Akita H., Ito R., Khalil I.A., Futaki S., & Harashima H. Quantitative three-dimensional analysis of the intracellular trafficking of plasmid DNA transfected by a nonviral gene delivery system using confocal laser scanning microscopy. *Mol. Ther.* **2004** 9(3) 443-451.

(276) Kamiya H., Fujimura Y., Matsuoka I., & Harashima H. Visualization of intracellular trafficking of exogenous DNA delivered by cationic liposomes. *Biochem. Biophys. Res. Commun.* **2002** 298(4) 591-597.

(277) Bieber T., Meissner W., Kostin S., Niemann A., & Elsasser H.P. Intracellular route and transcriptional competence of polyethylenimine-DNA complexes. *J. Control Release* **2002** 82(2-3) 441-454.

(278) Godbey W.T., Wu K.K., & Mikos A.G. Tracking the intracellular path of poly(ethylenimine)/DNA complexes for gene delivery. *Proc. Natl. Acad. Sci. U. S. A* **1999** 96(9) 5177-5181.

(279) Kogure K., Moriguchi R., Sasaki K., Ueno M., Futaki S., & Harashima H. Development of a non-viral multifunctional envelope-type nano device by a novel lipid film hydration method. *J. Control Release* **2004** 98(2) 317-323.

(280) Bettinger T., Remy J.S., & Erbacher P. Size reduction of galactosylated PEI/DNA complexes improves lectin-mediated gene transfer into hepatocytes. *Bioconjug. Chem.* **1999** 10(4) 558-561.

(281) Diebold S.S., Kursa M., Wagner E., Cotten M., & Zenke M. Mannose polyethylenimine conjugates for targeted DNA delivery into dendritic cells. *J. Biol. Chem.* **1999** 274(27) 19087-19094.

(282) Erbacher P., Bousser M.T., Raimond J., Monsigny M., Midoux P., & Roche A.C. Gene transfer by DNA/glycosylated polylysine complexes into human blood monocyte-derived macrophages. *Hum. Gene Ther.* **1996** 7(6) 721-729.

(283) Duverger E., Carpentier V., Roche A.C., & Monsigny M. Sugar-dependent nuclear import of glycoconjugates from the cytosol. *Exp. Cell Res.* **1993** 207(1) 197-201.

(284) Duverger E., Pellerin-Mendes C., Mayer R., Roche A.C., & Monsigny M. Nuclear import of glycoconjugates is distinct from the classical NLS pathway. *J. Cell Sci.* **1995** 108(Pt 4) 1325-1332.

(285) Niikura K., Nishio T., Akita H. *et al.* Accumulation of O-GlcNAc-displaying CdTe quantum dots in cells in the presence of ATP. *Chembiochem.* **2007** 8(4) 379-384.

(286) Fajac I., Grosse S., Briand P., & Monsigny M. Targeting of cell receptors and gene transfer efficiency: a balancing act. *Gene Ther.* **2002** 9(11) 740-742.

(287) Fajac I., Thevenot G., Bedouet L. *et al.* Uptake of plasmid/glycosylated polymer complexes and gene transfer efficiency in differentiated airway epithelial cells. *J. Gene Med.* **2003** 5(1) 38-48.

(288) Grosse S., Tremeau-Bravard A., Aron Y., Briand P., & Fajac I. Intracellular rate-limiting steps of gene transfer using glycosylated polylysines in cystic fibrosis airway epithelial cells. *Gene Ther.* **2002** 9(15) 1000-1007.

(289) Guinez C., Morelle W., Michalski J.C., & Lefebvre T. O-GlcNAc glycosylation: a signal for the nuclear transport of cytosolic proteins? *Int. J. Biochem. Cell Biol.* **2005** 37(4) 765-774.

(290) Menon R.P., Strom M., & Hughes R.C. Interaction of a novel cysteine and histidine-rich cytoplasmic protein with galectin-3 in a carbohydrate-independent manner. *FEBS Lett.* **2000** 470(3) 227-231.

(291) Moutsatsos I.K., Wade M., Schindler M., & Wang J.L. Endogenous lectins from cultured cells: nuclear localization of carbohydrate-binding protein 35 in proliferating 3T3 fibroblasts. *Proc. Natl. Acad. Sci. U. S. A* **1987** 84(18) 6452-6456.

(292) Masuda T., Akita H., Nishio T. *et al.* Development of lipid particles targeted via sugar-lipid conjugates as novel nuclear gene delivery system. *Biomaterials* **2008** 29(6) 709-723.

(293) Trotman L.C., Mosberger N., Fornerod M., Stidwill R.P., & Greber U.F. Import of adenovirus DNA involves the nuclear pore complex receptor CAN/Nup214 and histone H1. *Nat. Cell Biol.* **2001** 3(12) 1092-1100.

(294) Hatakeyama H., Akita H., Kogure K. *et al.* Development of a novel systemic gene delivery system for cancer therapy with a tumor-specific cleavable PEG-lipid. *Gene Ther.* **2007** 14(1) 68-77.

(295) Khalil I.A., Kogure K., Futaki S. *et al.* Octaarginine-modified multifunctional envelope-type nanoparticles for gene delivery. *Gene Ther.* **2007** 14(8) 682-689.

(296) Khalil I.A., Kogure K., Futaki S., & Harashima H. High density of octaarginine stimulates macropinocytosis leading to efficient intracellular trafficking for gene expression. *J. Biol. Chem.* **2006** 281(6) 3544-3551.

(297) Mazzanti M., Bustamante J.O., & Oberleithner H. Electrical dimension of the nuclear envelope. *Physiol Rev.* **2001** 81(1) 1-19.

(298) Danker T. & Oberleithner H. Nuclear pore function viewed with atomic force microscopy. *Pflugers Arch.* **2000** 439(6) 671-681.

(299) Stehno-Bittel L., Perez-Terzic C., & Clapham D.E. Diffusion across the nuclear envelope inhibited by depletion of the nuclear Ca2+ store. *Science* **1995** 270(5243) 1835-1838.

(300) Wang H. & Clapham D.E. Conformational changes of the in situ nuclear pore complex. *Biophys. J.* **1999** 77(1) 241-247.

(301) Oberleithner H., Schillers H., Wilhelmi M., Butzke D., & Danker T. Nuclear pores collapse in response to CO2 imaged with atomic force microscopy. *Pflugers Arch.* **2000** 439(3) 251-255.

(302) Enss K., Danker T., Schlune A., Buchholz I., & Oberleithner H. Passive transport of macromolecules through Xenopus laevis nuclear envelope. *J. Membr. Biol.* **2003** 196(3) 147-155.

(303) Shahin V., Danker T., Enss K., Ossig R., & Oberleithner H. Evidence for Ca2+- and ATP-sensitive peripheral channels in nuclear pore complexes. *FASEB J.* **2001** 15(11) 1895-1901.

(304) Oberleithner H., Schafer C., Shahin V., & Albermann L. Route of steroid-activated macromolecules through nuclear pores imaged with atomic force microscopy. *Biochem. Soc. Trans.* **2003** 31(Pt 1) 71-75.

(305) Schafer C., Shahin V., Albermann L. *et al.* Aldosterone signaling pathway across the nuclear envelope. *Proc. Natl. Acad. Sci. U. S. A* **2002** 99(10) 7154-7159.

(306) Shahin V., Ludwig Y., Schafer C., Nikova D., & Oberleithner H. Glucocorticoids remodel nuclear envelope structure and permeability. *J. Cell Sci.* **2005** 118(Pt 13) 2881-2889.

(307) Buchholz I., Enss K., Schafer C., Schlune A., Shahin V., & Oberleithner H. Transient permeability leak of nuclear envelope induced by aldosterone. *J. Membr. Biol.* **2004** 199(3) 135-141.

(308) Shulga N. & Goldfarb D.S. Binding dynamics of structural nucleoporins govern nuclear pore complex permeability and may mediate channel gating. *Mol. Cell Biol.* **2003** 23(2) 534-542.

(309) Schafer C., Ludwig Y., Shahin V. *et al.* Ethanol alters access to the cell nucleus. *Pflugers Arch.* **2007** 453(6) 809-818.

(310) Ribbeck K. & Gorlich D. The permeability barrier of nuclear pore complexes appears to operate via hydrophobic exclusion. *EMBO J.* **2002** 21(11) 2664-2671.

(311) Vandenbroucke R.E., Lucas B., Demeester J., De Smedt S.C., & Sanders N.N. Nuclear accumulation of plasmid DNA can be enhanced by non-selective gating of the nuclear pore. *Nucleic Acids Res.* **2007** 35(12) e86.

Chapter 2

Cellular Entry Pathway and Gene Transfer Capacity of Tat-modified Lipoplexes

This chapter is published:

Roosmarijn E. Vandenbroucke[1], Stefaan C. De Smedt[1], Joseph Demeester[1], Niek N. Sanders[1]; *Biochim Biophys Acta.* 2007 Mar;1768(3):571-9.

[1] Laboratory of General Biochemistry and Physical Pharmacy, Department of Pharmaceutics Ghent University, Ghent, Belgium.

ABSTRACT

Several reports have shown a fast and efficient translocation of Tat-modified lipoplexes (LPXs) and particles into the cell cytoplasm. However, neither the uptake mechanism nor the biological effect of Tat-modified LPXs has been studied in detail. In this report we show that the increase in gene transfer of Tat-modified LPXs depends on the amount of cationic lipid in the LPXs and on the way Tat was coupled to the LPXs. We demonstrate that the cellular uptake of both Tat-modified and unmodified LPXs is very fast and, in contrast to previous publications, temperature-dependent. Additionally, after internalization Tat-modified as well as unmodified LPXs end up in lysosomal vesicles, indicating the involvement of clathrin-mediated endocytosis. Furthermore, chlorpromazine, a specific inhibitor of clathrin-dependent endocytosis, strongly inhibits the cellular uptake and biological activity of both the Tat-modified and unmodified LPXs. We also found that the uptake and biological activity of these LPXs are diminished when cholesterol in the cell membrane was bound by filipin, an inhibitor of the lipid-raft mediated pathway. Considering these data, we conclude that Tat-modified and unmodified LPXs are mainly internalized via a cholesterol-dependent clathrin-mediated pathway.

Chapter 2

Cellular Entry Pathway and Gene Transfer Capacity of Tat-modified Lipoplexes

INTRODUCTION

Gene therapy may become an important strategy in the treatment of various diseases. However, the clinical applications of gene therapy depend largely on the development of suitable gene transfer vehicles. Although generally not as efficient as viral vectors, non-viral systems, such as lipids, have the advantages of being less toxic, safer, non restrictive in DNA size, potentially targetable, and easy to produce in relatively large amounts. However, poor transfection efficiencies presently limit their usefulness for gene therapy applications, caused by critical steps such as endosomal release and nuclear uptake [1].

Viruses, such as influenza viruses and adenoviruses, have developed peptides that warrant their escape from endosomes by membrane fusion or disruption upon the acidification of the endosomes. Such viral peptides and also synthetic polymers capable to disrupt endosomes upon acidification have been applied to enhance non-viral gene delivery (reviewed by [1-4]). However, it has been shown that an excessive disruption of endosomes by endosomolytic agents may be harmful to the cell [5]. Alternatively, to circumvent the endosomal escape barrier, it has been proposed to bypass the endosomal pathway by using cell penetrating peptides (CPPs) that rapidly translocate cargoes across the cell membrane [6-8]. Peptides derived from the HIV-1 transactivator of transcription protein or 'Tat', have been shown to facilitate both *in vitro* and *in vivo* the intracellular delivery of cargoes of various sizes and physicochemical properties (recently reviewed by [8-10]). These Tat peptides, typically having a positive charge at physiological pH, consist of a short stretch of basic amino acids (GRKKRRQRRR), which is responsible for the translocation across cellular membranes and is called the protein transduction domain (PTD) sequence [11]. Additionally, this sequence also functions as a nuclear localization signal [12].

Initially it was believed that the uptake of Tat peptide or Tat peptide conjugated cargoes occurs in a receptor-independent [13,14] and temperature-independent manner [11,15-17]. However, this is

currently questioned by the increasing evidence that the original data might originate from artefacts in the experimental procedure for fixation and removal of membrane-bound material [18]. Until now, the precise entry mechanism of Tat peptides and Tat peptide conjugated cargoes is still controversial (reviewed by [19]). Both clathrin-mediated endocytosis [20-23], caveolae-mediated endocytosis [24-27] and macropinocytosis [14,28] have been suggested. Possibly the mechanism of cellular entry depends on the cell type, the Tat sequence, physicochemical properties of the cargo, the amount of Tat peptides on the surface of the cargo, and the way Tat peptides are bound to the cargo [9].

The ability of Tat peptides to translocate cargoes across cell membranes is an attractive feature that could bring significant advantages to the cellular delivery of proteins, therapeutic DNA or small interfering RNA (siRNA) molecules [24,29,30]. However, in contrast to Tat peptides conjugated to proteins, the biological effect and the cellular entry mechanism of Tat/plasmid DNA (Tat/pDNA) conjugates and in particular Tat-modified lipoplexes (LPXs) [30-33] have not been studied in detail. Therefore, in this work we aimed to determine (**1**) whether the attachment of Tat peptides to LPXs could enhance their transfection efficiency, (**2**) whether the uptake of the Tat-modified LPXs is energy dependent, and (**3**) the cellular entry mechanism and intracellular routing of the Tat-modified LPXs.

MATERIALS & METHODS

Materials

Dulbecco's modified Eagle's medium (DMEM), L-glutamine (L-Gln), heat-inactivated fetal bovine serum (FBS), and penicilline-streptomycine (P/S) were supplied by GibcoBRL (Merelbeke, Belgium). The Tat peptide AA 37-72 (CFITKALGISYGRKKRRQRRRAPQGSQ-THQVSLSKQ) was obtained from the Centralised Facility for AIDS Reagents, EU Programme EVA (European Vaccine Against AIDS). The secreted alkaline phosphatase (SEAP) expression plasmid (pMet7 hβ_c SEAP) was a kind gift from Prof. Tavernier (Ghent University, Belgium). 1,2-Dioleolyl-3-trimethylammonium-propane (chloride salt) (DOTAP), 1,2-dioleoyl-*sn*-glycero-3-phosphoethanolamine (DOPE) and 1,2-distearoyl-sn-glycero-3-phosphatidylethanolamine-N-[maleimide(polyethylene glycol)2000] (DSPE-PEG_{2000}-MAL) were purchased from Avanti Polar Lipids (AL, USA).

Cell culture

Cos-7 cells (African green monkey kidney cells; ATCC number CRL-1651) were cultured in Dulbecco's modified Eagle's medium (DMEM) containing 2 mM L-Gln, 10 % heat inactivated FBS, 100 U/ml P/S and grown at 37°C in a humidified atmosphere containing 5% CO_2.

Preparation of cationic liposomes

Cationic liposomes composed of DOTAP:DOPE:DSPE-PEG_{2000}-MAL with molar ratios of 5:5:0.2, 3:7:0.2, and 1:9:0.2 (containing 50 mol%, 30 mol% and 10 mol% DOTAP, respectively) were prepared as described previously [34]. Briefly, appropriate amounts of lipids were dissolved in chloroform and mixed. To obtain FITC labeled liposomes 0.01 mol% FITC-DOPE was added to the mixture. The chloroform was subsequently removed by rotary evaporation at 37°C followed by flushing the obtained lipid film with nitrogen during 30 min at room temperature. The dried lipids were then hydrated by adding Hepes buffer (20 mM, pH 7.4) till a final lipid concentration of 10.2 mM. After mixing in the presence of glass beads, liposome formation was allowed overnight at 4°C. Thereafter, the formed liposomes were extruded 11 times through two stacked 100 nm polycarbonate membrane filters (Whatman, Brentfort, UK) at room temperature using an Avanti Mini-Extruder (Avanti Polar Lipids).

Preparation of Tat-modified and unmodified LPXs

To prepare 'post Tat-LPXs', the liposomes, with or without FITC-DOPE, were mixed with the appropriate amount of pDNA, in a +/- charge ratio of 4:1 and incubated at room temperature for 30 min. The final concentration of pDNA in the LPX dispersion was 0.126 µg/µl. Subsequently, Tat peptides were coupled to the MAL-group, present at the end of the PEG chains in DSPE-PEG_{2000}-MAL. Therefore, the Tat AA 37-72 peptide was first incubated under a nitrogen flow for 2 hrs with a 10-fold molar excess of TCEP (tris-2(carboxyethyl)phosphine) to reduce the disulfide bonds. Again under a nitrogen flow, the 'activated' Tat AA 37-72 peptide was added to the LPXs in a 4-fold molar excess compared to the DSPE-PEG_{2000}-MAL and incubated overnight at 4°C on a shaker.

To prepare 'pre Tat-LPXs', the same protocol was used, except that the Tat peptide was coupled to the liposomes before they were complexed with the pDNA.

The unmodified LPXs (i.e. LPXs without Tat) were prepared as the 'pre or post Tat-LPXs', but without the addition of Tat AA 37-72 peptide.

Size and zeta potential measurements

The average particle size and the zeta potential (ζ) of the liposomes and LPXs were measured by photon correlation spectroscopy (PCS) (Autosizer 4700, Malvern, Worcestershire, UK) and by particle electrophoresis (Zetasizer 2000, Malvern, Worcestershire, UK), respectively. The liposome and LPX dispersions were diluted 40-fold in 20 mM Hepes buffer pH 7.4 before the particle size and zeta potential were measured.

Agarose gel electrophoresis

To determine the extent of pDNA association to the liposomes and the release of the pDNA from the liposomes after incubation with SDS, agarose gel electrophoresis was used. 18 µl of the Tat-modified and unmodified LPXs, prepared as described above, were mixed with 2 µl 20 µg/µl SDS or 2 µl dH_2O and loaded together with 5 µl 5 x loading solution (30 % glycerol, 0.02 % bromophenol blue) on a 1 % agarose gel prepared in TBE buffer (10.8 g/l Tris base, 5.5 g/l boric acid and 0.58 g/l EDTA). The samples were subjected to electrophoresis at 80 V during 45 min and the DNA was visualized by UV transillumination using EtBr (0.5 µl/ml) staining prior to photography.

Cytotoxicity assay

The cytotoxicity of the LPXs was determined using the tetrazolium salt based colorimetric MTT assay (EZ4U, Biomedica, Vienna, Austria) according to the manufacturer's instructions. Briefly, 2.5×10^4 cells/cm^2 were seeded in a 96-well plate and allowed to adhere. After 24 hrs, cells were washed twice with serum free medium and incubated with LPXs, containing 0.18 µg pDNA per cm^2 in serum free medium. After 2 hrs, the complexes were removed and cells were washed with culture medium. Finally, to each well, 20 µl substrate was added together with 180 µl culture medium and after 4 hrs incubation at 37°C the concentration of reduced formazan was measured at 450 nm and 630 nm on a Wallac Victor^2 absorbance plate reader (Perkin Elmer-Cetus Life Sciences, Boston, MA).

Transfection experiments

Cells were seeded into 24-well plates (2.5×10^4 cells/cm^2) and allowed to attach overnight. The culture medium was removed from the cells and they were washed twice with serum free medium. Subsequently, the LPXs (with and without bound Tat peptide) were diluted in serum free medium and the diluted LPXs, containing 0.18 µg pDNA per cm^2, were added to the 24-well plates.

Cells were incubated at 37°C for 2 hr and, after a washing step with culture medium, the medium was replaced by 1 ml culture medium, and further incubated at 37°C.

For the transfection experiments at 4°C the cells, grown overnight as described above, were cooled down to 4°C during 30 min. Subsequently, pre-cooled solutions for washing and for the transfection were used. After addition of the complexes, the cells were incubated at 4°C and after 2 hrs, cells were washed with culture medium.

For treatment with uptake inhibitors, cells were pre-incubated for 1 hr at 37°C in DMEM with chlorpromazine (10 µg/ml) [35], filipin III (10 µg/ml) [36] before the complexes were added. In a recent study we have demonstrated that these inhibitors, at their respective concentrations, predominately block clathrin or raft mediated pathways without causing drastic cytotoxic effects [37]. After removal of the LPXs and addition of culture medium, cells were further incubated in an incubator. After 48 hrs the SEAP activity in the culture medium and the total protein concentration in the cells was measured.

Gene expression analysis

To determine the SEAP activity in the medium, 100 µl of the culture medium above the cells was taken and incubated at 65°C for 30 mins. Subsequently 100 µl dilution buffer (0.1 M glycine, 1 mM $MgCl_2$, 0.1 mM $ZnCl_2$, pH 10.4) and 15 µl 4-methylumbelliferyl phosphate (4-MUP, 5.1 µg/µl in distilled water) was added to the culture medium in a 96-well plate. The obtained mixtures were then incubated at 37°C and the fluorescence ($\lambda_{ex}/\lambda_{em}$ = 360/449 nm) was followed during 45 min on a Wallac Victor^2 fluorescence plate reader (Perkin Elmer-Cetus Life Sciences, Boston, MA). The fluorescence obtained after 30 min was used for comparing the gene transfer capacity of the different LPXs.

Finally, after removing the culture medium, the cells were washed twice with PBS to remove dead cells and serum proteins. Thereafter, cells were lysed with lysis buffer (10 % glycerol, 2.3 % w/v SDS, 0.125 M Tris-HCl, pH 6.8), sonicated for 30 min and the protein concentration was determined by BioRad DC protein assay.

Cell binding and cellular uptake experiments

2.5×10^4 cells/cm^2 were seeded onto sterile glass bottom culture dishes (MatTek Corporation, MA, USA) and allowed to adhere for 1 day. For lysosome staining, the cells were incubated during 30 min at 37°C with 50 pM of the lysosomal marker LysoTracker® Red (Molecular Probes, Eugene, OR, U.S.A.). For 4°C experiments, cells were cooled in the refrigerator during 30 min,

washed with pre-cooled DMEM and incubated with the LPXs at 4°C. At different time points samples were analyzed.

In the experiments with cellular uptake inhibitors, the cells were pre-incubated for 1 hr at 37°C in DMEM with chlorpromazine (10 µg/ml) [35], filipin III (10 µg/ml) [36]. Subsequently, the cells were washed twice with DMEM before the appropriate amount of fluorescent Tat-modified or unmodified LPXs and inhibitor-containing serum free medium was added. Immediately after adding LPXs, the cells were visualized on different time points by confocal laser scanning microscopy (CLSM) (BioRad MRC 1024; Hemel Hempstadt, UK). After capturing the image with a 60 x water immersion objective and a krypton/argon laser (488 nm and 547 nm) for the excitation of the FITC label and the LysoTracker® Red, pseudocoloring was performed by using the digital imaging system Confocal Assistant (CAS; BioRad; Hemel Hempstadt, UK).

Statistical analysis data

The experimental data in this report (zeta potential, DLS, cytotoxicity and transfection) are expressed as mean ± standard deviation (SD). One way ANOVA was used to determine whether data groups differed significantly from each other. A p-value lower than 0.05 was considered statistically significant.

RESULTS & DISCUSSION

Preparation and physicochemical characterization of unmodified and Tat-modified LPXs

PEGylated DOTAP:DOPE:DSPE-PEG_{2000}-MAL LPXs bearing covalently bound Tat peptides at the end of their PEG chains and containing increasing amounts of DOTAP (10, 30 and 50 mol%) were obtained via two strategies: Tat peptides were either coupled to the PEG chains of the PEGylated liposomes before complexing them with pDNA ('**pre Tat-LPXs**') or after complexing them with pDNA ('**post Tat-LPXs**'). The latter approach ensured that the Tat peptides were presented on the surface of the LPXs, a prerequisite for Tat peptides to promote the internalization of cargoes [38]. Moreover, to prevent that steric hindrance could abolish the interaction of Tat with the cell membrane [30], we attached the Tat peptides via a 2 kDa PEG spacer to the LPXs by the aid of DSPE-PEG_{2000}-MAL moieties. The maleimide (MAL) groups on these PEG chains are known to react specifically with sulfhydryl groups at neutral pH creating a stable thioether bond with the N-terminal cysteine of the Tat peptide. A schematic representation of the Tat-modified LPXs is shown in Fig. 1.

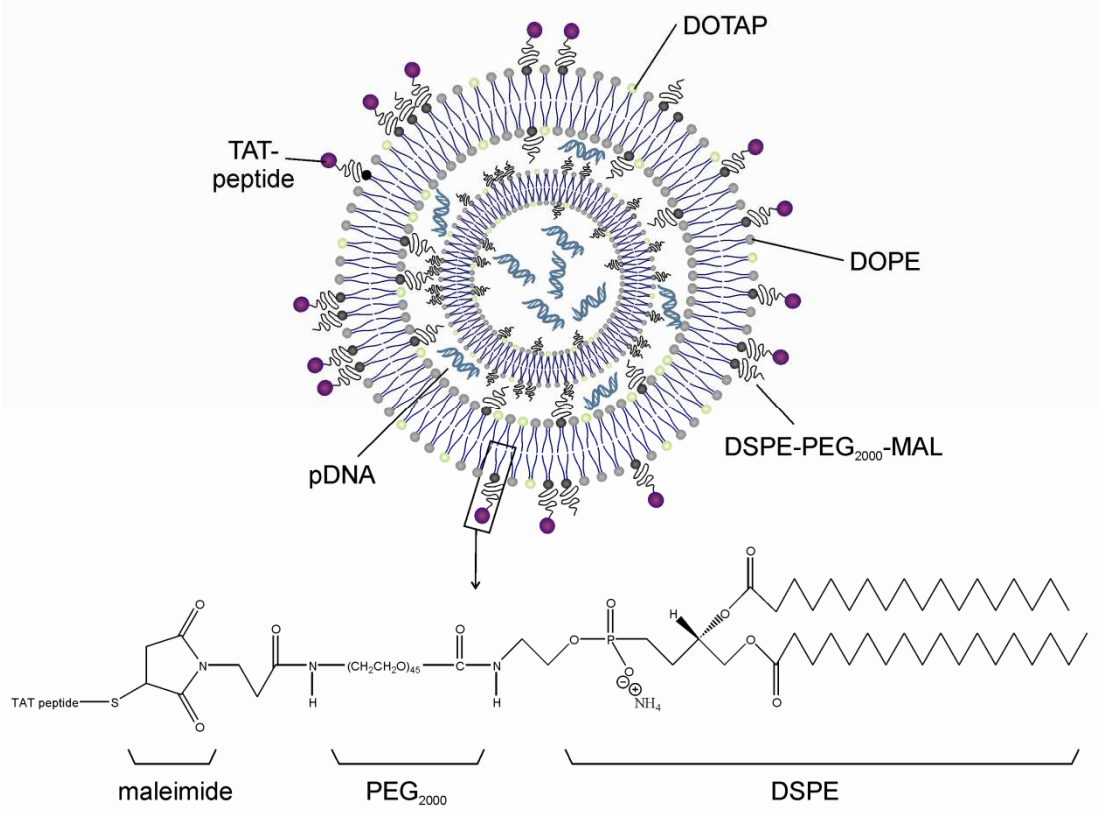

Figure 1. Schematic representation of the Tat-modified DOTAP:DOPE:DSPE-PEG_{2000}-MAL LPXs.

To assess the DNA binding capacity of the cationic liposomes and the ability of SDS to release the pDNA from the LPXs agarose gel electrophoresis experiments were performed (Fig. 2).

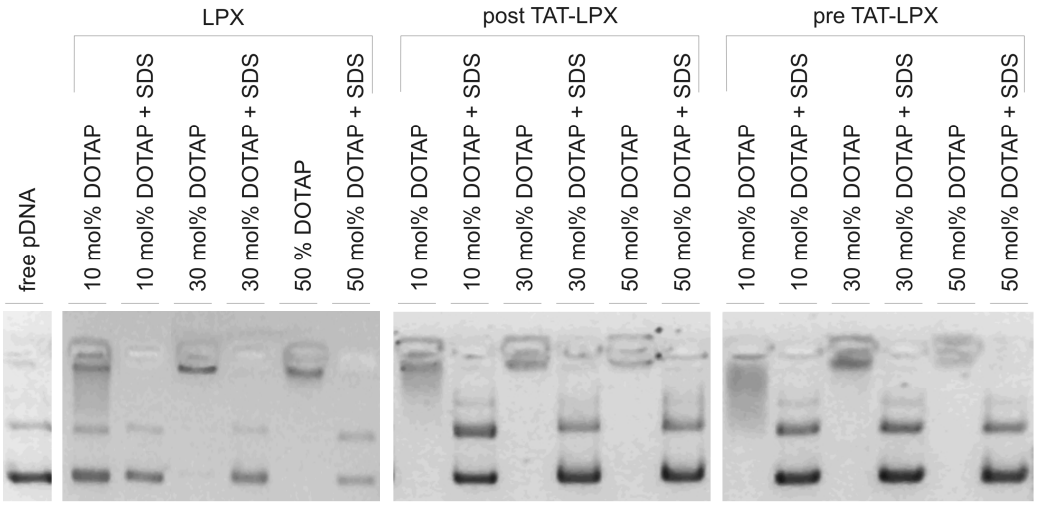

Figure 2. Agarose gelelectrophoresis of unmodified, pre and post Tat-LPX containing 10, 30 and 50 mol% DOTAP before and after addition of SDS.

LPXs containing 30 and 50 mol% DOTAP showed, both in the presence and absence of Tat, a complete complexation of the pDNA. 10 mol% DOTAP LPXs lacking the Tat peptide failed to bind all

the pDNA. Coupling of Tat peptides to these 10 mol% DOTAP LPXs retarded the pDNA on the agarose gel, but did not result in a full complexation. Finally, the release properties in the presence of SDS of the different types of LPXs were not altered by Tat peptides.

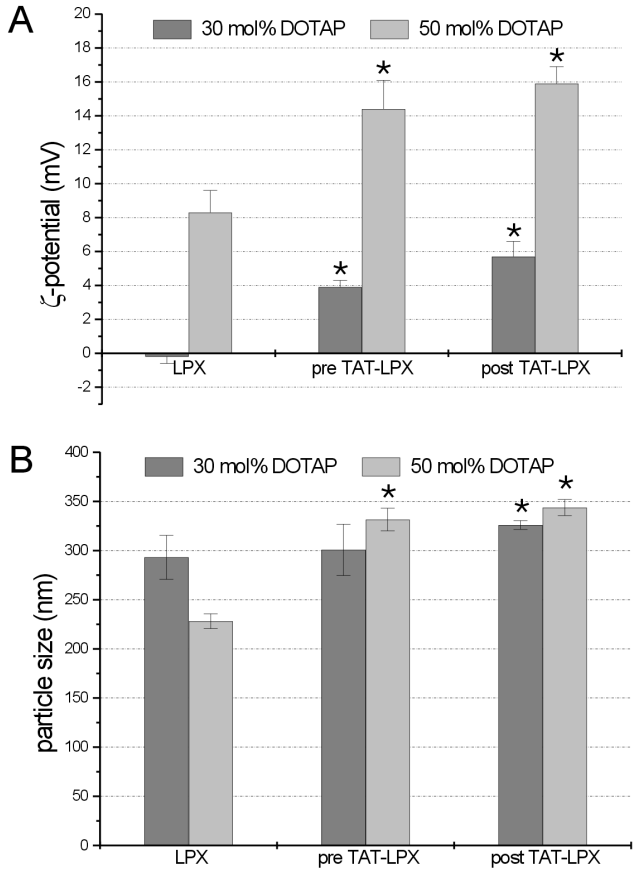

Figure 3. Zeta potential (A) and size (B) measurement of the unmodified and Tat-modified LPXs containing 30 mol% (dark grey) and 50 mol% (light grey) DOTAP. The size and zeta potential of the 10 mol% DOTAP LPXs could not be measured accurately due to the presence of large aggregates and/or a too high polydispersity. All data are shown as mean ± SD with n=4 for DLS and n=5 for zeta potential data. The asterix (*) represents data points that significantly differ ($p<0.05$; ANOVA) from the data of unmodified LPXs.

The effect of the attachment of Tat peptides to the LPXs was further evaluated by comparing the particle size and surface charge of Tat-modified and unmodified LPXs. Fig. 3A and 3B show that the attachment of Tat-peptides to the LPXs causes, in the case of both the 'pre Tat-LPXs' (pre Tat-LPX) and the 'post Tat-LPXs' (post Tat-LPX), a significant ($p<0.05$; ANOVA) increase in particle size and surface charge. The latter is an indication that cationic Tat peptides were indeed attached to the surface of the PEGylated LPXs. The particle size and surface charge of the 10 mol% DOTAP LPXs could not be determined accurately, due to large aggregates and/or a too high polydispersity. This is not surprising as huge amounts of free pDNA were present in the 10 mol% DOTAP LPXs (Fig. 2).

Cytotoxicity

Several groups have reported a significant cytoxicity of free Tat peptides [9,39,40]. Therefore, we characterized the cytotoxicity of our LPXs by measuring the mitochondrial activity. Linking of Tat peptides to the LPXs slightly increased their cytoxicity (Fig. 4). It is currently unclear via which mechanism Tat causes cell toxicity, however, it has been shown in HeLa cells that the α-helix structure, present in the Tat AA 37-72 peptide, plays an important role [11].

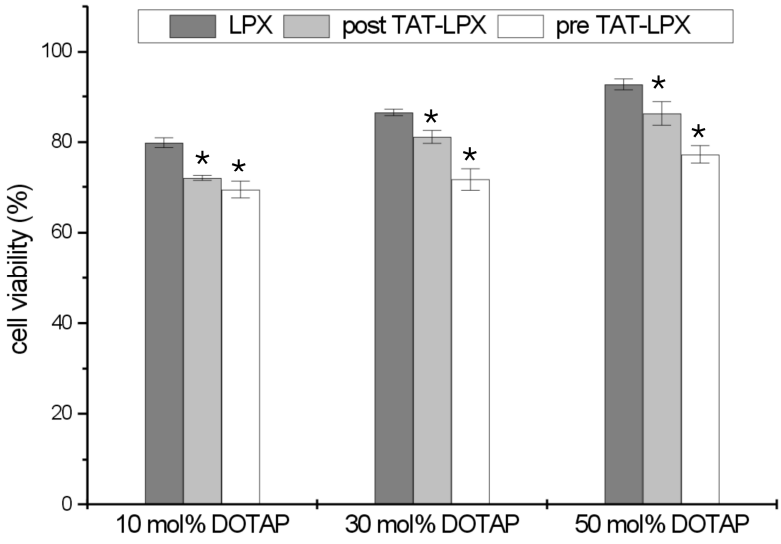

Figure 4. Cytotoxicity of unmodified and Tat-modified LPXs containing 10, 30 or 50 mol% DOTAP relatively to untreated cells. Data are shown as mean ± SD with n=3. The asterix (*) represents data points that significantly differ ($p<0.05$; ANOVA) from the data of unmodified LPXs.

Furthermore, except for the pre Tat-LPX containing 10 and 30 mol% DOTAP, the cytotoxicity of the LPXs slightly increased when they contain lower amounts of DOTAP and thus higher amounts of DOPE. DOPE is a fusogenic lipid that disrupts endosomal membranes during their acidification [41]. A higher DOPE content in the LPXs probably results in an increased endosomal breakdown, which, as previously been suggested for polyethyleneimine [5], may explain the increased cytotoxicity.

Transfection capacity of unmodified and Tat-modified LPXs

The transfection efficiency of the unmodified LPXs, the 'pre Tat-LPX' and the 'post Tat-LPX' were subsequently compared. To correct for the above observed cytotoxicity of the LPXs, the results of the transfection experiments were expressed relatively to the total cell protein content.

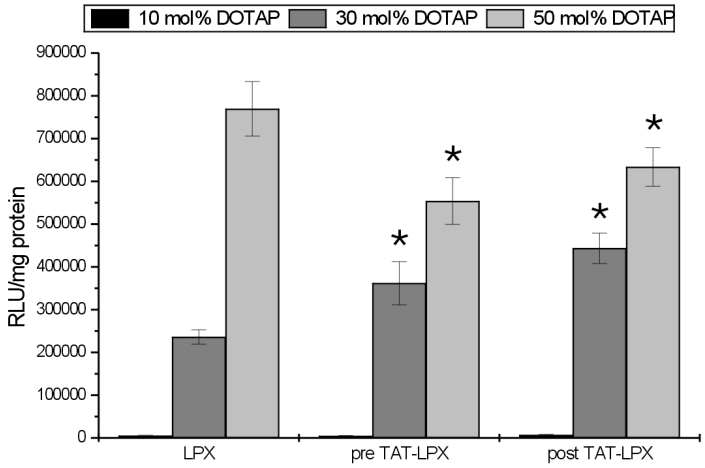

Figure 5. Transfection efficiency of the unmodified, pre and post Tat-LPX containing 10 (black), 30 (dark grey) or 50 mol% (light grey) DOTAP. Data are shown as mean ± SD and n=3. The asterix (*) represents data points that significantly differ ($p<0.05$; ANOVA) from the data of unmodified LPXs.

Fig. 5 reveals the following trends. First, the transfection capacity of the LPXs increased with increasing DOTAP content: the gene expression of the 50 mol% DOTAP LPXs without Tat peptide was 3.3-fold and with Tat peptide 1.4-fold higher than the gene expression of the corresponding 30 mol% DOTAP LPXs. Second, Tat peptide enhanced the gene expression of the 30 mol% DOTAP LPXs. 'Post Tat' modification of these LPXs gave the best results and led to a doubling of the transfection efficacy. This effect of Tat is slightly smaller than the effect of Tat seen on the gene expression of the LPXs used in the work of Torchilin et al. [42]. This may be explained by the lower initial gene expression of the LPXs in the latter work, which made it more likely that Tat could increase their gene expression. Additionally, the fact that in Torchilin's work a shorter Tat peptide was used may also explain the slight difference in gene expression. Third, Fig. 5 shows that the Tat peptide could not further enhance the gene transfer capacity of the (well transfecting) 50 mol% DOTAP LPXs. The 'post modification' of the 30 mol% DOTAP LPXs with Tat gave also slightly higher transfection efficiencies compared to the 'pre modification'. This may indicate that the preceding attachment of Tat to the liposomes complicated an efficient complexation of the pDNA. Finally, the unmodified 10 mol% DOTAP LPXs did not transfect the cells, which is explained by their poor DNA binding capacity (see Fig. 2). Also Tat-modified 10 mol% LPXs showed low transfection efficiency despite the reduced amount of free DNA caused by electrostatic binding of the Tat peptides to the free pDNA. However, we (unpublished data) and others have shown [43,44] that such Tat/pDNA complexes do not posses significant gene transfer capacities. Consequently, this explains why addition of Tat peptides to the 10 mol% DOTAP LPXs did not enhance their gene expression. Considering the low gene expression of the 10 mol% LPXs we decided to exclude them in our further work.

Tat peptide modified LPXs enter Cos-7 cells in an energy dependent manner and turn up in acidic vesicles

The ability of Tat peptides to enhance the uptake of liposomes and other types of nanoparticles was demonstrated by several groups at the beginning of this millennium [29,30,43,45]. Later on, Torchilin et al. [42] showed that the cellular uptake and gene expression of LPXs was also enhanced when Tat peptides were coupled to their surface. In all these reports it was proposed that the Tat-modified particles penetrate the cell membrane in an energy independent manner. In contrast, Fretz et al. [31] showed that OVCAR cells internalize Tat peptide modified liposomes by energy dependent endocytosis. To determine whether the Tat-modified LPXs under investigation in this study follow an energy dependent or independent pathway, we focused on the cellular uptake of FITC-labelled LPXs at 4°C and 37°C by confocal scanning fluorescence microscope (Fig. 6). To elucidate whether the LPXs end-up in acidic vesicles, the cells were pre-incubated with LysoTracker® Red, a compound known to localize primarily in the acidic compartments of cells [46]. The experiments were performed using living cells, as previous reports have shown that cell fixation may lead to an artificial uptake of Tat-modified proteins [18].

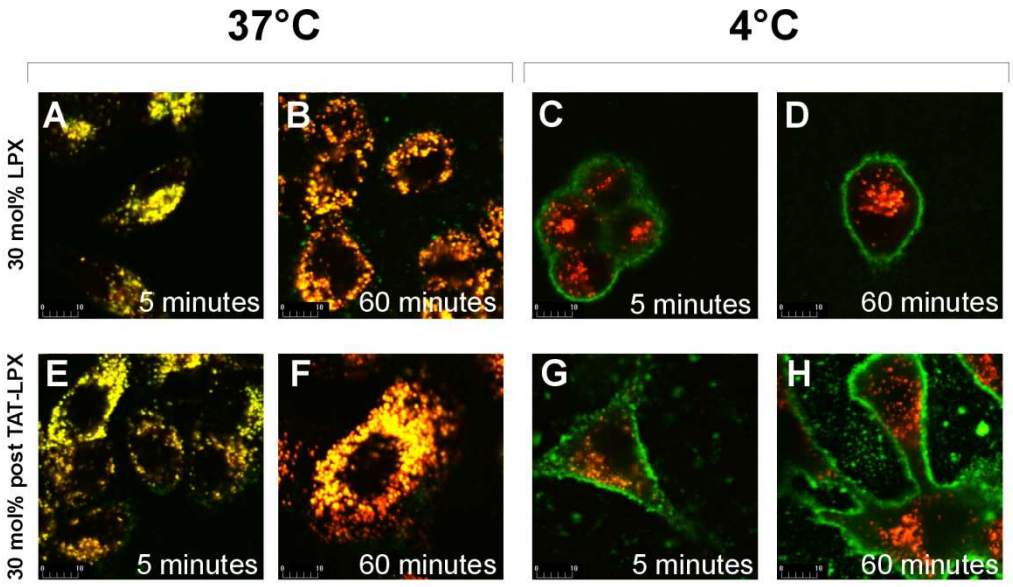

Figure 6. Confocal laser scanning microscopy images of FITC-labeled unmodified and Tat-modified LPXs (containing 30 mol% DOTAP) incubated with the cells at 37°C (A, B, E and F) and at 4°C (C, D, G and H). The red fluorescence in the cells originates from LysoTracker® Red. Yellow indicates co-localization of the green fluorescent from the LPXs with the red fluorescence from the Lysotracker® Red. Scale bar represents 10 µm. Similar results were obtained with the 50 mol% DOTAP LPXs.

Fig. 6A, 6B, 6E and 6F show that after incubation at 37°C, both the unmodified and Tat peptide modified LPXs were rapidly (even within 5 min) taken up by the cells. However, at 4°C the uptake was negligible for both types of LPXs (Fig. 6C, 6D, 6G and 6H). In contrast to previous reports

this clearly demonstrates that the uptake of the Tat-modified LPXs occurs, like for unmodified LPXs, via an energy-dependent process. To further confirm the energy dependency of the cellular uptake of the LPXs, we performed transfection experiments at 4°C. As expected from the data above, gene expression of both the Tat-modified and unmodified LPXs was reduced to about 3 % of the gene expression measured at 37°C (data not shown).

Both the Tat-modified and the unmodified LPXs appeared in the cells in a punctuated pattern and strongly co-localized with LysoTracker®, a marker of acidic organelles (Fig. 6A, 6B, 6E and 6F). This implies that the LPXs were most likely internalized via a clathrin-mediated pathway as lysosomes are the end point of a clathrin-mediated rather than a lipid raft-mediated internalization pathway. Additionally, the very fast internalization observed for the LPXs, is also typical for a clathrin-mediated uptake mechanism [47-49]. To further strengthen this conclusion we subsequently studied the effect of specific inhibitors of clathrin- and lipid raft-mediated endocytosis on the cellular uptake and gene expression of the LPXs. The fact that at least a portion of our LPXs turns up in lysosomes may be surprising as they contain DOPE, a helper lipid that is known to promote the endosomal escape of DNA and hence to avoid degradation of the pDNA by lysosomal enzymes [50-52].

Cholesterol-dependent clathrin-mediated endocytosis is the productive route for gene expression of Tat-modified and unmodified LPXs

Cells can internalize extracellular material via several mechanisms. The best characterized is the clathrin-coated pits pathway, which leads to intracellular vesicles that can either recycle back to the cell membrane or move, while they undergo a gradual acidification, along the microtubili to the perinuclear region [53]. Less defined are the lipid raft-mediated internalization mechanisms, among which the caveolae-mediated pathway is the best described (reviewed by [54]). Lipid rafts are dynamic regions of the plasma membrane which are enriched in cholesterol, sphingomyelin, glycolipids, GPI-anchored proteins and other membrane proteins. For caveolae-mediated uptake it is known that this pathway leads to neutral vesicles which stay after their formation near the cell surface before they are transported via the golgi apparatus to the endoplasmatic reticulum. It is obvious that the distinctive intracellular routing profile and properties of the vesicles occurring from the different pathways may either favour or disfavour non-viral gene expression. Nevertheless, the cellular pathways by which non-viral gene complexes enter mammalian cells have gained the attention of only a few groups [48,49,55]. Therefore, elucidating the entry mechanism is of interest for both the Tat-modified and unmodified LPXs.

To study the role of the clathrin- and lipid raft-mediated endocytosis in the uptake and gene expression of Tat-modified and unmodified LPXs, we performed transfection experiments in the

presence of a specific inhibitor of respectively clathrin-mediated (i.e. chlorpromazine) [35] and lipid raft-mediated endocytosis (i.e. filipin) [36]. Chlorpromazine is an amphiphilic drug that prevents the recycling of clathrin proteins from formed endosomes back to the cell membrane and inhibits in this manner the formation of new clathrin-coated pits. On the other hand, filipin binds strongly to cholesterol which is especially present in the lipid raft domains of the cell membrane, which will prevent lipid raft-mediated endocytosis. However, also other entry pathways may be inhibited as cholesterol is present all over the cell membrane.

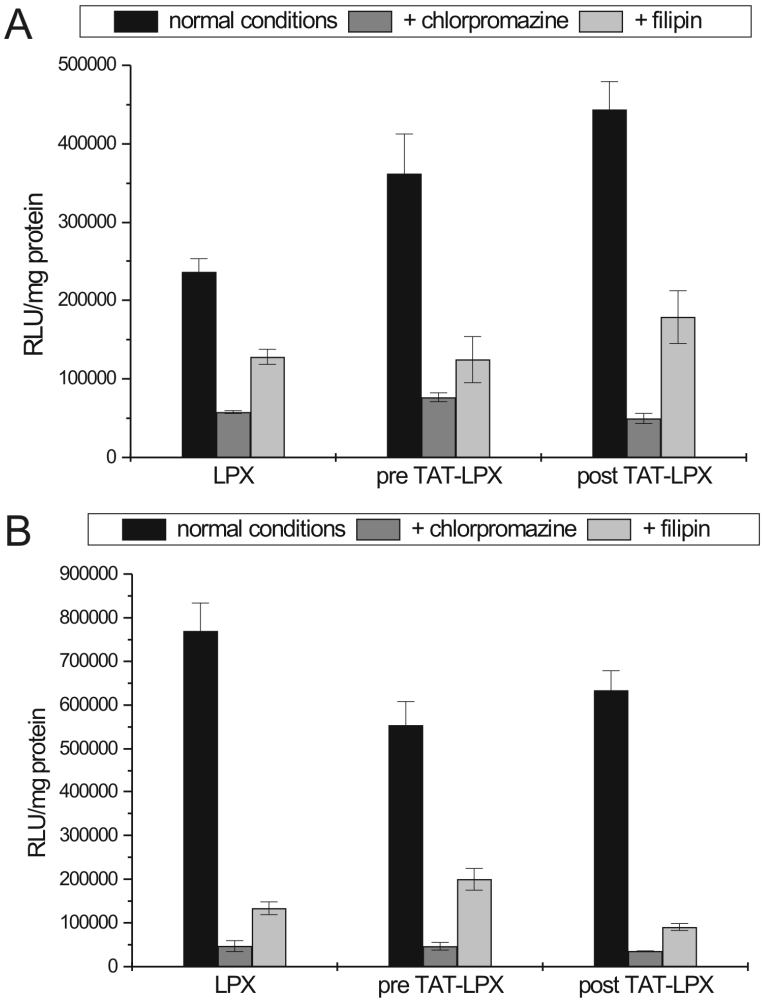

Figure 7. Transfection efficiency of the unmodified, pre Tat- and post Tat-LPX containing 30 mol% (A) or 50 mol% (B) DOTAP in the absence or presence of uptake inhibitors chlorpromazine and filipin. Data are shown as mean ± SD and n=3.

The gene expression of the Tat-modified and unmodified LPXs in the presence of chlorpromazine and filipin is shown in Fig. 7. Chlorpromazine significantly ($p < 0.05$; ANOVA) inhibits the gene expression of the 30 mol% (>86 % inhibition) and the 50 mol% (>92 % inhibition) DOTAP LPXs. Surprisingly, also filipin lowered the gene expression of both the Tat-modified and unmodified

LPXs significantly ($p<0.05$; ANOVA): the inhibition ranged between 46 % (for the unmodified LPXs) and 66 % (for the Tat-modified LPXs). The effect of filipin on the gene expression was significant lower ($p<0.05$; ANOVA) than the effect of chlorpromazine. In the light of the clear indications for a clathrin-mediated uptake mechanism of our LPXs (i.e. fast internalization and co-localization with acidic organelles), we suspect that the effect of filipin is due to its limited selectivity. Indeed, as cholesterol is required for the formation of curved coated pits [56,57] the binding of filipin to cholesterol might consequently also inhibit clathrin-mediated endocytosis. This hypothesis is in agreement with the work of Zuhorn et al. [49] who showed that depletion of cell membrane cholesterol by methyl-β-cyclodextrin, a compound previously proposed to selectively inhibit caveolae-mediated endocytosis [58,59], strongly inhibited cholesterol-dependent clathrin-mediated endocytosis of LPXs by Cos-7 cells. Therefore, we speculate here that our LPXs are internalized via cholesterol-dependent clathrin-mediated endocytosis and that this entry mechanism is also sensitive to filipin. However, we have to remark that we cannot totally exclude from our data that a small portion of the LPXs are also taken up via caveolae-mediated endocytosis.

It has been shown that the entry mechanism may depend on the size of the nanoparticles. Indeed, polystyrene nanoparticles with a diameter less than 200 nm were exclusively internalized via clathrin-coated pits, whereas those of 500 nm entered the cells via caveolae [47]. The average diameter of our LPXs, as determined by DLS, was around 300 nm. However, the size distribution of these LPXs typically ranged between 100 and 350 nm, with more than 70 % of the LPXs having a diameter smaller than 200 nm. Therefore, from the size of the LPXs a clathrin-mediated endocytosis pathway and to a lesser extend a caveolae-mediated pathway could be expected.

Finally, fluorescence confocal microscopy experiments showed a nice correlation between the decrease in gene expression caused by chlorpromazine or filipin and the amount of internalized LPXs in the presence of the respective uptake inhibitors (Fig. 8). In normal conditions (Fig. 8A and 8B), the 30 mol% LPXs clearly co-localize with the lysosomes, while the presence of chlorpromazine (Fig. 8C and 8D) almost completely blocks the co-localization. In contrast, filipin (Fig. 8E and 8F) partially inhibits the uptake of the complexes. Similar results were obtained with the 50 mol% LPXs.

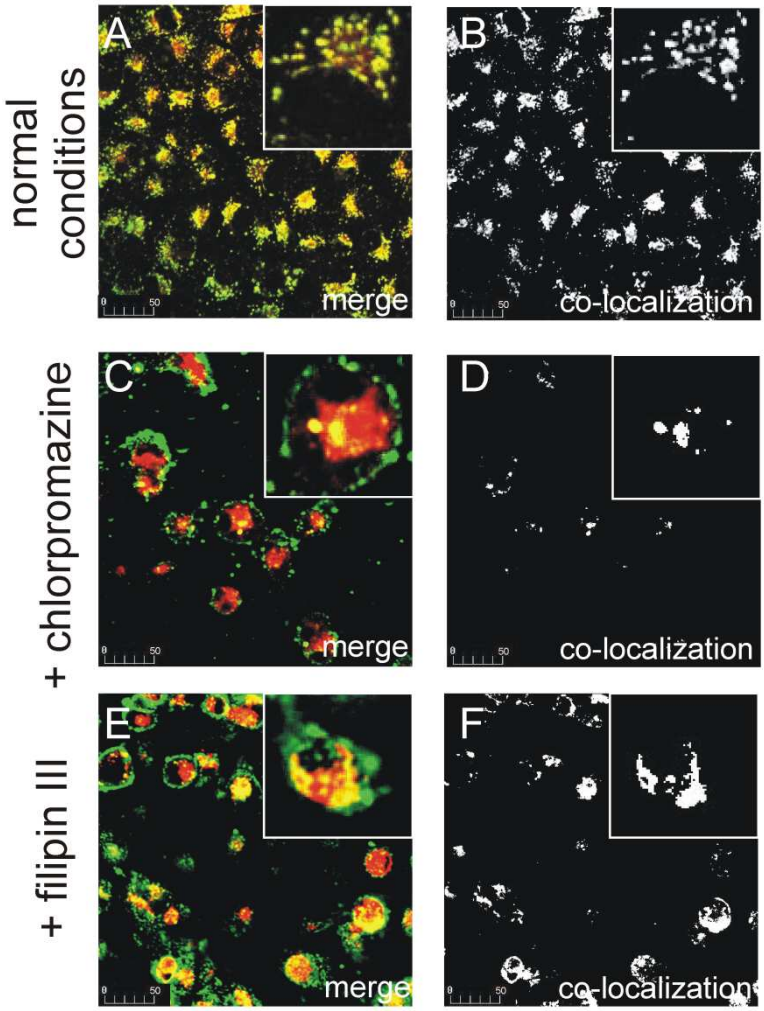

Figure 8. Confocal laser scanning microscopy images of Cos-7 cells incubated with FITC-labeled unmodified and Tat-modified 30 mol% DOTAP LPXs in normal conditions (A and B), in the presence of chlorpromazine (C and D) and in the presence of filipin (E and F). As marker of acidic organelles, LysoRed® tracker was used. The left panel (A, C and E) shows the merged images with the complexes represented as green and the lysosomes as red and the right panel (B, D, F) shows in white the co-localization of red and green signals. Scale bar represents 50 µm. The inserts show, at a higher magnification, the co-localization of LysoRed® tracker and LPXs in one cell.

CONCLUSION

In conclusion, our study shows that the gene transfer of LPXs containing 30 mol% DOTAP can be enhanced by coupling Tat peptides to their surface. Post modification of pre-formed LPXs with Tat gives the best results. In contrast, addition of Tat to LPXs containing 50 mol% DOTAP does not improve their gene transfer. In contrast to previous reports [30] we clearly demonstrate that the uptake of both Tat-modified and unmodified LPXs is energy dependent. Furthermore, by using cellular uptake inhibitors we suppose that the Tat-modified and unmodified LPXs enter the cytoplasm mainly via cholesterol-dependent clathrin-mediated endocytosis, a pathway previously postulated by Zuhorn et al. [49] for the cellular uptake of cationic LPXs.

ACKNOWLEDGMENTS

Ghent University (UG-BOF) and FWO (grant G.0310.02) are acknowledged for their support. Niek Sanders is a postdoctoral fellow of FWO (Fund for Scientific Research-Flanders). The financial support of this institute is acknowledged with gratitude.

REFERENCES

(1) Wiethoff C.M. & Middaugh C.R. Barriers to nonviral gene delivery. *J. Pharm. Sci.* **2003** 92(2) 203-217.

(2) Zuhorn I.S. & Hoekstra D. On the mechanism of cationic amphiphile-mediated transfection. To fuse or not to fuse: is that the question? *J. Membr. Biol.* **2002** 189(3) 167-179.

(3) Cho Y.W., Kim J.D., & Park K. Polycation gene delivery systems: escape from endosomes to cytosol. *J. Pharm. Pharmacol.* **2003** 55(6) 721-734.

(4) Carlisle R.C. Use of adenovirus proteins to enhance the transfection activity of synthetic gene delivery systems. *Curr. Opin. Mol. Ther.* **2002** 4(4) 306-312.

(5) Clamme J.P., Krishnamoorthy G., & Mely Y. Intracellular dynamics of the gene delivery vehicle polyethylenimine during transfection: investigation by two-photon fluorescence correlation spectroscopy. *Biochim. Biophys. Acta* **2003** 1617(1-2) 52-61.

(6) Frankel A.D. & Pabo C.O. Cellular uptake of the tat protein from human immunodeficiency virus. *Cell* **1988** 55(6) 1189-1193.

(7) Mann D.A. & Frankel A.D. Endocytosis and targeting of exogenous HIV-1 Tat protein. *EMBO J.* **1991** 10(7) 1733-1739.

(8) Trehin R. & Merkle H.P. Chances and pitfalls of cell penetrating peptides for cellular drug delivery. *Eur. J. Pharm. Biopharm.* **2004** 58(2) 209-223.

(9) Brooks H., Lebleu B., & Vives E. Tat peptide-mediated cellular delivery: back to basics. *Adv. Drug Deliv. Rev.* **2005** 57(4) 559-577.

(10) Gupta B., Levchenko T.S., & Torchilin V.P. Intracellular delivery of large molecules and small particles by cell-penetrating proteins and peptides. *Adv. Drug Deliv. Rev.* **2005** 57(4) 637-651.

(11) Vives E., Brodin P., & Lebleu B. A truncated HIV-1 Tat protein basic domain rapidly translocates through the plasma membrane and accumulates in the cell nucleus. *J. Biol. Chem.* **1997** 272(25) 16010-16017.

(12) Efthymiadis A., Briggs L.J., & Jans D.A. The HIV-1 Tat nuclear localization sequence confers novel nuclear import properties. *J. Biol. Chem.* **1998** 273(3) 1623-1628.

(13) Suzuki T., Futaki S., Niwa M., Tanaka S., Ueda K., & Sugiura Y. Possible existence of common internalization mechanisms among arginine-rich peptides. *J. Biol. Chem.* **2002** 277(4) 2437-2443.

(14) Wadia J.S., Stan R.V., & Dowdy S.F. Transducible TAT-HA fusogenic peptide enhances escape of TAT-fusion proteins after lipid raft macropinocytosis. *Nat. Med.* **2004** 10(3) 310-315.

(15) Schwarze S.R. & Dowdy S.F. In vivo protein transduction: intracellular delivery of biologically active proteins, compounds and DNA. *Trends Pharmacol. Sci.* **2000** 21(2) 45-48.

(16) Derossi D., Calvet S., Trembleau A., Brunissen A., Chassaing G., & Prochiantz A. Cell internalization of the third helix of the Antennapedia homeodomain is receptor-independent. *J. Biol. Chem.* **1996** 271(30) 18188-18193.

(17) Mi Z., Mai J., Lu X., & Robbins P.D. Characterization of a class of cationic peptides able to facilitate efficient protein transduction in vitro and in vivo. *Mol. Ther.* **2000** 2(4) 339-347.

(18) Lundberg M. & Johansson M. Positively charged DNA-binding proteins cause apparent cell membrane translocation. *Biochem. Biophys. Res. Commun.* **2002** 291(2) 367-371.

(19) Futaki S. Oligoarginine vectors for intracellular delivery: design and cellular-uptake mechanisms. *Biopolymers* **2006** 84(3) 241-249.

(20) Fischer R., Kohler K., Fotin-Mleczek M., & Brock R. A stepwise dissection of the intracellular fate of cationic cell-penetrating peptides. *J. Biol. Chem.* **2004** 279(13) 12625-12635.

(21) Potocky T.B., Menon A.K., & Gellman S.H. Cytoplasmic and nuclear delivery of a TAT-derived peptide and a beta-peptide after endocytic uptake into HeLa cells. *J. Biol. Chem.* **2003** 278(50) 50188-50194.

(22) Richard J.P., Melikov K., Brooks H., Prevot P., Lebleu B., & Chernomordik L.V. Cellular Uptake of Unconjugated TAT Peptide Involves Clathrin-dependent Endocytosis and Heparan Sulfate Receptors. *J. Biol. Chem.* **2005** 280(15) 15300-15306.

(23) Vendeville A., Rayne F., Bonhoure A., Bettache N., Montcourrier P., & Beaumelle B. HIV-1 Tat enters T cells using coated pits before translocating from acidified endosomes and eliciting biological responses. *Mol. Biol. Cell* **2004** 15(5) 2347-2360.

(24) Eguchi A., Akuta T., Okuyama H. *et al.* Protein transduction domain of HIV-1 Tat protein promotes efficient delivery of DNA into mammalian cells. *J. Biol. Chem.* **2001** 276(28) 26204-26210.

(25) Ferrari A., Pellegrini V., Arcangeli C., Fittipaldi A., Giacca M., & Beltram F. Caveolae-mediated internalization of extracellular HIV-1 tat fusion proteins visualized in real time. *Mol. Ther.* **2003** 8(2) 284-294.

(26) Fittipaldi A., Ferrari A., Zoppe M. *et al.* Cell membrane lipid rafts mediate caveolar endocytosis of HIV-1 Tat fusion proteins. *J. Biol. Chem.* **2003** 278(36) 34141-34149.

(27) Renigunta A., Krasteva G., Konig P. *et al.* DNA transfer into human lung cells is improved with Tat-RGD peptide by caveoli-mediated endocytosis. *Bioconjug. Chem.* **2006** 17(2) 327-334.

(28) Kaplan I.M., Wadia J.S., & Dowdy S.F. Cationic TAT peptide transduction domain enters cells by macropinocytosis. *J. Control Release* **2005** 102(1) 247-253.

(29) Lewin M., Carlesso N., Tung C.H. *et al.* Tat peptide-derivatized magnetic nanoparticles allow in vivo tracking and recovery of progenitor cells. *Nat. Biotechnol.* **2000** 18(4) 410-414.

(30) Torchilin V.P., Rammohan R., Weissig V., & Levchenko T.S. TAT peptide on the surface of liposomes affords their efficient intracellular delivery even at low temperature and in the presence of metabolic inhibitors. *Proc. Natl. Acad. Sci. U. S. A* **2001** 98(15) 8786-8791.

(31) Fretz M.M., Koning G.A., Mastrobattista E., Jiskoot W., & Storm G. OVCAR-3 cells internalize TAT-peptide modified liposomes by endocytosis. *Biochim. Biophys. Acta* **2004** 1665(1-2) 48-56.

(32) Torchilin V.P. & Levchenko T.S. TAT-liposomes: a novel intracellular drug carrier. *Curr. Protein Pept. Sci.* **2003** 4(2) 133-140.

(33) Torchilin V.P., Levchenko T.S., Rammohan R., Volodina N., Papahadjopoulos-Sternberg B., & D'Souza G.G. Cell transfection in vitro and in vivo with nontoxic TAT peptide-liposome-DNA complexes. *Proc. Natl. Acad. Sci. U. S. A* **2003** 100(4) 1972-1977.

(34) Sanders N.N., Van Rompaey E., De Smedt S.C., & Demeester J. Structural alterations of gene complexes by cystic fibrosis sputum. *Am. J. Respir. Crit Care Med.* **2001** 164(3) 486-493.

(35) Wang L.H., Rothberg K.G., & Anderson R.G. Mis-assembly of clathrin lattices on endosomes reveals a regulatory switch for coated pit formation. *J. Cell Biol.* **1993** 123(5) 1107-1117.

(36) Schnitzer J.E., Oh P., Pinney E., & Allard J. Filipin-sensitive caveolae-mediated transport in endothelium: reduced transcytosis, scavenger endocytosis, and capillary permeability of select macromolecules. *J. Cell Biol.* **1994** 127(5) 1217-1232.

(37) von Gersdorff K., Sanders N.N., Vandenbroucke R., De Smedt S.C., Wagner E., & Ogris M. The Internalization Route Resulting in Successful Gene Expression Depends on both Cell Line and Polyethylenimine Polyplex Type. *Mol. Ther.* **2006** 14(5) 745-753.

(38) Brooks H., Lebleu B., & Vives E. Tat peptide-mediated cellular delivery: back to basics. *Adv. Drug Deliv. Rev.* **2005** 57(4) 559-577.

(39) Vives E., Brodin P., & Lebleu B. A truncated HIV-1 Tat protein basic domain rapidly translocates through the plasma membrane and accumulates in the cell nucleus. *J. Biol. Chem.* **1997** 272(25) 16010-16017.

(40) Sabatier J.M., Vives E., Mabrouk K. *et al.* Evidence for neurotoxic activity of tat from human immunodeficiency virus type 1. *J. Virol.* **1991** 65(2) 961-967.

(41) Guo X. & Szoka F.C., Jr. Steric stabilization of fusogenic liposomes by a low-pH sensitive PEG--diortho ester--lipid conjugate. *Bioconjug. Chem.* **2001** 12(2) 291-300.

(42) Torchilin V.P. Fluorescence microscopy to follow the targeting of liposomes and micelles to cells and their intracellular fate. *Adv. Drug Deliv. Rev.* **2005** 57(1) 95-109.

(43) Hyndman L., Lemoine J.L., Huang L., Porteous D.J., Boyd A.C., & Nan X. HIV-1 Tat protein transduction domain peptide facilitates gene transfer in combination with cationic liposomes. *J. Control Release* **2004** 99(3) 435-444.

(44) Siprashvili Z., Scholl F.A., Oliver S.F. *et al.* Gene transfer via reversible plasmid condensation with cysteine-flanked, internally spaced arginine-rich peptides. *Hum. Gene Ther.* **2003** 14(13) 1225-1233.

(45) Tseng Y.L., Liu J.J., & Hong R.L. Translocation of liposomes into cancer cells by cell-penetrating peptides penetratin and tat: a kinetic and efficacy study. *Mol. Pharmacol.* **2002** 62(4) 864-872.

(46) Olson F., Hunt C.A., Szoka F.C., Vail W.J., & Papahadjopoulos D. Preparation of liposomes of defined size distribution by extrusion through polycarbonate membranes. *Biochim. Biophys. Acta* **1979** 557(1) 9-23.

(47) Rejman J., Oberle V., Zuhorn I.S., & Hoekstra D. Size-dependent internalization of particles via the pathways of clathrin- and caveolae-mediated endocytosis. *Biochem. J.* **2004** 377(Pt 1) 159-169.

(48) Rejman J., Bragonzi A., & Conese M. Role of clathrin- and caveolae-mediated endocytosis in gene transfer mediated by lipo- and polyplexes. *Mol. Ther.* **2005** 12(3) 468-474.

(49) Zuhorn I.S., Kalicharan R., & Hoekstra D. Lipoplex-mediated transfection of mammalian cells occurs through the cholesterol-dependent clathrin-mediated pathway of endocytosis. *J. Biol. Chem.* **2002** 277(20) 18021-18028.

(50) Farhood H., Serbina N., & Huang L. The role of dioleoyl phosphatidylethanolamine in cationic liposome mediated gene transfer. *Biochim. Biophys. Acta* **1995** 1235(2) 289-295.

(51) Wrobel I. & Collins D. Fusion of cationic liposomes with mammalian cells occurs after endocytosis. *Biochim. Biophys. Acta* **1995** 1235(2) 296-304.

(52) Zhou X. & Huang L. DNA transfection mediated by cationic liposomes containing lipopolylysine: characterization and mechanism of action. *Biochim. Biophys. Acta* **1994** 1189(2) 195-203.

(53) Schmid S.L. Clathrin-coated vesicle formation and protein sorting: an integrated process. *Annu. Rev. Biochem.* **1997** 66511-548.

(54) Nichols B. Caveosomes and endocytosis of lipid rafts. *J. Cell Sci.* **2003** 116(Pt 23) 4707-4714.

(55) Goncalves C., Mennesson E., Fuchs R., Gorvel J.P., Midoux P., & Pichon C. Macropinocytosis of polyplexes and recycling of plasmid via the clathrin-dependent pathway impair the transfection efficiency of human hepatocarcinoma cells. *Mol. Ther.* **2004** 10(2) 373-385.

(56) Mousavi S.A., Malerod L., Berg T., & Kjeken R. Clathrin-dependent endocytosis. *Biochem. J.* **2004** 377(Pt 1) 1-16.

(57) Subtil A., Gaidarov I., Kobylarz K., Lampson M.A., Keen J.H., & McGraw T.E. Acute cholesterol depletion inhibits clathrin-coated pit budding. *Proc. Natl. Acad. Sci. U. S. A* **1999** 96(12) 6775-6780.

(58) Rothberg K.G., Heuser J.E., Donzell W.C., Ying Y.S., Glenney J.R., & Anderson R.G. Caveolin, a protein component of caveolae membrane coats. *Cell* **1992** 68(4) 673-682.

(59) Sieczkarski S.B. & Whittaker G.R. Dissecting virus entry via endocytosis. *J. Gen. Virol.* **2002** 83(Pt 7) 1535-1545.

Chapter 3

Ultrasound Assisted siRNA Delivery using PEG-siPlex Loaded Microbubbles

This chapter is published:

Roosmarijn E. Vandenbroucke[1], Ine Lentacker[1], Joseph Demeester[1], Stefaan C. De Smedt[1] and Niek N. Sanders[1]; *Journal of Controlled Release.* 2008 Mar 20;126(3):265-73

[1] Laboratory of General Biochemistry and Physical Pharmacy, Department of Pharmaceutics Ghent University, Ghent, Belgium.

ABSTRACT

Short interfering RNA (siRNA) attracts much attention for the treatment of various diseases. However, its delivery, especially via systemic routes, remains a challenge. Indeed, naked siRNAs are rapidly degraded, while complexed siRNAs massively aggregate in the blood or are captured by macrophages. Although this can be circumvented by PEGylation, we found that PEGylation had a strong negative effect on the gene silencing efficiency of siRNA-liposome complexes (siPlexes). Recently, ultrasound combined with microbubbles has been used to deliver naked siRNA but the gene silencing efficiency is rather low and very high amounts of siRNA are required. To overcome the negative effects of PEGylation and to enhance the efficiency of ultrasound assisted siRNA delivery, we coupled PEGylated siPlexes (PEG-siPlexes) to microbubbles. Ultrasound radiation of these microbubbles resulted in massive release of unaltered PEG-siPlexes. Interestingly, PEG-siPlexes loaded on microbubbles were able to enter cells after exposure to ultrasound, in contrast to free PEG-siPlexes, which were not able to enter cells rapidly. Furthermore, these PEG-siPlex loaded microbubbles induced, in the presence of ultrasound, much higher gene silencing than free PEG-siPlexes. Additionally, the PEG-siPlex loaded microbubbles only silenced the expression of genes in the presence of ultrasound, which allows space and time controlled gene silencing.

Chapter 3

Ultrasound Assisted siRNA Delivery using PEG-siPlex Loaded Microbubbles

INTRODUCTION

RNA interference (RNAi), a naturally occurring process of sequence-specific post-transcriptional gene silencing, is an important biological process for modulating gene expression. The silencing effect of RNAi is highly potent and requires only that the sequence of the target RNA is known. One approach to evoke RNAi in target cells is by the delivery of chemically synthesized siRNAs, which results in a sequence-specific, robust silencing of the targeted gene [1]. The potential of siRNA molecules as therapeutic agent in the treatment of e.g. cancer, viral infections, arthritis, Huntington's disease and hypercholesterolemia has been widely studied [2]. However, cells do not readily take up siRNAs. Therefore, clinical applications of siRNA largely depend on the development of delivery systems that can bring intact siRNA into the cytoplasm of the target cells of a patient.

Strategies that have been considered for *in vivo* delivery of synthetic siRNA in laboratory animals are hydrodynamic injection of naked siRNA [3] or siRNA conjugates [4], electroporation [5-8] and the use of cationic carriers [9-15]. However, several aspects limit the applicability of these methods in humans. Indeed, hydrodynamic injection, which involves the intravascular injection of large volumes, generates high pressure in the vascular system and therefore often results in heart failure. Additionally, undesirable gene suppression may be induced in non-target organs. Electroporation allows targeting, but requires the insertion of electrodes into the target area, and hence invasive procedures that limit its range of application. Cationic siRNA delivery carriers, such as cationic lipids and polymers, are often cytotoxic and/or not very efficient. Furthermore, they are often not suited for systemic application since their positively charged surface makes them vulnerable to non-specific interactions with blood compounds, leading to life-threatening aggregates and a rapid clearance by the mononuclear phagocyte system [10,16]. A common approach for reducing these undesired interactions is by masking the cationic surface of the nanoparticles with hydrophilic polymers, such as poly(ethylene glycol) (PEG). This prevents the aggregation of these nucleic acid containing

nanoparticles in blood and prolongs their circulation time [17-20]. However, it has been observed by many groups that shielding the surface of non-viral gene delivery systems with polymers like PEG leads to a drastic reduction in gene transfer, due to a reduced cellular uptake or limited endosomal release [21,22].

The use of ultrasound energy has intensively been studied for pDNA delivery [23-30]. Recently, ultrasound in combination with microbubbles has also been used in two reports to deliver naked siRNA [31,32]. However, the gene silencing efficiency in these studies was rather low and very high amounts of siRNA were required. Nevertheless, ultrasound assisted drug delivery is considered as rather safe as ultrasound, in combination with microbubbles, is routinely used in the clinic for diagnostic purposes. It is believed that ultrasound, especially when combined with microbubbles, causes small (100 to a few 100 nm large) transient pores in the cell membrane which allows large molecules to enter the cell cytoplasm [33]. These perforations are caused by microjets that are generated by the ultrasound induced cavitation, i.e. alternate growing and shrinking of microbubbles, and implosion of microbubbles. The lifetime of these pores in the cell membranes is very short, i.e. milliseconds to seconds [34], making high concentrations of nucleic acids in the surrounding of the cells beneficial to ensure that a significant amount of nucleic acids can enter the cells through these short-living pores. Consequently, as recently shown by our group for pDNA, microbubbles that at the same time perforate cells and release massive amounts of nucleic acids containing nanoparticles near these perforations may drastically enhance the cellular uptake and hence the biological activity of nucleic acids [26].

Therefore, the aim of this study was to evaluate (a) the loading and release of PEGylated siRNA-liposome complexes (PEG-siPlexes) on/off ultrasound responsive microbubble, and (b) the cellular distribution and gene silencing efficiency of the PEG-siPlex loaded microbubbles after ultrasound radiation.

MATERIALS & METHODS

Cell culture

HuH-7 and HuH-7_eGFPLuc cells were cultured in Dulbecco's modified Eagle's medium supplemented with F12 (DMEM:F12) containing 2 mM L-glutamine (L-Gln), 10 % heat-inactivated fetal bovine serum (FBS) and 100 U/ml penicilline/streptomycine (P/S) at 37°C in a humidified atmosphere containing 5 % CO_2. All cell culture products were purchased from Invitrogen (Merelbeke, Belgium).

HuH-7_eGFPLuc cells stably expressing eGFP-Luciferase were generated by transfecting HuH-7 cells with the vector pEGFPLuc (Clontech, Palo Alto, USA). The vector was linearized using the restriction enzyme *Dra*III and transfected using linear poly(ethyleneimine) (PEI) 22 kDa. Transfected cells were incubated in fresh medium for 72 hrs and then selected with 60 to 400 µg/ml G418. After several days, surviving cells were seeded at low densities into 6-well plates in order to generate separate colonies. Single cell clones were then isolated and expanded. The generated clones were analyzed for the percentage of GFP-positive (eGFPLuc stably transfected) cells. Clones with the highest number of GFP-positive cells were then further selectively grown up under the above described selective conditions and this procedure was repeated until all cells were positive for GFP.

SiRNA

Atto488-labeled and non labeled siRNA duplexes against firefly luciferase and control siRNA duplexes were purchased from Eurogentec (Seraing, Belgium) and dissolved in RNase free water at a final concentration of 20 µM.

Preparation and characterization of lipid microbubbles

1,2-Dipalmitoyl-sn-glycero-3-phosphocholine (DPPC) and 1,2-distearoyl-sn-glycero-3-phosphoethanolamine-N-[biotinyl(polyethylene glycol)2000] (ammonium salt) (DSPE-PEG_{2000}-biotin) were purchased from Avanti Polar Lipids (Alabaster, AL).

Lipid microbubbles were prepared from liposomes composed of DPPC and DSPE-PEG_{2000}-biotin with molar ratios of 95:5. Therefore, as described previously [35], appropriate amounts of lipids were dissolved in chloroform and mixed. The chloroform was subsequently removed by rotary evaporation at 37°C followed by flushing the obtained lipid film with nitrogen during 30 min at room temperature. The dried lipids were then hydrated by adding Hepes buffer (20 mM, pH 7.4) till a final lipid concentration of 5 mg/ml. After mixing in the presence of glass beads, liposome formation was allowed overnight at 4°C. Thereafter, the DPPC:DSPE-PEG_{2000}-biotin liposomes were extruded through two stacked 0.200 µm polycarbonate membrane filters (Whatman; Brentfort, UK) at 55°C using an Avanti Mini-Extruder (Avanti Polar Lipids). Subsequently, the liposome suspension was sonicated with a 20 kHz probe (Branson 250 sonifier, Branson Ultrasonics Corp.; Danbury, CT) in the presence of perfluorobutane gas (MW 238 g/mol; F2 chemicals; Preston, Lancashire, UK). After sonication, the lipid microbubbles were washed with 3 ml Hepes buffer by 5 min centrifugation at 470 g. The amount of microbubbels per ml was determined by light microscopy and equalled 4 x 10^8

microbubbles/ml. The size distribution of the microbubbles was determined by laser diffraction (Mastersizer S, Malvern; Worcestershire, UK).

Preparation of avidin coated lipid microbubbles

Avidinylated microbubbles were prepared by incubating them at room temperature with 500 µl avidin (10 mg/ml). After 10 min of incubation, the microbubbbles were washed with 3 ml Hepes buffer by 5 min centrifugation at 470 g and finally resuspended in 10 ml. For the preparation of red labelled lipid microbubbles, the microbubbles were incubated with the unlabelled avidin supplemented with 50 µl Cy5-labelled streptavidin (1 mg/ml) (Zymed Laboratories; San Francisco, CA).

Preparation and characterization of liposomes and PEG-siPlexes

The cationic lipid 1,2-dioleoyl-3-trimethylammonium-propane (chloride salt) (DOTAP) and the helper lipid 1,2-dioleoyl-sn-glycero-3-phosphoethanolamine (DOPE) were purchased from Avanti Polar Lipids. Cationic liposomes containing DOTAP and DOPE in a 1:1 molar ratio, supplemented with 0 to 15 mol% DSPE-PEG_{2000}-biotin, were prepared at a final DOTAP concentration of 5 mM. All liposomes were prepared as described above for the DPPC:DSPE-PEG_{2000}-biotin liposomes, however extrusion occurred through two stacked 0.100 µm polycarbonate membrane filters at room temperature. To obtain (PEG-)siPlexes, equal volumes of siRNA solution and extruded liposomes were mixed in a N:P ratio of 20:1. Subsequently, the obtained mixture was vortexed for 5 sec and incubated at room temperature for 30 min.

The average particle size and the zeta potential (ζ) of the (PEGylated) liposomes and siPlexes were measured by photon correlation spectroscopy (PCS) (Malvern zetasizer nano ZS; Malvern) and by particle electrophoresis (Malvern zetasizer nano ZS; Malvern), respectively. Therefore, the liposome and PEG-siPlex dispersions were diluted 40-fold in 20 mM Hepes buffer. The size of the liposomes was independent of the degree of PEGylation and averaged 120 nm. In contrast, the zeta potential clearly dropped with increasing degree of PEGylation, varying from ~50 mV for the 0 mol% and ~20 mV for the 5 mol% DSPE-PEG_{2000}-biotin containing DOTAP:DOPE liposomes The size and zeta potential of the siPlexes are displayed in Fig. 5.

Preparation and characterization of siPlexes loaded microbubbles

130 µl siPlex dispersion was mixed with 1 ml microbubbles, vortexed shortly and incubated at room temperature for 5 min. Subsequently, the size distribution of the siPlex loaded microbubbles was determined as described for the non-loaded microbubbles. The time-dependent stability of the (PEG-)siPLex loaded microbubbles was followed for 36 hrs at room temperature via light microscopy using a motorized Nikon TE2000-E inverted microscope (Nikon Benelux, Brussels, Belgium). The small microbubbles (< 2 µm) were stable for at least 24 hrs and the larger ones for at least 36 hrs.

Gel electrophoresis

(PEG-)siPlexes, before binding to the microbubbles and after ultrasound induced release from the microbubbles, were loaded on a native 20 % polyacrylamide gel (PAGE). All samples were supplemented with 10 % glycerol and subjected to electrophoresis at 100 V for 2 hrs. Finally, the siRNA was stained with 1:10000 diluted SYBR-green II dye (Molecular Probes; Merelbeke, Belgium) and visualized by UV transillumination.

Confocal laser scanning microscopy

The Cy5-streptavidin coated microbubbles and Atto488-siRNA containing siPlexes were visualized using a Nikon C1si confocal laser scanning module attached to a motorized Nikon TE2000-E inverted microscope (Nikon Benelux; Brussels, Belgium). Images were captured with a 60 x objective lens using the 488 nm line from an Ar-ion laser for the excitation of Atto488-siRNA and the 639 nm laser line from a diode laser for the excitation of Cy5-streptavidin.

Cellular distribution of PEG-siPlexes in HuH-7 cells

Atto488-siRNA containing PEG-siPlexes (with 5 mol% DSPE-PEG_{2000}-biotin) were prepared as described above. HuH-7 cells were grown in OptiCells™ and incubated for 20 min with the free PEG-siPlexes or with the PEG-siPlexes loaded microbubbles, immediately followed by ultrasound treatment. The ultrasound settings were the same as in the transfection experiments (see below). After one wash step with phosphate buffered saline (PBS; Invitrogen), cells were treated for 10 min with Draq5 (Biostatus Limited; Leicestershire, UK), to stain the nucleus, and TRITC-concanavalin A (Molecular Probes), to stain the cellular membrane. Subsequently, the cellular distribution of the Atto488-siRNA was visualized using a Nikon EZC1-si confocal laser scanning microscope equipped

with a 60 x objective. The 488 nm line of the Ar-ion laser was used to excite the Atto488 label and the 639 nm line from a diode laser to excite Draq5 and TRITC-concanavalin A.

Transfection experiments

HuH-7_eGFPLuc cells were seeded in OptiCell™ units (Biocrystal; Westerville, OH) at 4 x 10^4 cells/cm^2, and allowed to attach overnight in a humidified incubator at 37°C and 5 % CO_2. The culture medium was removed from the cells and after a washing step with PBS, the free siPlexes or siPlex loaded microbubbles, both dissolved in OptiMEM (Invitrogen) and containing 50 nM siRNA, were added to the OptiCell™ units. Subsequently, the OptiCell™ units were placed in a water bath at 37°C with an absorbing rubber at the bottom as shown in Fig. 1B and immediately subjected to ultrasound radiation for 10 sec with a sonitron 2000 (RichMar; Inola, OK) equipped with a 22 mm probe. It has been reported that standing waves can influence the ultrasound assisted transfection efficiency dramatically [36]. In our ultrasound set up (Fig. 1B) standing waves are eliminated as much as possible by (1) using the ultrasound transparent OptiCell™ units, (2) placing an absorbing rubber at the bottom of the water bath and (3) degassing the water. In all experiments the same ultrasound settings were applied: 1 MHz, 10 % duty cycle (DC) and an ultrasound intensity of 2 W/cm^2 during 10 sec. After 2 hrs incubation of the cells (at 37°C) with the free siPlexes or siPlex loaded microbubbles, the transfection medium was removed, cells were washed twice with PBS and culture medium was added. After 48 hrs incubation, discs (22 mm in diameter) were cut from the OptiCell™ membrane, transferred to a 24-well plate and lysed with 80 µl 1x CCLR buffer (Promega; Leiden, The Netherlands) to measure both the luciferase activity and the total protein concentration.

Luciferase activity was determined with the Promega luciferase assay kit according to the manufacturer's instructions in relative light units (RLU). Briefly, 100 µl substrate was added to 20 µl cell lysate and after a 2 sec delay, the luminescence was measured during 10 sec with a GloMax™ 96 luminometer. To correct for the amount of cells per well, the protein concentration was determined with the BCA kit (Pierce; Rockford, IL). Therefore, 200 µl mastermix, containing 50 parts reagent A to 1 part B, was mixed with 20 µl cell lysate or BSA (to make the standard curve). After 30 min incubation at 37°C, the absorbance at 590 nm was measured with a Wallac Victor^2 absorbance plate reader (Perkin Elmer; Waltham, MA).

RESULTS & DISCUSSION

Preparation and characterization of PEG-siPlex loaded microbubbles

As schematically depicted in Fig. 1A, the first goal of this work was to attach PEGylated siRNA-liposome complexes (PEG-siPlexes) to gas-filled microbubbles via a biotin-avidin-biotin bridge. Therefore, we first prepared perfluorobutane filled lipid microbubbles by sonication of a DPPC:DSPE-PEG_{2000}-biotin liposome dispersion in the presence of perfluorobutane gas. The lipid coating prevents a rapid diffusion of the perfluorobutane gas out of the microbubbles. To assure that biotin molecules were present at the outer surface of the microbubbles, we incubated them with Cy5 labelled streptavidin. As shown by the confocal images in Fig. 2A and 2B, after removal of the unbound streptavidin, a thin fluorescent layer of streptavidin molecules surrounding the gas-filled microbubbles could be observed, which indicates the formation of biotin-avidin linkages. This suggests that the DSPE- PEG_{2000}-biotin molecules in the lipid shell are oriented with their hydrophobic tails to the perfluorobutane gas core while their hydrophilic head groups are exposed to the surrounding aqueous medium, as previously suggested by Unger [37].

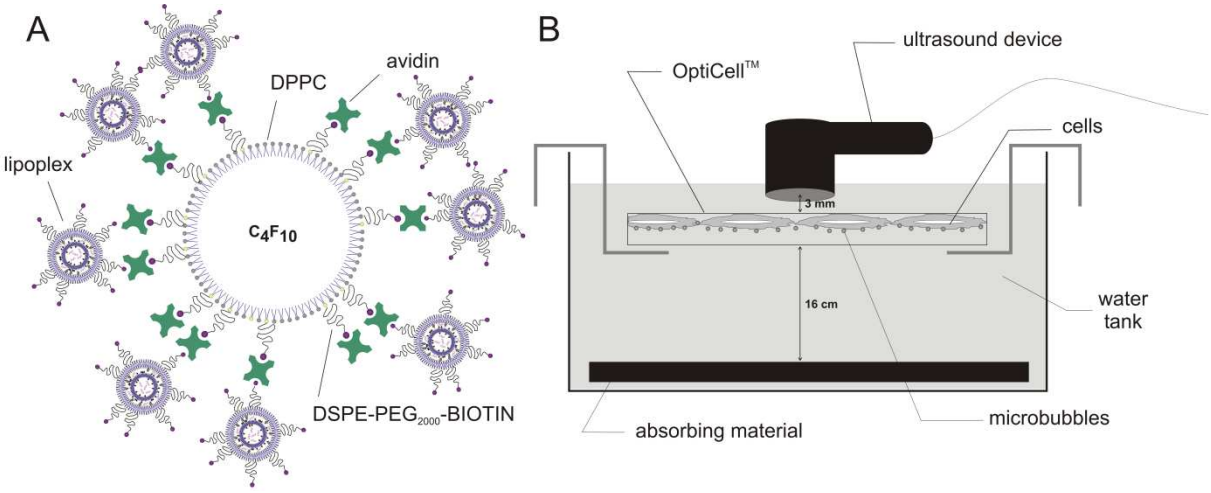

Figure 1. (A) Schematic overview of a PEG-siPlex loaded microbubble. The white disk surrounded by lipids (95 mol% DPPC and 5 mol% DSPE-PEG_{2000}-biotin) represents an avidinylated lipid microbubble with its perfluorobutane (C_4F_{10}) gas core. PEG-siPlexes with increasing amounts of DSPE-PEG_{2000}-biotin were attached to these avidinylated microbubbles via a biotin-avidin-biotin bridge. (B) Experimental setup used in the transfection experiments. An OptiCell™ unit containing a monolayer of HuH-7 cells on one of their membranes was placed in a water tank with a rubber plate, designed to minimize ultrasound reflection or scattering, at the bottom. In all experiments the same ultrasound settings were applied: 10 sec, 1 MHz, 10 % duty cycle and an ultrasound intensity of 2 W/cm^2. The ultrasound was delivered vertically to the cells which were present on the upper membrane of the OptiCell™ unit, closest to the ultrasound probe. Different regions of the OptiCell™ unit were sonicated separately by moving the ultrasound device.

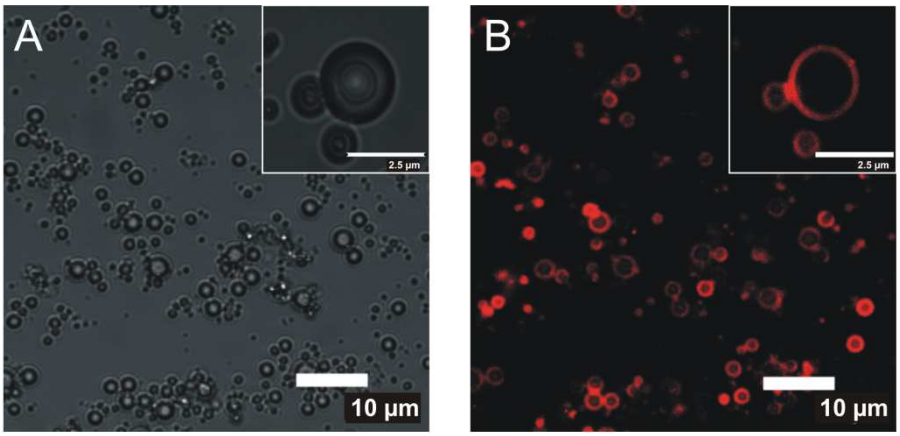

Figure 2. Transmission image (A) and confocal laser scanning microscopy image (B) of avidinylated microbubbles coated with Cy5-streptavidin (red). The inserts display a close-up of three microbubbles.

In a next step, we prepared DOTAP:DOPE based siPlexes containing increasing amounts of DSPE-PEG_{2000}-biotin (0, 2, 5 and 15 mol%). In all cases, a N:P ratio of 20:1 was chosen as non-PEGylated siPlexes showed at this ratio the highest gene silencing effect in HuH-7 cells (data not shown). The ability of the siPlexes to bind siRNA was analyzed by PAGE (Fig. 3A). In case of the 0, 2 and 5 mol% DSPE-PEG_{2000}-biotin containing siPlexes, no free siRNA could be detected. This implies that all the siRNA is complexed with the liposomes, which are too large to migrate into the gel network. In contrast, a smear of siRNA was observed in case of the 15 mol% PEG-siPlexes, indicating only a partial siRNA complexation in these siPlexes.

Subsequently, the ability of the different siPlexes to bind to the surface of the biotinylated microbubbles was tested. Therefore, the biotinylated microbubbles were first incubated with avidin. An excess of avidin was used to avoid massive clustering of the microbubbles, due to avidin mediated bridging. After removal of the unbound avidin, siPlexes, containing Atto488 labelled siRNA, were added to the avidinylated microbubbles. The confocal images in Fig. 3B till 3E show that the amount of DSPE-PEG_{2000}-biotin in the siPlexes clearly influences to which extent the microbubble surface becomes covered with siPlexes. Non-PEGylated siPlexes (Fig. 3B), thus not containing DSPE-PEG_{2000}-biotin, only showed some non-specific binding to the avidinylated microbubbles. In contrast, the PEGylated siPlexes, containing DSPE-PEG_{2000}-biotin, clearly bound to the avidinylated surface of the microbubbles. The surface of the microbubbles became only partially covered with siPlexes containing 2 mol% DSPE-PEG_{2000}-biotin (Fig. 3C), probably due to the limited degree of biotinylation of the siPlexes. In contrast, the microbubble surface was almost completely coated with siPlexes when they contained 5 mol% DSPE-PEG_{2000}-biotin (Fig. 3D). The 15 mol% containing PEG-siPlexes also showed an efficient coating of the surface of the microbubbles. However, as these siPlexes showed

incomplete complexation of the siRNA, previously shown by gel electrophoresis experiments (Fig. 3A, lane 5), these siPlexes were further excluded from the study.

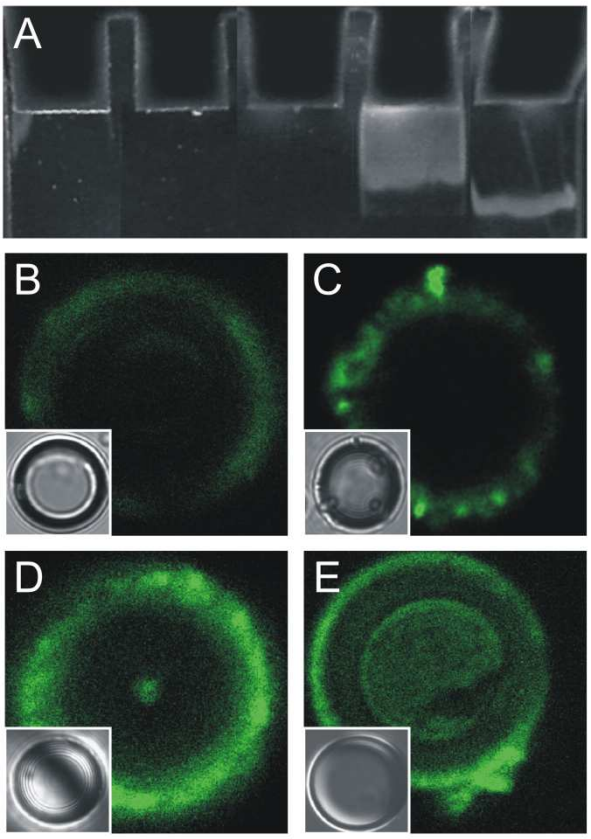

Figure 3. (A) Polyacrylamide gel after electrophoresis of siPlexes containing 0 mol% (lane 1), 2 mol% (lane 2), 5 mol% (lane 3) and 15 mol% DSPE-PEG_{2000}-biotin (lane 4) before attachment to the microbubbles. As a reference, free siRNA was loaded in lane 5 and each lane contains 0.3 µg siRNA. (B-E) Confocal laser scanning microscopy images and corresponding transmission images (inserts) of avidinylated microbubbles incubated with siPlexes containing 0 mol% (B), 2 mol% (C), 5 mol% (D) and 15 mol% DSPE-PEG_{2000}-biotin (E). The siPlexes were visualized by using Atto488-siRNA.

Subsequently we studied the size distribution of the siPlex coated microbubbles by laser diffraction to assure that the microbubbles had the optimal size distribution for cavitation. Fig. 4 shows the size distribution of microbubbles incubated with non-PEGylated siPlexes and microbubbles loaded with PEGylated siPlexes. In both cases, the diameter of the microbubbles varied between 0,5 and 10 µm, which is an appropriate size to favour cavitation upon exposure to clinically relevant ultrasound energy. Fig. 4 (arrow) also shows a significant amount of sub-micron particles in case of the non-PEGylated siPlexes, indicating the presence of non bound siPlexes. In contrast, this sub-micron peak was not visible in case of the microbubbles loaded with PEGylated siPlexes (Fig. 4, grey circles). These results are in agreement with the confocal images shown in Fig. 3B and 3D. Similar size

distributions were found for microbubbles that were loaded with 2 mol% DSPE-PEG_{2000}-biotin containing siPlexes (data not shown).

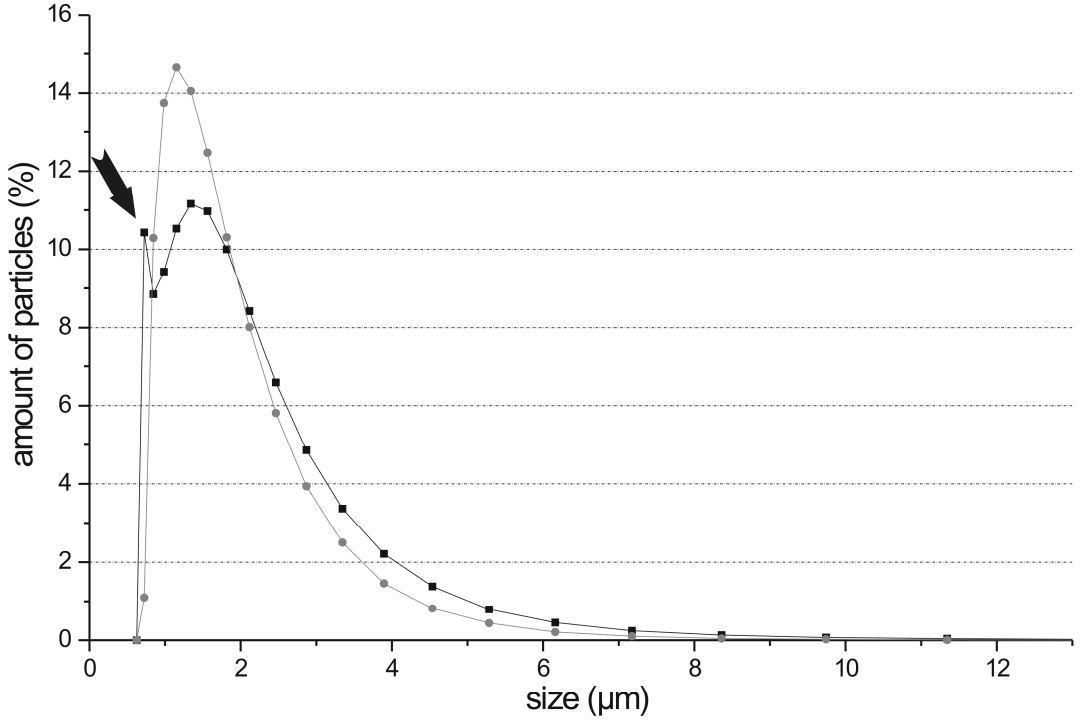

Figure 4. Size distribution measured by laser diffraction of microbubbles after addition of non-PEGylated siPlexes (black squares) and attachment of 5 mol% DSPE-PEG_{2000}-biotin containing siPlexes (grey circles). The data are the mean of three measurements and error bars represent standard deviations. Arrow indicates a peak of sub-micron sized particles.

Ultrasound induced release of PEG-siPlexes from microbubbles

It has been shown that coupling of polystyrene beads to the surface of microbubbles via a biotin-avidin bridge, results in local delivery of the beads upon ultrasound radiation [38]. However, in contrast to these inert beads, self-assembled siPlexes may undergo physicochemical alterations during the ultrasound triggered release, which may influence their biological performance. Therefore, we determined the size, zeta potential and siRNA complexation of the siPlexes before attachment to the microbubbles and after ultrasound triggered release from the microbubbles.

The dark grey bars in Fig. 5A show that, before binding to the microbubble surface the size of the siPlexes was independent of the PEGylation degree and averaged 130 nm. In contrast, the surface charge lowered with increasing degree of PEGylation (dark grey bars in Fig. 5B) varying from 50 mV for the non-PEGylated to 20 mV for the siPlexes containing 5 mol% DSPE-PEG_{2000}-biotin. Fig. 5A also shows that binding and subsequent ultrasound assisted release of the PEG-siPlexes from

the microbubbles (light grey bars) had only a limited effect on the size of these PEG-siPlexes with a maximal increase of ~20 nm, in contrast to the clear increase in size of the non-PEGylated siPlexes.

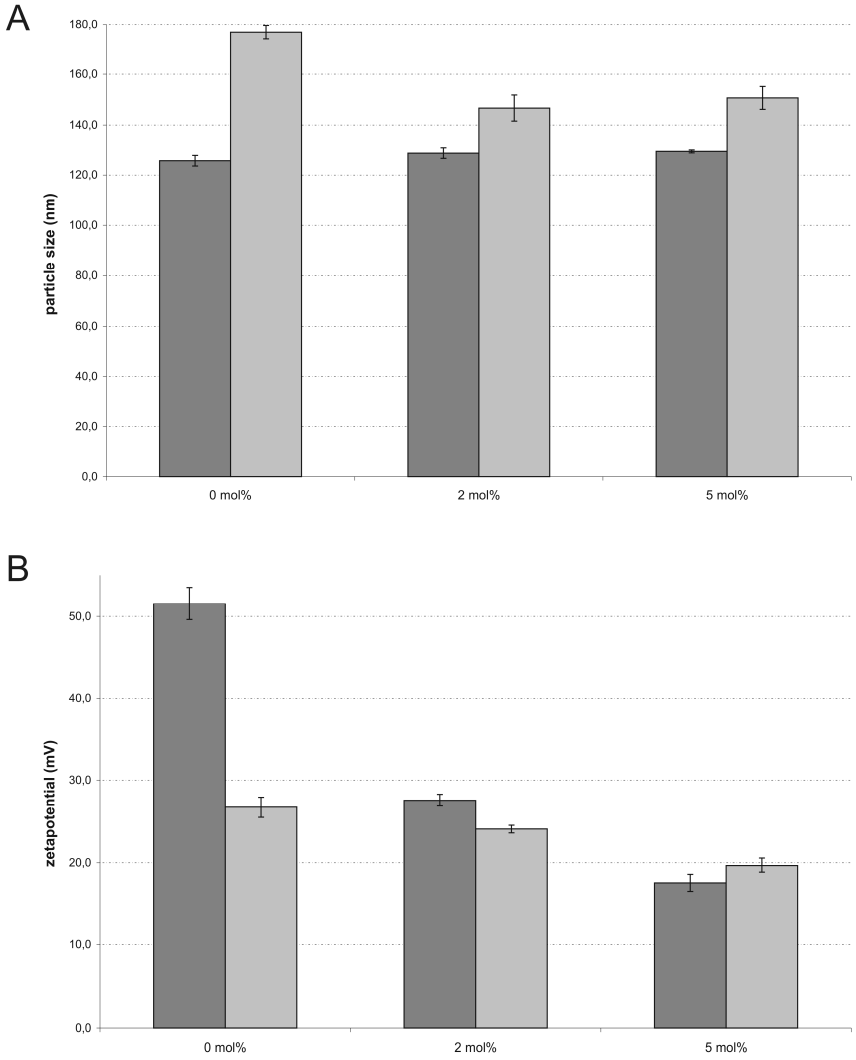

Figure 5. (A) Size and (B) zeta potential of the siPlexes containing 0 mol%, 2 mol% and 5 mol% DSPE-PEG_{2000}-biotin before attachment to the microbubbles (dark grey bars) and after ultrasound assisted release from the siPlex loaded microbubbles (light grey bars). The data are the means of three independent measurements and the error bars represent standard deviations.

As observed for the size, the zeta potential (Fig. 5B) of the PEG-siPlexes after being released from the microbubbles by ultrasound was not significantly altered, while the zeta potential of the non-PEGylated siPlexes was significantly lower. The change in size and zeta potential of the non-PEGylated siPlexes may be due the binding of negatively charged DSPE-PEG_{2000}-biotin lipids from the imploded microbubbles to the non-PEGylated siPlexes.

Clearly, to keep their biological performance, the siPlexes may not dissociate (i.e. release their siRNA) upon exposure to ultrasound, as free siRNA is prone to nuclease degradation. Gel electrophoresis revealed that ultrasound energy did not dissociate the siPlexes (data not shown). In conclusion, ultrasound mediated implosion of the PEG-siPlex loaded microbubbles and the induced

microjets did not drastically influence the size, zeta potential and the complexation properties of the released PEG-siPlexes.

Cellular distribution of PEG-siPlexes

Next we studied the cellular distribution of PEG-siPlexes. Fig. 6A till 6C show HuH-7 cells incubation with 5 mol% PEG-siPlexes. The z-scan in Fig. 6A reveals that these PEG-siPlexes, after 20 min incubation at 37°C, were still located on top of the HuH-7 cells. This was confirmed by the images in Fig. 6B and 6C. In these images, the green labelled PEG-siPlexes (Fig. 6C) show exactly the same cellular distribution as the red labelled plasma membrane (Fig. 6B). This confirms that PEGylation indeed has an effect on the cellular uptake of siPlexes [39], as non-PEGylated siPlexes were clearly taken up by the cells after 20 min (data not shown). Ultrasound irradiation did not change the cellular distribution of these free PEG-siPlexes (data not shown). Interestingly, PEG-siPlexes released from siPlex loaded microbubbles by ultrasound showed a totally different cellular distribution (Fig. 6D till 6F). In this case, the green labelled PEG-siPlexes were localized inside the cells as shown by the z-scan (Fig. 6D) and the membrane colouring (Fig. 6E and 6F). These results suggest that PEG-siPlexes enter the cells via a different mechanism when they are released from the PEG-siPLex loaded microbubbles by ultrasound. Although further research is needed, we suppose that they enter cells via the transient cell membrane perforations that arise during the exposure to ultrasound [40]. Indeed, such pores, which have been reported to be a few hundreds of nanometers in size [34,41], are large enough to allow the passage of the PEG-siPlexes released from the microbubbels. This implies that the negative effects of PEGylation on the cellular uptake as well as on the endosomal escape of PEG-siPlexes can be circumvented by attaching them to microbubbles and subsequently expose these siPlex loaded microbubbles to ultrasound.

Gene silencing efficiency of PEG-siPlex loaded microbubbles

Finally, we determined whether siRNA delivered by ultrasound mediated implosion of the PEG-siPLex loaded microbubbles could inhibit constitutive luciferase expression in HuH-7eGFPLuc cells (Fig. 7). The black bars in Fig. 7 show that the silencing capacity of the free siPlexes declines dramatically with increasing PEGylation degree. SiPlexes with a PEGylation degree of 2 mol% already showed a 3-fold reduced gene silencing capacity compared to the non-PEGylated siPlexes.

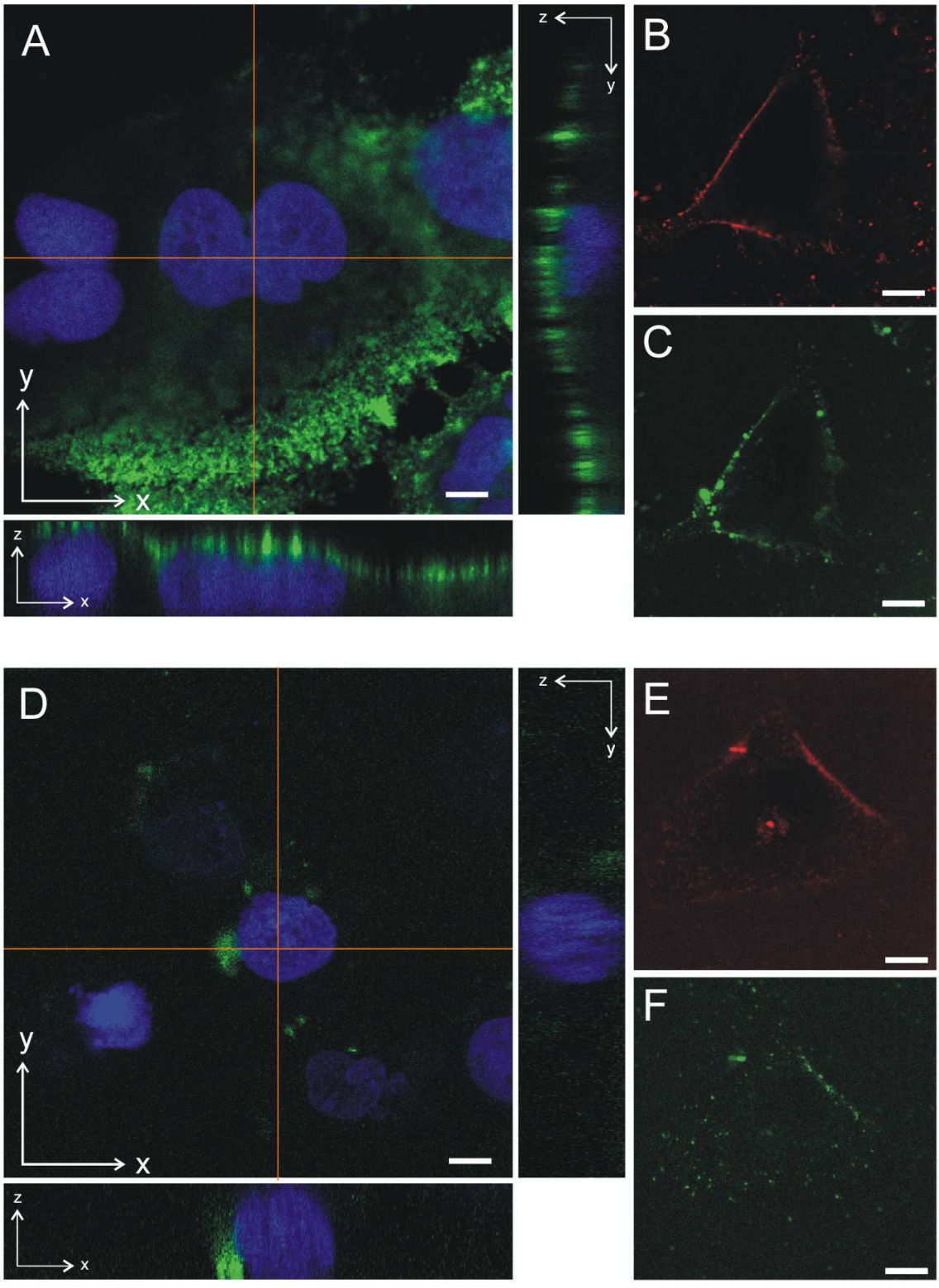

Figure 6. Cellular uptake and intracellular distribution of PEG-siPlexes (A till C) and ultrasound irradiated PEG-siPlex loaded microbubbles (D till F). All PEG-siPlexes contain 5 mol% DSPE-PEG_{2000}-biotin. Images A and D display confocal images and z-scans, at the positions indicated by the red lines, through HuH-7 cells with Draq5 labelled nuclei (blue) and incubated for 20 minutes with Atto488-labelled siPlexes (green). Confocal image (B) and (E) show the localisation of TRITC-concanavalin A (red), a plasma membrane marker. Confocal image (C) and (F) show the localisation of Atto488-labelled siPlexes (green) in the cells shown in image (B) and (E), respectively. The scale bars represent 10 µm.

Increasing the PEGylation degree to 5 mol% even completely blocked the silencing capacity of the siPlexes. This negative effect of PEGylation has intensively been studied for pDNA delivery and some groups suggest that the loss in transfection efficiency of highly PEGylated lipoplexes is due to a reduced cellular binding and uptake [41,42], while others believe that the PEG-lipids inhibit the endosomal release of the nucleic acids into the cytoplasm [39,43-46]. The white bars in Fig. 7 show that the negative effect of PEGylation on the gene silencing efficiency of the siPlexes containing 5 mol% DSPE-PEG_{2000}-biotin can be completely counteracted by loading of these PEG-siPlexes on the surface of microbubbles followed by exposure of these microbubbles to ultrasound. Attachment of siPlexes containing 2 mol% DSPE-PEG_{2000}-biotin to the microbubbles and subsequent exposure to ultrasound resulted in a similar silencing as the corresponding free PEG-siPlexes. For these PEG-siPlexes the number of PEG-siPlexes bound to the microbubbles is probably not enough to further increase their gene silencing efficiency. Indeed, as shown in Fig. 3C, the 5 mol% DSPE-PEG_{2000}-biotin containing siPlexes bind much more efficiently to the microbubble surface than the 2 mol% DSPE-PEG_{2000}-biotin containing siPlexes (Fig. 3B). Therefore, these data may indicate that the extent of gene silencing is governed by the amount of PEG-siPlexes that are released near the cell perforations. Fig. 7 (dark grey bars) also shows that applying ultrasound energy, in the absence of microbubbles, could not enhance the gene silencing efficiency of the different siPlexes. Furthermore, microbubbles loaded with 5 mol% PEG-siPlexen were not able to cause gene silencing in the absence of ultrasound (Fig. 7; light grey bars). This implies that the PEG-siPlex loaded microbubbles described in this work allow ultrasound controlled, i.e. targeted, intracellular delivery of siRNA.

CONCLUSION

In conclusion, we developed a novel delivery system in which PEG-siPlexes are attached to ultrasound responsive microbubbles via a biotin-avidin-biotin bridge. Exposure of these PEG-siPlex loaded microbubbles to ultrasound resulted in a massive release of unaltered PEG-siPlexes. Furthermore, PEG-siPlexes (containing 5 mol% DSPE-PEG_{2000}-biotin) loaded on microbubbles were able to enter cells rapidly after exposure to ultrasound, while free PEG-siPlexes did not enter cells. Moreover, these PEG-siPlex loaded microbubbles caused, in the presence of ultrasound, a much higher gene silencing than free PEG-siPlexes. Interestingly, in the absence of ultrasound these PEG-siPlex loaded microbubbles did not cause any gene silencing. Therefore, the developed siRNA delivery system allows both space and time controlled gene silencing. Furthermore, the PEG-siPlex loaded microbubbles are expected to be suitable for systematic applications as ultrasound in combination with microbubbles is considered as a safe and already used in the clinic for diagnostic

purposes. Additionally, PEG-siPlexes are known not to aggregate in serum which is important to avoid blockage of small blood capillaries by aggregates [47]. The developed siRNA delivery system may also allow the treatment of patients with metastasized tumours. Indeed, a recently developed device that combines magnetic resonance imaging (MRI) and ultrasound can both track down the metastasized tumours and guide the ultrasound energy to these tumours [48]. So, the siRNA delivery system presented in this work may open up new perspectives for ultrasound controlled *in vivo* delivery of siRNA.

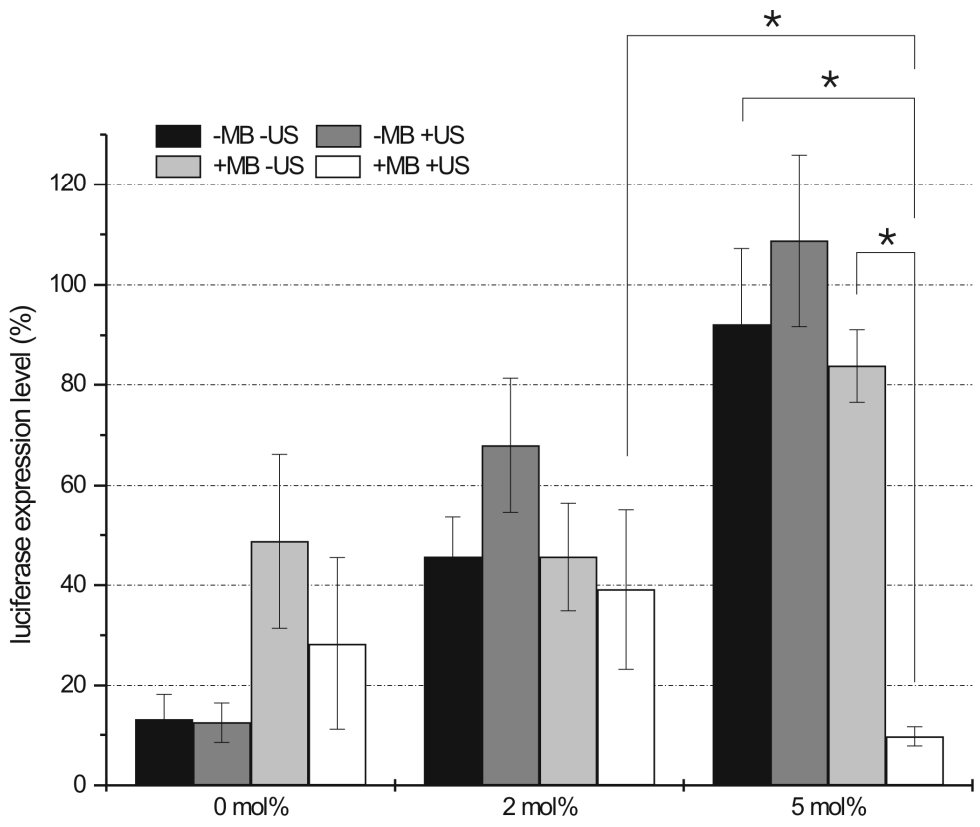

Figure 7. Silencing efficiency of free siPlexes and PEG-siPlexes in the absence and presence of ultrasound, and PEG-siPlex loaded microbubbles in the presence of ultrasound. The PEGylation (DSPE-PEG_{2000}-biotin) degree of the siPlexes is represented in the x-axis. The black and the dark grey bars represent the gene silencing efficiency of free siPlexes in the absence and presence of ultrasound, respectively. The light grey and white bars represent the gene silencing of the siPlexes loaded on the microbubbles in the absence or presence of ultrasound. In all cases, the following ultrasound settings were used: 1 MHz, 10 % DC, 2 W/cm^2, 10 sec. The results are expressed as percentage of luciferase expression compared to mock siRNA transfected cells. The asterixes (*) represent significant differences with $p<0.05$. (MB = microbubble; US = ultrasound)

ACKNOWLEDGMENTS

Niek Sanders is supported by the Fund for Scientific Research-Flanders (FWO). The financial support of this institute is acknowledged with gratitude. This work was supported by grants from Ghent University (BOF), FWO and the European Union (MediTrans). The HuH-7_eGFPLuc cells were kindly provided by Prof. Ernst Wagner, LMU University Munich.

REFERENCES

(1) Elbashir S.M., Harborth J., Lendeckel W., Yalcin A., Weber K., & Tuschl T. Duplexes of 21-nucleotide RNAs mediate RNA interference in cultured mammalian cells. *Nature* **2001** 411(6836) 494-498.

(2) Aagaard L. & Rossi J.J. RNAi therapeutics: principles, prospects and challenges. *Adv. Drug Deliv. Rev.* **2007** 59(2-3) 75-86.

(3) Lewis D.L. & Wolff J.A. Systemic siRNA delivery via hydrodynamic intravascular injection. *Adv. Drug Deliv. Rev.* **2007**

(4) Lee S.H., Kim S.H., & Park T.G. Intracellular siRNA delivery system using polyelectrolyte complex micelles prepared from VEGF siRNA-PEG conjugate and cationic fusogenic peptide. *Biochem. Biophys. Res. Commun.* **2007** 357(2) 511-516.

(5) Akaneya Y., Jiang B., & Tsumoto T. RNAi-induced gene silencing by local electroporation in targeting brain region. *J. Neurophysiol.* **2005** 93(1) 594-602.

(6) Golzio M., Mazzolini L., Ledoux A. *et al.* In vivo gene silencing in solid tumors by targeted electrically mediated siRNA delivery. *Gene Ther.* **2007** 14(9) 752-759.

(7) Kishida T., Asada H., Gojo S. *et al.* Sequence-specific gene silencing in murine muscle induced by electroporation-mediated transfer of short interfering RNA. *J. Gene Med* **2004** 6(1) 105-110.

(8) Takabatake Y., Isaka Y., Mizui M. *et al.* Exploring RNA interference as a therapeutic strategy for renal disease. *Gene Ther.* **2005** 12(12) 965-973.

(9) Chien P.Y., Wang J., Carbonaro D. *et al.* Novel cationic cardiolipin analogue-based liposome for efficient DNA and small interfering RNA delivery in vitro and in vivo. *Cancer Gene Ther.* **2005** 12(3) 321-328.

(10) Eliyahu H., Servel N., Domb A.J., & Barenholz Y. Lipoplex-induced hemagglutination: potential involvement in intravenous gene delivery. *Gene Ther.* **2002** 9(13) 850-858.

(11) Howard K.A., Rahbek U.L., Liu X. *et al.* RNA Interference in Vitro and in Vivo Using a Novel Chitosan/siRNA Nanoparticle System. *Mol. Ther.* **2006**

(12) Schiffelers R.M., Ansari A., Xu J. *et al.* Cancer siRNA therapy by tumor selective delivery with ligand-targeted sterically stabilized nanoparticle. *Nucleic Acids Res.* **2004** 32(19) e149.

(13) Sorensen D.R., Leirdal M., & Sioud M. Gene silencing by systemic delivery of synthetic siRNAs in adult mice. *J. Mol. Biol.* **2003** 327(4) 761-766.

(14) Thomas M., Lu J.J., Ge Q., Zhang C., Chen J., & Klibanov A.M. Full deacylation of polyethylenimine dramatically boosts its gene delivery efficiency and specificity to mouse lung. *Proc. Natl. Acad. Sci. U. S. A* **2005** 102(16) 5679-5684.

(15) Urban-Klein B., Werth S., Abuharbeid S., Czubayko F., & Aigner A. RNAi-mediated gene-targeting through systemic application of polyethylenimine (PEI)-complexed siRNA in vivo. *Gene Ther.* **2005** 12(5) 461-466.

(16) Sakurai F., Nishioka T., Yamashita F., Takakura Y., & Hashida M. Effects of erythrocytes and serum proteins on lung accumulation of lipoplexes containing cholesterol or DOPE as a helper lipid in the single-pass rat lung perfusion system. *Eur. J. Pharm. Biopharm.* **2001** 52(2) 165-172.

(17) Choi Y.H., Liu F., Kim J.S., Choi Y.K., Park J.S., & Kim S.W. Polyethylene glycol-grafted poly-L-lysine as polymeric gene carrier. *J. Control Release* **1998** 54(1) 39-48.

(18) Kunath K., von H.A., Petersen H. *et al.* The structure of PEG-modified poly(ethylene imines) influences biodistribution and pharmacokinetics of their complexes with NF-kappaB decoy in mice. *Pharm. Res.* **2002** 19(6) 810-817.

(19) Ogris M., Brunner S., Schuller S., Kircheis R., & Wagner E. PEGylated DNA/transferrin-PEI complexes: reduced interaction with blood components, extended circulation in blood and potential for systemic gene delivery. *Gene Ther.* **1999** 6(4) 595-605.

(20) Tam P., Monck M., Lee D. *et al.* Stabilized plasmid-lipid particles for systemic gene therapy. *Gene Ther.* **2000** 7(21) 1867-1874.

(21) Wasungu L. & Hoekstra D. Cationic lipids, lipoplexes and intracellular delivery of genes. *J. Control Release* **2006** 116(2) 255-264.

(22) Zuhorn I.S., Engberts J.B., & Hoekstra D. Gene delivery by cationic lipid vectors: overcoming cellular barriers. *Eur. Biophys. J.* **2007** 36(4-5) 349-362.

(23) Bekeredjian R., Chen S., Frenkel P.A., Grayburn P.A., & Shohet R.V. Ultrasound-targeted microbubble destruction can repeatedly direct highly specific plasmid expression to the heart. *Circulation* **2003** 108(8) 1022-1026.

(24) Duvshani-Eshet M., Adam D., & Machluf M. The effects of albumin-coated microbubbles in DNA delivery mediated by therapeutic ultrasound. *J. Control Release* **2006** 112(2) 156-166.

(25) Kinoshita M., McDannold N., Jolesz F.A., & Hynynen K. Targeted delivery of antibodies through the blood-brain barrier by MRI-guided focused ultrasound. *Biochem. Biophys. Res. Commun.* **2006** 340(4) 1085-1090.

(26) Lentacker I., De Smedt S.C., Demeester J., Van Marck V., Bracke M., & Sanders N.N. Lipoplex-Loaded Microbubbles for Gene Delivery: A Trojan Horse Controlled by Ultrasound. *Adv. Funct. Mater.* **2007** 17(12) 1910-1916.

(27) Manome Y., Nakayama N., Nakayama K., & Furuhata H. Insonation facilitates plasmid DNA transfection into the central nervous system and microbubbles enhance the effect. *Ultrasound Med. Biol.* **2005** 31(5) 693-702.

(28) Newman C.M., Lawrie A., Brisken A.F., & Cumberland D.C. Ultrasound gene therapy: on the road from concept to reality. *Echocardiography.* **2001** 18(4) 339-347.

(29) Pislaru S.V., Pislaru C., Kinnick R.R. *et al.* Optimization of ultrasound-mediated gene transfer: comparison of contrast agents and ultrasound modalities. *Eur. Heart J.* **2003** 24(18) 1690-1698.

(30) Vannan M., McCreery T., Li P. *et al.* Ultrasound-mediated transfection of canine myocardium by intravenous administration of cationic microbubble-linked plasmid DNA. *J. Am. Soc. Echocardiogr.* **2002** 15(3) 214-218.

(31) Kinoshita M. & Hynynen K. A novel method for the intracellular delivery of siRNA using microbubble-enhanced focused ultrasound. *Biochem. Biophys. Res. Commun.* **2005** 335(2) 393-399.

(32) Tsunoda S., Mazda O., Oda Y. *et al.* Sonoporation using microbubble BR14 promotes pDNA/siRNA transduction to murine heart. *Biochem. Biophys. Res. Commun.* **2005** 336(1) 118-127.

(33) Ogawa K., Tachibana K., Uchida T. *et al.* High-resolution scanning electron microscopic evaluation of cell-membrane porosity by ultrasound. *Med Electron Microsc.* **2001** 34(4) 249-253.

(34) Mehier-Humbert S., Bettinger T., Yan F., & Guy R.H. Ultrasound-mediated gene delivery: kinetics of plasmid internalization and gene expression. *J. Control Release* **2005** 104(1) 203-211.

(35) Sanders N.N., Van R.E., De Smedt S.C., & Demeester J. Structural alterations of gene complexes by cystic fibrosis sputum. *Am. J. Respir. Crit Care Med.* **2001** 164(3) 486-493.

(36) Kinoshita M. & Hynynen K. Key factors that affect sonoporation efficiency in in vitro settings: the importance of standing wave in sonoporation. *Biochem. Biophys. Res. Commun.* **2007** 359(4) 860-865.

(37) Unger E.C., Porter T., Culp W., Labell R., Matsunaga T., & Zutshi R. Therapeutic applications of lipid-coated microbubbles. *Adv. Drug Deliv. Rev.* **2004** 56(9) 1291-1314.

(38) Lum A.F., Borden M.A., Dayton P.A., Kruse D.E., Simon S.I., & Ferrara K.W. Ultrasound radiation force enables targeted deposition of model drug carriers loaded on microbubbles. *J. Control Release* **2006** 111(1-2) 128-134.

(39) Mishra S., Webster P., & Davis M.E. PEGylation significantly affects cellular uptake and intracellular trafficking of non-viral gene delivery particles. *Eur. J. Cell Biol.* **2004** 83(3) 97-111.

(40) Prentice P., Cuschieri A., Dholakia K., Prausnitz M., & Campbell P. Membrane disruption by optically controlled microbubble cavitation. *Nature Physics* **2005** 1107-110.

(41) Schlicher R.K., Radhakrishna H., Tolentino T.P., Apkarian R.P., Zarnitsyn V., & Prausnitz M.R. Mechanism of intracellular delivery by acoustic cavitation. *Ultrasound Med. Biol.* **2006** 32(6) 915-924.

(42) Deshpande M.C., Davies M.C., Garnett M.C. *et al.* The effect of poly(ethylene glycol) molecular architecture on cellular interaction and uptake of DNA complexes. *J. Control Release* **2004** 97(1) 143-156.

(43) Audouy S. & Hoekstra D. Cationic lipid-mediated transfection in vitro and in vivo (review). *Mol. Membr. Biol.* **2001** 18(2) 129-143.

(44) Meyer O., Kirpotin D., Hong K. *et al.* Cationic liposomes coated with polyethylene glycol as carriers for oligonucleotides. *J. Biol. Chem.* **1998** 273(25) 15621-15627.

(45) Shi F., Wasungu L., Nomden A. *et al.* Interference of poly(ethylene glycol)-lipid analogues with cationic-lipid-mediated delivery of oligonucleotides; role of lipid exchangeability and non-lamellar transitions. *Biochem. J.* **2002** 366(Pt 1) 333-341.

(46) Song L.Y., Ahkong Q.F., Rong Q. *et al.* Characterization of the inhibitory effect of PEG-lipid conjugates on the intracellular delivery of plasmid and antisense DNA mediated by cationic lipid liposomes. *Biochim. Biophys. Acta* **2002** 1558(1) 1-13.

(47) Buyens K., Lucas B., Raemdonck K. *et al.* A fast and sensitive method for measuring the integrity of siRNA-carrier complexes in full human serum. *J. Control Release* **2007**

(48) Moonen C.T. Spatio-temporal control of gene expression and cancer treatment using magnetic resonance imaging-guided focused ultrasound. *Clin. Cancer Res.* **2007** 13(12) 3482-3489.

Chapter 4

Pitfalls in the Use of Inhibitors to Study Endocytic Uptake of Gene Complexes

This chapter is *submitted*:

Roosmarijn E. Vandenbroucke[1], Dries Vercauteren[1], Joseph Demeester[1], Arwyn T. Jones[2], Stefaan C. De Smedt[1], Kevin Braeckmans[1] and Niek N. Sanders[1]

[1] Laboratory of General Biochemistry and Physical Pharmacy, Department of Pharmaceutics, Ghent University, Ghent, Belgium.

[2] Welsh School of Pharmacy, Cardiff University, Redwood Building, King Edward the VII Avenue, Cardiff CF10 3XF, UK

ABSTRACT

Several types of endocytosis have been demonstrated to be involved in the uptake of nucleic acid containing particles, varying according to cell type, type of carrier and particle size. As the intracellular processing can differ strongly depending on the precise uptake mechanism, unravelling this uptake mechanism of individual non-viral gene carriers in a specific cell line model can open up possibilities to correlate uptake to intracellular processing and subsequently to transfection efficiency. Consequently, several research groups have tried to quantitatively assess the contribution of each endocytic pathway to the uptake of non-viral gene delivery vehicles through the use of endocytosis inhibitors. Such chemicals are easy to apply and are presumed to inhibit specific endocytic pathways. However, in this work, we show that one should take extra care when using inhibitors to specifically perturb endocytic pathways as the inhibitory efficiency appears to be strongly cell type dependent, and so is the concentration threshold of cellular toxicity. Moreover, the inhibition is not always as efficient and specific as has been claimed in recent literature. We also demonstrate that the chemical compounds can exhibit side effects such as dramatic changes in cellular morphology. Taken together, we conclude that the use of endocytosis inhibitors is still a very useful approach to study the uptake mechanisms of nucleic acid containing particles, but only when the appropriate control experiments are performed to assure inhibitor toxicity, efficacy and specificity. Additionally, combining these inhibitors with other tools such as fluorescent dual colour colocalization studies or suppression of specific endocytic pathways through the use of dominant negative mutants or RNAi, will assure to draw correct and reliable conclusions.

Chapter 4

Pitfalls in the Use of Inhibitors to study Endocytic Uptake of Gene Carriers

INTRODUCTION

Successful gene delivery relies mainly on the development of non-toxic gene carriers that can deliver foreign genetic material efficiently to target cells. Although more effective, the clinical use of viral carriers is mainly limited due to safety issues. As a safe(r) alternative, non-viral gene carriers, such as cationic liposomes or polymers, can be used. However, their low transfection efficiency is a major limiting factor. A deep mechanistic understanding of the pathways involved in the cellular uptake of these non-viral delivery vehicles may therefore help to design more effective gene carriers.

The majority of the reports suggest that endocytosis is the preferred route of cell entry of non-viral gene carriers [1]. As shown in Fig. 1, endocytosis can be classified in two broad categories: phagocytosis and pinocytosis [2]. Phagocytosis is typically restricted to specialized cells whereas pinocytosis occurs in all cell types. Therefore, endocytosis and pinocytosis are mostly used in the same context and considered to be synonyms. The study of the different pinocytotic pathways is still an evolving field and no current classification system is completely satisfactory. Nowadays, one primarily distinguishes macropinocytosis, clathrin-dependent (CDE) and clathrin-independent (CIE) endocytosis. Additionally, under CIE, one can make a further distinction between dynamin-dependent and -independent endocytosis [3].

CDE is the major and best characterized endocytic pathway and is claimed to be the preferred pathway for particles up to 200 nm in size [4]. A local, clathrin-associated invagination of the plasmamembrane (PM), a coated pit, pinches off to form a membrane-derived clathrin-coated vesicle. This is followed by fission of the mature vesicle which is dependent on the activity of the

GTPase dynamin [5] and the immediate release of the clathrin coat, resulting in vesicles of 60 to 200 nm in size [6]. The presence of cholesterol is shown to be essential for CDE [7]. Actin plays an accessory role during CDE, but disrupting the actin filaments does not inhibit the endocytic process [8]. By fusion with the sorting (early) endosomes, CDE typically ends up in the acidifying and degrading endolysosomal pathway resulting in hydrolytic and enzymatic destruction of the endocytosed macromolecules. The majority of the internalized receptors, such as the transferrin receptor, are recycled to the PM through tubulating of the sorting endosome (SE), either directly or via the endocytic recycling compartment (ERC) [9]. In contrast, endocytosed macromolecules are retained in the lumen of the SE whose pH is subsequently lowered to pH 5.9 [10]. After 5-10 min, the SE stops receiving newly formed vesicles and matures into a late endosome (LE). At this point, the endosome exhibits intralumenal membrane structures, subsequently often referred to as multivesicular body [11], and is actively transported on microtubules to the periphery of the nucleus. At this stage, the pH has dropped to pH 4.5-5.5 [10]. As a final phase of the degrading endolysosomal pathway, the LE fuses with the prelysosomal vesicles, which contain the hydrolyzing enzymes, to form mature hybrid degrading endolysosomes [12]. Certain macromolecules preferentially associate with this pathway and are specifically taken up in clathrin-coated vesicles. Examples are the Low Density Lipoprotein (LDL) receptor, the transferrin receptor and the Epidermal Growth Factor (EGF) receptor [7,13].

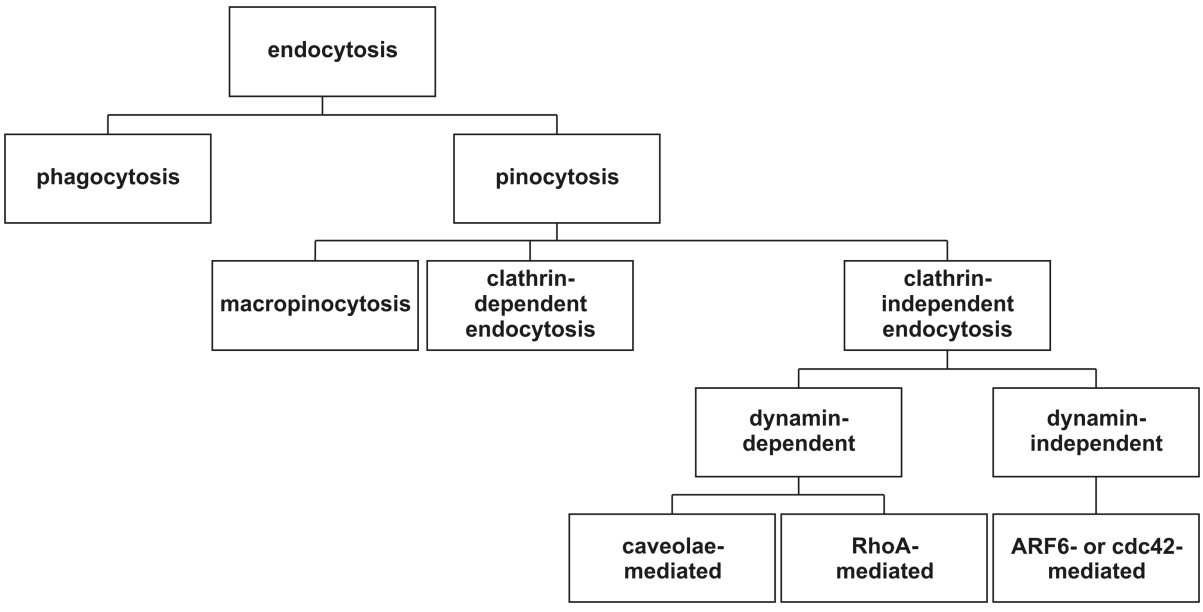

Figure 1. Overview of the known endocytic pathways in mammalian cells (see Chapter 1 Fig. 7 for more details).

Although the details of the CIE mechanism have not been completely elucidated, the current classification is based on the role of dynamin and several small GTPases [3] (see Fig. 1). Dynamin-independent CIE is subdivided in ADP-ribosylation factor 6 (ARF6-) and cell division cycle 42 (CDC42-)

regulated endocytosis. Dynamin-dependent CIE is subdivided in caveolae-mediated and RhoA-regulated endocytosis. All the CIE endocytic pathways are related by the fact that the endocytic vesicles bud from a liquid ordered membrane environment, called lipid rafts, enriched in unsaturated phospholipids, cholesterol, glycosphingolipids and certain proteins [14]. Additionally, all CIE processes strongly depend on the integrity of actin microfilaments [3]. Caveolae mediated endocytosis is probably the best characterized CIE pathway. Caveolae, not present in all cell types [15,16], are small (50-80 nm), smooth, flask-shaped invaginations of the PM that are characterized by the presence of caveolin [17]. Besides the flask-shape, some flexibility in morphology has been observed [18]. The post-endocytic trafficking of CIE is quite diverse and mostly dependent on the cargo. The cargoes taken up by the RhoA-, ARF6- and CDC42-regulated CIE end up in the SEs from where they are further sorted and translocated [3]. In contrast, the newly formed caveolin-containing vesicles, often named cavicles [19], fuse either with SEs or caveosomes [20]. Caveosomes are neutral endosomes which do not acidify [21], nor do they fuse with lysosomes [18]. Subsequently, the cargo can be translocated to the Golgi, the endoplasmatic reticulum (ER) or the LE [18,22]. Besides this non-degrading character, caveosomes exist longer than other endosomes [23]. For these reasons, this non-acidifying, non-degrading environment could be an interesting target for gene-delivery. Cholera toxin subunit B (CTB) is often being used as marker for this pathway [24], though it is currently known that a significant fraction of CTB is also taken up in clathrin-coated vesicles [25]. Albumin is preferentially taken up by CIE [26]. Lactosylceramid, a glycosphingolipid, is taken up by a clathrin-independent and dynamin- and caveolin-dependent mechanism [27-29]. Certain pathogens, like SV40 virus, use specifically this pathway to enter cells and to hijack the cell's machinery [23].

During macropinocytosis (MP), a third type of pinocytosis (see Fig. 1), membrane protrusions, often called ruffles, are formed which can subsequently fuse with each other or with the PM to enclose large volumes [30]. MP is a non-selective endocytic mechanism of suspended macromolecules resulting in vesicles with sizes up to 5 µm [31]. The process is actin-driven [32] and dependent on the presence of cholesterol [31]. Constitutive MP has been observed in dendritic cells, but in other non-phagocytic cells, MP is mostly a response to growth factor stimulation [30]. Once taken up, the intracellular itinerary differs from cell to cell. In macrophages, the formed macropinosomes shrink, acidify and fuse with lysosomes. In contrast, in epithelial cell lines, these vesicles do only partially acidify, do not fuse with lysosomes and are finally mostly exocytosed [33]. Ricine is a macromolecule which is preferentially taken up via macropinocytosis. [31]. Additionally, this pinocytic pathway is the alternative entry pathway for adenoviruses [34], the HIV-1 Tat peptide [35] and in general for large, solubilised molecules such as 50 kDa dextran [36].

Phagocytosis shares many features with MP, but instead of membrane ruffles that form a macropinosome, the fagosome is formed by actin-driven pseudopodia which ingest micron-sized

particles. This is an adsorptive type of endocytosis and is exclusive used by specialized cells such as macrophages and dendritic cells to engulf large structures (> 500 nm) such as bacteria, dead cells or yeast [37].

Several forms of endocytosis have been demonstrated to be involved in DNA uptake [38,39] and varies widely according to cell type (summarized in [3]), gene carrier [22] and particle size [4]. This specificity stresses why it is imperative to study the internalization of the individual non-viral gene carriers in the appropriate cell line model. Therefore, a quantitative assessment of the contribution of each endocytic pathway to the overall cellular uptake is essential to establish the intracellular pharmacokinetic models in the future [40] and to evaluate if it is feasible to relate the endocytic pathway to intracellular processing and transfection efficiency. There are several tools available to study endocytosis and trafficking of gene carriers. The present paper focuses on methods of perturbing endocytosis through the use of endocytosis inhibitors. We show that both the inhibitory efficiency and the concentration-threshold of cellular toxicity is strongly cell type dependent. In addition, the chemical compounds exhibit cell type dependent side effects and there is redundancy when inhibiting one pathway. Therefore in this paper, we bring a strongly cautionary message concerning the use of inhibitors for studying endocytic pathways.

MATERIALS & METHODS

Materials

Chlorpromazine, methyl-β-cyclodextrin (mBCD), nystatin, genistein, and filipin III were purchased from Sigma Aldrich (Bornem, Belgium) and cytochalasin D (cytoD) from Biosource (Nivelles, Belgium). Dulbecco's modified Eagle's medium (DMEM), OptiMEM, L-glutamine (L-Gln), foetal bovine serum (FBS), penicillin-streptomycin (5000 IU/ml penicillin and 5000 µg/ml streptomycin) (P/S) and phosphate buffered saline (PBS) were supplied by GibcoBRL (Merelbeke, Belgium). Human transferrin-AlexaFluor633 (hTF) and BODIPY FL C_5-lactosylceramide (LacCer) were purchased from Molecular Probes (Merelbeke, Belgium). Other chemicals used were commercially available and were reagent grade products.

Cell culture

Cos-7 cells (African green monkey kidney fibroblast cell line; ATCC number CRL-1651) and Vero cells (African green monkey kidney epithelial cell line; ATCC number CCL-81) were cultured in

DMEM containing 10 % FBS, 2 mM L-Gln and 2 % P/S. HuH-7 cells (human hepatocellular carcinoma cell line; HSRRB number JCRB 0403) were cultured in DMEM:F12 supplemented with 10 % FBS, 2 mM L-Gln and 2 % P/S. The D407 RPE (retinal pigment epithelium) cell line [41] were a kind gift from Dr Richard Hunt (University of South Carolina, Medical School, Columbia, USA) and were cultured in DMEM with high glucose concentration (4500 mg/l), 5 % FBS, 2 mM L-Gln and 2 % P/S. All cells were grown at 37 °C in a humidified atmosphere containing 5 % CO_2.

Cytotoxicity analysis

The cytotoxicity of the different inhibition protocols was evaluated using the non-radioactive EZ4U cell proliferation and cytotoxicity assay kit (Biomedica, Vienna, Austria). This assay is based on the principle of the classical MTT test where less coloured tetrazolium salts are reduced into intensely coloured formazan derivatives by mitochondrial enzymes which are rapidly inactivated within a few minutes after cell death. The assay was performed according to the manufacturer's instructions. Briefly, cells were seeded at 10^5 cells/well in a 24-well plate for 24 hrs. Next, the cells were incubated in OptiMEM with various concentrations of the described inhibitors for 30 min (in case of cytoD) or 2 hrs (in case of all other inhibitors). In case of potassium depletion, cells were washed once with potassium-free buffer (140 mM NaCl, 20 mM Hepes, 1 mM $CaCl_2$, 1 mM $MgCl_2$, 1 mg/ml D-glucose, pH 7.4), then with hypotonic buffer (1:1 potassium-free buffer and H_2O) during 5 min and again 3 times with potassium-free buffer. It is important to note that filipin should be freshly prepared. Subsequently, the cells were immediately incubated with the EZ4U substrate (40 µl substrate with 260 µl culture medium per well) which contains the tetrazolium salts. After 3 hrs at 37°C, the absorbance of the coloured formazan was measured on a Wallac Victor² Plate reader (Perkin Elmer-Cetus Life Sciences, Boston, MA, USA) at 460 nm and corrected for the absorbance measured at 630 nm which represents nonspecific absorbance like fingerprints and cell debris.

Inhibition and specificity studies

For the inhibition and specificity studies, cells were seeded at a cell density of 2.5 x 10^4 cells per cm² on sterile MatTek coverslip (1.5)-bottom dishes (MatTek corporation, MA, USA) 24 hrs prior to the experiment. The cells were subsequently incubated with the appropriate concentration of inhibitor in OptiMEM for the appropriate time. For potassium depletion, cells were washed once with potassium-free buffer, then with hypotonic buffer during 5 min and again 3 times with potassium-free buffer. Next, cells were incubated with 25 µg/ml hTf or 1.35 µM LacCer for 10 min at

37°C in the presence of the appropriate inhibitor or buffer. hTF and LacCer uptake in the different conditions was qualitatively evaluated by the use of confocal laser scanning microscopy (CLSM).

Confocal laser scanning microscopy (CLSM)

The internalisation of the fluorescently tagged biomarkers hTF and LacCer was visualized and evaluated with a Nikon C1 confocal laser scanning module attached to a motorized Nikon TE2000-E inverted microscope (Nikon Benelux, Brussels, Belgium) equipped with a Plan Apo VC 60x 1.4 NA oil immersion objective and suitable optical elements to acquire differential interference contrast (DIC) transmission images. Bodipy FL (LacCer) was excited with the Argon ion 488 nm laser line and emission light was collected using a 500-530 nm band pass filter. AlexaFluor 633 (hTF) was excited with the diode 639 nm laser line and emission light was collected using a 655 nm long pass filter.

RESULTS

The cytotoxicity of endocytosis inhibitors is cell type dependent

To establish an optimal protocol for the use of endocytosis inhibitors on different cell lines, it is imperative to evaluate the *in vitro* cellular toxicity to determine the upper limit in terms of concentration and incubation time that can be applied. Different concentrations of each inhibitor were tested on the HuH-7, Vero, Cos-7 and RPE cell lines and the cellular toxicity was subsequently assessed with the MTT based EZ4U test. The inhibitor was in all cases diluted in OptiMEM and incubated with the cells for 2 hrs, except for cytoD, where the incubation time was reduced to 30 min. In case of K^+-depletion, the cytotoxicity was determined following the treatment with the different buffers as described in materials and methods. As a positive control, cells were exposed for 2 hrs to 20 mg/ml phenol solution in OptiMEM and as negative control for 2 hrs to OptiMEM. The cytotoxicity, expressed as a percentage of cell viability, was calculated from the measured absorbance values after correction for the positive control and normalization to the negative control and is depicted in Fig. 2.

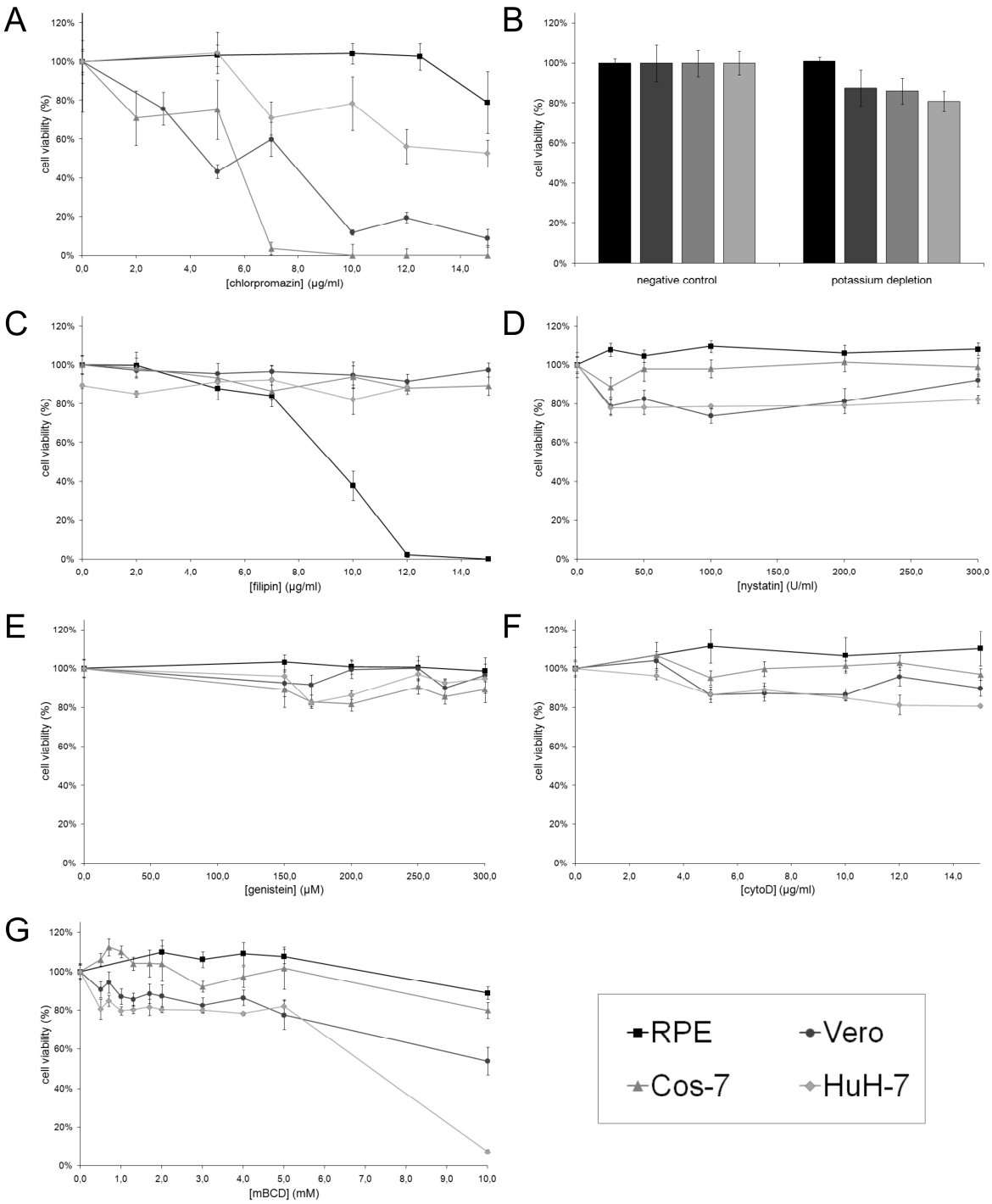

Figure 2. *In vitro* cytotoxicity of the endocytosis inhibitors (A) chlorpromazine, (B) K^+-depletion, (C) filipin, (D) nystatin, (E) genistein (F) cytoD and (G) mBCD after 2 hrs incubation with RPE, Vero, Cos-7 and HuH-7 cells.

The cytotoxicity results exhibit some noteworthy effects. Cos-7 and Vero cells, both African green monkey kidney cells, were very sensitive to chlorpromazine (Fig. 2A). These cell lines showed a clear increase in cytotoxicity after 2 hrs incubation with chlorpromazine concentrations above 2 µg/ml. In contrast, chlorpromazine concentrations up to 5 and 12 µg/ml did not affect the viability of HuH-7 and RPE cells, respectively (Fig. 2A). In general, while K^+-depletion was not toxic to RPE

cells, a limited toxicity was found for the other cell lines (Fig. 2B). Filipin, up to 14 µg/ml, was not toxic to HuH-7, Vero and Cos-7 cells, while it was toxic for RPE cells at concentrations above 7 µg/ml (Fig. 2C). None of the tested nystatin, genistein and cytoD concentrations had a noticeable effect on the viability of the four tested cell lines (Fig. 2D till F). mBCD was slightly cytotoxic to RPE and Cos-7 cells at a concentration of 10 mM, while Vero and especially HuH-7 cells were more sensitive to mBCD (Fig. 2G). Indeed, mBCD became very toxic for HuH-7 cells at concentrations above 5 mM. Based on these results we conclude that several of the tested endocytosis inhibitors show a cell type dependent cytotoxicity profile.

Selecting the appropriate inhibition conditions based on cytotoxicity and efficacy experiments

To determine the optimal concentration to inhibit specific endocytic pathways, we evaluated the (inhibition of the) uptake of biomarkers which are known to be specifically taken up either by CDE or CIE. hTf was used as a specific biomarker for CDE and LacCer for CIE. hTf is a plasma glycoprotein that binds extracellular iron. After binding with its cellular receptor hTf is taken up via CDE. After the first acidification step in the SEs, the transferrin-receptor complex releases the bound iron and the hTf-receptor complex recycles to the PM, either directly or indirectly via the ERC, followed by hTF-receptor dissociation [42]. To study CIE specific uptake, we used LacCer as a lipid biomarker. LacCer is a glycosphingolipid that resides preferably in lipid rafts, i.e. a liquid ordered environment present in biological membranes and is taken up via a clathrin-independent and dynamin-dependent endocytic mechanism [27]. It is stated that the lipid is preferably taken up via a caveolin-1 dependent mechanism [28]. K^+-depletion and chlorpromazine are reported to inhibit CDE, whilst mBCD, cytoD, nystatin, genistein and filipin have extensively been used to inhibit CIE. To test the specificity of these inhibitors we qualitatively evaluated, via CLSM, the uptake of the biomarkers hTf and LacCer. Different inhibitor concentrations and incubation times were evaluated to optimize the inhibition conditions. As an example, the effect of RPE cell exposure to different mBCD conditions on the LacCer uptake is shown in Fig. 3. Fig. 3A shows the negative control where the cells were incubated only with LacCer for 10 min. It can clearly be observed that the uptake of LacCer is increasingly inhibited with increasing concentrations of mBCD. Moreover, an increasing incubation time with the cyclodextrin also exhibited a stronger inhibition (Fig. 3B till H). Higher incubation times and concentrations are not recommended because of toxic effects which are evident from the major morphological changes in Fig. 3H. This is in agreement with the cytotoxicity results after mBCD exposure to RPE cells as was shown Fig. 2. Finally, based on the biodistribution of the biomarker in the various conditions, one can decide on the optimal concentration and incubation time for a specific inhibition protocol. In case of mBCD, this would be an incubation of 2 hrs with 5 mM mBCD in

OptiMEM. Similarly we have tested the efficiency of different inhibitors on the uptake of hTf and LacCer by different cell lines, the results of which are summarized in Table 1. This information was used for the inhibition and specificity studies further on.

Table 1. Uptake of the hTF and LacCer biomarkers in cells in the presence of endocytosis inhibitors.

Treatment			RPE		HuH-7		Cos-7		Vero	
[Conc]	Compound	Time (hrs)	hTf	LacCer	hTf	LacCer	hTf	LacCer	hTf	LacCer
	K^+-depletion		++	+	+	-	-	-	-	+
5 µg/ml	Chlorpromazine	2	ND	ND	ND	ND	+	+	++	-
10 µg/ml	Chlorpromazine	2	++	-	++	-	ND	ND	ND	ND
5 mM	mBCD	2	++	++	+	++	++	++	+	+
5 µg/ml	cytoD	0.5	-	++	-	++	-	+	-	+
300 U/ml	Nystatin	2	-	-	-	-	-	+	-	-
400 µM	Genistein	2	-	-	-	++	-	++	-	-
10 µg/ml	Filipin	2	-	++	-	++	-	++	-	+

-: no inhibition; +: noticeable inhibition; ++: strong inhibition; ND: not determined

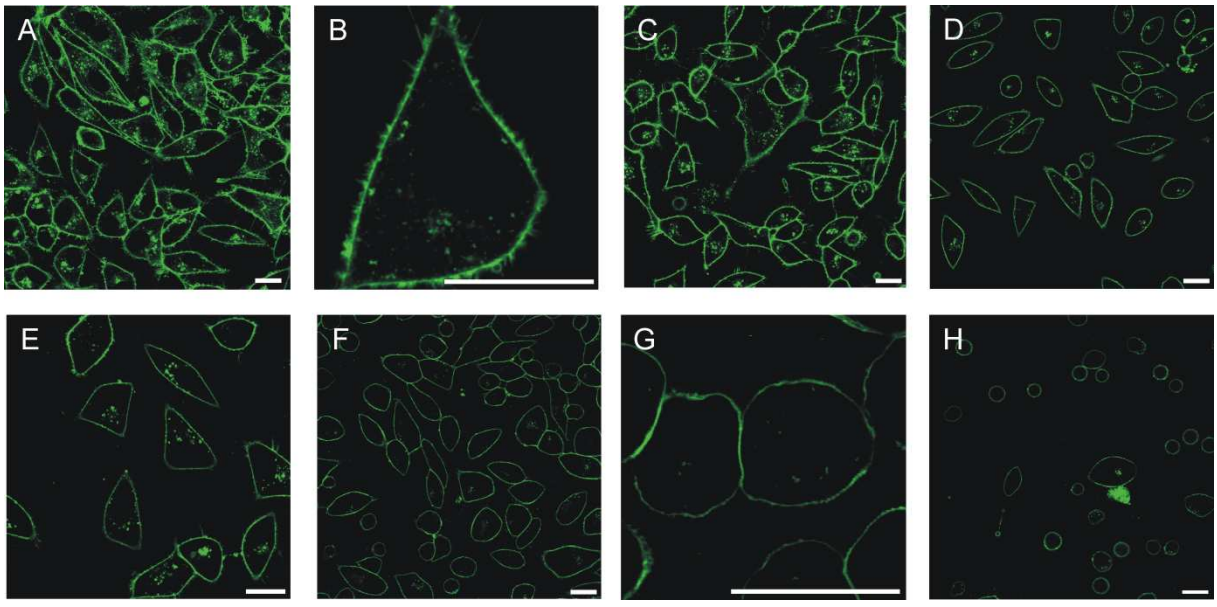

Figure 3. Optimization of the concentration of mBCD to inhibit CIE in RPE cells. Cells were incubated with different mBCD concentrations for different incubation times to find the optimal inhibition conditions. The inhibition of CIE was evaluated based on the uptake of the LacCer biomarker (green). (A) control (B) 30 min 2.5 mM mBCD (C) 1 hr 2.5 mM mBCD (D) 3 hrs 2.5 mM mBCD (E) 1 hr 5 mM mBCD (F) 2 hrs 5 mM mBCD (G) 3 hrs 5 mM mBCD (H) 2 hrs 10 mM mBCD. The scalebar represents 20 µm.

The inhibitor effect is clearly cell type dependent

From the results in Table 1 it is clear that the inhibition efficiency of biomarker uptake is definitely cell type dependent. While a certain inhibitor protocol resulted in a good inhibition in one

cell line, it had no inhibiting effect in another one. For example, as shown in Fig. 4, 2 hrs incubation with 400 µM genistein inhibited the uptake of LacCer in HuH-7 and Cos-7 cells, but had no noticeable effect on the LacCer uptake by Vero and RPE cells. Each time, a comparison was made with the corresponding negative control in the absence of genistein (Fig. 4A till D). These control images show that after 10 min incubation, LacCer is mainly found in vesicular structures inside the cytoplasm, concentrated at the nuclear periphery. Fig. 4E till 4H show the uptake of LacCer after incubation with genistein. Numerous LacCer containing intracellular vesicles could be observed in Vero (Fig. 4F) and RPE cells (Fig. 4G). In contrast, almost no intracellular LacCer could be observed in HuH-7 (Fig. 4E) and Cos-7 (Fig. 4H) cells, indicating a cell type dependent inhibitory effect by genistein. Other examples of inhibitors which have a cell type dependent effect are nystatin and K^+-depletion. A 2 hrs treatment with 300 U/ml nystatin in OptiMEM could partially inhibit LacCer uptake in Cos-7 cells only. K^+-depletion inhibited the uptake of hTf in both RPE and HuH-7 cells, but not at all in Cos-7 and Vero cells.

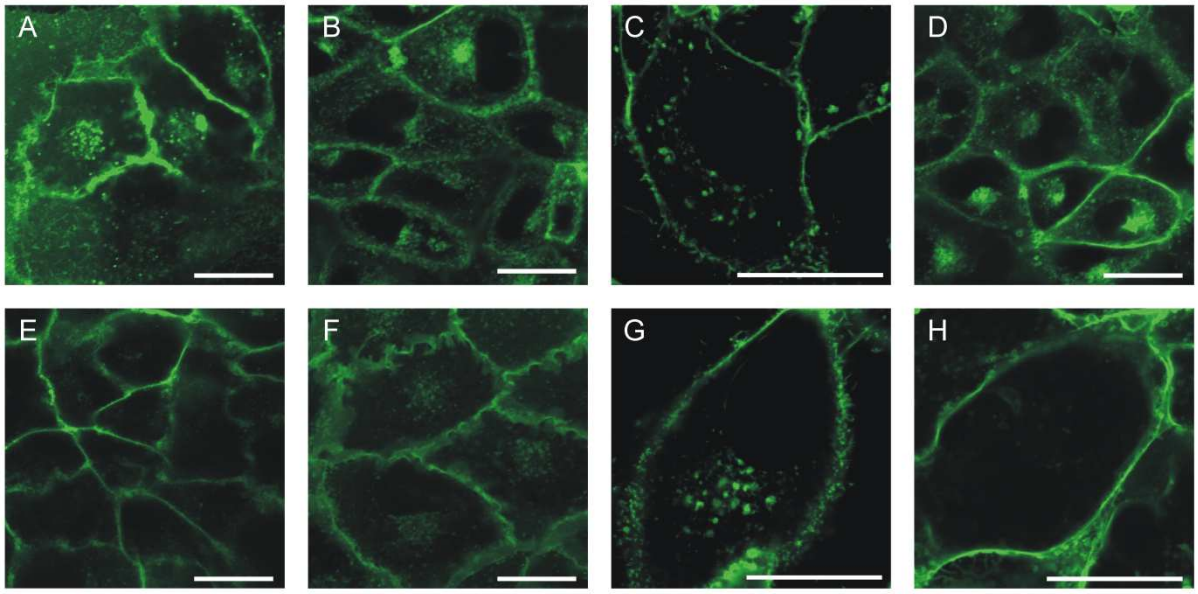

Figure 4. Cellular uptake of LacCer (green) by HuH-7 (A and E), Vero (B and F), RPE (C and G) and Cos-7 (D and H) cells. Images (A) till (D) are the control samples and (E) till (H) are the corresponding samples incubated with 400 µM genistein for 2 hrs. The scalebar represents 20 µm.

The inhibitor effect is not always as specific as claimed in literature

In the end, we would like to use the endocytosis inhibition protocols to have an idea about the endocytic pathways that are involved in the uptake of certain non-viral gene complexes. Therefore, it is necessary to evaluate the specificity of the applied inhibition protocol. This can be done by studying the effect of a certain inhibitor on the uptake of biomarkers which are expected not

to be blocked. Hence, in this research we tested the effect of the different inhibitors on the uptake of both hTf and LacCer biomarkers. If the inhibition protocol prevents the uptake of both hTf and LacCer, the inhibitor can be considered as nonspecific, limiting the application of the tested compound to study the internalization pathway of non-viral gene complexes. A summary of the specificity is represented in Table 1.

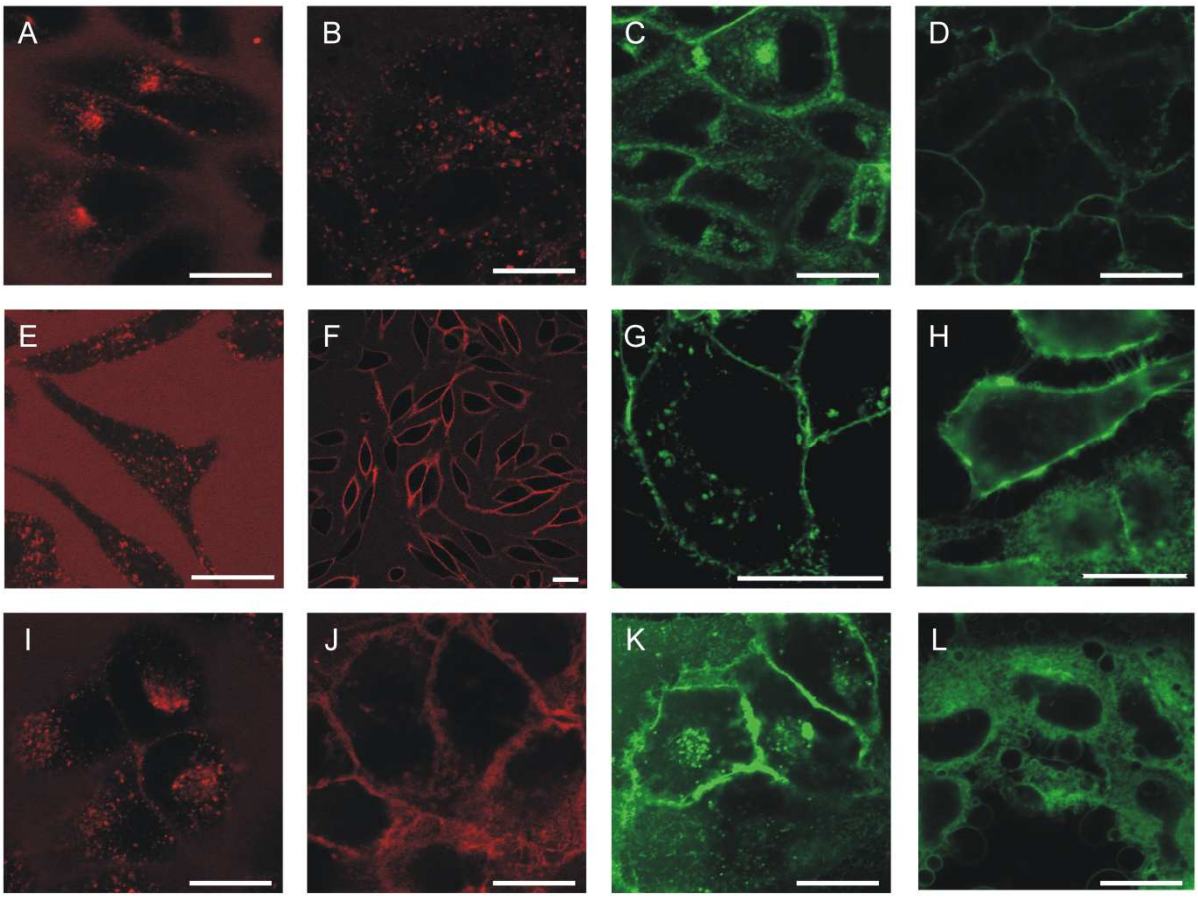

Figure 5. Effect of K^+-depletion on the cellular uptake of hTF (red) and LacCer (green) by Vero (A till D), RPE (E till H) and HuH-7 (I till L) cells. Images (A), (E) and (I) are the control samples for the LacCer uptake and (C), (G) and (K) for the hTF uptake. Images (B), (F), (J), (D), (H) and (L) are the corresponding samples after treatment with K^+-depletion. The scalebar represents 20 µm.

Despite what is often stated in literature, very few inhibitors exhibited specific inhibition of a single endocytic pathway in the studied cell lines. Based on our results, only the following protocols were shown to be specific (1) 2 hrs treatment of RPE and HuH-7 cells with 10 µg/ml chlorpromazine, (2) 5 µg/ml cytoD incubation during 30 min in all studied cell lines, (3) 2 hrs treatment of HuH-7 and Cos-7 cells with 400 µM genistein and (4) incubation with 10 µg/ml filipin during 2 hrs in all studied cell lines. It is for example clear that mBCD entirely lacks specificity. Although cyclodextrines have been used to specifically block caveolae-mediated endocytosis or lipid raft-mediated endocytosis (see Table 2), it is clear that incubation for 2 hrs with 5 mM mBCD blocks both CIE and CDE in the

four cell types which were studied (Table 1). Another example is K^+-depletion. The extraction of cellular potassium should, according to the literature, lead to specific CDE inhibition [43] (Table 2), but there is no specific CDE inhibition observed in any of the examined cell lines. Moreover, when evaluating the effect of K^+-depletion on Vero cells, the effect seems to be inversed, as CIE was clearly inhibited while CDE remained unaffected. Contrary to what is often claimed to be a specific CDE inhibitor, chlorpromazine was found to partially inhibit CIE uptake as well in Cos-7 cells (Table 1).

Table 2. Overview of the chemical compounds used to inhibit membrane traffic pathways and their application in studies on non-viral gene therapy

Agent	*Presumed effect*	*Comments*	*Original reference*	*Conditions*	*Cell type*	*Reference*
Chlorpromazine	Dissociation of clathrin and APs of PM	Pleiotropic effects, e.g. receptor recycling is affected Mechanism of action unknown Interacts with liposomal membranes	[44]	10 µg/ml 10 µg/ml, 30 min 10.66 µg/ml, 30 min 10 µg/ml, 30 min 10 µg/ml, 1 hr 7.5 µg/ml, 1 hr 10 µg/ml, 1 hr 10 µg/ml, 1 hr 20 µg/ml, 1 hr 10 µg/ml, 1 hr 35.5 µg/ml, 30 min	Cos-7 HepG2 HeLa A549 HuH-7, Cos-7 HeLa HUVEC Cos-7 Cos-7 Cos-7 CHO-DP12	[45] [46] [47] [48] [49] [49] [50] [50] [51] [52] [22]
Low potassium	Dissociation of clathrin of PM	Cell type differences	[43,53]	45 min in K^+-free buffer, wash 2 x with K^+-free buffer, 1 x with hypotonic buffer and 3 x with K^+-free buffer 1 x wash in K^+-free buffer, 1 x with hypotonic buffer, 3 x with K^+-free buffer	56FHTE8o$^-$	[54] [48]
Hypertonic medium	Same effect as K^+-depletion	Pleiotropic effects	[53,55]	0.45 M sucrose, 45 min	56FHTE8o$^-$	[54]
Monensin	Creates intracellular iso-pH		[56]	50 µM, 30 min, 4°C	HepG2	[46]
Chloroquine	Inhibits endosomal acidification	Leads to decrease in general endocytosis Leads to swelling of lysosomes and destabilisation of lysosomal membranes	[57]	100 µM, 0 min 200 µM, 20 min 500 µM, 30 min	K562 HUVEC Cos-7	[58] [50] [50]
Bafilomycin A1	V-ATPase inhibitor	Show stronger effects than chloroquine	[59,60]	125 nM, 30 min 175 nM 200 nM, 45 min 200 nM, 1 hr	HeLa HepG2 HUVEC Cos-7	[61] [62] [50] [50]
AlF_4	Blocks transport from ERC to PM		[13,63,64]			-
Jasplakinolide	binds and stabilizes actin		[65]			-
Latrunculine	Actin disruption		[66]			-
Cytochalasin B	Depolymerisation of actin filaments		[67]	5 µg/ml, 45 min	56FHTE8o$^-$	[54]

CytoD	Depolymerisation of actin filaments		[67]	20 µM, 30 min	Cos-7	[45]
				20 µMl	HepG2	[46]
				5 µM, 30 min	HeLa	[47]
				5 µM, 30 min	HUVEC	[50]
				10 µM, 30 min-5 hrs	Cos-7	[50]
				20 µM, 1 hr	HepG2	[68]
				20 µM, 1 hr	HeLa	[68]
				20 µM, 1 hr	EA.hy 926	[68]
Nocodazole	Depolymerisation of microtubules		[69]	33 µM	HepG2	[46]
				33 µM, 1 hr	B16-F10	[4]
				10 µM, 2 hrs	HUVEC	[50]
				15 µM, 2hrs	Cos-7	[50]
				10 µM, 60 min	Cos-7	[51]
Nystatin	Binds cholesterol in PM		[26]	25 µg/ml, 1 hr	Hek293, CHO	[70]
				25 µg/ml, 30 min	HeLa	[47]
				50 µg/ml, 45 min	ΣCFTE29o$^-$	[71]
Filipin III	Binds cholesterol in PM, inhibits uptake of CTB	Filipin cannot interact with with the cholesterol in coated pits Specificity might be lost at higher concentrations	[26]	1 µg/ml, 1 hr	Cos-7	[45]
				5 µg/ml, 1 hr	B16-F10	[4]
				5 µg/ml, 1 hr	Hek293, CHO, EA.hy 926	[70]
				5 µg/ml, 30 min	HeLa	[47]
				5 µg/ml, 30 min	A549, HeLa	[48]
				5 µg/ml, 45 min	ΣCFTE29o$^-$	[71]
				1 µg/ml, 1 hr	Cos-7, HeLa	[49]
				0.5 µg/ml, 1 hr	HuH-7	[49]
				10 µg/ml, 1 hr	HUVEC	[50]
				9 µg/ml, 1 hr	Cos-7	[50]
				1 µg/ml, 1 hr	Cos-7	[52]
				5 µg/ml, 30 min	CHO-DP12	[22]
Cyclodextrin	Extracts cholesterol out of PM	Changes in cell morphology	[7,72]	10 mM, 1 hr	Cos-7	[45]
				10 mM, 30 min	HepG2	[46]
				10 mM, 1 hr	Hek293, CHO, EA.hy 926	[70]
				5 mM, 30 min	HeLa	[47]
				6 mM, 15 min	HUVEC	[50]
				9 mM, 15 min	Cos-7	[50]
				164 µM, 15 min	Cos-7	[51]
				1 mM, 30 min	CHO-DP12	[22]
Genistein	Inhibits tyrosine-phosphorylation of cav-1 (inhibits cav and CDC42, not RhoA)		[24,73]	200 µg/ml, 30 min	HepG2	[46]
				200 µM, 1 hr	B16-F10	[4]
				200 µM, 30 min	A549	[48]
				200 µM, 1 hr	Cos-7	[51]
				200 µM, 30 min	CHO-DP12	[22]
Staurosporin	Inhibits PKC (inhibits cav)		[74]	200 nM	HeLa	[75]
Dynasore	Inhibits dynamin		[76]			-
Clostridium toxin B	Inhibits Rho GTPAse inhibitor, no effect on cav		[77] [78]			-
Amiloride and derivatives	Inhibits Na^+/H^+ ion exchange in PM and so membrane ruffling	More specific than PI 3-kinase inhibitors Lowers the cytoplasmic pH	[79,80]	100 µM, 5 min	HepG2	[46]
				10 µM, 1 hr	B16-F10	[4]
				5 mM, 30 min	HeLa	[47]
				250 µM, 30 min	HUVEC, Cos-7	[50]
				50 µM, 1 hr	Cos-7	[81]
				3 mM, 30 min	CHO-DP12	[22]
PI 3-kinase inhibitors: wortmannin,	Inhibits fusion of two membrane protrusions (blocks PI 3-kinase)	Inhibits evenly fusion of endosomes, irreversible Has influence on membrane recruitment of Rab5	[82]	100 nM, 30 min	HepG2	[46]
				100 nM, 1 hr	EA.hy 926	[68]
				30 nM, 1 hr	HUVEC, Cos-7	[50]
				50 nM, 1 hr	Cos-7	[51]
LY294002		More specific than	[83]	50 µM, 1 hr	HUVEC, Cos-7	[50]
			[84]	50 µM, 1 hr	Hek293, CHO,	

		wortmannin, reversible		50 µM, 1 hr	EA.hy 926 Cos-7 [51,68]
Antimycin A + NaF + NaN_3	Restricts metabolic activity of the cell		[85]	1 µg/ml + 10 mM + 0.1 %, 30 min	HeLa [61]
Z-Phe-Phe-Gly	Fusion inhibiting peptide		[86]	100 µM, 30 min	A431 [87]

cav-1 : caveoline-1; AP: adaptor proteins; CTB: cholera toxin subunit B; PKC: protein kinase C; PI 3-kinase: phosphatidylinositol-3-kinase; LY294002: 2-(4-morpholinyl)-8-phenyl-4H-1-benzopyran-4-one

The application of inhibitors can have pronounced effects on cellular morphology

Besides the risk for cytotoxic effects, nonspecific inhibition of endocytic pathways and cell type dependent specificity and efficiency, several other pronounced side effects have been reported as summarized in Table 2. Although we did not evaluate these side effects by biochemical assays in this work, from our DIC images we can clearly observed major effects of the inhibitors on the morphology of the cells, which did not always correlate with the cytotoxic effects displayed in Fig. 2.

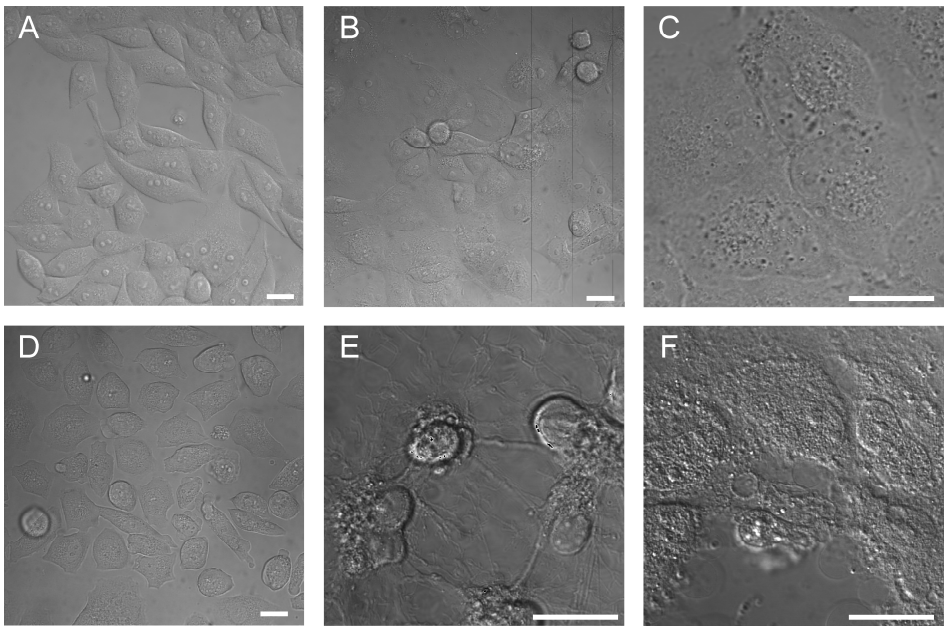

Figure 6. DIC images of RPE (A and D), Cos-7 (B and E) and HuH-7 (C and F) cells before (A till C) and after (D till F) exposure to different endocytosis inhibitors: (D) chlorpromazine (10 µg/ml), (E) cytoD (5 µg/ml) and (F) K^+-depletion. The scalebar represents 20 µm.

Fig. 6 shows the morphological effects on the Cos-7 cells after (1) K^+-depletion on the Cos-7,cells (2) cytoD (5 µg/ml, 30 min) on the HuH-7 cells and (3) chlorpromazine (10 µg/ml, 2 hrs) on the RPE cells. These morphological effects seem to be very pronounced for each condition and were similar for all tested cell lines.

DISCUSSION

A thorough mechanistic understanding of the intracellular pharmacokinetics, which is mainly determined by the endocytic pathways used by the gene carrier complexes, is of great importance for the design of efficient non-viral gene delivery carriers. Quantitative insight into the contribution of different endocytic pathways to the cellular uptake of carriers can be very helpful to achieve this goal since it will allow to correlate the effects of specific carrier characteristics with differences in intracellular processing. The internalization and post-endocytic trafficking of gene carrier complexes can be studied by different approaches. Besides imaging the intracellular localization at different time points by the use of electron microscopy, several other methods have been described. A very powerful strategy to define the rate-limiting steps in transfection is to quantify the fraction of therapeutic DNA in the different intracellular compartments. This can be achieved by subcellular fractionating [54], by confocal image assisted three-dimensional integrated quantification (CIDIC) [88], by particle tracking [89] or by modelling [90].

To define association with a certain intracellular compartment one can also use fluorescent dual colour colocalization studies. In this approach, the accuracy of the achieved information relies on the specificity and proper use of the fluorescently tagged biological marker, which is preferably associated with a certain pathway. Examples are hTF for CDE [7] and LacCer for CIE [27]. Although some of the available biomarkers can be used to specifically label a certain endocytic pathway, it must be stressed that the post-endocytic itinerary can show a lot of variability depending on the properties of the internalized macromolecule or structure. Additionally, it is known that intense interactions between the different pathways can occur, e.g. LacCer is specifically taken up via CIE, but after less than 15 min, colocalization with hTf containing vesicles can be observed, which are believed to be mainly the SEs [13]. This is also seen in own experiments (data not shown). Furthermore, these probes may also themselves affect the localization and/or metabolism of the targeted compartment or structure that they are used as a reporter for, as reviewed in [91]. However, careful application of these probes, especially when several ones are being combined, can lead to accurate information regarding intracellular trafficking of gene complexes. Finally, it must be said that the arsenal on available reliable biomarkers which are specifically taken up are very limited.

Alternatively, quantification of the uptake and the intracellular trafficking of gene complexes can also be established by perturbing specific cellular uptake mechanisms. This can be achieved by using endocytosis inhibitors or by creating transient or stable knock out mutants; the latter two of which are often referred to as ‘biological inhibitors’. Transient knock outs can be created by using the RNA interference (RNAi) silencing mechanism or by introducing dominant negative proteins. In the

first strategy crucial genes involved in a specific uptake pathway are silenced, which can lead to the inhibition of a specific pathway [92-95]. In the second strategy, cells are transiently transfected or transduced with DNA which encodes for a dominant negative protein that interferes with a specific uptake process, again resulting in uptake inhibition. Several examples of transient knock outs or biological inhibitors are summarized in Table 3.

Table 3. Biological inhibitors used to study endocytosis and post-endocytic trafficking

Strategy	*Presumed effect*	*Original reference*	*Gene therapy related reference*
DN-Eps15	Inhibits CDE	[96]	DN-Eps15
DN-AP-2 (D3Δ2)	Inhibits CDE	[96]	DN-AP-2 (D3Δ2)
DN-AP180	Inhibits CDE	[97]	DN-AP180
DN-dyn2 (K44A)	Blocks dynamin-dependent endocytosis	[27,98-101]	DN-dyn2 (K44A)
DN-cav-1	Inhibits caveolae-mediated CIE	[3]	DN-cav-1
DN-clathrin HC	Inhibits CDE	[102]	DN-clathrin HC
KO-AP-2	Inhibits CDE	[93]	KO-AP-2
KO-clathrin HC	Inhibits CDE	[93]	KO-clathrin HC
KO-epsin	Inhibits CDE	[95]	KO-epsin
KO-cav-1	Inhibits caveolae-mediated CIE	[92]	KO-cav-1
DN-ARF6	Inhibits ARF6-regulated CIE	[3]	DN-ARF6
DN-RhoA	Inhibits RhoA-regulated CIE	[3]	DN-RhoA
DN-CDC42	Inhibits CDC42-regulated CIE	[3]	DN-CDC42
DN-Rab5(S34N)	Inhibits trafficking from early endocytic vesicles to SE	[103]	DN-Rab5(S34N)

DN: dominant negative; KO: RNAi knock out

In this paper, we have focused on the use of inhibitors to selectively block different endocytic pathways. In the 90's, a number of pharmacological treatments have been discovered that differentially affect the pinocytic pathways [104]. In Table 2 a summary is given of the most important chemical compounds which have been used in literature to interfere with endocytic pathways, together with references out the research field of non-viral gene delivery with the therein used concentration and cell type. Although the ease of use makes these inhibitors very popular to study endocytic pathways, there are some serious considerations to be made before using them, as it can be extremely tricky to extrapolate the inhibition protocols from literature to your specific experimental setup. As we have shown in this paper, the treatment with endocytosis inhibitors exhibits extreme cell type variations, lacks in several cell lines specificity and often causes side effects on the cellular morphology.

First, we have clearly shown that almost all tested inhibitors exhibit cell type dependent cytotoxic effects. E.g. high chlorpromazine concentrations had no effect on the RPE cell viability, while all other tested cell lines, especially the Cos-7 cells, appeared to be very sensitive to it. In contrast, filipin was only toxic for RPE cells and also mBCD showed cell specific cytotoxicity, especially at high concentrations. Finally, although the effect was limited, K^+-depletion decreased the cell viability of both HuH-7, Cos-7 and Vero cells, but not of RPE cells. Taking in account these observed toxicity effects, using endocytosis inhibitors to study the uptake of non-viral gene complexes will be even more complicated, as it is very likely that the cells will not survive the stress of both pre-incubation with the inhibitor and a subsequent incubation with often cytotoxic cationic gene complexes again in the presence of inhibitor. Secondly, very few endocytic inhibitors are specific to a single pathway, making it necessary to implement different types of inhibition to determine the contribution of a specific cell entry pathway to non-viral uptake. E.g. mBCD showed (partial) inhibition of both CDE and CIE in all tested cell lines, while Huth et al. have reported an enhanced liposome uptake after mBCD treatment [50]. In our experiments, some treatments did show good specificity, e.g. filipin and chlorpromazine, although the first treatment was shown to be slightly toxic in case of RPE cells and the latter one even in all tested cell lines, again limiting the reliability of the observed effects. Finally, we have also shown that most inhibitors exhibit pronounced effects on the cellular morphology. For several inhibitors it is already known that they exhibit side effects, including effects on post-endocytic trafficking of gene carrier complexes [45]. Therefore, one must be vigilant of possible side effects when using endocytosis inhibitors, as this can often lead to contradictory results [105]. It is e.g. known that amyloride lowers the cytosolic pH [106], while other examples are summarized in Table 2, column 3. It is clear that a detailed knowledge of the effects of inhibitors on cells is an absolute prerequisite for a reliable interpretation of the obtained results.

Regardless the approach you choose, the complete inhibition of endocytic pathway will rarely be achieved. It should also be realized that different pathways may be operating simultaneously or may be upregulated when one pathway is blocked, i.e. inhibition of one route may lead to an increased uptake via an alternative route [107]. Finally it should be noted that the existence of unknown endocytic processes or even worse, the induction of non-natural pathways due to the cellular manipulations, cannot be excluded. Based on our results, we can state that performing the correct control experiments to test the efficacy of the inhibitors is of key importance to be able to come to reliable conclusions. In literature, however, there are only very few publications in which the efficiency and/or specificity of endocytosis inhibitors have been tested [47-49].

While it is clear that endocytosis inhibitors should be used with care, we still believe they provide for an elegant and practical way to study the role of specific endocytic pathways, especially when they are combined with other approaches like biological inhibitors or colocalization studies. It

will be very important for new and hopefully more specific endocytosis inhibitors to become available, such as e.g. the recently discovered dynasore [76]. Also the further development of new specific biomarkers will be useful and even necessary. It has for instance been shown that cholera toxin, which was thought to be a specific biomarker for caveolae-mediated endocytosis, is not exclusively taken up via caveolae [25], this is in contrast to others who claim that the cholera toxin uptake is not inhibited by chlorpromazine in Cos-7 [50]. We expect that new suitable biomarkers will become available when recombinant proteins will be found which are specifically taken up through macropinocytosis, CIE or caveolae-mediated uptake.

CONCLUSION

In this work we have given experimental evidence in combination with information from literature that care should be taken when using chemical inhibitors to study endocytic processes. The inhibitory effect is extremely cell type dependent and so is the concentration threshold of cellular toxicity. Moreover, the chemical compounds can exhibit severe side effects on cellular morphology and the inhibition is not always as specific for a certain endocytic pathway as is sometimes stated in literature. In any case it is clear that the specificity is cell type dependent. Therefore, treatments with endocytosis inhibitors which have been applied successfully on one cell line should not be blindly transferred to other cell lines without performing the necessary control experiments. On the other hand we would like to point out that the use of chemical inhibitors for studying intracellular trafficking of gene carrier complexes does not have to be banned completely as long as proper care is taken. For different cell types the inhibitor efficacy and specificity can be tested by using suitable biomarkers. To conclude, we plead for an approach where several complementary methods are combined, such as the combination of inhibition experiments with biomarker colocalization studies. We believe this is the only way to avoid erroneous conclusions and to come to reliable information regarding intracellular trafficking of gene carriers.

ACKNOWLEDGMENTS

Dries Vercauteren is a doctoral fellow of the Institute for the Promotion of Innovation through Science and Technology in Flanders (IWT), Belgium. Niek N. Sanders is supported by the Fund for Scientific Research - Flanders (FWO). The European Commission is thanked for funding through the Integrated 6th Framework Programme MediTrans.

REFERENCES

(1) Wattiaux R., Laurent N., Wattiaux-De Coninck S., & Jadot M. Endosomes, lysosomes: their implication in gene transfer. *Advanced Drug Delivery Reviews* **2000** 41(2) 201-208.

(2) Conner S.D. & Schmid S.L. Regulated portals of entry into the cell. *Nature* **2003** 422(6927) 37-44.

(3) Mayor S. & Pagano R.E. Pathways of clathrin-independent endocytosis. *Nat Rev Mol Cell Biol* **2007** 8(8) 603-612.

(4) Rejman J., Oberle V., Zuhorn I.S., & Hoekstra D. Size-dependent internalization of particles via the pathways of clathrin-and caveolae-mediated endocytosis. *Biochemical Journal* **2004** 377159-169.

(5) Mousavi S.A., Malerod L., Berg T., & Kjeken R. Clathrin-dependent endocytosis. *Biochemical Journal* **2004** 3771-16.

(6) Kirchhausen T. CLATHRIN. *Annual Review of Biochemistry* **2000** 69(1) 699-727.

(7) Rodal S.K., Skretting G., Garred O., Vilhardt F., van Deurs B., & Sandvig K. Extraction of Cholesterol with Methyl-beta -Cyclodextrin Perturbs Formation of Clathrin-coated Endocytic Vesicles. *Mol. Biol. Cell* **1999** 10(4) 961-974.

(8) Fujimoto L.M., Roth R., Heuser J.E., & Schmid S.L. Actin assembly plays a variable, but not obligatory role in receptor-mediated endocytosis in mammalian cells. *Traffic* **2000** 1(2) 161-171.

(9) Maxfield F.R. & Mcgraw T.E. Endocytic recycling. *Nature Reviews Molecular Cell Biology* **2004** 5(2) 121-132.

(10) Van Dyke R.W. Acidification of lysosomes and endosomes. *Subcell. Biochem.* **1996** 27331-360.

(11) Katzmann D.J., Odorizzi G., & Emr S.D. Receptor downregulation and multivesicular-body sorting. *Nature Reviews Molecular Cell Biology* **2002** 3(12) 893-905.

(12) Luzio J.P., Pryor P.R., & Bright N.A. Lysosomes: fusion and function. *Nat Rev Mol Cell Biol* **2007** 8(8) 622-632.

(13) Sharma D.K., Choudhury A., Singh R.D., Wheatley C.L., Marks D.L., & Pagano R.E. Glycosphingolipids internalized via caveolar-related endocytosis rapidly merge with the clathrin pathway in early endosomes and form microdomains for recycling. *J. Biol. Chem.* **2003** 278(9) 7564-7572.

(14) Simons K. & Toomre D. Lipid rafts and signal transduction. *Nature Reviews Molecular Cell Biology* **2000** 1(1) 31-39.

(15) Fra A.M., Williamson E., Simons K., & Parton R.G. Detergent-Insoluble Glycolipid Microdomains in Lymphocytes in the Absence of Caveolae. *J. Biol. Chem.* **1994** 269(49) 30745-30748.

(16) Fujimoto T., Kogo H., Nomura R., & Une T. Isoforms of caveolin-1 and caveolar structure. *J Cell Sci* **2000** 113(19) 3509-3517.

(17) Smart E.J., Graf G.A., McNiven M.A. *et al.* Caveolins, liquid-ordered domains, and signal transduction. *Molecular and Cellular Biology* **1999** 19(11) 7289-7304.

(18) Pelkmans L. Secrets of caveolae- and lipid raft-mediated endocytosis revealed by mammalian viruses. *Biochimica et Biophysica Acta-Molecular Cell Research* **2005** 1746(3) 295-304.

(19) Mundy D.I., Machleidt T., Ying Y.s., Anderson R.G.W., & Bloom G.S. Dual control of caveolar membrane traffic by microtubules and the actin cytoskeleton. *J Cell Sci* **2002** 115(22) 4327-4339.

(20) Pelkmans L., Burli T., Zerial M., & Helenius A. Caveolin-Stabilized Membrane Domains as Multifunctional Transport and Sorting Devices in Endocytic Membrane Traffic. *Cell* **2004** 118(6) 767-780.

(21) Parton R.G. & Richards A.A. Lipid rafts and caveolae as portals for endocytosis: New insights and common mechanisms. *Traffic* **2003** 4(11) 724-738.

(22) Wong A.W., Scales S.J., & Reilly D.E. DNA Internalized via Caveolae Requires Microtubule-dependent, Rab7-independent Transport to the Late Endocytic Pathway for Delivery to the Nucleus. *J. Biol. Chem.* **2007** 282(31) 22953-22963.

(23) Pelkmans L., Kartenbeck J., & Helenius A. Caveolar endocytosis of simian virus 40 reveals a new two-step vesicular-transport pathway to the ER. *Nature Cell Biology* **2001** 3(5) 473-483.

(24) Parton R.G., Joggerst B., & Simons K. Regulated internalization of caveolae. *J. Cell Biol.* **1994** 127(5) 1199-1215.

(25) Torgersen M.L., Skretting G., van Deurs B., & Sandvig K. Internalization of cholera toxin by different endocytic mechanisms. *J Cell Sci* **2001** 114(20) 3737-3747.

(26) Schnitzer J.E., Oh P., Pinney E., & Allard J. Filipin-Sensitive Caveolae-Mediated Transport in Endothelium - Reduced Transcytosis, Scavenger Endocytosis, and Capillary-Permeability of Select Macromolecules. *Journal of Cell Biology* **1994** 127(5) 1217-1232.

(27) Puri V., Watanabe R., Singh R.D. *et al.* Clathrin-dependent and -independent internalization of plasma membrane sphingolipids initiates two Golgi targeting pathways. *Journal of Cell Biology* **2001** 154(3) 535-547.

(28) Singh R.D., Puri V., Valiyaveettil J.T., Marks D.L., Bittman R., & Pagano R.E. Selective Caveolin-1-dependent Endocytosis of Glycosphingolipids. *Mol. Biol. Cell* **2003** 14(8) 3254-3265.

(29) Marks D.L., Singh R.D., Choudhury A., Wheatley C.L., & Pagano R.E. Use of fluorescent sphingolipid analogs to study lipid transport along thepathway endocytic. *Methods* **2005** 36(2) 186-195.

(30) Jones A.T. Macropinocytosis: searching for an endocytic identity and role in the uptake of cell penetrating peptides. *Journal of Cellular and Molecular Medicine* **2007** 11(4) 670-684.

(31) Grimmer S., van Deurs B., & Sandvig K. Membrane ruffling and macropinocytosis in A431 cells require cholesterol. *J Cell Sci* **2002** 115(14) 2953-2962.

(32) Hacker U., Albrecht R., & Maniak M. Fluid-phase uptake by macropinocytosis in Dictyostelium. *J Cell Sci* **1997** 110105-112.

(33) Swanson J.A. & Watts C. Macropinocytosis. *Trends in Cell Biology* **1995** 5(11) 424-428.

(34) Meier O. & Greber U.F. Adenovirus endocytosis. *Journal of Gene Medicine* **2004** 6S152-S163.

(35) Wadia J.S., Stan R.V., & Dowdy S.F. Transducible TAT-HA fusogenic peptide enhances escape of TAT-fusion proteins after lipid raft macropinocytosis. *Nature Medicine* **2004** 10(3) 310-315.

(36) Lai S.K., Hida K., Man S.T. *et al.* Privileged delivery of polymer nanoparticles to the perinuclear region of live cells via a non-clathrin, non-degradative pathway. *Biomaterials* **2007** 28(18) 2876-2884.

(37) Desjardins M. & Griffiths G. Phagocytosis: latex leads the way. *Current Opinion in Cell Biology* **2003** 15(4) 498-503.

(38) Khalil I.A., Kogure K., Akita H., & Harashima H. Uptake Pathways and Subsequent Intracellular Trafficking in Nonviral Gene Delivery. *Pharmacol Rev* **2006** 58(1) 32-45.

(39) Medina-Kauwe L.K., Xie J., & Hamm-Alvarez S. Intracellular trafficking of nonviral vectors. *Gene Ther* **2005** 12(24) 1734-1751.

(40) Banks G.A., Roselli R.J., Chen R., & Giorgio T.D. A model for the analysis of nonviral gene therapy. *Gene Therapy* **2003** 10(20) 1766-1775.

(41) Davis A.A., Bernstein P.S., Bok D., Turner J., Nachtigal M., & Hunt R.C. A Human Retinal-Pigment Epithelial-Cell Line That Retains Epithelial Characteristics After Prolonged Culture. *Investigative Ophthalmology & Visual Science* **1995** 36(5) 955-964.

(42) Widera A., Norouziyan F., & Shen W.C. Mechanisms of TfR-mediated transcytosis and sorting in epithelial cells and applications toward drug delivery. *Advanced Drug Delivery Reviews* **2003** 55(11) 1439-1466.

(43) Larkin J.M., Donzell W.C., & Anderson R.G. Potassium-dependent assembly of coated pits: new coated pits form as planar clathrin lattices. *J. Cell Biol.* **1986** 103(6) 2619-2627.

(44) Wang L.H., Rothberg K.G., & Anderson R.G. Mis-assembly of clathrin lattices on endosomes reveals a regulatory switch for coated pit formation. *J. Cell Biol.* **1993** 123(5) 1107-1117.

(45) Zuhorn I.S., Kalicharan R., & Hoekstra D. Lipoplex-mediated transfection of mammalian cells occurs through the cholesterol-dependent clathrin-mediated pathway of endocytosis. *J. Biol. Chem.* **2002** 277(20) 18021-18028.

(46) Goncalves C., Mennesson E., Fuchs R., Gorvel J.P., Midoux P., & Pichon C. Macropinocytosis of Polyplexes and Recycling of Plasmid via the Clathrin-Dependent Pathway Impair the Transfection Efficiency of Human Hepatocarcinoma Cells[ast]. *Mol Ther* **2004** 10(2) 373-385.

(47) Mano M., Teodosio C., Paiva A., Simoes S., & de Lima M.C.P. On the mechanisms of the internalization of S4(13)-PV cell-penetrating peptide. *Biochemical Journal* **2005** 390603-612.

(48) Rejman J., Bragonzi A., & Conese M. Role of clathrin- and caveolae-mediated endocytosis in gene transfer mediated by lipo- and polyplexes. *Molecular Therapy* **2005** 12(3) 468-474.

(49) von Gersdorff K., Sanders N.N., Vandenbroucke R., De Smedt S.C., Wagner E., & Ogris M. The internalization route resulting in successful gene expression depends on polyethylenimine both cell line and polyplex type. *Molecular Therapy* **2006** 14(5) 745-753.

(50) Huth U.S., Schubert R., & Peschka-Suss R. Investigating the uptake and intracellular fate of pH-sensitive liposomes by flow cytometry and spectral bio-imaging. *Journal of Controlled Release* **2006** 110(3) 490-504.

(51) van der Aa M.A.E.M., Huth U.S., Hafele S.Y. *et al.* Cellular uptake of cationic polymer-DNA complexes via caveolae plays a pivotal role in gene transfection in COS-7 cells. *Pharmaceutical Research* **2007** 24(8) 1590-1598.

(52) Vandenbroucke R.E., De Smedt S.C., Demeester J., & Sanders N.N. Cellular entry pathway and gene transfer capacity of TAT-modified lipoplexes. *Biochimica et Biophysica Acta-Biomembranes* **2007** 1768(3) 571-579.

(53) Hansen S.H., Sandvig K., & Vandeurs B. Clathrin and Ha2 Adapters - Effects of Potassium-Depletion, Hypertonic Medium, and Cytosol Acidification. *Journal of Cell Biology* **1993** 121(1) 61-72.

(54) Colin M., Maurice M., Trugnan G. *et al.* Cell delivery, intracellular trafficking and expression of an integrin-mediated gene transfer vector in tracheal epithelial cells. *Gene Therapy* **2000** 7(2) 139-152.

(55) Heuser J.E. & Anderson R.G. Hypertonic media inhibit receptor-mediated endocytosis by blocking clathrin-coated pit formation. *J. Cell Biol.* **1989** 108(2) 389-400.

(56) Tartakoff A.M. Perturbation of Vesicular Traffic with the Carboxylic Ionophore Monensin. *Cell* **1983** 32(4) 1026-1028.

(57) Gonzaleznoriega A., Grubb J.H., Talkad V., & Sly W.S. Chloroquine Inhibits Lysosomal-Enzyme Pinocytosis and Enhances Lysosomal Enzyme-Secretion by Impairing Receptor Recycling. *Journal of Cell Biology* **1980** 85(3) 839-852.

(58) Cotten M., Langle-Rouault F., Kirlappos H. *et al.* Transferrin-Polycation-Mediated Introduction of DNA into Human Leukemic Cells: Stimulation by Agents that Affect the Survival of Transfected DNA or Modulate Transferrin Receptor Levels. *PNAS* **1990** 87(11) 4033-4037.

(59) Bowman E.J., Siebers A., & Altendorf K. Bafilomycins: A Class of Inhibitors of Membrane ATPases from Microorganisms, Animal Cells, and Plant Cells. *PNAS* **1988** 85(21) 7972-7976.

(60) Drose S. & Altendorf K. Bafilomycins and concanamycins as inhibitors of V-ATPases and P-ATPases. *Journal of Experimental Biology* **1997** 200(1) 1-8.

(61) Simoes S., Slepushkin V., Pires P., Gaspar R., de Lima M.C.P., & Duzgunes N. Human serum albumin enhances DNA transfection by lipoplexes and confers resistance to inhibition by serum. *Biochimica et Biophysica Acta-Biomembranes* **2000** 1463(2) 459-469.

(62) Kichler A., Leborgne C., Coeytaux E., & Danos O. Polyethylenimine-mediated gene delivery: a mechanistic study. *Journal of Gene Medicine* **2001** 3(2) 135-144.

(63) Sternweis P.C. & Gilman A.G. Aluminum - A Requirement for Activation of the Regulatory Component of Adenylate-Cyclase by Fluoride. *Proceedings of the National Academy of Sciences of the United States of America-Biological Sciences* **1982** 79(16) 4888-4891.

(64) Sheff D.R., Daro E.A., Hull M., & Mellman I. The receptor recycling pathway contains two distinct populations of early endosomes with different sorting functions. *Journal of Cell Biology* **1999** 145(1) 123-139.

(65) Bubb M.R., Senderowicz A.M., Sausville E.A., Duncan K.L., & Korn E.D. Jasplakinolide, a cytotoxic natural product, induces actin polymerization and competitively inhibits the binding of phalloidin to F-actin. *J. Biol. Chem.* **1994** 269(21) 14869-14871.

(66) Coue M., Brenner S.L., Spector I., & Korn E.D. Inhibition of actin polymerization by latrunculin A. *FEBS Lett.* **1987** 213(2) 316-318.

(67) Sampath P. & Pollard T.D. Effects of Cytochalasin, Phalloidin, and Ph on the Elongation of Actin-Filaments. *Biochemistry* **1991** 30(7) 1973-1980.

(68) Manunta M., Nichols B.J., Hong Tan P., Sagoo P., Harper J., & George A.J.T. Gene delivery by dendrimers operates via different pathways in different cells, but is enhanced by the presence of caveolin. *Journal of Immunological Methods* **2006** 314(1-2) 134-146.

(69) Peterson J.R. & Mitchison T.J. Small molecules, big impact: A history of chemical inhibitors and the cytoskeleton. *Chemistry & Biology* **2002** 9(12) 1275-1285.

(70) Manunta M., Tan P.H., Sagoo P., Kashefi K., & George A.J.T. Gene delivery by dendrimers operates via a cholesterol dependent pathway. *Nucl. Acids Res.* **2004** 32(9) 2730-2739.

(71) Grosse S., Aron Y., Thevenot G., Francois D., Monsigny M., & Fajac I. Potocytosis and cellular exit of complexes as cellular pathways for gene delivery by polycations. *Journal of Gene Medicine* **2005** 7(10) 1275-1286.

(72) Subtil A., Gaidarov I., Kobylarz K., Lampson M.A., Keen J.H., & Mcgraw T.E. Acute cholesterol depletion inhibits clathrin-coated pit budding. *Proceedings of the National Academy of Sciences of the United States of America* **1999** 96(12) 6775-6780.

(73) Orlandi P.A. & Fishman P.H. Filipin-dependent inhibition of cholera toxin: Evidence for toxin internalization and activation through caveolae-like domains. *Journal of Cell Biology* **1998** 141(4) 905-915.

(74) Tamaoki T., Nomoto H., Takahashi I., Kato Y., Morimoto M., & Tomita F. Staurosporine, A Potent Inhibitor of Phospholipid/Ca++Dependent Protein-Kinase. *Biochemical and Biophysical Research Communications* **1986** 135(2) 397-402.

(75) Kopatz I., Remy J.S., & Behr J.P. A model for non-viral gene delivery: through syndecan adhesion molecules and powered by actin. *Journal of Gene Medicine* **2004** 6(7) 769-776.

(76) Macia E., Ehrlich M., Massol R., Boucrot E., Brunner C., & Kirchhausen T. Dynasore, a cell-permeable inhibitor of dynamin. *Developmental Cell* **2006** 10(6) 839-850.

(77) Aktories K., Schmidt G., & Just I. Rho GTPases as targets of bacterial protein toxins. *Biological Chemistry* **2000** 381(5-6) 421-426.

(78) Sabharanjak S., Sharma P., Parton R.G., & Mayor S. GPI-anchored proteins are delivered to recycling endosomes via a distinct cdc42-regulated, clathrin-independent pinocytic pathway. *Developmental Cell* **2002** 2(4) 411-423.

(79) Hewlett L.J., Prescott A.R., & Watts C. The Coated Pit and Macropinocytic Pathways Serve Distinct Endosome Populations. *Journal of Cell Biology* **1994** 124(5) 689-703.

(80) Dangoria N.S., Breau W.C., Anderson H.A., Cishek D.M., & Norkin L.C. Extracellular simian virus 40 induces an ERK/MAP kinase-independent signalling pathway that activates primary response genes and promotes virus entry. *Journal of General Virology* **1996** 772173-2182.

(81) Walsh M., Tangney M., O'Neill M.J. *et al.* Evaluation of Cellular Uptake and Gene Transfer Efficiency of Pegylated Poly-L-lysine Compacted DNA: Implications for Cancer Gene Therapy. *Mol. Pharmaceutics* **2006** 3(6) 644-653.

(82) Araki N., Johnson M.T., & Swanson J.A. A role for phosphoinositide 3-kinase in the completion of macropinocytosis and phagocytosis by macrophages. *Journal of Cell Biology* **1996** 135(5) 1249-1260.

(83) Arcaro A. & Wymann M.P. Wortmannin Is A Potent Phosphatidylinositol 3-Kinase Inhibitor - the Role of Phosphatidylinositol 3,4,5-Trisphosphate in Neutrophil Responses. *Biochemical Journal* **1993** 296297-301.

(84) Vlahos C.J., Matter W.F., Hui K.Y., & Brown R.F. A Specific Inhibitor of Phosphatidylnositol 3-Kinase, 2-(4-Morpholinyl)-8-Phenyl-4H-1-Benzopyran-4-One (Ly294002). *J. Biol. Chem.* **1994** 269(7) 5241-5248.

(85) Lee K.D., Nir S., & Papahadjopoulos D. Quantitative-Analysis of Liposome-Cell Interactions Invitro - Rate Constants of Binding and Endocytosis with Suspension and Adherent J774-Cells and Human Monocytes. *Biochemistry* **1993** 32(3) 889-899.

(86) Kelsey D.R., Flanagan T.D., Young J., & Yeagle P.L. Peptide Inhibitors of Enveloped Virus-Infection Inhibit Phospholipid Vesicle Fusion and Sendai Virus Fusion with Phospholipid-Vesicles. *J. Biol. Chem.* **1990** 265(21) 12178-12183.

(87) Almofti M.R., Harashima H., Shinohara Y., Almofti A., Baba Y., & Kiwada H. Cationic liposome-mediated gene delivery: Biophysical study and mechanism of internalization. *Archives of Biochemistry and Biophysics* **2003** 410(2) 246-253.

(88) Akita H., Ito R., Khalil I.A., Futaki S., & Harashima H. Quantitative three-dimensional analysis of the intracellular trafficking of plasmid DNA transfected by a nonviral gene delivery system using confocal laser scanning microscopy. *Molecular Therapy* **2004** 9(3) 443-451.

(89) Suh J., Wirtz D., & Hanes J. Efficient active transport of gene nanocarriers to the cell nucleus. *Proceedings of the National Academy of Sciences of the United States of America* **2003** 100(7) 3878-3882.

(90) Dinh A.T., Pangarkar C., Theofanous T., & Mitragotri S. Understanding intracellular transport processes pertinent to synthetic gene delivery via stochastic simulations and sensitivity analyses. *Biophys. J.* **2007** 92(3) 831-846.

(91) Watson P., Jones A.T., & Stephens D.J. Intracellular trafficking pathways and drug delivery: fluorescence imaging of living and fixed cells. *Advanced Drug Delivery Reviews* **2005** 57(1) 43-61.

(92) Nichols B.J. A distinct class of endosome mediates clathrin-independent endocytosis to the Golgi complex. *Nature Cell Biology* **2002** 4(5) 374-378.

(93) Hinrichsen L., Harborth J., Andrees L., Weber K., & Ungewickell E.J. Effect of clathrin heavy chain- and alpha -adaptin specific small interfering RNAs on endocytic accessory proteins and receptor trafficking in HeLa cells. *J. Biol. Chem.* **2003**M307290200.

(94) Huang F.T., Khvorova A., Marshall W., & Sorkin A. Analysis of clathrin-mediated endocytosis of epidermal growth factor receptor by RNA interference. *J. Biol. Chem.* **2004** 279(16) 16657-16661.

(95) Vanden Broeck D. & De Wolf M.J.S. Selective blocking of clathrin-mediated endocytosis by RNA interference: epsin as target protein. *Biotechniques* **2006** 41(4) 475-484.

(96) Benmerah A., Bayrou M., Cerf-Bensussan N., & utry-Varsat A. Inhibition of clathrin-coated pit assembly by an Eps15 mutant. *J Cell Sci* **1999** 112(9) 1303-1311.

(97) Ford M.G.J., Pearse B.M.F., Higgins M.K. *et al.* Simultaneous binding of PtdIns(4,5)P-2 and clathrin by AP180 in the nucleation of clathrin lattices on membranes. *Science* **2001** 291(5506) 1051-1055.

(98) Damke H., Baba T., Vanderbliek A.M., & Schmid S.L. Clathrin-Independent Pinocytosis Is Induced in Cells Overexpressing A Temperature-Sensitive Mutant of Dynamin. *Journal of Cell Biology* **1995** 131(1) 69-80.

(99) Pelkmans L., Puntener D., & Helenius A. Local actin polymerization and dynamin recruitment in SV40-induced internalization of caveolae. *Science* **2002** 296(5567) 535-539.

(100) Nabi I.R. & Le P.U. Caveolae/raft-dependent endocytosis. *J. Cell Biol.* **2003** 161(4) 673-677.

(101) Damke H., Baba T., Warnock D.E., & Schmid S.L. Induction of mutant dynamin specifically blocks endocytic coated vesicle formation. *J. Cell Biol.* **1994** 127(4) 915-934.

(102) Liu S.H., Marks M.S., & Brodsky F.M. A Dominant-negative Clathrin Mutant Differentially Affects Trafficking of Molecules with Distinct Sorting Motifs in the Class II Major Histocompatibility Complex (MHC) Pathway. *J. Cell Biol.* **1998** 140(5) 1023-1037.

(103) Roberts R.L., Barbieri M.A., Pryse K.M., Chua M., & Stahl P.D. Endosome fusion in living cells overexpressing GFP-rab5. *J Cell Sci* **1999** 112(21) 3667-3675.

(104) Lamaze C. & Schmid S.L. The Emergence of Clathrin-Independent Pinocytic Pathways. *Current Opinion in Cell Biology* **1995** 7(4) 573-580.

(105) Zuhorn I.S., Engberts J.B.F.N., & Hoekstra D. Gene delivery by cationic lipid vectors: overcoming cellular barriers. *European Biophysics Journal with Biophysics Letters* **2007** 36(4-5) 349-362.

(106) Comolli R., Zanoni L., Mauri C., & Leonardi M.G. Amiloride Inhibits Protein-Synthesis and Lowers the Intracellular Ph in Exponential Growing Yoshida Rat Ascites Hepatoma (Ah 130)-

Cells - Evidence for A Role of the Na+/H+ Exchanger. *Cell Biology International Reports* **1985** 9(11) 1017-1025.

(107) Hoekstra D., Rejman J., Wasungu L., Shi F., & Zuhorn I. Gene delivery by cationic lipids: in and out of an endosome. *Biochemical Society Transactions* **2007** 3568-71.

Chapter 5

Prolonged Gene Silencing in Hepatoma Cells & Primary Hepatocytes after siRNA Delivery with Biodegradable PbAEs

This chapter is *in revision*:

Roosmarijn E. Vandenbroucke[1], Bruno. G. De Geest[1], Stefan Bonné[2], Mathieu Vinken[3], Tamara Van Haecke[3], Harry Heimberg[2], Ernst Wagner[4], Vera Rogiers[3], Stefaan C. De Smedt[1], Joseph Demeester[1] and Niek N. Sanders[1]; *Journal of Gene Medicine*

[1] Laboratory of General Biochemistry and Physical Pharmacy, Ghent University, Harelbekestraat 72, B-9000 Ghent, Belgium.

[2] Diabetes Research Center, Vrije Universiteit Brussel, Laarbeeklaan 103, B-1090 Brussels, Belgium.

[3] Department of Toxicology, Dermato-Cosmetology and Pharmacognosy, Vrije Universiteit Brussel, Laarbeeklaan 103, B-1090 Brussels, Belgium.

[4] Department of Pharmacy, Ludwig-Maximilians-Universität München, Butenandtstrasse 5-13, D-81377 Munich, Germany.

ABSTRACT

SiRNA mediated inhibition of oncogenes or viral genes may offer great opportunities for the treatment of several diseases such as hepatocellular carcinoma and viral hepatitis. However, the development of siRNAs as therapeutic agents strongly depends on the availability of safe and effective intracellular delivery systems. Poly(β-amino esters) (PbAEs) are, in contrast to many other cationic polymers evaluated in siRNA delivery, biodegradable into smaller, non-toxic molecules. We show for the first time that PbAE:siRNA complexes, containing 1,4-butanediol (PbAE1) or 1,6-hexanediol (PbAE2) diacrylate-based polymers, induced efficient gene silencing in both hepatoma cells and primary hepatocytes without causing significant cytotoxicity. Furthermore, carriers that slowly release the siRNA into the cytoplasm and hence induce a prolonged gene silencing are of major clinical interest, especially in fast dividing tumour cells. Therefore, we also studied the duration of gene silencing in the hepatoma cells and found that it was maintained for at least 5 days after siRNA delivery with PbAE2, the polymer with the slowest degradation kinetics. From the time-dependent cellular distribution of these PbAE:siRNA complexes we suggest that the slowly degrading PbAE2 causes a sustained endosomal release of siRNA during a much longer period than PbAE1. This may support the hypothesis that the endosomal release mechanism of PbAE:siRNA complexes is based on an increase of osmotic pressure in the endosomal vesicles after polymer hydrolysis. In conclusion, our results show that both PbAEs, and especially PbAE2, open up new perspectives for the development of efficient biodegradable siRNA carriers suitable for clinical applications.

Chapter 5

Prolonged Gene Silencing in Hepatoma Cells & Primary Hepatocytes after siRNA Delivery with Biodegradable PbAEs

INTRODUCTION

Hepatocellular carcinoma (HCC) is worldwide one of the most prevalent human cancers, with ~600 000 new cases diagnosed annually and almost as many deaths [1]. For the vast majority of HCC cases no effective therapy is available. Hence, new treatment approaches for HCC are urgently needed [2]. The major cause of HCC is chronic hepatitis B (HBV) and hepatitis C virus (HCV) infection. The former can be prevented by vaccination and also different treatments are currently available, e.g. with nucleo(s)(t)ide analogues [3]. In contrast, there is no vaccine available against HCV infection and all HCV treatments so far rely on the antiviral activity of pegylated interferon alfa (IFN-α) that is administered alone or in combination with ribavirin [4]. Unfortunately, only a part of the HCV patients clear the virus during therapy and for the non-responders currently no alternative treatment exists [5]. Clearly, more effective treatments are needed against HCV and HCC. Therefore, the selective inhibition of highly active genes involved in liver oncogenesis [6] or HCV genes involved in viral replication [7-14] via RNA interference (RNAi) may offer great improvement in the treatment of HCC and HCV infections.

RNAi is a naturally occurring post-transcriptional sequence-specific gene silencing mechanism that is initiated by double-stranded RNAs (dsRNAs) that are homologous in sequence to the target mRNA [15]. These dsRNAs are enzymatically processed into 21-22 nucleotide small interfering RNAs (siRNAs) by the RNase III-like cellular enzyme Dicer [16]. The generated siRNAs are subsequently incorporated into a silencing complex called RNA-induced silencing complex (RISC) that scans and cleaves mRNA in a sequence-specific manner [17].

Therapeutic RNAi applications mainly depend on the availability of safe delivery systems that cause a sufficient cellular delivery of siRNA. DNA molecules encoding short hairpin RNAs (shRNAs)

that are subsequently processed by Dicer into siRNAs, are often used to demonstrate the therapeutic potential of RNAi. Both viral and non-viral carriers have been used to deliver these DNAs. However, viral delivery of DNA encoding shRNA is, due to safety and production concerns, not feasible for therapeutic applications. Non-viral carriers are no suitable alternative as they lack the ability to efficiently deliver DNA into the nucleus [18]. Additionally, it was suggested that HCV has evolved mechanisms to inhibit Dicer-dependent cleavage of longer dsRNAs like shRNAs [19,20]. Therefore, to avoid the necessity of nuclear uptake involved with DNA delivery and safety concerns involved with viral carriers, the most desirable approach seems to be the cytoplasmic delivery of synthetic siRNAs by means of non-viral carriers. So far, non-viral carriers for delivering synthetic siRNA are mostly based on transfection with cationic lipids [21-25]. Cationic polymers, such as polyethylenimine (PEI) and chitosan, have also been tested as delivery agents [26-29] but they are often less efficient [30] and more cytotoxic [31].

Poly(β-amino esters) (PbAEs) are polyamines that are synthesized by Michael addition of either primary amines or bis (secondary amines) to diacrylate esters (Fig. 1A) [32]. PbAEs are fully biodegradable via hydrolysis of their backbone esters to yield small molecular weight bis(β-amino acid) and diol products, which along with the parent polymer are significantly less toxic than many other polycations, such as PEI and poly(L-lysine) [33]. Anderson et al. identified a library of PbAEs that transfect pDNA in Cos-7 cells as good as or even better than PEI [34]. Additionally, several of the synthesized PbAEs were shown to be effective for *in vivo* pDNA delivery [35-37]. Therefore, in this work, different PbAEs were synthesized and for the first time their capacity to deliver siRNA and to evoke a biological siRNA effect was tested. Two PbAEs that successfully delivered the siRNA in the cells were identified: PbAE1 (polymer 1; Fig. 1B) and PbAE2 (polymer 2; Fig. 1C). These were obtained by conjugation of respectively 1,4-butanediol diacrylate (PbAE1) and 1,6-hexanediol diacrylate (PbAE2) to 4,4'-trimethylenedipiperidine. Both polymers showed a strong gene silencing effect in both human hepatoma cells and primary rat hepatocytes. Furthermore, in contrast to PbAE1, PbAE2 was able to induce a prolonged gene silencing effect in the hepatoma cells.

MATERIALS & METHODS

Materials

4,4'-Trimethylenedipiperidine, anhydrous dichloromethane (CH_2Cl_2), tetrahydrofurane (THF), triethylamine, insulin, glucagon, kanamycin monosulfate, streptomycin sulfate and ampicillin sodium salt were purchased from Sigma-Aldrich (Bornem, Belgium). Hydrocortisone hemisuccinate came

from Upjohn (Windsor, United Kingdom). 1,4-Butanediol diacrylate and 1,6-hexanediol diacrylate were purchased from Alfa Aesar Organics (Karlsruhe, Germany). SiRNA against firefly (Photinus pyralis) luciferase (pGL3), Alexa488-labelled pGL3 siRNA, negative control siRNA and jetSI™-ENDO were purchased from Eurogentec (Seraing, Belgium). All siRNAs were purchased in their annealed form, dissolved in RNase free water at a concentration of 20 µM, aliquoted and stored at -80°C. Dulbecco's modified Eagle medium (DMEM), OptiMEM, L-glutamine (L-Gln), heat-inactivated fetal bovine serum (FBS), G418 (geneticine) and penicillin/streptomycin (P/S) were obtained from Invitrogen (Merelbeke, Belgium).

Synthesis of PbAE1 and PbAE2

All glassware was flame-dried under vacuum before use. 37.8 mmol 1,4-butanediol diacrylate (in case of PbAE1) or 1,6-hexanediol diacrylate (in case of PbAE2) and 37.8 mmol 4,4'-trimethylenedipiperidine were separately dissolved in 50 ml CH_2Cl_2. The 4,4'-trimethylenedipiperidine solution was added dropwise to the 1,4-butanediol diacrylate (or 1,6-hexanediol diacrylate) solution under vigorous stirring. The reaction mixture was placed in an oil bath at 50°C and the polymerisation was allowed to proceed during 48 hrs under a nitrogen atmosphere. After cooling to room temperature, the reaction product was precipitated in diethyl ether saturated with HCl. The precipitate was filtered and thoroughly washed with diethyl ether. A white powder was obtained after overnight drying under vacuum. The molecular weight of the polymers was determined by size exclusion chromatography using a Waters GPC system equipped with two PLgel 5 micron MIXED-D, 300 x 7.5 mm columns (Polymer Laboratories, St.-Katelijne-Waver, Belgium). THF / 0.1 M triethylamine was used as mobile phase at a flow rate of 1 ml/min. The molecular weight of the polymers was calculated relative to polystyrene standards. ^{1}H-NMR (300 mHz) spectra were recorded on a Varian Mercury 300 spectrometer in $CDCl_3$ as solvent. The obtained chemical shifts δ were 4.12 (4H), 2.87 (4H), 2.52 (4H), 1.97 (4H), 2.63 (8H), 1.16 (12H) and 4.06 (4H), 2.91 (4H), 2.71 (4H), 2.55 (4H), 2.01 (4H), 1.65 (8H), 1.37 (4H), 1.22 (12H) for PbAE1 and PbAE2, respectively.

Preparation of siRNA complexes

The synthesized PbAEs were dissolved in acetate buffer (100 mM, pH 5.4) at different concentrations depending on the desired nitrogen to phosphate (N:P) ratio (10:1, 20:1 and 30:1) of the PbAE:siRNA complexes and prior use filtered through a 0.22 µm membrane syringe filter. The PbAE:siRNA complexes were formed by adding an equal volume of PbAE solution to 0.5 µM siRNA,

followed by vigorously mixing. The resulting PbAE:siRNA complexes were incubated at room temperature for at least 30 min before addition to the cells.

JetSI™-ENDO:siRNA complexes were prepared as described by the manufacturer. Briefly, the jetSI™-ENDO solution was diluted into OptiMEM and vigorously vortexed. After incubation at room temperature for 10 min, the jetSI™-ENDO mixture was added all at once to an equal volume of a 0.5 µM siRNA solution, immediately vortexed for 10 sec and incubated at room temperature for 15 min before addition to the cells.

Characterization of siRNA complexes

The average particle size and the zeta potential of the different siRNA complexes were measured by photon correlation spectroscopy (PCS) (Autosizer 4700, Malvern, Worcestershire, UK) and particle electrophoresis (Zetasizer 2000, Malvern), respectively. Before measurement, the jetSI™-ENDO:siRNA and PbAE:siRNA complexes were diluted 2-fold in 20 mM Hepes buffer pH 7.4 and 0.1 M acetate buffer pH 5.4, respectively. The control JetSI™-ENDO:siRNA complexes had a size of 221 ± 5 nm and a zeta potential of 23 ± 4 mV. The results for the PbAE:siRNA complexes are summarized in Table 1.

Native polyacrylamide gelelectrophoresis (PAGE) was used to study the complexation state of siRNA in the jetSI™-ENDO:siRNA and PbAE:siRNA complexes. Loading buffer containing 10 % glycerol was added to the siRNA complexes, containing 0.3 µg siRNA, and these samples were consequently loaded on a gel that contained 20 % polyacrylamide in TBE buffer (89 mM Tris·borate pH 8.3 and 2 mM EDTA). The PAGE gel was subjected to electrophoresis at 100 V for 2 hrs and the siRNA was visualized by UV transillumination using 1:10 000 diluted SYBR® Green II RNA stain (Molecular Probes, Merelbeke, Belgium) prior to photography.

Production of recombinant adenoviruses

For the generation of recombinant adenovirus the AdEasy™ Adenoviral Vector system (Stratagene, La Jolla, CA) was employed. The *firefly* luciferase open reading frame (ORF) was cloned in the pShuttle-CMV vector and was constitutively expressed under control of the CMV promoter. Subsequently, recombinant, replication-deficient adenoviruses expressing luciferase (Adluc) were generated following the standard protocol as described by He et al. [38].

Gene silencing in primary hepatocytes

As human primary hepatocytes are difficult to obtain because of their increasing use in transplantation, rat primary hepatocytes were used in this study. These hepatocytes were isolated from outbred adult male Sprague-Dawley rats (200–250 g; Iffa Credo), with free access to food and water, as described previously [39]. Cell integrity was tested by trypan blue exclusion.

For gene silencing experiments, rat hepatocytes were cultured (37°C, 5 % CO_2, 100 % humidity) as a monolayer in 24-well plates at a density of 6 x 10^4 cells per cm² in DMEM containing 0.5 U/ml insulin, 7 ng/ml glucagon, 10 % FBS and 1 % antibiotic mix (sodium ampicillin (10 µg/ml), kanamycin monosulfate (50 µg/ml), benzyl penicillin (7.3 IU/ml) and streptomycin sulfate (50 µg/ml) [40]. After 4 hrs, the medium was renewed with the same medium as described above but supplemented with 7.5 µg/ml hydrocortisone hemisuccinate and incubated overnight. Prior to transfection with the siRNA complexes, the hepatocytes were transduced with replication-deficient adenoviruses expressing firefly luciferase at a multiplicity of infection (MOI) of 50. Subsequently, 30 min after addition of the adenoviral vectors, the PbAE:siRNA or jetSI™-ENDO:siRNA complexes, containing 25 pmol siRNA, were added to the cells and incubated for 4 hrs at a final concentration of 50 nM. The remaining viruses and siRNA complexes were removed and replaced by 1 ml culture medium. Thirty hours later, cells were lysed with 80 µl passive lysis buffer (PLB; Promega, Leiden, The Netherlands) under vigorous shaking. Luciferase activity was determined with the Promega luciferase assay kit according to the manufacturer's instructions and expressed in relative light units (RLU). Briefly, 100 µl substrate was added to 20 µl sample and after a 2 sec delay, the luminescence was measured during 10 sec with the GloMax™ 96 luminometer with injector. To correct for the amount of cells per well, the protein concentration was determined with the BCA kit (Pierce, Rockford, IL). Two hundred microliter mastermix, containing 50 parts reagent A to 1 part B, was mixed with 20 µl cell lysate, incubated at 37°C for 30 min and measured on a Wallac Victor² absorbance plate reader (PerkinElmer Life Sciences, Boston, MA) at 590 nm. For each carrier, the RLU value per mg protein of the anti-luciferase siRNA transfected cells was compared to the RLU value per mg protein of the mock siRNA transfected cells and expressed as luciferase expression level (%).

Gene silencing in human hepatoma cells

The human hepatoma cell lines HuH-7 and HuH-7_eGFPLuc, stably expressing firefly luciferase, were cultured (37°C and 5 % CO_2) in DMEM:F12 supplemented with 2 mM L-Gln, 10 % heat-inactivated FBS and 100 U/ml P/S.

HuH-7_eGFPLuc cells stably expressing eGFP-Luciferase were generated by transfecting HuH-7 cells with the vector pEGFPLuc (Clontech, Palo Alto, USA) as previously described [41].

For gene silencing experiments, HuH-7_eGFPLuc cells were seeded into 24-well plates at a density of 5 x 10^4 cells per cm^2 and allowed to attach overnight. Cells were washed with PBS and to each well the siRNA complexes, containing 25 pmol siRNA, were added at a final concentration of 50 nM. After 4 hrs, the remaining complexes were removed and replaced by 1 ml culture medium. Thirty hours later, cells were lysed with 80 µl CCLR buffer (Promega), and luciferase activity and protein concentration were determined as described above.

For the long term gene silencing experiments, cells were seeded in 24-wells at a density of 5 x 10^4 cells per cm^2 and allowed to attach overnight. All transfection experiments were performed as described above, but in duplex. Twenty four hours later, one sample was lysed (day 1) while the parallel sample was trypsinized and 1:5 diluted into four 24-wells. These were incubated at 37°C and cells were lysed at day 2, 3, 4 or 5. After collection of all samples, luciferase activity and protein concentration were determined as described above. To correct for the dilution of the cells after trypsinization, the RLU value per mg protein of the anti-luciferase transfected cells was compared to similarly treated cells, transfected with mock siRNA and expressed as luciferase expression level (%).

Cytotoxicity assay

The influence of the siRNA complexes on the cell viability was determined using the CellTiter-Glo® Assay (Promega) and the tetrazolium salt-based colorimetric MTT assay (EZ4U; Biomedica, Vienna, Austria). 5 x 10^4 cells per cm^2 were seeded into 96-well plates and allowed to adhere. After 24 hrs, cells were washed with PBS and incubated either with the PbAE:siRNA complexes, the jetSI™-ENDO:siRNA complexes or free carrier. After 4 hrs, the remaining siRNA complexes or carriers were removed from the cells and replaced by culture medium. For the CellTiter-Glo® Assay, the 96-well plate was incubated at 37°C for 24 hrs, subsequently incubated at room temperature for 30 min and 100 µl CellTiter-Glo® reagent was added to each well. After shaking the plate for 2 min and 10 min incubation at room temperature, the luminescence was measured on a GloMax™ 96 luminometer with 1 sec integration time. In case of the EZ4U assay, medium was removed after 24 hrs and 20 µl EZ4U substrate, along with 180 µl culture medium, was added to each well. After 4 hrs incubation at 37°C reduced formazan was measured at 450 nm and 630 nm on a Wallac Victor^2 absorbance plate reader.

Confocal microscopy

Primary hepatocytes or HuH-7 cells were seeded on sterile glass bottom culture dishes (MatTek Corporation, Ashland, MA) at a density of 5×10^4 cells per cm^2 and allowed to attach overnight. PbAE:siRNA and jetSI™-ENDO:siRNA complexes, containing Alexa488-labelled siRNA, were prepared and added to the cells as described above. The distribution of the fluorescence in the cells was visualized using a Nikon C1si confocal laser scanning module attached to a motorized Nikon TE2000-E inverted microscope (Nikon Benelux, Brussels, Belgium). A non-confocal diascopic DIC (differential interference contrast) image was collected simultaneously with the confocal images. For lysosome staining, cells were incubated for 60 min with 1:15 000 diluted Lysotracker Red® (Molecular Probes) prior to image recording. Images were captured with a Nikon Plan Apochromat 60 x oil immersion objective lens (numerical aperture of 1.4) using the 488 nm and 639 nm line from an Ar-ion and a diode laser for the excitation of the Alexa488-siRNA and Lysotracker Red®, respectively.

RESULTS & DISCUSSION

Synthesis and characterization of PbAEs

Different PbAEs were synthesized (Fig. 1A) and the structures of the most efficient PbAEs for siRNA delivery are shown in Fig. 1B and 1C. Polymer 1 (PbAE1; Fig. 1B) and polymer 2 (PbAE2; Fig. 1C) were obtained by reaction between 4,4'-trimethylenedipiperidine and respectively 1,4-butanediol diacrylate and 1,6-hexanediol diacrylate. The structure of PbAE1 and PbAE2 was verified by ^{1}H NMR spectroscopy and the integration of the peaks yielded values as expected for the proposed chemical structures (see Materials and Methods). As these PbAEs were not soluble at a neutral or basic pH, they were dissolved in acetate buffer with pH 5.4. The average molecular weight of the polymers was determined by size exclusion chromatography and found to be 18 kDa for PbAE1 and 22 kDa for PbAE2.

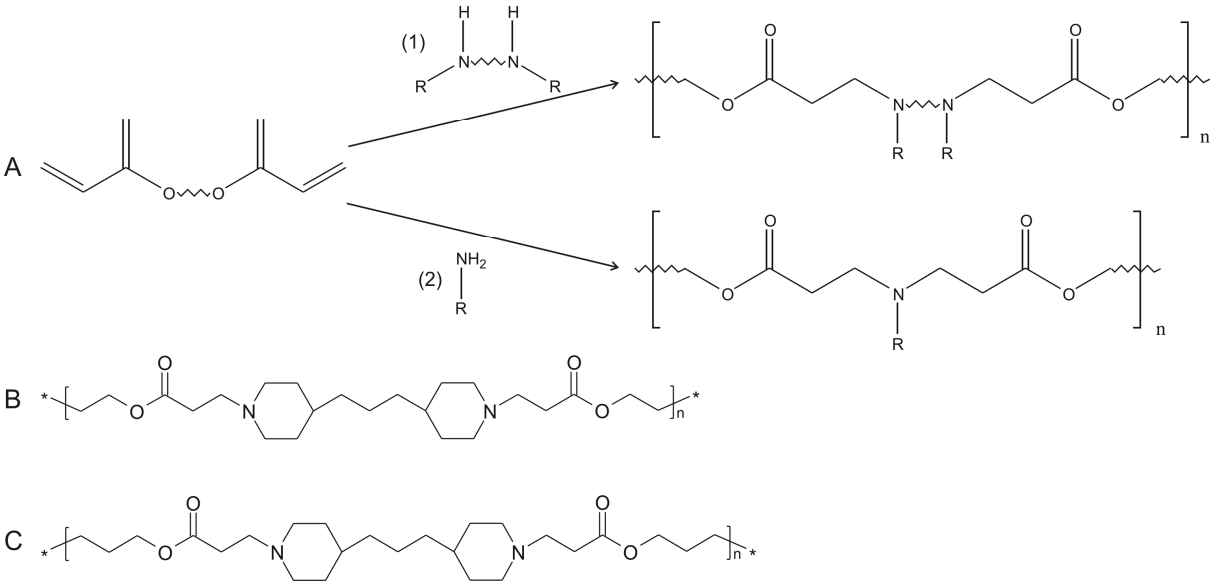

Figure 1. The synthesis of PbAEs by Michael addition between a bis (secondary amine) (1) or a primary amine (2) and a diacrylate is schematically represented in (A). PbAE1 (B) and PbAE2 (C) were synthesized by a Michael addition between 4,4'-trimethylenedipiperidine and 1,4-butanediol diacrylate, and between 4,4'-trimethylenedipiperidine and 1,6-hexanediol diacrylate, respectively.

Characterization and cytotoxicity of the PbAE:siRNA complexes

The ability of PbAEs to complex siRNA was tested via polyacrylamide gel electrophoresis (PAGE) (Fig. 2).

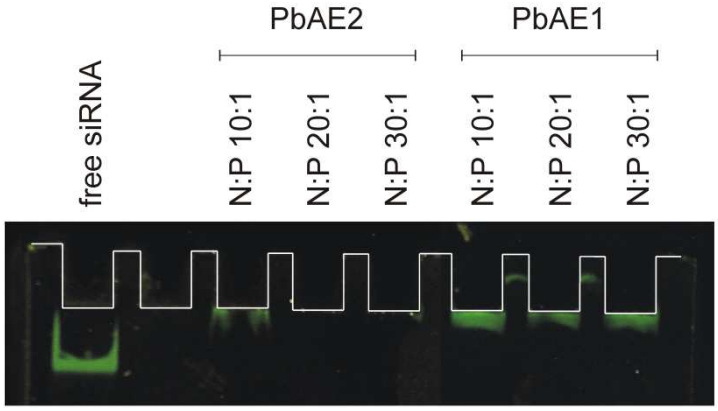

Figure 2. Native 20 % PAGE of free (i.e. non-complexed) siRNA, PbAE1:siRNA and PbAE2:siRNA complexes with N:P ratios 10:1, 20:1 and 30:1. In all lanes 0.3 µg siRNA was loaded after addition of 10 % glycerol and the samples were subsequently subjected to electrophoresis at 100 V for 2 hrs. The siRNA was visualized after staining the gel with SYBR® Green via UV illumination.

As no bands were present at the position of free siRNA, both PbAE1 and PbAE2 were able to bind siRNA. In case of PbAE2 N:P ratio 20:1 and 30:1 no fluorescence signal was visible in the lanes, which indicates that no free siRNA is present in these complexes. However, the lanes containing the PbAE1:siRNA complexes showed, independent of the N:P ratio, a siRNA band just beneath the slots.

Similarly, PbAE2:siRNA complexes with a N:P ratio 10:1 also displayed some traces of siRNA at this position. This may indicate the presence of partially complexed siRNA that is able to enter the gel, but that migrates slower than the free siRNA. Alternatively, the electric field may have caused a dissociation of these PbAE:siRNA complexes, generating free siRNA that entered the gel at a later time point than the free siRNA present in the first lane. Nevertheless, these observations indicate that PbAE2 forms tighter complexes with siRNA than PbAE1.

Besides the ability to bind siRNA, we also determined the size and zeta potential of the PbAE:siRNA complexes (Table 1). PbAE1:siRNA complexes were, except at N:P ratio 30:1, smaller than PbAE2:siRNA complexes and their zeta potential clearly increased as a function of the N:P ratio. In contrast, the zeta potential of PbAE2:siRNA complexes was more or less independent of the N:P ratio. In general, both PbAEs were able to form relatively small siRNA complexes with a positive surface charge, a feature known to facilitate cellular binding and uptake.

Table 1. The particle size and zeta potential of the different PbAE:siRNA complexes. As indicated, PbAE:siRNA complexes were made at three different nitrogen to phosphate (N:P) ratios. Mean values with corresponding standard deviations are shown (n = 5).

	particle size (nm)	zeta potential (mV)
PbAE1:siRNA		
N:P 10:1	326 ± 14	15 ± 3
N:P 20:1	315 ± 6	20 ± 2
N:P 30:1	380 ± 9	31 ± 1
PbAE2:siRNA		
N:P 10:1	517 ± 29	23 ± 3
N:P 20:1	457 ± 24	13 ± 3
N:P 30:1	374 ± 23	18 ± 3

Before performing siRNA transfection experiments, the cytotoxicity of PbAEs (data not shown) and PbAE:siRNA complexes (Fig. 3) was assessed by quantifying the intracellular ATP levels after transfection. Measuring ATP levels is a sensitive marker of cell viability. Indeed, within minutes after a loss of membrane integrity, cells lose the ability to synthesize ATP. Additionally, endogenous ATPases destroy any remaining ATP. We found that the free PbAEs and PbAE:siRNA complexes only slightly reduced cell viability, with a maximal cytotoxicity of ~20 % in case of PbAE2:siRNA N:P 30:1. JetSI^{TM}-ENDO:siRNA complexes, which are commonly used for *in vitro* siRNA delivery and which are claimed to lack cytotoxicity, did indeed not decrease cell viability. Furthermore, we also performed an MTT-based cell viability test (EZ4U assay), a test that relies on the ability of live but not dead cells to reduce MTT into a colorimetric formazan product by active mitochondrial dehydrogenases. In this approach none of the free polymers or complexes showed significant cytotoxicity (data not shown) which can be explained by the fact that this test only detects severe cytotoxicity effects, in contrast to the ATP-based cytotoxicity test.

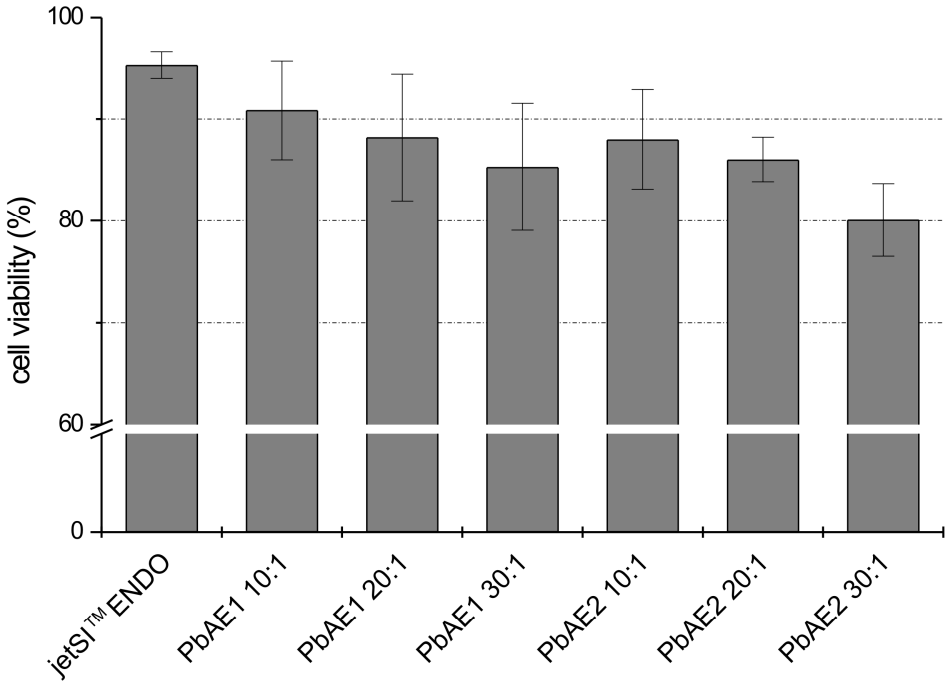

Figure 3. Cell viability of HuH-7_eGFPLuc cells incubated with JetSI™-ENDO:siRNA, PbAE1:siRNA and PbAE2:siRNA complexes. The siRNA complexes were removed from the cells after 4 hrs and the cell viability of the cells was determined after 24 hrs by measuring the intracellular ATP levels. The metabolic activity of non-treated cells was arbitrarily set at 100 % an all data are shown as mean ± SD (n=3).

Cellular uptake of PbAE:siRNA complexes by primary hepatocytes

To tackle viral hepatitis, the siRNA molecules must be delivered to primary hepatocytes. Although numerous mechanical, electrical, and chemical delivery methods have been applied, efficient transfer of siRNAs into primary cells is restricted to only a few cell types [42]. To study cellular uptake, one of the first steps in siRNA delivery, we visualized the cellular entry of the PbAE:siRNA complexes in primary hepatocytes via confocal laser scanning microscopy (CLSM). PbAE:siRNA complexes containing Alexa-488 labelled siRNA (green colour in Fig. 4) were incubated during 4 hrs with primary hepatocytes and the lysosomes were visualized using the Lysotracker Red® (red colour in Fig. 4). Fig. 4 (A through I) shows the outcome of a typical uptake experiment analysed by CLSM. After 4 hrs, all siRNA complexes gave rise to a punctuated green non-homogeneous distribution pattern of the siRNA inside the cell, which is indicative of an endocytotic uptake mechanism. This is confirmed by co-localization of the green pattern with the red labelled lysosomes. PbAE:siRNA complexes are thus clearly taken up by the hepatocytes by endocytosis, but they do not show a clear cytoplasmic localization of the siRNA after 4hrs and not even at 24 hrs (data not shown), which is needed to evoke a RNAi-mediated inhibitory effect.

Gene silencing in primary rat hepatocytes

The ability of PbAE:siRNA complexes to induce gene silencing of viral genes was tested in primary rat hepatocytes transduced with replication-deficient adenoviruses expressing *firefly* luciferase. As a control, complexes containing non-specific siRNA, i.e. siRNA with no known target in the cells, were added to the cells under identical conditions to ascertain that the reduction in gene expression was due to a specific siRNA effect and not to non-specific effects like interferon induction. The gene silencing observed 30 hrs after the adenoviral transduction was independent of the N:P ratio and equalled ~55% and ~65% for the PbAE1:siRNA and PbAE2:siRNA complexes, respectively (Fig. 5). Our lipid-based reference siRNA complexes (JetSI^{TM}-ENDO:siRNA complexes) were much less efficient and silenced only 30% of the luciferase expression in primary hepatocytes. Additionally, both polymers were also used to target the endogenous connexin (Cx) proteins Cx32 and Cx43, the building stones of gap junctions controlling direct communication between cells. In both cases a strong gene silencing was observed by western blotting (data not shown).

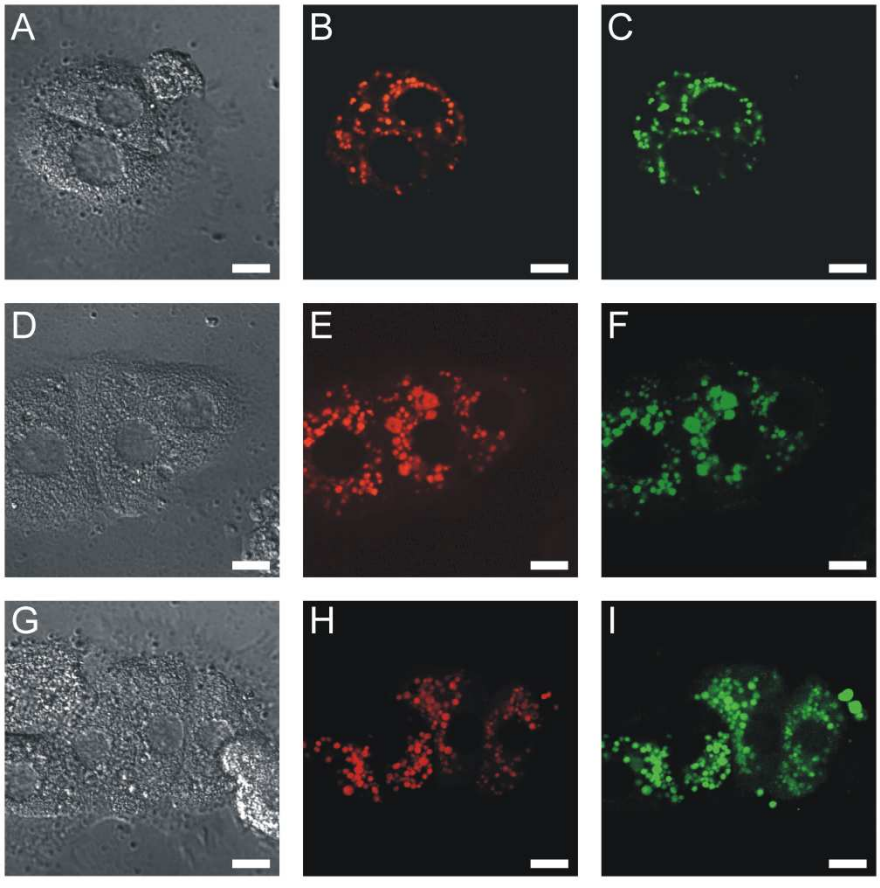

Figure 4. Confocal images of the cellular uptake of jetSI^{TM}-ENDO:siRNA (A till C), PbAE1:siRNA (N:P 10:1) (D till F) and PbAE2:siRNA (N:P 30 ratio) complexes (G till I) 4 hrs after addition to primary rat hepatocytes. (A), (D) and (G) are non-confocal DIC images. Images (B), (E) and (H) display Lysotracker® Red labelled lysosomes and (C), (F) and (I) display Alexa488-labelled siRNA. Microscopical analysis was performed using a confocal laser scanning microscope. The white bar equals 10 µm.

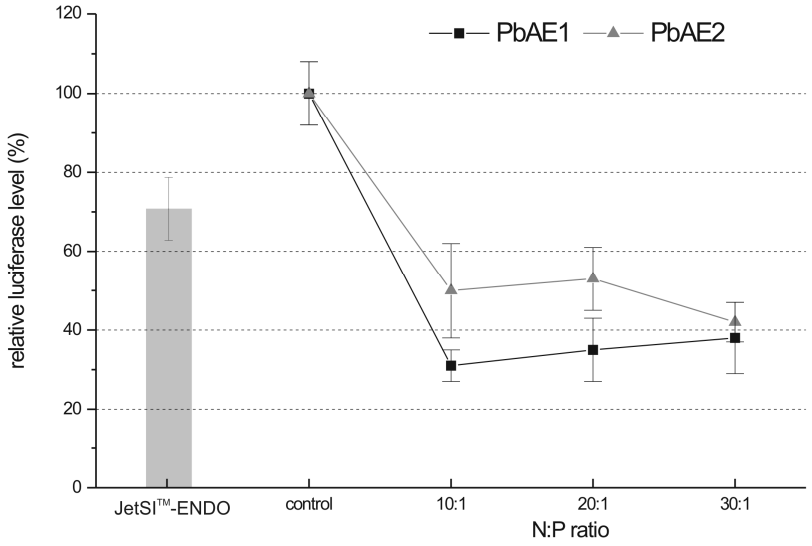

Figure 5. Relative luciferase levels in primary rat hepatocytes transfected with jetSI™-ENDO:siRNA, PbAE1:siRNA and PbAE2:siRNA complexes containing anti-luciferase siRNA. The gene silencing efficiency was obtained by comparison with mock siRNA-containing complexes, for which the luciferase level was arbitrarily set at 100 % and data are shown as mean ± SD (n=3). The represented control is the average of all mock transfected samples.

These results imply that, although not clearly visible by CLSM after 4 hrs (Fig. 4) and not even after 24 hrs (data not shown), a portion of the siRNA molecules must be released from the endosomes after endocytotic uptake. Because of the recycling of the siRNA after degradation of a target mRNA, it can be expected that very low amounts of siRNA in the cytosol can cause an efficient gene silencing. Indeed, it has been calculated that ~300 siRNA molecules per cell are sufficient to reduce luciferase activity with 50 % [43]. Such small amounts of cytosolic siRNA are most likely not visible via CLSM. Therefore, the absence of visible siRNA in the cytosol of our cells does not exclude that a small fraction is present in the cytosol that is causing the observed gene silencing effect. Since no fusogenic function is present in our polymers and based on the physicochemical properties, two possible mechanisms may mediate endosomal escape of the siRNA. First, PbAE:siRNA complexes may disrupt endosomes via the proton sponge mechanism that is considered to be responsible for the high transfection efficiency of PEI-based DNA complexes. The 'proton sponge' nature of PEI is thought to act as a strong buffer that prevents the pH drop inside endosomes. The endosomes try to overcome this high buffer capacity of PEI by pumping in more protons. To maintain charge neutrality, the influx of protons is accompanied by an influx of chloride ions. These ion influxes cause a drastic increase of the ionic strength inside the endosomes, which leads to an osmotic swelling and finally a physical rupture of the endosomes, resulting in the escape of PEI based DNA complexes from the endosomes [44]. Alternatively, endosomal escape of our siRNA may also occur via an increase of the

colloidal osmotic pressure in the endosomes after degradation of the PbAE into low molecular weight fragments, as suggested by Murthy et al [45].

Gene silencing in hepatoma cells

In contrast to e.g. viral HCV RNA, the candidate target genes for siRNA therapeutics in tumour cells are stably and massively expressed. Therefore, we also tested the gene silencing efficiency of the PbAE:siRNA complexes in human hepatoma (HuH-7) cells that stably express the eGFP-luciferase fusion protein (HuH-7_eGFPLuc). In several reports, the targeted gene that needs to be silenced is introduced in the cells via the same carrier as the siRNA. In such experiments an efficient gene silencing is highly expected as the gene and the siRNA are co-delivered to the same cells. Furthermore, it was recently questioned whether simultaneous transfection of an exogenous gene and the siRNA is suitable to quantify RNA interference [46]. Additionally, it is currently unknown whether siRNA-mediated knockdown of transiently expressed proteins is an acceptable quantitative surrogate for stably expressed proteins [47]. In conclusion, targeting a stably expressed gene can be considered as a model for oncogene silencing and targeting a transient gene as a model for viral gene silencing, if the viral genome is not integrated in the host's genome. Therefore, the stably transfected hepatoma cells used in this work are the most appropriate model for silencing of genes in tumour cells.

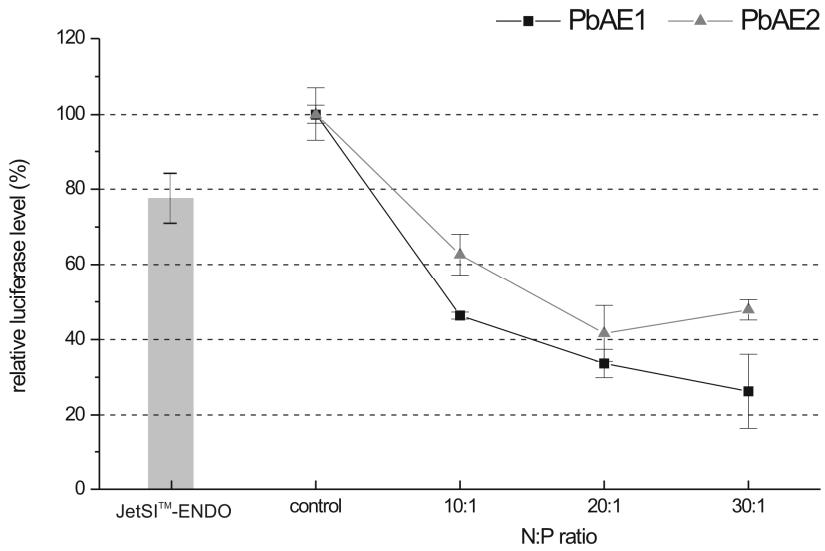

Figure 6. Relative luciferase levels of HuH-7_eGFPLuc cells transfected with jetSI™-ENDO:siRNA, PbAE1:siRNA and PbAE2:siRNA complexes containing anti-luciferase siRNA. The gene silencing efficiency was obtained by comparison with mock siRNA-containing complexes, for which the luciferase level was arbitrarily set at 100 % and data are shown as mean ± SD (n=3). The represented control is the average of all mock transfected samples.

As demonstrated in Fig. 6, the extent of gene silencing of the PbAE:siRNA complexes depends on the N:P ratio. The gene silencing increased as a function of the N:P ratio and a gene silencing of ~75 % was obtained at a N:P ratio 30:1. PbAE1:siRNA complexes with a higher N:P ratios were due to cytotoxicity concerns not tested. The gene silencing of the PBAE2:siRNA complexes was also higher at higher N:P ratios, but at the highest N:P ratios it stagnated at ~60 %. With the jetSI^{TM}-ENDO:siRNA complexes a gene silencing efficacy of only 20 % could be detected.

Prolonged gene silencing in hepatoma cells

A major disadvantage of the current available non-viral carriers for synthetic siRNA delivery is that the period of effective gene silencing is very brief. It has been demonstrated that the rapid restoration of gene expression after delivery of synthetic siRNA is mainly due to dilution of the siRNA during cell division, and not to a rapid intracellular degradation of siRNA by nucleases [48]. This implies that prolonged gene silencing after siRNA delivery is of major importance for siRNA delivery to especially tumour cells, which exhibit rapid growth with doubling times on the order of only a few days. Therefore, carriers that slowly release their siRNA in the cytoplasm could be of interest for therapeutic siRNA delivery to tumour cells. The only difference between PbAE1 and PbAE2 is the 4- or 6-carbon linkers situated between the esters in the repeat units, which implies variations in both charge density and hydrophobicity. It was found that these relatively minor changes in polymer structure do play an important role in determining the hydrolysis rate of the polymers when incubated in physiologically relevant media. Polyelectrolyte complexes containing PbAE1 and PbAE2 eroded completely in ~50 hrs and ~6 days, respectively [49]. Therefore, we wanted to analyze whether this difference in degradation rate could also influence the gene silencing kinetics of both PbAE1:siRNA and PbAE2:siRNA complexes. As discussed above, obtaining a sustained gene silencing is, due to dilution of the siRNA during cell division, most challenging in dividing cells. Hence, we monitored gene silencing up to 5 days after siRNA transfection in the HuH-7 hepatoma cells that stably expressed luciferase.

In Fig. 7, huge differences in the gene silencing kinetics between both PbAE:siRNA complexes are shown. After siRNA delivery with PbAE1, we observed a gradual recovery of the gene expression (Fig. 7A). The rate of recovery inversely correlated with the N:P ratio of these siRNA complexes. Indeed, at an N:P ratio 10:1, the luciferase expression started to recover at day 2 and was completely restored at day 5. In contrast, the onset of recovery at N:P ratios 20:1 and 30:1 occurred later and at day 5 the luciferase level reached ~90% and ~60%, respectively. An increase in N:P ratio, and thus in polymer concentration, probably leads to more tight complexes that release their siRNA more slowly. This may explain why PbAE1:siRNA complexes with a higher N:P ratio can suppress gene expression

during longer periods. In sharp contrast to the PBAE1:siRNA complexes, the gene silencing was almost completely maintained until day 5 when PbAE2:siRNA complexes with a N:P 20 and especially 30:1 were used. A small recovery in luciferase expression was observed when PbAE2:siRNA complexes at a N:P ratio of 10:1 were used. The observation that PbAE2 forms stronger complexes with the siRNA (see discussion of Fig. 2 above) is probably not the main reason for the more prolonged gene silencing observed with PbAE2. Indeed, at a N:P ratio of 10 PbAE2 also formed, like PbAE1, 'weaker' complexes with siRNA that were still able to cause a prolonged gene silencing (Fig. 7B).

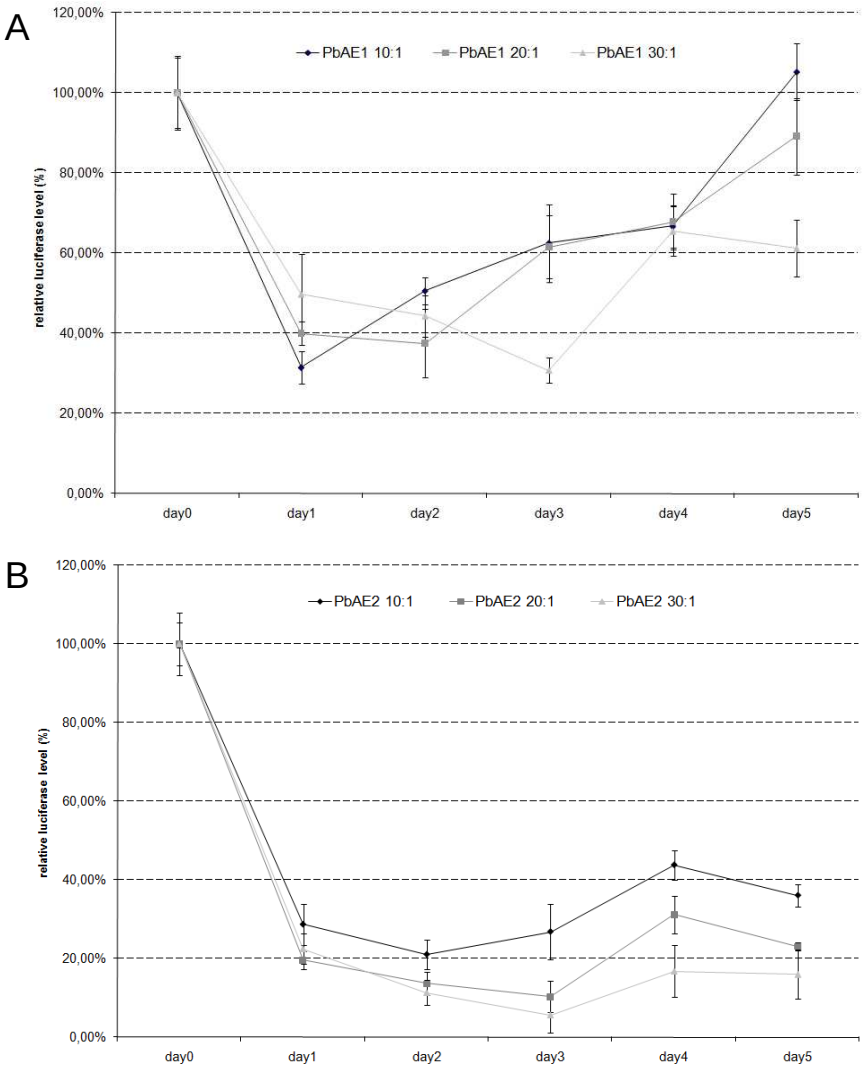

Figure 7. Long term gene silencing in HuH-7_eGFPLuc cells transfected with PbAE1:siRNA (A) and PbAE2:siRNA complexes (B) containing anti-luciferase siRNA. The gene silencing efficiency was obtained by comparison with mock siRNA-containing complexes, for which the luciferase level was arbitrarily set at 100 % and data are shown as mean ± SD (n=3).

Time-dependent intracellular fate of siRNA delivered via PbAE

To get more insight into the intracellular mechanisms that govern the prolonged gene silencing after siRNA delivery via PBAE2, we compared the time-dependent intracellular distribution of PbAE1:siRNA (N:P 10) and PbAE2:siRNA (N:P 30) complexes. PbAE1:siRNA (N:P 10) and PbAE2:siRNA (N:P 30) complexes containing Alexa-488 labelled siRNA (green colour in Fig. 8) were added to cultured HuH-7 cells and the intracellular fluorescence was monitored for 5 days. To visualize the lysosomes we again used Lysotracker Red® (red colour in Fig. 8).

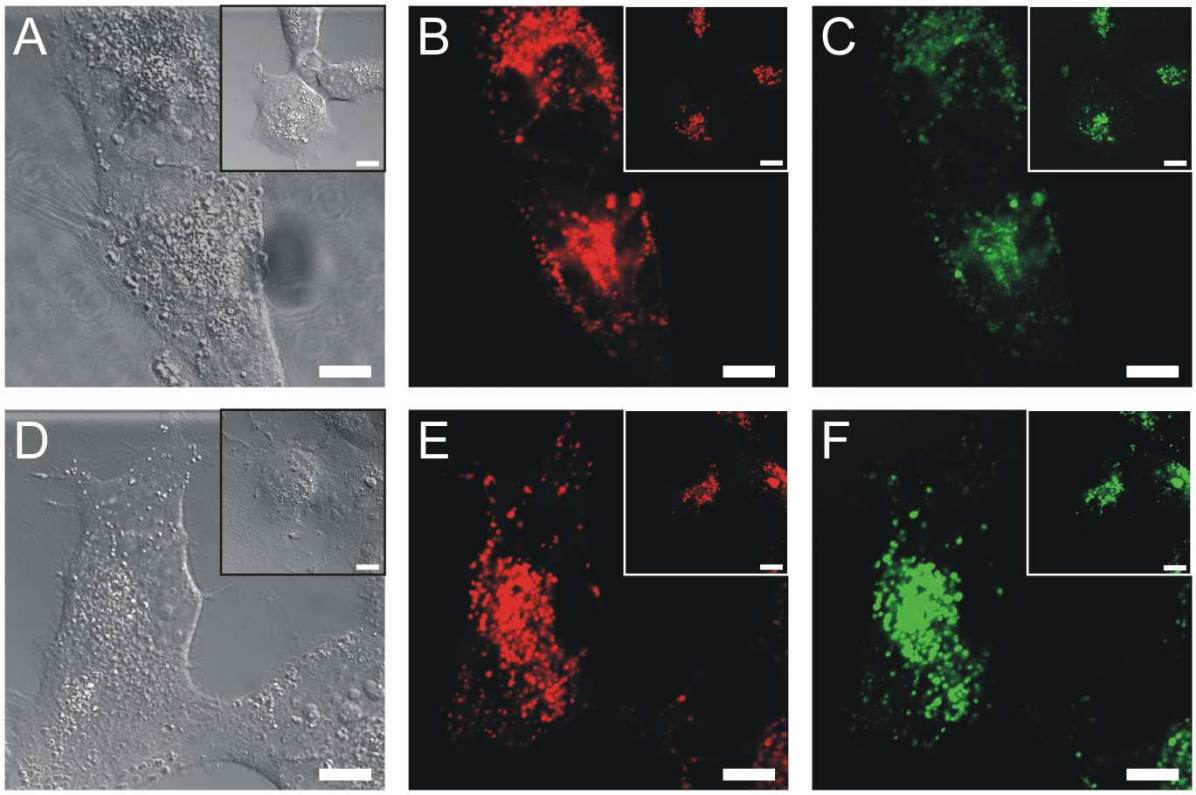

Figure 8. Confocal images of the cellular distribution of siRNA 24 hrs (insert) and 5 days after addition of PbAE1:siRNA N:P ratio 10:1 (A-C) and PbAE2:siRNA complexes N:P 30:1 (D-F) to HuH-7 cells. (A) and (D) are non-confocal DIC images, (B) and (E) display Lysotracker Red® labelled lysosomes and (C) and (F) show Alexa488-labelled siRNA.

The inserts in Fig. 8 show the intracellular distribution of the labelled siRNA 24 hrs after transfection. After 24 hrs, a punctuated pattern, that co-localized with the Lysotracker Red®, was observed with both PbAE:siRNA complexes. However, 5 days after transfection, a clear difference in the intracellular siRNA distribution pattern was visible. The intracellular fluorescence of the siRNA after delivery via PbAE1 (N:P 10) became weaker and the dotted fluorescence signal was replaced by a more diffuse distribution of the fluorescence. In contrast, the intracellular fluorescence of the siRNA after delivery via PbAE2 (N:P 30) showed at day 5 a similar intensity and intracellular

localization, i.e. in vesicles, as after 24 hrs. As stated above, a vesicular localization of the siRNA is not necessarily expected to result in a good RNAi effect, as the RNAi machinery is present in the cytosol. Therefore, the siRNA or the siRNA complexes will have to escape from the endosomes.

With the slow degrading polymer (PbAE2) the siRNA remained in vesicles up to day 5 (Fig. 8E and 8F), while the siRNA signal became more weak and diffuse at day 5 with the fast degrading polymer (PbAE1) (Fig. 8B and 8C). If we correlate these observations with the duration of gene silencing (Fig. 7), it is tempting to speculate that the endosomal release kinetics of siRNA, and hence the duration of the gene silencing, are driven by the degradation kinetics of the PbAEs. This is in line with the hypothesis that the endosomal escape of the siRNAs or PbAE:siRNA complexes occurs via the above explained colloidal osmotic pressure hypothesis in which the osmotic pressure in the endosomes is due to the formation of small PbAE degradation products. The prolonged gene silencing with PBAE2 also implies that not all endosomes are ruptured at the same time. Such a continuous rupture of endosomes is very likely to occur as the kinetics of the osmotic pressure increase in the endosomes will also depend on the amount of PbAE in the endosomes and the latter is expected to vary from endosome to endosome. Therefore, the siRNA filled vesicles can be considered as a depot from which siRNA is continuously released in the cytoplasm during a time period that is mainly determined by the degradation kinetics of the PbAE.

CONCLUSION

Inhibition of highly active genes involved in liver oncogenesis or viral replication via siRNA delivery may offer great opportunities for the treatment of several diseases, such as HCC and HCV infections. Unfortunately, clinical applications of siRNAs are currently limited because no safe and efficient delivery systems are available. In this study we showed for the first time that biodegradable polymers (PbAEs) were able to induce efficient siRNA-mediated gene silencing of a viral (transduced*)* gene in primary rat hepatocytes and a stably expressed gene in hepatoma cells without causing significant cytotoxicity. However, besides the development of carriers that efficiently deliver the siRNA, there is also major clinical interest for siRNA carriers that slowly release the siRNA in the cytoplasm and hence induce a prolonged gene silencing effect. We showed that, in contrast to PbAE1, PbAE2 was also able to induce a long term gene silencing in the hepatoma cells (up to 5 days). Interestingly, the prolonged gene silencing of PbAE2-based siRNA complexes correlated with the slower degradation kinetics of PbAE2 and a prolonged vesicular localization of the siRNA. This supports the hypothesis that the release of the PBAE:siRNA complexes or siRNA is based on an increase in colloidal osmotic pressure in the endosomal vesicles after polymer hydrolysis. In this way,

the siRNA filled endosomal vesicles act as a siRNA depot from which siRNA is continuously released in the cytoplasm during a time period that is mainly determined by the degradation kinetics of the PbAE. We conclude that both PbAEs, and especially PbAE2, open up new perspectives for the development of efficient biodegradable siRNA carriers suitable for clinical applications.

ACKNOWLEDGMENTS

The HuH-7_eGFPLuc cells were kindly provided by Prof. Ernst Wagner, LMU University Munich. Niek N. Sanders, Tamara Van Haecke, Harry Heimberg, Mathieu Vinken and Stefan Bonné are supported by the Fund for Scientific Research - Flanders (FWO). The financial support of this institute is acknowledged with gratitude. This work was supported by grants from Ghent University (BOF), FWO and the European Union (MediTrans).

REFERENCES

(1) Thorgeirsson S.S. & Grisham J.W. Molecular pathogenesis of human hepatocellular carcinoma. *Nat. Genet.* **2002** 31(4) 339-346.

(2) Bruix J., Boix L., Sala M., & Llovet J.M. Focus on hepatocellular carcinoma. *Cancer Cell* **2004** 5(3) 215-219.

(3) Hadziyannis S.J. New developments in the treatment of chronic hepatitis B. *Expert. Opin. Biol. Ther.* **2006** 6(9) 913-921.

(4) Koike K. Antiviral treatment of hepatitis C: present status and future prospects. *J. Infect. Chemother.* **2006** 12(5) 227-232.

(5) Tarantino G., Conca P., Sorrentino P., & Ariello M. Metabolic factors involved in the therapeutic response of patients with hepatitis C virus-related chronic hepatitis. *J. Gastroenterol. Hepatol.* **2006** 21(8) 1266-1268.

(6) Cho-Rok J., Yoo J., Jang Y.J. *et al.* Adenovirus-mediated transfer of siRNA against PTTG1 inhibits liver cancer cell growth in vitro and in vivo. *Hepatology* **2006** 43(5) 1042-1052.

(7) Wu J. & Nandamuri K.M. Inhibition of hepatitis viral replication by siRNA. *Expert. Opin. Biol. Ther.* **2004** 4(10) 1649-1659.

(8) Wilson J.A. & Richardson C.D. Future promise of siRNA and other nucleic acid based therapeutics for the treatment of chronic HCV. *Infect. Disord. Drug Targets.* **2006** 6(1) 43-56.

(9) Smolic R., Volarevic M., Wu C.H., & Wu G.Y. Potential applications of siRNA in hepatitis C virus therapy. *Curr. Opin. Investig. Drugs* **2006** 7(2) 142-146.

(10) Shlomai A. & Shaul Y. RNA interference--small RNAs effectively fight viral hepatitis. *Liver Int.* **2004** 24(6) 526-531.

(11) Romero-Lopez C., Sanchez-Luque F.J., & Berzal-Herranz A. Targets and tools: recent advances in the development of anti-HCV nucleic acids. *Infect. Disord. Drug Targets.* **2006** 6(2) 121-145.

(12) Randall G. & Rice C.M. Interfering with hepatitis C virus RNA replication. *Virus Res.* **2004** 102(1) 19-25.

(13) Radhakrishnan S.K., Layden T.J., & Gartel A.L. RNA interference as a new strategy against viral hepatitis. *Virology* **2004** 323(2) 173-181.

(14) Gomez J., Nadal A., Sabariegos R., Beguiristain N., Martell M., & Piron M. Three properties of the hepatitis C virus RNA genome related to antiviral strategies based on RNA-therapeutics: variability, structural conformation and tRNA mimicry. *Curr. Pharm. Des* **2004** 10(30) 3741-3756.

(15) Fire A., Xu S., Montgomery M.K., Kostas S.A., Driver S.E., & Mello C.C. Potent and specific genetic interference by double-stranded RNA in Caenorhabditis elegans. *Nature* **1998** 391(6669) 806-811.

(16) Bernstein E., Caudy A.A., Hammond S.M., & Hannon G.J. Role for a bidentate ribonuclease in the initiation step of RNA interference. *Nature* **2001** 409(6818) 363-366.

(17) Elbashir S.M., Lendeckel W., & Tuschl T. RNA interference is mediated by 21- and 22-nucleotide RNAs. *Genes Dev.* **2001** 15(2) 188-200.

(18) Vandenbroucke R.E., Lucas B., Demeester J., De Smedt S.C., & Sanders N.N. Nuclear accumulation of plasmid DNA can be enhanced by non-selective gating of the nuclear pore. *Nucleic Acids Res.* **2007**

(19) Randall G., Grakoui A., & Rice C.M. Clearance of replicating hepatitis C virus replicon RNAs in cell culture by small interfering RNAs. *Proc. Natl. Acad. Sci. U. S. A* **2003** 100(1) 235-240.

(20) Seo M.Y., Abrignani S., Houghton M., & Han J.H. Small interfering RNA-mediated inhibition of hepatitis C virus replication in the human hepatoma cell line Huh-7. *J. Virol.* **2003** 77(1) 810-812.

(21) Yano J., Hirabayashi K., Nakagawa S. *et al.* Antitumor activity of small interfering RNA/cationic liposome complex in mouse models of cancer. *Clin. Cancer Res.* **2004** 10(22) 7721-7726.

(22) Takahashi Y., Nishikawa M., Kobayashi N., & Takakura Y. Gene silencing in primary and metastatic tumors by small interfering RNA delivery in mice: quantitative analysis using melanoma cells expressing firefly and sea pansy luciferases. *J. Control Release* **2005** 105(3) 332-343.

(23) Sorensen D.R., Leirdal M., & Sioud M. Gene silencing by systemic delivery of synthetic siRNAs in adult mice. *J. Mol. Biol.* **2003** 327(4) 761-766.

(24) Sioud M. & Sorensen D.R. Cationic liposome-mediated delivery of siRNAs in adult mice. *Biochem. Biophys. Res. Commun.* **2003** 312(4) 1220-1225.

(25) Hassani Z., Lemkine G.F., Erbacher P. *et al.* Lipid-mediated siRNA delivery down-regulates exogenous gene expression in the mouse brain at picomolar levels. *J. Gene Med.* **2005** 7(2) 198-207.

(26) Howard K.A., Rahbek U.L., Liu X. *et al.* RNA Interference in Vitro and in Vivo Using a Novel Chitosan/siRNA Nanoparticle System. *Mol. Ther.* **2006**

(27) Schiffelers R.M., Ansari A., Xu J. *et al.* Cancer siRNA therapy by tumor selective delivery with ligand-targeted sterically stabilized nanoparticle. *Nucleic Acids Res.* **2004** 32(19) e149.

(28) Thomas M., Lu J.J., Ge Q., Zhang C., Chen J., & Klibanov A.M. Full deacylation of polyethylenimine dramatically boosts its gene delivery efficiency and specificity to mouse lung. *Proc. Natl. Acad. Sci. U. S. A* **2005** 102(16) 5679-5684.

(29) Urban-Klein B., Werth S., Abuharbeid S., Czubayko F., & Aigner A. RNAi-mediated gene-targeting through systemic application of polyethylenimine (PEI)-complexed siRNA in vivo. *Gene Ther.* **2005** 12(5) 461-466.

(30) Koping-Hoggard M., Tubulekas I., Guan H. *et al.* Chitosan as a nonviral gene delivery system. Structure-property relationships and characteristics compared with polyethylenimine in vitro and after lung administration in vivo. *Gene Ther.* **2001** 8(14) 1108-1121.

(31) Clamme J.P., Krishnamoorthy G., & Mely Y. Intracellular dynamics of the gene delivery vehicle polyethylenimine during transfection: investigation by two-photon fluorescence correlation spectroscopy. *Biochim. Biophys. Acta* **2003** 1617(1-2) 52-61.

(32) Lynn D.M. & Langer R. Degradable poly(beta-amino esters): Synthesis, characterization, and self-assembly with plasmid DNA. *Journal of the American Chemical Society* **2000** 122(44) 10761-10768.

(33) Lynn D.M., Anderson D.G., Putnam D., & Langer R. Accelerated discovery of synthetic transfection vectors: parallel synthesis and screening of a degradable polymer library. *J. Am. Chem. Soc.* **2001** 123(33) 8155-8156.

(34) Anderson D.G., Lynn D.M., & Langer R. Semi-automated synthesis and screening of a large library of degradable cationic polymers for gene delivery. *Angewandte Chemie-International Edition* **2003** 42(27) 3153-3158.

(35) Greenland J.R., Liu H., Berry D. *et al.* Beta-amino ester polymers facilitate in vivo DNA transfection and adjuvant plasmid DNA immunization. *Mol. Ther.* **2005** 12(1) 164-170.

(36) Little S.R., Lynn D.M., Ge Q. *et al.* Poly-beta amino ester-containing microparticles enhance the activity of nonviral genetic vaccines. *Proc. Natl. Acad. Sci. U. S. A* **2004** 101(26) 9534-9539.

(37) Peng W., Anderson D.G., Bao Y., Padera R.F., Jr., Langer R., & Sawicki J.A. Nanoparticulate delivery of suicide DNA to murine prostate and prostate tumors. *Prostate* **2007** 67(8) 855-862.

(38) He T.C., Zhou S., da Costa L.T., Yu J., Kinzler K.W., & Vogelstein B. A simplified system for generating recombinant adenoviruses. *Proc. Natl. Acad. Sci. U. S. A* **1998** 95(5) 2509-2514.

(39) Papeleu P., Vanhaecke T., Henkens T. *et al.* Isolation of rat hepatocytes. *Methods Mol. Biol.* **2006** 320229-237.

(40) Henkens T., Vanhaecke T., Papeleu P. *et al.* Rat hepatocyte cultures: conventional monolayer and cocultures with rat liver epithelial cells. *Methods Mol. Biol.* **2006** 320239-246.

(41) Vandenbroucke R.E., Lentacker I., Demeester J., De Smedt S.C., & Sanders N.N. Ultrasound assisted siRNA delivery using PEG-siPlex loaded microbubbles. *J. Control Release* **2007**

(42) Ovcharenko D., Jarvis R., Hunicke-Smith S., Kelnar K., & Brown D. High-throughput RNAi screening in vitro: from cell lines to primary cells. *RNA.* **2005** 11(6) 985-993.

(43) Veldhoen S., Laufer S.D., Trampe A., & Restle T. Cellular delivery of small interfering RNA by a non-covalently attached cell-penetrating peptide: quantitative analysis of uptake and biological effect. *Nucleic Acids Res.* **2006** 34(22) 6561-6573.

(44) Behr J.P. The proton sponge: A trick to enter cells the viruses did not exploit. *Chimia* **1997** 51(1-2) 34-36.

(45) Murthy N., Xu M., Schuck S., Kunisawa J., Shastri N., & Frechet J.M. A macromolecular delivery vehicle for protein-based vaccines: acid-degradable protein-loaded microgels. *Proc. Natl. Acad. Sci. U. S. A* **2003** 100(9) 4995-5000.

(46) Tagami T., Barichello J.M., Kikuchi H., Ishida T., & Kiwada H. The gene-silencing effect of siRNA in cationic lipoplexes is enhanced by incorporating pDNA in the complex. *Int. J Pharm.* **2007** 333(1-2) 62-69.

(47) Grayson A.C., Ma J., & Putnam D. Kinetic and efficacy analysis of RNA interference in stably and transiently expressing cell lines. *Mol. Pharm.* **2006** 3(5) 601-613.

(48) Bartlett D.W. & Davis M.E. Insights into the kinetics of siRNA-mediated gene silencing from live-cell and live-animal bioluminescent imaging. *Nucleic Acids Res.* **2006** 34(1) 322-333.

(49) Zhang J., Fredin N.J., Janz J.F., Sun B., & Lynn D.M. Structure/property relationships in erodible multilayered films: influence of polycation structure on erosion profiles and the release of anionic polyelectrolytes. *Langmuir* **2006** 22(1) 239-245.

Chapter 6

Electrostatic HIV-1 Tat/pDNA Complexes as Non-viral Gene Delivery Vehicles

ABSTRACT

Non-viral gene delivery generally results in low transgene expression, likely due to poor intranuclear DNA delivery. In this study, we tried to improve the nuclear import by complexing pDNA with the NLS containing HIV-1 Tat peptide. We first showed that the peptide was indeed able to mediate nuclear translocation of BSA macromolecules and that the peptide could electrostatically interact with the pDNA, resulting in polydisperse particles. However, the formed Tat/pDNA complexes failed to significantly increase the transfection efficiency compared to naked pDNA transfection. Moreover, transfection efficiency could not significantly be enhanced after addition of the lysosomotropic compound chloroquine and cytoplasmic injected Tat/pDNA complexes did not translocate into the nucleus. Both observations indicate that the Tat peptide, once complexed with pDNA, was unable to interact with the nuclear import machinery, which was confirmed by a negative GST pull down assay. Taken together, these data demonstrate that the NLS containing HIV-1 Tat peptide is unable to improve nuclear import of pDNA by electrostatic interaction, probably because the NLS of the peptide is masked after electrostatic binding to pDNA.

Chapter 6

Electrostatic HIV-1 Tat/pDNA Complexes as Non-viral Gene Delivery Vehicles

INTRODUCTION

Despite the several advantages of non-viral gene delivery carriers compared to their viral counterparts, low transfection efficiency still limits the usefulness of these vectors for clinical gene therapy applications. One important drawback in non-viral DNA delivery is nuclear import, as the nuclear membrane forms a closed barrier for DNA molecules. This nuclear import process is especially relevant in post-mitotic and quiescent cells, as these cells lack nuclear envelope (NE) breakdown. Because many cells that are targeted in gene therapy do not divide or divide very slowly, the entry of plasmids into the nucleus becomes a major limiting step in non-viral DNA transfer.

In non-dividing cells, the only way to pass the NE, is through the nuclear pore complexes (NPCs) and this transport can be either passive or active, and both are size restricted. Molecules > 20-40 kDa require active transport [1], mediated by a nuclear localization signal (NLS), which interacts with components of the nuclear transport system, thereby initiating nuclear import [2,3]. The classical NLSs consist of one or two clusters of mostly basic amino acids and the uptake is initiated by binding of the NLS to members of the importin family. Most classical NLSs interact first with importin α and subsequently bind to the importin β receptor, anchoring the cargo-importin complex to the NPC and resulting in transportation into the nucleus via the NPC by an energy-dependent process [4]. The nuclear import of some proteins with classical NLS, e.g. the HIV-1 Tat protein, is mediated by direct binding to importin β, without the need of importin α [5].

Conjugating an NLS peptide to DNA could thus improve nuclear import of exogenous DNA, thereby improving transfection efficiency [6,7]. In 1999 indeed, it was reported that covalent attachment of an NLS peptide to linear DNA could result in a 300-fold increase in transfection efficiency [8].

The HIV-1 transactivator protein Tat is an 86-amino-acid protein that regulates viral transcription by recruiting cellular factors to the HIV promoter, by interaction with protein kinase

complexes, acetyltransferases, protein phosphatases and other factors (reviewed by [9]). The protein possesses a high net positive charge at physiological pH, with nine amino acids being either arginine or lysine. This short stretch of amino acids highly enriched in basic residues is responsible for the NLS activity [10].

Here, we evaluated the capacity of the HIV-1 Tat AA 37-72 (Tat) peptide to (1) transport large cargos (FITC-BSA) into the nucleus, (2) condense pDNA into small particles by electrostatic interactions, (3) induce nuclear localization of pDNA and (4) increase the pDNA transfection efficiency.

MATERIALS & METHODS

Materials

Dulbecco's modified Eagle's medium (DMEM), L-glutamine (L-Gln), heat inactivated fetal bovine serum (FBS) and 100 U/ml penicilline-streptomycine (P/S) were supplied by GibcoBRL (Merelbeke, Belgium). The HIV-1 Tat peptide AA 37-72 (CFITKALGISYGRKKRRQRRRAPQGS-QTHQVSLSKQ) was obtained from the EU Programme EVA (European Vaccine Against AIDS) Centralised Facility. The secreted alkaline phosphatase (SEAP) expression plasmid (pMet7 hβ_c SEAP) was a kind gift from Prof. Tavernier (Ghent University, Belgium).

Cell culture

Cos-7 cells (African green monkey kidney fibroblast-like cell line; ATCC number CRL-1651) and Vero cells (African green monkey kidney epithelial cells; ATCC number CCL-81) were cultured in Dulbecco's modified Eagle's medium (DMEM) containing 2 mM L-Gln, 10 % heat inactivated FBS and 1 % P/S. All cells were grown at 37°C in a humidified atmosphere containing 5 % CO_2.

Preparation of FITC-BSA-Tat conjugates

FITC-BSA was covalently coupled to the Tat peptide via a NHS-PEG-MAL linker (Shearwaters, Huntsville, AL). In a first step, 3.54 x 10^{-8} mol FITC-BSA was incubated with a 10-fold molar excess of NHS-PEG-MAL in 0.1 M $NaHCO_3$ pH 8.3. After 1 hr, the reaction was stopped by adding $HONH_2$.HCl and the excess of non-reacted linker was removed using a Microcon® column (MWCO 30 kDa). The pH of the FITC-BSA-NHS-PEG-MAL solution was adjusted with 50 mM Hepes buffer pH 6.8, until it

reached pH 7. In a second step, the Tat peptide was incubated with a 10-fold excess of TCEP in Hepes buffer pH 7, to reduce the disulfide bonds and added to the FITC-BSA-NHS-PEG-MAL solution in a 10-fold molar excess. The non-reacted Tat peptide was removed using Microcon® column (MWCO 30 kDa). Finally, the presence of the Tat peptide on the FITC-BSA molecule was confirmed by SDS-PAGE, followed by Western blotting.

Recombinant protein expression and purification

All GST pull down assays were performed using the purified recombinant *S. cerevisiae* proteins Srp1p (importin α) and Kap95p (importin β). Importin α and the SV40 NLS-GFP (SV40_eGFP) were expressed in *E. coli* and purified by nickel affinity chromatography as described previously [11]. Briefly, both His_6 tagged proteins were overexpressed at 30°C in the *Escherichia coli* strain BL21 (DE3). The *E. coli* cells were grown in LB medium containing 30 µg/ml kanamycin, and expression was induced at an optical density of 0.6 (600 nm) by addition of 0.2 mM isopropyl-1-thio-β-D-galactopyranoside for 5 hrs. Cells were harvested by centrifugation and resuspended in buffer A (20 mM Tris-HCl pH 8.0, 100 mM NaCl, 1 mM EDTA, 1 mM β-mercaptoethanol, 1 mM phenylmethylsulfonyl fluoride, and 0.1% igepal). Following French press cell lysis and separation of cell debris by high speed centrifugation, the soluble supernatant was loaded onto a Hitrap nickel chelator column (GE Healthcare Bio-Sciences AB, Uppsala, Sweden), washed with buffer B (50 mM Na_2HPO_4 pH 7.4, 0.25 M NaCl), and eluted with a 0.5 M imidazole gradient. GST-importin β was expressed in *E. coli*. A total of 10 ml of saturated overnight cultures of transformed *E. coli*, was diluted 1:100 with Luria–Bertani medium (LB) containing ampicillin (100 µg/ml), and allowed to grow overnight at 30°C. After centrifugation at 3800 rpm for 20 min at 4°C, the pellet was resuspended in a 1/50 culture volume of lysis buffer (50 mM Tris pH 8.0, 200 mM NaCl, 2.5 mM EDTA and 0.1 % Tween20). Then 1/50 000 0.1 M phenylmethylsulfonyl fluoride (PMSF) was added and the suspension was dissolved by vortexing and disrupted by French press. Cell debris was removed by centrifugation for 30 min at 4°C at 15 000 rpm. The crude lysate was added to equilibrated Glutathione Sepharose 4B beads (GE Healthcare Bio-Sciences AB) for 2 hrs at 4°C. The beads were subsequently washed 5 times for 10 min at 4°C. Once with lysis buffer, once with wash buffer (50 mM Tris pH 8.0, 200 mM NaCl), once with high-salt buffer (50 mM Tris pH 8.0, 500 mM NaCl) and finally twice with wash buffer. The beads, loaded with GST-importin β, were equilibrated in an elution buffer (50 mM Tris–HCl pH 8.0 and 0.1 % Triton X-100) and the fusion protein was eluted by the addition of 1 bed volume of ice-cold elution buffer containing 15 mM reduced glutathione, after being shaken overnight at 4°C.

In all cases, the supernatant was separated from the beads by centrifugation, analyzed by 10 % SDS-PAGE and visualized by Coomassie™ brilliant blue staining. Subsequently, protein concentration was determined by using a bradford protein assay and all proteins were stored at -80°C at a concentration of 10 mg/ml in PBS containing 10 % glycerol.

GST pull down assay

GST-importin β was incubated with Glutathione Sepharose 4B beads at a concentration of 0.5 mg/ml. Subsequently, 100 µl GST-importin β bearing beads were incubated with the appropriate components (importin α and/or eGFP_SV40 or Tat peptide) in a total volume of 500 µl PBSMT (1 x PBS, 5 mM $MgCl_2$, 0.5 % Triton X-100) for 3 hrs at 4°C and then washed three times with PBSMT and twice with PBSM. Both unbound and bound fractions were subsequently analyzed on a Precast 10-20 % gradient SDS-PAGE gel (BioRad) and visualized by Coomassie™ brilliant blue staining.

Preparation of the Tat/pDNA complexes

The pMet7 hβ_c SEAP plasmid (5 803 bp) has 11 606 negative charges, against 10 positive charges of one Tat molecule. The Tat/pDNA complexes were prepared by mixing 2.6 nM pDNA in a 1:1 volume ratio with the Tat peptide in different plus:minus ratios. The mixtures were prepared in 20 mM Hepes buffer pH 7.4 and incubated at room temperature for at least 30 min.

Agarose gel electrophoresis assay

For the agarose gel electrophoresis assay, Tat/pDNA complexes were prepared as described in the previous section and 5 x loading solution (30 % glycerol, 0.02 % bromophenol blue) was added. Subsequently, all samples were loaded on a 1 % agarose gel and run for 45 min at 80 V in 1 x TBE buffer (10.8 g/l Tris base, 5.5 g/l boric acid and 0.58 g/l EDTA). Subsequently, the gel was soaked in 0.5 µl/ml EtBr for 20 min, washed and visualized by UV transillumination.

Microinjection experiments

For microinjection experiments, 2.5 x 10^5 cells per cm^2 were seeded onto sterile glass bottom culture dishes (MatTek Corporation, MA, USA) and allowed to adhere for 1 day. Microinjection experiments were performed using a Femtojet® microinjector and an Injectman® NI 2 micromanipulator (Eppendorf). All injections were performed in the cytoplasm of the cells.

Immediately after injection, CLSM (BioRad MRC 1024; Hemel Hempstadt, UK) was used to visualize the fluorescence distibution in the cells.

Confocal laser scanning microscopy (CLSM)

Confocal images were captured with a 60 x water immersion objective and a krypton/argon laser (488 nm) for the excitation of the FITC label or YOYO-1® iodide (Molecular Probes). Emission light was collected using a 500-530 nm band pass filter and pseudocoloring was performed by using a digital imaging system, Confocal Assistant (CAS; BioRad; Hemel Hempstadt, UK).

Size and zeta potential measurement

The average particle size and the zeta potential were measured by dynamic light scattering (DLS), using an Autosizer 4700 (Malvern, Worcestershire, UK), and by particle electrophoresis, using a Zetasizer 2000 (Malvern, Worcestershire, UK), respectively. Before measurement, the pDNA/Tat solutions were diluted 40-fold with 20 mM Hepes buffer pH 7.4.

Cytotoxicity analysis

The cytotoxicity of the Tat/pDNA complexes was determined using the tetrazolium salt based colorimetric MTT assay (EZ4U, Biomedica, Vienna, Austria) according to the manufacturer's instructions. Briefly, 2.5 x 10^4 cells/cm^2 were seeded in a 24-well plate and allowed to adhere. After 24 hrs, cells were washed twice with serum free medium and incubated with Tat/pDNA complexes, containing 0.18 µg pDNA per cm^2 in serum free medium. After 2 hrs, the complexes were removed and cells were washed with culture medium. Finally, 40 µl EZ4U substrate with 260 µl culture medium was added per well and after 4 hrs incubation at 37°C the concentration of reduced formazan was measured at 450 nm on a Wallac Victor^2 absorbance plate reader (Perkin Elmer-Cetus Life Sciences, Boston, MA). Additionally, the absorbance was measured at 630 nm to correct for cell debris.

Transfection experiments

Cells were seeded into 6-well plates at 2.5 x 10^4 cells/cm^2 and allowed to attach overnight. The culture medium was removed from the wells and after two wash steps with serum free medium, the Tat/pDNA complexes, containing 1.6 µg plasmid DNA, were added to each well. In the

chloroquine experiments, the serum free medium was supplemented with 100 µM chloroquine [12,13]. Cells were incubated at 37°C for 2 hrs and then the medium was replaced by 1 ml culture medium. SEAP activity was measured after 48 hrs incubation at 37°C.

Reporter gene analysis

To measure SEAP activity, 110 µl of the medium was incubated at 65°C for 30 min with 990 µl dilution buffer (0.1 M glycine, 1 mM $MgCl_2$, 0.1 mM $ZnCl_2$, pH 10.4) and 15 µl of 5.1 µg/µl 4-methylumbelliferyl phosphate substrate (4-MUP, Sigma) in a cuvette. Samples were then incubated at room temperature for 30 min and sample fluorescence ($\lambda_{ex}/\lambda_{em}$ = 360/449 nm) was measured using the SLM-Aminco Bowman spectrofluorimeter (Urbana, IL).

Cy5 pDNA labelling

pDNA was covalently labelled with Cy5 using the *Label*IT kit of Mirus Corporation (Madison, WI, USA) according to the manufacturer's recommendations. Briefly, The Cy5 containing *Label*IT reagent and 100 µg pDNA were mixed in 1 ml Hepes buffer (20 mM Hepes, pH 7.4) at Cy5:pDNA ratio (w:w) of 0.5:1 and incubated at 37°C for 1 hr. Subsequently, the labelled pDNA was separated from unattached label by precipitation in the presence of ethanol and 0.5 M NaCl and reconstituted in Hepes buffer.

YOYO-1® GST pull down assay

Glutathione Sepharose 4B beads (5 µl) were incubated with increasing amounts of pDNA in the presence of 1:1000 YOYO-1® iodide and diluted into a total volume of 100 µl with distilled water to determine the linear range of the assay. Subsequently, the GST pull down assay was performed as described earlier, but this time in the presence of Tat/pDNA complexes (containing 7.5 µg pDNA) and 5 µl beads was analyzed on the presence of pDNA on a Wallac Victor^2 fluorescence plate reader (λ_{ex} = 485 nm and λ_{em} = 530 nm).

RESULTS & DISCUSSION

FITC-BSA-Tat and nuclear import

As mentioned in literature, molecules > 20-40 kDa are excluded from the nucleus as they cannot pas the NPC channels by passive diffusion [1]. The used Tat peptide contains a basic amino acids stretch that functions as an NLS, resulting in active nuclear transport after interaction with importin β. To test the functionality of the Tat peptide, we coupled it to FITC-BSA, a macromolecule with a molecular weight of ~68 kDa and consequently unable to passively cross the NE. Both molecules, FITC-BSA and FITC-BSA-Tat, were microinjected in the cytoplasm of Vero cells and their intracellular distribution was followed during time by CLSM. (Fig. 1). After 30 min, a strong fluorescence signal was visible in all nuclei of cells that were microinjected with FITC-BSA-Tat (Fig. 1B and 1D). In contrast, no fluorescence was present in the nuclei of cells microinjected with FITC-BSA (Fig. 1A and 1C). This experiment clearly shows that the used Tat peptide was indeed able to efficiently translocate macromolecules through the nuclear membrane that are normally excluded.

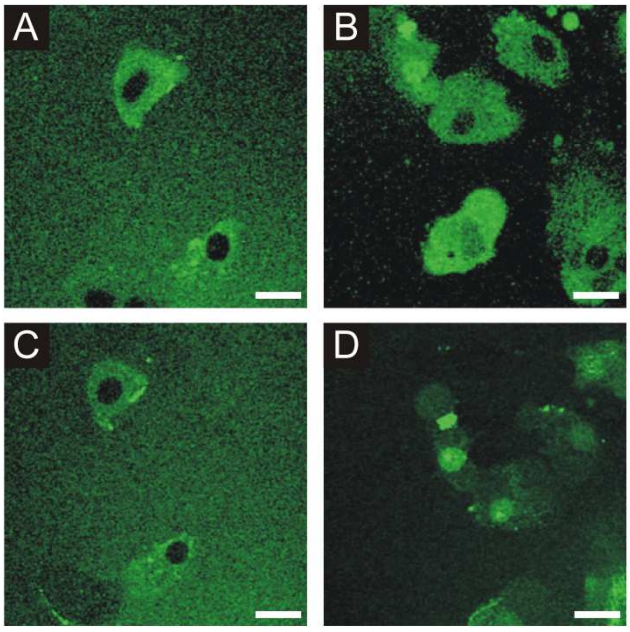

Figure 1. CLSM images of the cellular localization of FITC-BSA (A,C) and FITC-BSA-Tat (B,D) 5 min (A,B) and 30 min (C,D) after cytoplasmic microinjection. The scalebar represents 10 µm.

As nuclear uptake by NLS-containing cargos is mediated by importins, we further confirmed Tat functionality by using a GST pull down assay to analyze the ability of the Tat peptide to interact with its transporter molecule importin β. Recombinant importine β, containing a GST tag, was purified and subsequently incubated with glutathione beads. After incubation, the Tat peptide was

added to the importin β bearing beads (with or without the presence of importin α), allowing importin β-Tat interaction. After washing, both bound and unbound fraction were analyzed on PAGE, together with a control sample, i.e. SV40_eGFP incubated with importin β beads in the presence or absence of importin α. As shown in Fig. 2, the Tat-peptide was indeed present in the bound fraction of the importin β bound beads, both in the presence and absence of importin α proving the Tat peptide-importin β interaction. The control sample, SV40_eGFP NLS, could only be found in the bound fraction when both importin α and β were present, which is in agreement with literature.

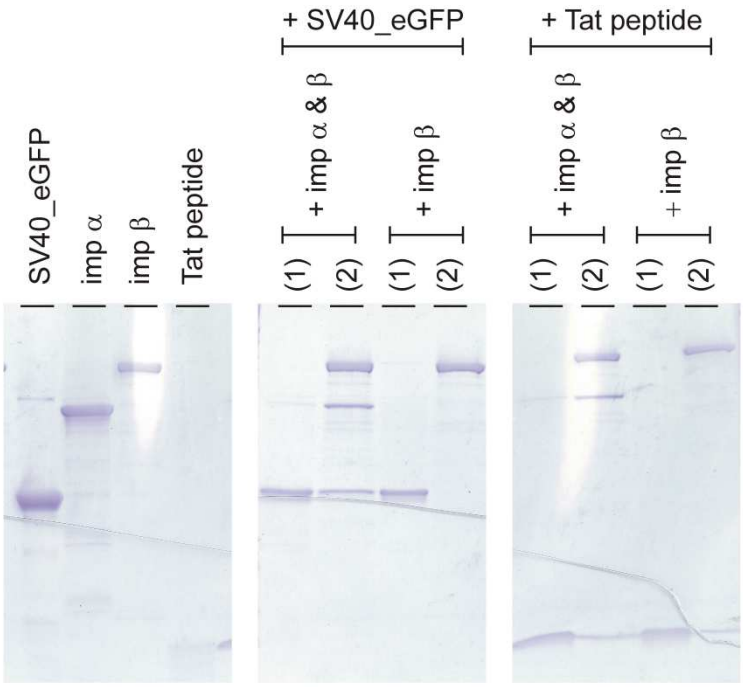

Figure 2. Coomassie brilliant blue staining of a precast 10-20 % gradient SDS-PAGE gel loaded with (1) unbound and (2) bound fractions of the control sample (SV40_eGFP) and Tat peptide sample incubated with GST-importin β (imp β) bound glutathione beads in the presence or absence of importin α (imp α).

Characterization of Tat/pDNA complexes

As the Tat peptide is strongly positively charged at physiological pH, it should have DNA binding ability by interacting with the negatively charged phosphate backbone of nucleic acids. To determine this DNA binding ability, increasing amounts of Tat peptide were incubated with a constant amount of pDNA, and the resulting effect on DNA mobility was analyzed via agarose gel electrophoresis (Fig. 3A). Additionally, the pDNA condensation ability of the Tat peptide was analyzed by measuring the fluorescence intensity of PicoGreen® after addition to the Tat/pDNA complexes (Fig. 3B).

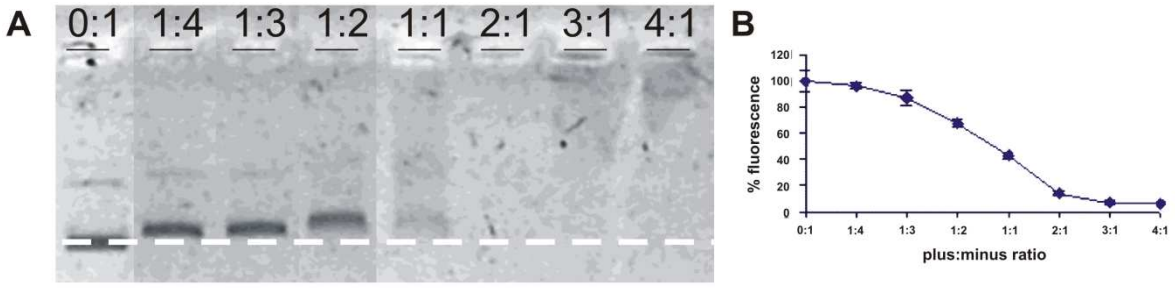

Figure 3. (A) pDNA mobility shift analysis of Tat/pDNA complexes. The pDNA (0.5 µg/ml) was electrophoresed alone or after pre-incubation with the Tat peptide in the indicated plus:minus ratio. (B) PicoGreen® fluorescence measurement after incubation of pDNA with increasing amounts of Tat.

As shown in Fig. 3A, the pDNA mobility in the agarose gel decreased when increasing amounts of Tat were added to the pDNA. At a plus:minus ratio of 2:1, the pDNA was completely immobilized. This retardation of pDNA was expected, as binding between Tat peptide and pDNA will neutralize the negatively charged pDNA and consequently decrease its mobility during electrophoresis. Additionally, if large Tat/pDNA complexes are formed, the DNA will become completely immobilized inside the slots of the gel. The data in Fig. 3A clearly show that the Tat peptide can indeed bind to the pDNA.

Furthermore, the complexation degree of the Tat/pDNA complexes was measured with a condensation assay (Fig. 3B). An increasing pDNA complexation degree will result in a gradual decrease of PicoGreen® fluorescence as this pDNA intercalating molecule cannot penetrate into tight complexes. Based on the obtained graph (Fig. 3B), we can conclude that at a plus:minus ratio of 2:1 all pDNA is complexed into tight complexes, compared to ~60 % and 0 % at a 1:1 and 0:1 plus:minus ratio, respectively.

To know whether the observed condensation is the result of the formation of (homogenous) particles, the Tat/pDNA complexes were also analyzed by particle size and zeta potential measurements. Particle size measurements via DLS were not possible on Tat/pDNA complexes with plus:minus ratios of 0:1 to 3:1. Only at a plus:minus ratio 4:1 we could measure the particle size and here we observed particles varying from 100 to 1000 nm. As an alternative, we used CLSM to visualize the Tat/pDNA complexes, by using YOYO-1® iodide labeled pDNA. Fig. 4 shows that an increasing amount of positive charges leads to an increase in particle size. We also noticed a concentration dependency of the particle size. If we used Tat/pDNA mixtures that were 10 times more concentrated, particle size was at least ten times higher and showed a higher polydispersity (data not shown).

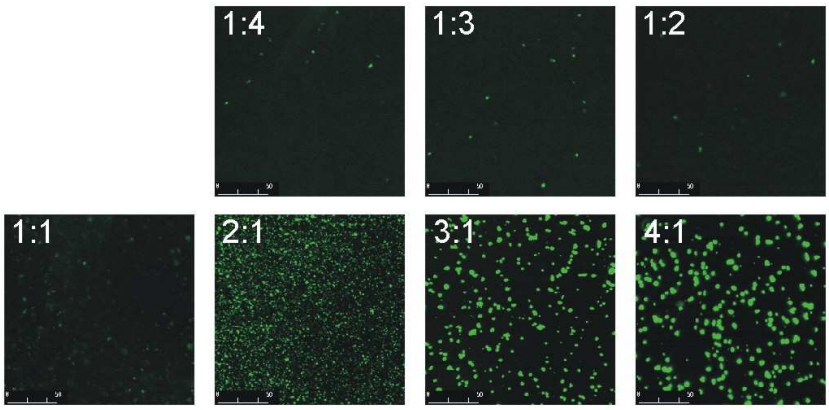

Figure 4. CSLM of YOYO-1® labelled Tat/pDNA complexes at different plus:minus ratios.

The zeta potential measurements of the Tat/pDNA complexes are shown in Fig. 5 and can be explained by the complex three dimensional structure of the pDNA. If no Tat peptide is added, the surface charge is strongly negative. If a small amount of positively charged Tat is added to the plasmid DNA, the surface charge almost reaches neutrality, since almost all added Tat peptides electrostatically interact with the first encountered, available negative charges of the pDNA at the outside of the supercoiled structure. When more Tat peptide is added, according to the zeta potential measurements, this suddenly causes a decrease in surface charge. This may be explained by a conformational change of the pDNA, leading to a higher exposure of negative groups at the outside upon addition of more Tat. Above a 1:1 plus:minus ratio, we observed a continuous increase in zeta potential, since the electrostatic Tat/pDNA interactions can't cause additional conformational changes in the pDNA, but only results in more charge neutralization. A plus:minus ratio of 3:1 eventually results in positively charged particles.

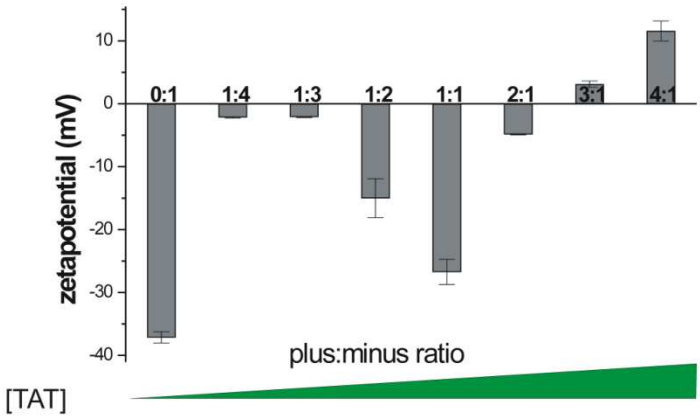

Figure 5. Zeta potential of Tat/pDNA complexes at different plus:minus ratios. If no Tat peptide is added, the surface charge is strongly negative. If a small amount of positively charged Tat is added to the plasmid DNA, the surface charge almost reaches neutrality. When more Tat peptide is added, this causes again a decrease in surface charge and beyond a 1:1 plus:minus ratio, we observed a continuous increase in zeta potential.

Cytotoxicity of the Tat/pDNA complexes

One important feature of gene carrier complexes is that they should be non-toxic when incubated with cells. The cytotoxicity of Tat/pDNA complexes was analyzed by incubating them with Vero cells and measuring the cell viability after 2 hrs using the MTT based EZ4U test. Fig. 6 clearly shows that none of the Tat/pDNA complexes exhibited severe cytotoxicity.

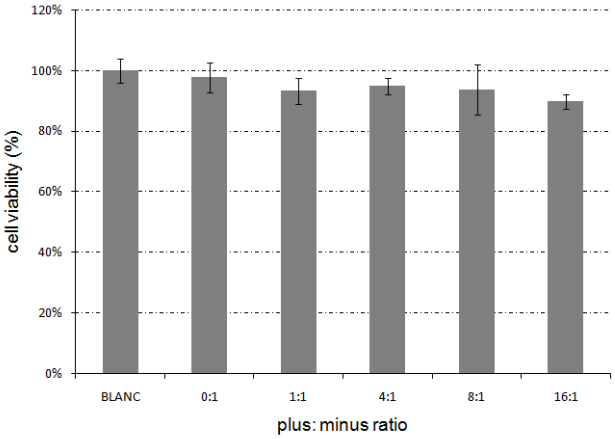

Figure 6. Cytotoxicity of Tat/pDNA complexes on Vero cells with different plus:minus ratios.

Transfection efficiency, cellular uptake and nuclear transport of Tat/pDNA complexes

We examined the transfection efficiency of the Tat/pDNA complexes both in Vero and Cos-7 cells by evaluating the expression of the complexed reporter gene, SEAP. Different plus:minus ratios were used. As seen in Fig. 7, the obtained transfection results were disappointing as the increase in transfection efficiency was rather limited compared to naked pDNA transfection.

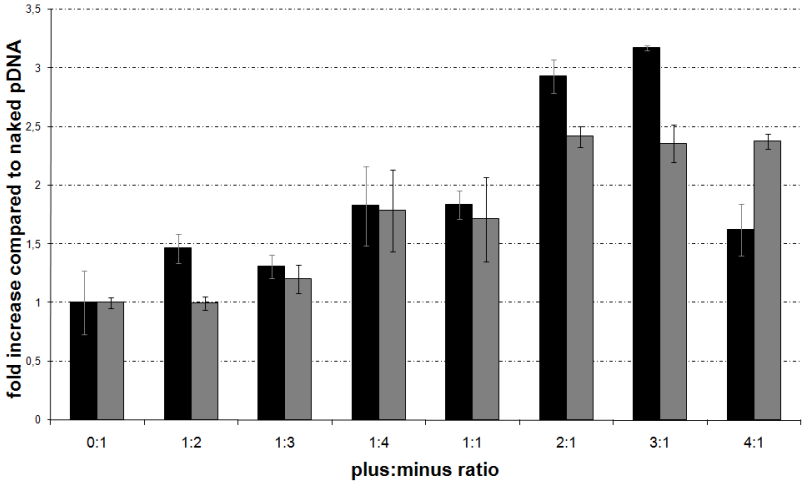

Figure 7. Transfection efficiency of Tat/pDNA complexes with different plus:minus ratios compared to naked pDNA in Cos-7 (black) and Vero cells (grey).

Measuring the transfection efficiency means measuring the end result of both cellular and nuclear transport of the pDNA. As transfection efficiency was barely enhanced, we analyzed both processes separately. To study the cellular uptake, Cy5 labelled pDNA was complexed with the Tat peptide in a plus:minus ratio of 2:1 and incubated with Vero cells. Subsequently, cellular distribution of the Cy5 labelled pDNA was evaluated by CLSM. After 3 hrs incubation, the Tat/pDNA complexes formed a punctuated pattern inside the cytoplasm (data not shown), indicating an endosomal uptake of the Tat/pDNA complexes. However, the Tat/pDNA complexes were apparently unable to escape from the endosomes as no cytoplasmic fluorescence signal was visible. The lysosomotropic compound chloroquine is known to mediated endosomal release [14], therefore Tat/pDNA transfection experiments were performed in the presence of chloroquine, but this had no effect on the transfection efficiency (data not shown). As endosomal release couldn't enhance the efficiency of the Tat/pDNA complexes, one of the major limiting factors of the transfection efficiency of these complexes is probably the nuclear import. Therefore, we evaluated the effect of Tat on the nuclear transport of pDNA by microinjection of free Cy5 labelled pDNA and Tat/Cy5-pDNA complexes (plus:minus ratio 2:1). In both experiments, there was no nuclear signal visible, even not after 1 hr (data not shown), indicating the absence of nuclear pDNA import.

Relation nuclear import and importin β binding

We confirmed in Fig. 1 that Tat has the ability to translocate the FITC-BSA molecule through the nuclear membrane. However, when the peptide is electrostatically mixed with pDNA, no enhancement in transfection efficiency could be observed. The absence of nuclear uptake of pDNA after cytoplasmic injection of the Tat/pDNA complexes may indicate that (1) pDNA is a too large cargo for Tat or (2) Tat loses its NLS capacity after electrostatic binding to pDNA. To elucidate whether the latter hypothesis this true, we analyzed if the Tat peptide, complexed with the pDNA, is still able to interact with importin β by using the abovementioned pull down assay. Importin β bearing beads were mixed with Tat/Cy5-pDNA complexes and subsequently, the presence of fluorescent pDNA around the beads was analyzed using a fluorimeter. However, no pDNA could be detected around the beads, indicating the inability of the Tat/pDNA complexes to interact with importin β. This hypothesis was further confirmed by determining the presence of pDNA in the bound fraction using the DNA intercalating agent YOYO-1® iodide. First, the linearity of the test was studied in the presence of beads and between 0 and 15 ng pDNA a linear curve was obtained, making this approach useful to determine the amount of pDNA. In parallel, also the bound fraction was analyzed on the presence of pDNA but again no pDNA could be detected, indicating the inability of the Tat/pDNA complexes to interact with the importin β beads.

One can speculate about the reasons of the obtained results that are in contrast with research published by e.g. Zanta et al. who found that attachment of an NLS peptide to DNA could result in a 300-fold increase in transfection efficiency [8]. However, it should be mentioned that more studies were published in which coupling of an NLS peptide to DNA did not result in major increases in gene transfection. Attachment of the SV40 NLS to a specific region in the pDNA by using a peptide nucleic acid (PNA) molecule, resulted in a limited 5 to 8-fold increase [15]. Covalent association of NLS peptides to the pDNA by photoactivation didn't result in nuclear translocation after cytoplasmic injection [16]. Covalent linkage of the SV40 NLS to linear DNA did not enhance transfection efficiency of cationic polymer based gene delivery systems [17]. We demonstrated that Tat loses its importin β binding capacity when it is electrostatically bound to pDNA. The NLS domain in Tat is probably masked after electrostatic binding of Tat to the negatively charged pDNA, resulting in masking of the NLS domain. The latter has also been suggested by van der AA et al. [17]. This hypothesis is supported by the finding that introducing a spacer between DNA and peptide can be beneficial for the efficiency [18].

CONCLUSION

Efficient non-viral gene delivery requires efficient DNA transport into the nucleus. As the nuclear membrane forms a tight barrier for molecules larger than 20-40 kDa, such as DNA, nuclear import can be considered as one of the major limiting steps, especially in non-dividing cells. One strategy to overcome this barrier is the attachment of components of the active nuclear import machinery to the pDNA molecules. The positively charged Tat peptide contains a basic amino acids stretch exhibiting NLS function. To enhance nuclear uptake of pDNA we prepared non-toxic, electrostatic Tat/pDNA complexes with different plus:minus ratios. Cytoplasmic microinjection of Tat/pDNA complexes did not result in nuclear import of the labeled pDNA. Similarly, the transfection efficiency was barely increased when the pDNA was electrostatically complexed with the Tat peptide. In agreement with these results, an *in vitro* test to evaluate binding of the Tat/pDNA complexes with the nuclear import machinery was negative, although the Tat peptide itself was able to interact with importin β. So, despite the fact that the Tat peptide was able to mediate nuclear import of BSA (~68 kDa), the same peptide was unable to translocate pDNA into the nucleus, probably due to masking of the NLS domain after electrostatic interaction between Tat and pDNA. Taken together, the results of our study indicate that electrostatically coupling of an NLS to pDNA does not necessarily enhance transfection efficiency.

ACKNOWLEDGMENTS

Els Vanderleyden is thanked for the FITC-BSA-Tat coupling. The people at the Corbett Lab (Emory University, Atlanta, Georgia), especially Anita Corbett and Allison Lange, are thanked for all the help with the recombinant protein purification and GST pull down assays.

REFERENCES

(1) Macara I.G. Transport into and out of the nucleus. *Microbiol. Mol. Biol. Rev.* **2001** 65(4) 570-94, table.

(2) Gorlich D. & Kutay U. Transport between the cell nucleus and the cytoplasm. *Annu. Rev. Cell Dev. Biol.* **1999** 15607-660.

(3) Dingwall C. & Laskey R.A. Nuclear targeting sequences--a consensus? *Trends Biochem. Sci.* **1991** 16(12) 478-481.

(4) Gorlich D. Transport into and out of the cell nucleus. *EMBO J.* **1998** 17(10) 2721-2727.

(5) Truant R. & Cullen B.R. The arginine-rich domains present in human immunodeficiency virus type 1 Tat and Rev function as direct importin beta-dependent nuclear localization signals. *Mol. Cell Biol.* **1999** 19(2) 1210-1217.

(6) Hebert E. Improvement of exogenous DNA nuclear importation by nuclear localization signal-bearing vectors: a promising way for non-viral gene therapy? *Biol. Cell* **2003** 95(2) 59-68.

(7) Escriou V., Carriere M., Scherman D., & Wils P. NLS bioconjugates for targeting therapeutic genes to the nucleus. *Adv. Drug Deliv. Rev.* **2003** 55(2) 295-306.

(8) Zanta M.A., Belguise-Valladier P., & Behr J.P. Gene delivery: a single nuclear localization signal peptide is sufficient to carry DNA to the cell nucleus. *Proc. Natl. Acad. Sci. U. S. A* **1999** 96(1) 91-96.

(9) Nekhai S. & Jeang K.T. Transcriptional and post-transcriptional regulation of HIV-1 gene expression: role of cellular factors for Tat and Rev. *Future. Microbiol.* **2006** 1417-426.

(10) Efthymiadis A., Briggs L.J., & Jans D.A. The HIV-1 Tat nuclear localization sequence confers novel nuclear import properties. *J. Biol. Chem.* **1998** 273(3) 1623-1628.

(11) Fanara P., Hodel M.R., Corbett A.H., & Hodel A.E. Quantitative analysis of nuclear localization signal (NLS)-importin alpha interaction through fluorescence depolarization. Evidence for auto-inhibitory regulation of NLS binding. *J. Biol. Chem.* **2000** 275(28) 21218-21223.

(12) Ferrari V. & Cutler D.J. Kinetics and thermodynamics of chloroquine and hydroxychloroquine transport across the human erythrocyte membrane. *Biochem. Pharmacol.* **1991** 41(1) 23-30.

(13) Abes S., Williams D., Prevot P., Thierry A., Gait M.J., & Lebleu B. Endosome trapping limits the efficiency of splicing correction by PNA-oligolysine conjugates. *J. Control Release* **2006** 110(3) 595-604.

(14) Shiraishi T. & Nielsen P.E. Enhanced delivery of cell-penetrating peptide-peptide nucleic acid conjugates by endosomal disruption. *Nat. Protoc.* **2006** 1(2) 633-636.

(15) Branden L.J., Mohamed A.J., & Smith C.I. A peptide nucleic acid-nuclear localization signal fusion that mediates nuclear transport of DNA. *Nat. Biotechnol.* **1999** 17(8) 784-787.

(16) Ciolina C., Byk G., Blanche F., Thuillier V., Scherman D., & Wils P. Coupling of nuclear localization signals to plasmid DNA and specific interaction of the conjugates with importin alpha. *Bioconjug. Chem.* **1999** 10(1) 49-55.

(17) van der Aa M.A., Koning G.A., d'Oliveira C. *et al.* An NLS peptide covalently linked to linear DNA does not enhance transfection efficiency of cationic polymer based gene delivery systems. *J. Gene Med.* **2005** 7(2) 208-217.

(18) Nagasaki T., Myohoji T., Tachibana T., Futaki S., & Tamagaki S. Can nuclear localization signals enhance nuclear localization of plasmid DNA? *Bioconjug. Chem.* **2003** 14(2) 282-286.

Chapter 7

Nuclear Accumulation of Plasmid DNA can be Enhanced by Non-selective Gating of the Nuclear Pore

This chapter is published:

Roosmarijn E. Vandenbroucke[1], Bart Lucas[1], Joseph Demeester[1], Stefaan C. De Smedt[1] and Niek N. Sanders[1]; *Nucleic Acid Research*. 2007;35(12):e86.

[1] Laboratory of General Biochemistry and Physical Pharmacy, Department of Pharmaceutics Ghent University, Ghent, Belgium.

ABSTRACT

One of the major obstacles in non-viral gene transfer is the nuclear membrane. Attempts to improve the transport of DNA to the nucleus through the use of nuclear localisation signals or importin β have achieved limited success. It has been proposed that the nuclear pore complexes (NPCs) through which nucleocytoplasmic transport occurs are filled with a hydrophobic phase through which hydrophobic importins can dissolve. Therefore, considering the hydrophobic nature of the NPC channel, we evaluated whether a non-selective gating of nuclear pores by *trans*-cyclohexane-1,2-diol (TCHD), an amphipathic alcohol that reversibly collapses the permeability barrier of the NPCs, could be obtained and used as an alternative method to facilitate nuclear entry of plasmid DNA. Our data demonstrate for the first time that TCHD makes the nucleus permeable for both high molecular weight dextrans and plasmid DNA (pDNA) at non-toxic concentrations. Furthermore, in line with these observations, TCHD enhanced the transfection efficacy of both naked DNA and lipoplexes. In conclusion, based on the proposed structure of NPCs we succeeded to temporarily open the NPCs for macromolecules as large as pDNAs and demonstrated that this can significantly enhance non-viral gene delivery.

Chapter 7

Nuclear Accumulation of Plasmid DNA can be Enhanced by Non-selective Gating of the Nuclear Pore

INTRODUCTION

Viral vectors are efficient DNA delivery systems as they possess natural mechanisms to enter cells, to escape from endosomes and to transport their DNA into the nucleus. However, they also display important disadvantages, such as immunogenic response and safety risks when administered to patients. Non-viral carriers lack these disadvantages, but poor transfection efficiencies currently limit the usefulness of these vectors for gene therapy applications. The low gene transfer capacity of non-viral vectors is mainly due to their inability to translocate the therapeutic DNA into the cell nucleus. Indeed, it has been shown that microinjection of plasmid DNA (pDNA) in the cytoplasm of non-dividing cells resulted in <1 % gene expression, while a massive gene expression occurred when the pDNA was injected in the nucleus [1-3]. In dividing cells the nuclear envelope disassembles on a regular base, which offers an opportunity for DNA to enter the nucleus [4-6]. However, the DNA that is waiting in the cytoplasm for the next cell division is sensitive to degradation by nucleases. Therefore, methods that can enhance the nuclear uptake of DNA into nuclei of both non-dividing and dividing cells are urgently needed in non-viral-based gene therapy.

Nucleocytoplasmic transport proceeds through the nuclear pore complexes (NPCs) which form channels in the nuclear envelope with a diameter of approximately 40 nm [7,8]. Vertebrate NPCs have a mass of ~125 MDa and contain 30-50 different proteins, which are called nucleoporins. Small molecules with a molecular weight up to 30 kDa can passively diffuse through the NPC. In contrast, the translocation of larger macromolecules into the nucleus occurs via an active mechanism involving nuclear transport receptors. The majority of the nuclear transport pathways are mediated by receptors of the importin family. Proteins or other cargo molecules that carry a classical nuclear localization sequence (NLS) are recognized by importin α, which subsequently forms a complex

through its importin β binding domain with importin β [9]. NLSs can be highly diverse in nature and range from the short bipartite classical NLS to extended protein domains, as is the case for histones or ribosomal proteins [10]. To promote the nuclear import of DNA, NLS peptides, NLS containing proteins and even importin β [11] have been attached to DNA via several strategies: electrostatic [12-17] or covalent [18-22] binding, via protein-DNA interaction [23,24], via PNA clamps [25-28] and coupled to polymers [29-31], lipids [32-37] or recombinant lambda phage [38]. Nevertheless, all these attempts to improve the transport of DNA to the nucleus through the use of NLSs or importin β have achieved only limited success.

It has recently been shown that the nuclear uptake of macromolecules can be enhanced significantly by addition of the amphipathic molecule *trans*-cyclohexane-1,2-diol (TCHD) [39]. The mechanism by which TCHD causes nuclear localization of macromolecules can be explained based on the inner channel properties of the nuclear pores. It is believed that these nuclear pores are filled with a hydrophobic phase through which importins, but not inert hydrophilic substrates, can dissolve. The addition of TCHD causes a temporary, non-selective gating of the pore and allows passage of molecules which would otherwise be rejected from passage. In other words, a non-selective gating of the nuclear pore channel by TCHD renders the actual translocation through the pore channel independent of nuclear transport receptors. This can be explained by the fact that TCHD causes disruption of the hydrophobic interactions between the hydrophobic phenylalanine-glycine (FG) repeats of the nucleoporines, which consequently causes collapsing of the permeability barrier of the NPCs. Importantly, the effect of TCHD is reversible and does not cause damage of the nuclear pores [40].

In this paper we studied whether a non-selective gating of nuclear pores by amphipathic molecules like TCHD could also be used as an alternative method to facilitate nuclear entry of plasmid DNA. Therefore, we examined the effect of TCHD (a) on the nuclear import of macromolecules and pDNA and (b) on the transfection efficiency of naked pDNA and non-viral nanoparticles, such as poly- and lipoplexes (LPXs). In summary, we found that TCHD was able to make the nuclear membrane permeable for both high molecular weight dextrans and pDNA at non-toxic concentrations. Furthermore, TCHD enhanced the transfection efficiency of both naked pDNA and DOTAP:DOPE-based LPXs, but had no effect on the linear PEI-based polyplexes.

MATERIALS & METHODS

Materials

Dulbecco's modified Eagle's medium (DMEM), L-glutamine (L-Gln), heat-inactivated fetal bovine serum (FBS), Phosphate Buffered Saline (PBS) and penicillin/streptomycin (P/S) were supplied by GibcoBRL (Merelbeke, Belgium). The secreted alkaline phosphatase (SEAP) expression plasmid was a kind gift from Prof. Dr. Tavernier (Ghent University, Belgium) and 22 kDa linear poly(ethyleneimine) (PEI) from Prof. Dr. Wagner (University of Munich, Germany). The pGL3-control plasmid and luciferase assay kit were obtained from Promega (Leiden, The Netherlands). 158 kDa tetramethylrhodamine isothiocyanate labelled dextran (TRITC-dextran) and TCHD were purchased from Sigma Aldrich. 1,2-Dioleoyl-3-Trimethylammonium-Propane Chloride Salt (DOTAP), 1,2-Dioleoyl-*sn*-Glycero-3-Phosphoethanolamine (DOPE) and 1,2-Distearoyl-*sn*-Glycero-3-Phosphoethanolamine-N-[Amino(Polyethylene Glycol)2000] (DSPE-PEG_{2000}) were obtained from Avanti Polar Lipids (Alabaster, AL, US).

Cell culture

A549 (lung carcinoma cells; ATCC number CCL-185) and Vero (epithelial African green monkey kidney cells; ATCC number CCL-81) cells were cultured in DMEM containing 2 mM L-Gln, 10 % heat-inactivated FBS, 1 % P/S and grown at 37°C in a humidified atmosphere containing 5 % CO_2.

Fluorescent labelling of pDNA

Plasmid DNA was covalently labelled with Cy5 using the *Label*IT kit of Mirus Corporation (Madison, WI, USA) according to the manufacturer's recommendations. Briefly, *Label*IT reagent, containing Cy5, and 100 µg DNA were mixed in 1 ml Hepes buffer (20 mM Hepes, pH 7.4) at Cy5:DNA ratio (w:w) of 0.5:1 and incubated at 37°C for 1 hr. Subsequently, the labelled pDNA was separated from unattached label by precipitation in the presence of ethanol and 0.5 M NaCl and reconstituted in 20 mM Hepes buffer (pH 7.4).

Microinjection studies

Microinjection studies were conducted using a Femtojet® microinjector and an Injectman® NI 2 micromanipulator (Eppendorf, Hamburg, Germany). Vero cells were chosen for these microinjection experiments as they have a well defined nucleus and large cytoplasm. Vero cells (2.5×10^4 cells/cm^2) were plated onto sterile glass bottom culture dishes (MatTek Corporation, MA, USA) and allowed to adhere for 1 day. The cells were then washed with PBS and transferred into 2 ml serum free medium supplemented with 20 mM Hepes (pH 7.4) to improve the buffering capacity of the medium during microinjection. 5 µl 158 kDa TRITC-dextran (1 mg/ml) or Cy5 labelled pDNA (1 mg/ml) was back-loaded into Femptotip II microinjection needles and cells were injected using an injection pressure of 100 psi, a backpressure of 30–50 psi and injection duration of 0.5 sec. Where mentioned, the medium was replaced after microinjection by TCHD containing serum free medium, supplemented with 20 mM Hepes (pH 7.4).

To determine the cellular distribution, the fluorescence in the cells was visualized on different time points after microinjection using a Nikon C1si confocal laser scanning module attached to a motorized Nikon TE2000-E inverted microscope (Nikon Benelux, Brussels, Belgium). with a 60 x water immersion objective and the 561 nm and 638 nm laser lines for the excitation of the TRITC and Cy5 label, respectively. A non-confocal diascopic DIC (differential interference contrast) image was collected simultaneously with the confocal images.

For the z-scan analysis of the fluorescence after cytoplasmic microinjection of the Cy5 labelled pDNA (Cy5-pDNA), the confocal volume (~1 femtoliter) of a BioRad MRC 1024 CLSM (Hemel Hempstadt, UK) equipped with the ConfoCor 2 fluorescence correlation spectroscopy (FCS) setup (LSM510 ConfoCor 2, Zeiss, Göttingen, Germany) was positioned in a randomly selected site in the nucleus. The fluorescence, along the z-axis at this selected XY site and perpendicular to the cell surface, was recorded with the avalanche photodiodes of the ConfoCor 2 system before and every 10 min after addition of 1 % (w/v) TCHD dissolved in serum free medium supplemented with 20 mM Hepes (pH 7.4).

Preparation of polyplexes and lipoplexes

Polyplexes consisting of 22 kDa linear PEI were prepared as described by Fayazpour et al. [41]. Briefly, polyplexes were prepared in 20 mM Hepes pH 7.4 by adding the PEI all at once to the pDNA at a N/P ratio of 10. Subsequently, the mixture was vortexed for 10 sec and the polyplexes were allowed to equilibrate for 30 min at room temperature prior to use. The final pDNA concentration in the polyplexes was 0.126 µg/µl.

Liposomes composed of DOTAP:DOPE:DSPE-PEG_{2000} (molar ratio 5:5:0.2) were prepared as described previously [42]. Briefly, appropriate amounts of lipids were dissolved in chloroform and mixed. The chloroform was subsequently removed by rotary evaporation at 37°C followed by flushing the obtained lipid film with nitrogen during 30 min at room temperature. The dried lipids were then hydrated by adding Hepes buffer till a final lipid concentration of 10.2 mM. After mixing in the presence of glass beads, liposome formation was allowed overnight at 4°C. Thereafter, the formed liposomes were extruded 11 times through two stacked 100 nm polycarbonate membrane filters (Whatman, Brentfort, UK) at room temperature using an Avanti Mini-Extruder (Avanti Polar Lipids). The extruded liposomes were subsequently mixed with pDNA in a +/- charge ratio of 4 and incubated at room temperature for 30 min prior to use. The final pDNA concentration in the LPX dispersion was 0.126 µg/µl.

Size and zeta potential measurements

The average particle size and zeta potential of the liposomes, LPXs and polyplexes were measured by photon correlation spectroscopy (PCS) (Autosizer 4700, Malvern, Worcestershire, UK) and particle electrophoresis (Zetasizer 2000, Malvern), respectively. The liposome, lipoplex and polyplex dispersions were diluted 40-fold in Hepes buffer before the particle size and zeta potential were measured. The average (± standard error) of the liposomes and lipoplexes was 118 ± 1 nm and 242 ± 6 nm, respectively and their average zeta potential equaled 26 ± 4 mV and 14 ± 1 mV, respectively. The diameter and zeta potential of the linear PEI polyplexes were 165 ± 4 nm and 33 ± 2 mV.

Cell Viability Assay

The influence of TCHD on the cell viability was determined using the CellTiter-Glo® Assay (Promega). according to the manufacturer's instructions. Briefly, 2.5 x 10^4 cells/cm^2 were seeded in a 96-well plate and allowed to adhere. After 24 hrs, cells were washed with PBS and incubated with serum free medium containing increasing amounts of TCHD. After 1 hr, the TCHD was removed and replaced by culture medium. After 48 hrs, the plate was incubated at room temperature for 30 min and 100 µl CellTiter-Glo® reagent was added to each well. After shaking the plate for 10 min and 2 min incubation at room temperature, the luminescence was measured on a GloMax™ 96 luminometer with 1 sec integration time.

Transfection experiments

Cells were seeded into 24-well plates at 2.5 x 10^4 cells/cm^2 and allowed to attach overnight. Subsequently, the culture medium was removed, and after two washing steps with serum free medium, 0.4 µg pDNA, polyplexes or lipoplexes (both containing 0.4 µg pDNA) were added to each well. After 2 hrs the pDNA or non-viral nanoparticles were removed from the cells and the cells were post-incubated for 1 hr with serum-free medium containing increasing amounts of TCHD. Subsequently, this medium was replaced by culture medium and the cells were further incubated at 37°C. After 48 hrs both the SEAP (or luciferase) activity, as well as the total cellular protein concentration were measured.

To determine the SEAP activity, 100 µl of the culture medium above the cells was taken and incubated at 65 °C for 30 min. Subsequently, 100 µl dilution buffer (0.1 M glycine, 1 mM $MgCl_2$, 0.1 mM $ZnCl_2$, pH 10.4) and 15 µl 4-methylumbelliferyl phosphate (4-MUP, 5.1 µg/µl in distilled water) was added. The obtained mixtures were then incubated at 37°C and the fluorescence was measured on a Wallac Victor^2 fluorescence plate reader (Perkin Elmer-Cetus Life Sciences, Boston, MA) using an excitation and emission wavelength of 360 nm and 449 nm, respectively.

To determine the luciferase activity of the cells, cells were lysed with 80 µl 1 x CCLR buffer (Promega) and luciferase activity was determined with the Promega luciferase assay kit according to the manufacturer's instructions. Briefly, 100 µl substrate was added to 20 µl sample and after a 2 sec delay, the luminescence was measured during 10 sec with the GloMax^{TM} 96 luminometer.

To correct for the amount of cells per well, the protein concentration was determined with the BCA kit (Pierce, Rockford, IL, USA). 200 µl mastermix, containing 50 parts reagent A to 1 part B, was mixed with 20 µl cell lysate and incubated at 37°C for 30 min and the absorbance was measured on a Wallac Victor^2 absorbance plate reader (Perkin Elmer-Cetus Life Sciences) at 590 nm.

Statistics

The experimental data in this report are expressed as mean ± standard deviation (SD). One way ANOVA was used to determine whether data groups differed significantly from each other. A p-value lower than 0.05 was considered statistically significant.

RESULTS & DISCUSSION

TCHD facilitates the nuclear accumulation of dextrans and plasmid DNA

It has been demonstrated that TCHD enhances the rate of nuclear entry of the maltose binding protein [43]. However, this protein has a rather low molecular weight (40 kDa) and is consequently not totally excluded from the nucleus. Therefore, we studied whether TCHD could induce nuclear entry of higher molecular weight compounds like 158 kDa dextrans and especially pDNA, since nuclear transport of therapeutic genes forms an important bottle neck in non-viral gene delivery.

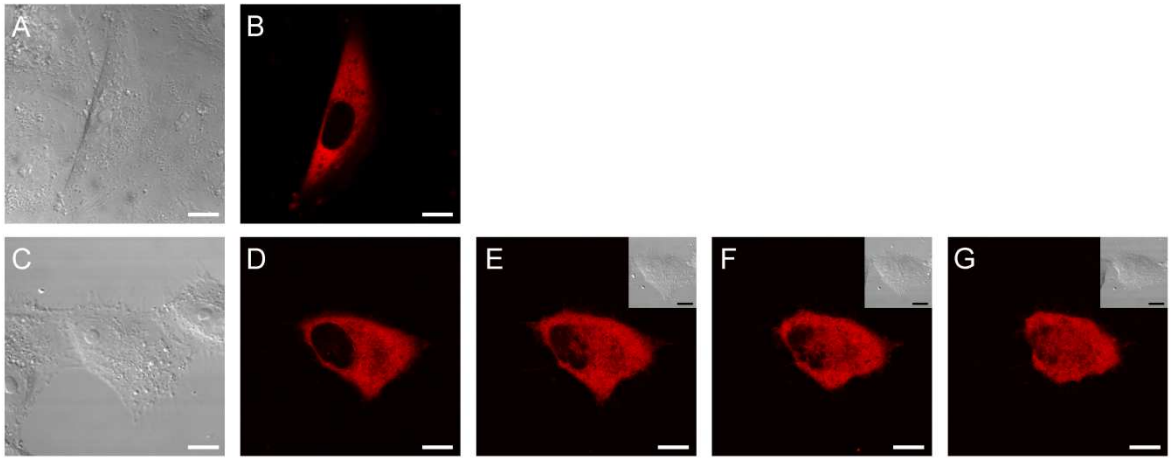

Figure 1. Non-confocal DIC (A, C and inserts in E till G) and confocal images (B and D till G) of Vero cells after cytosolic microinjection of 158 kDa TRITC-dextran. Images (A) and (B) represent a microinjected cell 60 min after microinjection. Images (C) till (G) represent another microinjected cell after 10 sec (D), 40 sec (E), 5 min (F) and 10 min (G) incubation with 1 % (w/v) TCHD.

In a first approach we microinjected 158 kDa TRITC-dextrans in the cytoplasm of Vero cells and followed their nuclear influx in the absence and presence of TCHD by confocal laser scanning microscopy (CLSM). In the absence of TCHD, no TRITC-dextran could be detected in the nucleus, not even after 1 hr of incubation (Fig. 1A and 1B). This is as expected, since it is well known that molecules larger than ~70 kDa can not move passively through the NPC network [44]. When TRITC-dextran microinjected cells were incubated with 1 % (w/v) TCHD containing medium, a rapid nuclear localisation of the TRITC-dextrans was detected (Fig. 1D till 1G). Indeed, as soon as 10 sec after addition of TCHD to the cells, TRITC-dextran was already detected in the nucleus. After 10 min the TRITC-dextran fluorescence was homogeneously distributed throughout the cell. These data clearly demonstrate that TCHD opens the NPCs what results in nuclear passage of macromolecules that

otherwise are excluded from the nucleus. We also co-injected TCHD (2 % w/v) and TRITC-dextran (158 kDa) in the cytosol, but under these conditions we could not observe nuclear localisation (data not shown). One likely explanation is that TCHD, which is an amphiphilic compound and contains a polar ethylene glycol moiety and an apolar butylene moiety, can rapidly cross cell membranes and thus becomes rapidly diluted in the surrounding medium [45].

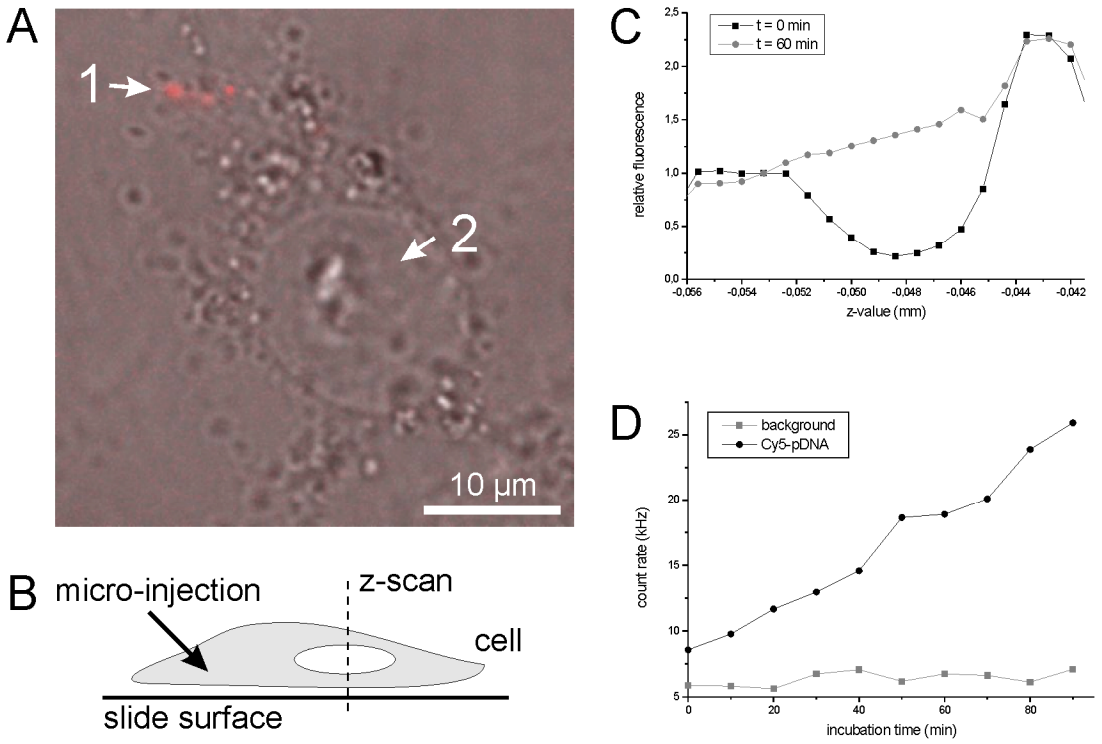

Figure 2. Effect of TCHD on the nuclear entry of microinjected Cy5-pDNA microinjected in the cytoplasm of Vero cells. A schematic overview of the experimental set up is shown in (B). (A) represents a microinjected cell with arrow (1) representing the place of cytoplasmic microinjection and arrow (2) the place where the z-scan was performed. The black squares (-■-) in (C) represent the z-scan through the cytosol and nucleus of a microinjected Vero at time point zero, so just after microinjection and before addition of TCHD. The grey circles (-●-) represent the z-scan 60 min after addition of 1 % (w/v) TCHD. In image (C), the center of the cell nucleus is located at z-value -0.048. The time dependent increase of Cy5-pDNA fluorescence in the nucleus after cytoplasmic injection of Cy5-pDNA without (-■-) and with (-●-) TCHD is shown in (D).

Next, we tested whether TCHD can also facilitate the nuclear uptake of pDNA, since pDNAs are much larger (2 to 10 MDa) than 158 kDa TRITC-dextran and have dimensions in the range of the inner diameter of the channels formed by the NPCs. When Cy5-pDNA was microinjected in the cytoplasm of Vero cells, a fluorescent spot was visible at the injection site (Fig. 2A, position 1). After 1 hr incubation with TCHD, we could not observe accumulation of the pDNA inside the nucleus by CLSM (data not shown). Importantly, during that time the fluorescent microinjection spot became more diffuse but remained visible, indicating a restricted mobility of pDNAs in the cytoplasm. This is in agreement with the observations by Lukacs et al. who showed that the diffusion of pDNA in the cytoplasm may be an important rate-limiting barrier in gene delivery utilizing non-viral vectors [46].

Hence, after 1 hr only a small fraction of the microinjected pDNA will have reached the nuclear membrane. Additionally, as stated above the inner diameter of the NPC is in the size range of pDNA. Therefore, even in the presence of TCHD the number of pDNA molecules that enter the nucleus is probably low and beyond the detection limit of the CLSM.

To monitor nuclear pDNA influx with higher sensitivity, we used a CLSM equipped with a fluorescence correlation spectroscopy (FCS) set up, which can detect as few as ~1 fluorescent molecule in a femtoliter range confocal volume [47]. We performed time dependent z-scans, perpendicular to the slide surface and through position 2 (Fig. 2A) before and after microinjection of Cy5-pDNA in the cytoplasm at position 1 (Fig. 2A), hereby crossing first a part of the cytoplasm beneath the nucleus, then the nucleus and finally the cytoplasm above the nucleus (Fig. 2B). The black squares in Fig. 2C show that after cytoplasmic microinjection of the Cy5-pDNA, a fluorescence signal could be detected in the cytoplasm, but not in the nucleus. The difference in fluorescence intensity detected below and above the nucleus is most likely due to a difference in distance from the cytosolic injection site. Subsequently, 1 % (w/v) TCHD was added to the cells and z-scans through position 2 were performed every 10 min. The z-scan after 60 min, represented by grey circles in Fig. 2C, shows a clear elevated Cy5-pDNA fluorescence signal in the nucleus compared to the fluorescence profile before addition of TCHD. Subsequently, we studied the pDNA influx in the nucleus in the presence and absence of TCHD. Therefore, the confocal volume of the FCS set up was parked in the middle of the nucleus (at z-value -0.048 mm). A gradual increase of Cy5-pDNA was observed when TCHD was added to the cells (Fig. 2D; black circles). In contrast, when no TCHD was present, no increase in fluorescence could be detected in the nucleus (Fig. 2D; grey squares). This demonstrates that the time dependent increase in fluorescence after addition of TCHD is not a result of passive diffusion of small degradation products of the Cy5-pDNA into the nucleus.

Cytotoxicity of TCHD

It has been demonstrated that the effect of 7 % (w/v) TCHD on the NPC permeability is reversible and that it does not cause denaturation or leakage of nucleoporins out of the NPCs [48]. Nevertheless, the reversible non-selective opening of NPCs may result into an unwanted leakage of cellular biomacromolecules from the cytoplasm into the nucleus or vice versa and hence interfere with essential cellular processes. Therefore, to ascertain that TCHD does not cause cytotoxic effects, we determined the cell viability 48 hrs after exposure to TCHD by the CellTiter-Glo® assay (Promega). This assay assesses the cytotoxicity by quantifying the intracellular ATP levels, which is a sensitive marker of cell viability as within minutes after a loss of membrane integrity, cells lose the ability to synthesize ATP and endogenous ATPases destroy any remaining ATP. Fig. 3 shows that incubation of

Vero and A549 cells during 1 hr with 1 % (w/v) TCHD slightly reduced the viability of these cells. These results demonstrate that the TCHD does not cause drastic cytotoxic effects under the conditions of the nuclear uptake experiments above, i.e. incubation of the cells with 1 % (w/v) TCHD for 1 hr. Furthermore, we noticed a cell dependent TCHD sensitivity. Indeed, TCHD at concentrations above 1 % (w/v) significantly decrease the viability of Vero cells whereas almost no cytotoxic effects are observed in A549 cells incubated with up to 3 % (w/v) TCHD.

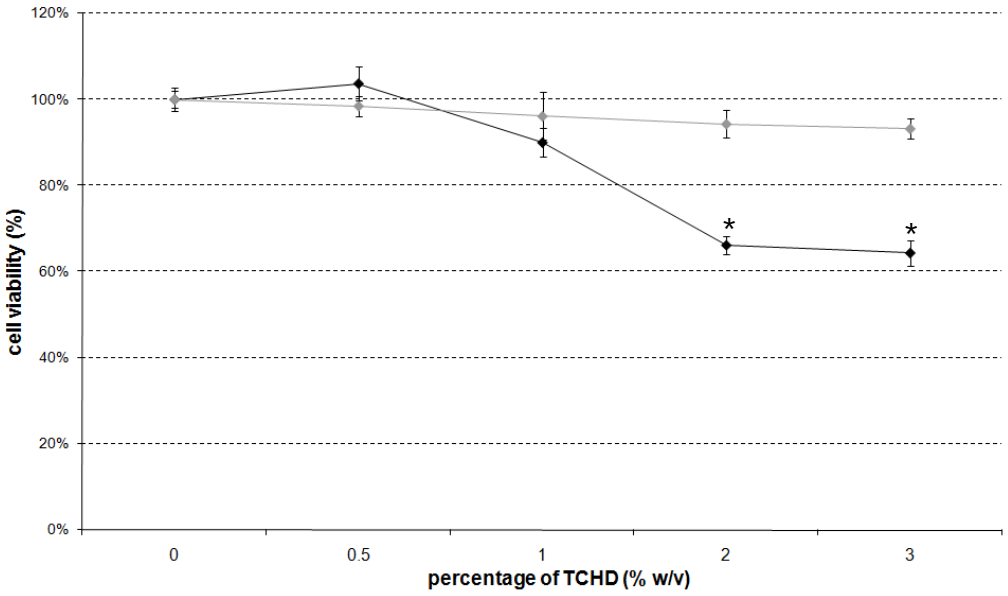

Figure 3. Cell viability of Vero (black) and A549 cells (grey) after 1 hr of incubation with TCHD. The asterix (*) represents data that significantly differ ($p<0.05$) from the data point 0 % (w/v) TCHD.

Influence of TCHD on the transfection efficiency of non-viral vectors

Since nuclear uptake of pDNA is considered as one of the major barriers in non-viral gene delivery and since we showed that TCHD could cause nuclear uptake of Cy5-pDNA, we wondered whether TCHD could enhance the transfection efficiency of naked pDNA, cationic polyplexes and lipoplexes. All transfection experiments were performed in two cell types, namely A549 cells (lung carcinoma cell line) and Vero cells (kidney epithelial cell line), using different TCHD concentrations.

The effect of TCHD on the transfection efficiency of naked pDNA was evaluated by incubating Vero and A549 cells with naked pDNA for 2 hr. Subsequently, pDNA that was not incorporated into the cells was removed by washing, and the cells were exposed to increasing percentages (w/v) of TCHD for 1 hr (Fig. 4). The incubation with TCHD clearly increased the gene expression. This increase reached a maximal value at a TCHD percentage of 0.5 % and 1.5 % in Vero (Fig. 4A) and A549 cells (Fig. 4B), respectively. At these optimal concentrations, a 3- and 66-fold increase in gene expression

was observed in Vero and A549 cells, respectively. At higher percentages no further increase and even a drop in gene expression was observed. Most likely this indicates that TCHD at these concentrations affects cellular processes that are not detected by the CellTiter-Glo® assay. Indeed, it has been shown that the sensitivity of the MTT assay depends on the mechanism causing cytotoxicity [49]. Between 0 and 1.5 % (w/v) TCHD, a gradual increase in gene expression was observed in A549 cells (Fig. 4B), which may indicate that the extent of NPC opening by TCHD is concentration dependent. Whether at 1.5 % (w/v) TCHD a maximal opening of the NPCs is reached is not certain, since above this concentration also cytotoxic effects can play a role. This also explains the lower effects of TCHD in Vero cells. Indeed, in these cells the optimal concentration of TCHD to increase gene transfer is 0.5 %. Based on the results in A549 cells, we can deduce that at such low TCHD concentration the opening of the NPC hasn't reached its maximum.

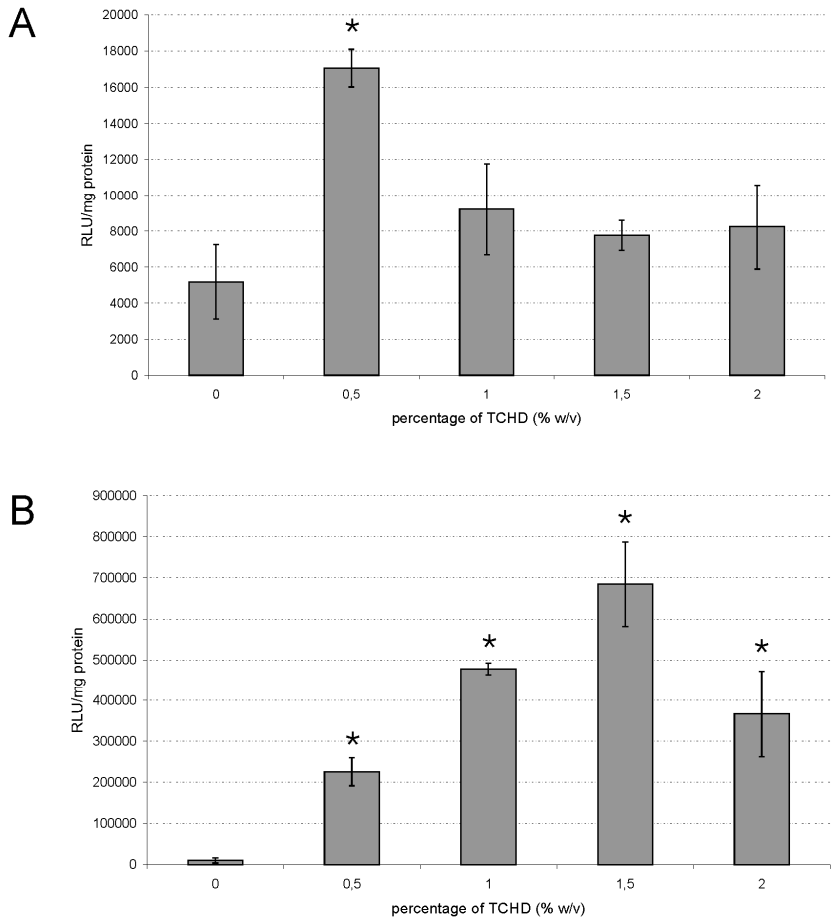

Figure 4. Transfection efficiency of naked pDNA in Vero (A) and A549 (B) cells post-incubated for 1 hr with different TCHD concentrations. The asterix (*) represents data that significantly differ ($p<0.05$) from the data point 0 % (w/v) TCHD.

When TCHD was incubated together with the naked pDNA, we also observed an increase in transfection efficiency, but the effect was less pronounced compared to the post-incubation experiments described above (data not shown). This could be expected as it takes some time for pDNA to become internalized by the cells and released from endocytotic vesicles into the cytoplasm. Additionally, as cytosolic nucleases degrade pDNA, the optimal moment to add TCHD to the cells is immediately after the release of the pDNA in the cytoplasm.

To exclude that the higher gene expression was due to a perforation of the cell membrane by TCHD, which would allow an increased internalization of pDNA through the plasma membrane, we tested whether TCHD causes cytoplasmic entry of 158 kDa TRITC-dextrans. Fig. 5 shows that TRITC-dextrans did not enter the cells in the absence nor in the presence of TCHD (1 % w/v). Consequently, we can state that after 1 hr incubation TCHD does not cause membrane perforation.

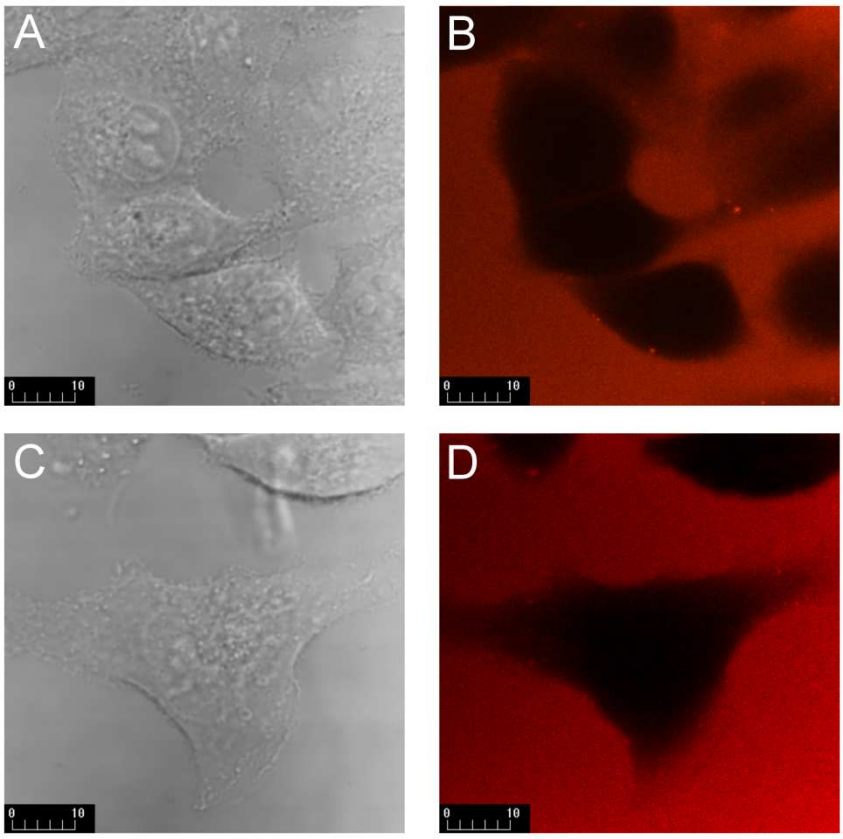

Figure 5. Transmission and CLSM images of Vero cells after 1 min (A and B) and 1 hr incubation (C and D) with 158 kDa TRITC-dextran in the presence of 1 % (w/v) TCHD.

In a next step, we analyzed the effect of TCHD on the transfection efficiency of linear PEI-based polyplexes, a quite efficient non-viral pDNA carrier that induces endosomal release via the proton sponge mechanism [50]. Surprisingly, none of the incubation protocols with TCHD resulted in a significant increase in gene expression mediated by linear PEI-based polyplexes even not when the Vero and A549 cells were post-incubated with 2 % (w/v) TCHD (Supplementary Fig. 1A and B).

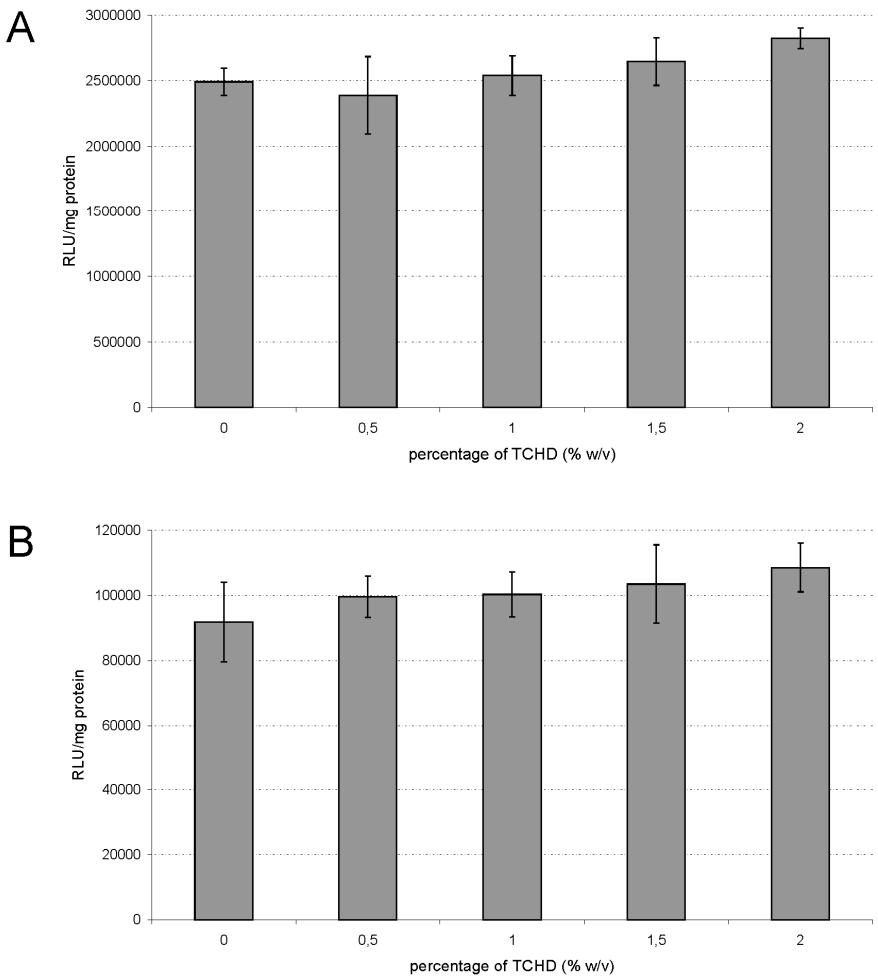

Supplementary Figure 1. Transfection efficiency of polyplexes in Vero (A) and A549 (B) cells post-incubated for 1 hr with different TCHD concentrations.

These data may indicate that, in agreement with Grosse et al., linear PEI based polyplexes are mainly released from the endosomes as intact complexes [51]. Because of the latter and taking into account the diameter of the linear PEI based polyplexes (~165 nm), TCHD is not expected to be able to enhance the nuclear transport and hence transfection efficacy of such linear PEI-based polyplexes.

The endosomal escape mechanism of DOTAP:DOPE-based lipoplexes is based on a different mechanism and results in the release of uncomplexed pDNA in the cytosol [52]. This implies that, when the free pDNA reaches the nuclear membrane, TCHD should be able to induce its nuclear translocation, similar to the naked pDNA transfections. Therefore, we analyzed the effect of TCHD on the transfection efficiency of DOTAP:DOPE-based lipoplexes. The same incubation protocols and cells were used as in the experiments above. Incubating the cells with TCHD for 1 hr immediately after incubation with the lipoplexes, indeed caused an increase in transfection efficiency in both Vero and A549 cells (Fig. 6A and 6B). A maximal increase was observed when the Vero and A549 cells were

incubated with 0.5 % and 1.5 % (w/v) TCHD, respectively. This increase is lower than observed with naked pDNA transfection, which can be attributed to cell division. Compared to naked pDNA transfection, transfection with lipoplexes introduces a higher amount of pDNA in the cytoplasm, which can translocate to the nucleus with higher probability either by entry through the pores or during cell division. Hence, the few extra copies that enter the nucleus after treating the cells with TCHD will not tremendously increase gene expression. In contrast, the amount of pDNA that reaches the cytoplasm and subsequently the nucleus is extremely low in case of naked pDNA transfection. Therefore, if TCHD can cause nuclear translocation of only one pDNA molecule, this effect is much more spectacular.

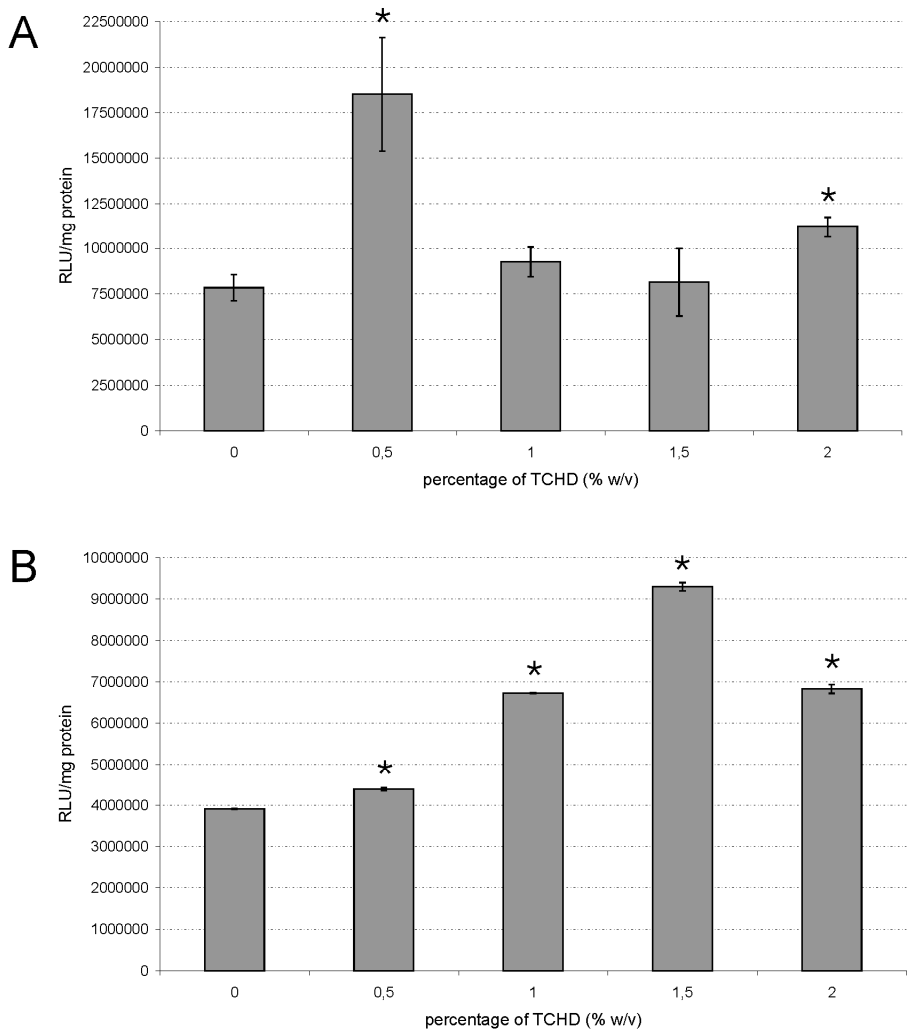

Figure 6. Transfection efficiency of lipoplexes in Vero (A) and A549 (B) cells post-incubated for 1 hr with different TCHD concentrations. The asterix (*) represents data that significantly differ ($p<0.05$) from the data point 0 % (w/v) TCHD.

CONCLUSION

In conclusion, our study demonstrates for the first time that the amphipathic alcohol TCHD can be employed to enhance the nuclear uptake of pDNA by reversibly collapsing the permeability barrier of the NPCs at non-toxic concentrations. Furthermore, our transfection data show that TCHD has huge potential to enhance especially naked gene transfer. Although less efficient than carrier mediated gene delivery, naked gene transfer is currently the most investigated non-viral gene delivery strategy in gene therapy clinical trials because of the higher safety profile, the simplicity of delivery, the lack of immune responses and nonspecific interactions in the body (with e.g. extracellular matrices) [53]. Naked gene transfer is considered for DNA vaccination, Duchenne muscular dystrophy, peripheral limb ischemia, and cardiac ischemia [54-57]. Therefore, strategies that can enhance naked gene transfer by enhancing nuclear uptake of DNA are of huge interest. Additionally, we also want to remark that TCHD is a metabolite of the drug candesartan cilexetil [58] and of the solvent cyclohexanone, a contaminant of intravenous dextrose and parenteral feeding solutions [59], which possibly makes TCHD a clinical acceptable adjuvant for naked gene transfer. However, toxicology and *in vivo* gene transfer studies are needed to confirm the usefulness of this approach for clinical applications.

ACKNOWLEDGMENTS

Niek Sanders is a Postdoctoral Fellow with the Fund for Scientific Research - Flanders (Belgium). The LSM510 ConfoCor 2 experiments were performed at the Advanced Light Microscopy Facility (Prof. R. Pepperkok) at the European Molecular Biology Laboratory (EMBL) in Heidelberg (Germany). Prof. K. Ribbeck is thanked for carefully reading the manuscript.

REFERENCES

(1) Capecchi M.R. High efficiency transformation by direct microinjection of DNA into cultured mammalian cells. *Cell* **1980** 22(2 Pt 2) 479-488.

(2) Dowty M.E., Williams P., Zhang G., Hagstrom J.E., & Wolff J.A. Plasmid DNA entry into postmitotic nuclei of primary rat myotubes. *Proc. Natl. Acad. Sci. U. S. A* **1995** 92(10) 4572-4576.

(3) Pollard H., Remy J.S., Loussouarn G., Demolombe S., Behr J.P., & Escande D. Polyethylenimine but not cationic lipids promotes transgene delivery to the nucleus in mammalian cells. *J. Biol. Chem.* **1998** 273(13) 7507-7511.

(4) Brunner S., Sauer T., Carotta S., Cotten M., Saltik M., & Wagner E. Cell cycle dependence of gene transfer by lipoplex, polyplex and recombinant adenovirus. *Gene Ther.* **2000** 7(5) 401-407.

(5) Mortimer I., Tam P., MacLachlan I., Graham R.W., Saravolac E.G., & Joshi P.B. Cationic lipid-mediated transfection of cells in culture requires mitotic activity. *Gene Ther.* **1999** 6(3) 403-411.

(6) Wilke M., Fortunati E., van den B.M., Hoogeveen A.T., & Scholte B.J. Efficacy of a peptide-based gene delivery system depends on mitotic activity. *Gene Ther.* **1996** 3(12) 1133-1142.

(7) Laskey R.A. CIBA Medal Lecture. Regulatory roles of the nuclear membrane. *Biochem. Soc. Trans.* **1998** 26(4) 561-567.

(8) Vasu S.K. & Forbes D.J. Nuclear pores and nuclear assembly. *Curr. Opin. Cell Biol.* **2001** 13(3) 363-375.

(9) Gorlich D., Henklein P., Laskey R.A., & Hartmann E. A 41 amino acid motif in importin-alpha confers binding to importin-beta and hence transit into the nucleus. *EMBO J.* **1996** 15(8) 1810-1817.

(10) Jakel S., Albig W., Kutay U. *et al.* The importin beta/importin 7 heterodimer is a functional nuclear import receptor for histone H1. *EMBO J.* **1999** 18(9) 2411-2423.

(11) Nagasaki T., Kawazu T., Tachibana T., Tamagaki S., & Shinkai S. Enhanced nuclear import and transfection efficiency of plasmid DNA using streptavidin-fused importin-beta. *J. Control Release* **2005** 103(1) 199-207.

(12) Collas P. & Alestrom P. Nuclear localization signals enhance germline transmission of a transgene in zebrafish. *Transgenic Res.* **1998** 7(4) 303-309.

(13) Subramanian A., Ranganathan P., & Diamond S.L. Nuclear targeting peptide scaffolds for lipofection of nondividing mammalian cells. *Nat. Biotechnol.* **1999** 17(9) 873-877.

(14) Liang M.R., Alestrom P., & Collas P. Glowing zebrafish: integration, transmission, and expression of a single luciferase transgene promoted by noncovalent DNA-nuclear transport peptide complexes. *Mol. Reprod. Dev.* **2000** 55(1) 8-13.

(15) Bremner K.H., Seymour L.W., Logan A., & Read M.L. Factors influencing the ability of nuclear localization sequence peptides to enhance nonviral gene delivery. *Bioconjug. Chem.* **2004** 15(1) 152-161.

(16) Mesika A., Kiss V., Brumfeld V., Ghosh G., & Reich Z. Enhanced intracellular mobility and nuclear accumulation of DNA plasmids associated with a karyophilic protein. *Hum. Gene Ther.* **2005** 16(2) 200-208.

(17) Arenal A., Pimentel R., Garcia C., Pimentel E., & Alestrom P. The SV40 T antigen nuclear localization sequence enhances nuclear import of vector DNA in embryos of a crustacean (Litopenaeus schmitti). *Gene* **2004** 33771-77.

(18) Sebestyen M.G., Ludtke J.J., Bassik M.C. *et al.* DNA vector chemistry: the covalent attachment of signal peptides to plasmid DNA. *Nat. Biotechnol.* **1998** 16(1) 80-85.

(19) Zanta M.A., Belguise-Valladier P., & Behr J.P. Gene delivery: a single nuclear localization signal peptide is sufficient to carry DNA to the cell nucleus. *Proc. Natl. Acad. Sci. U. S. A* **1999** 96(1) 91-96.

(20) Neves C., Byk G., Scherman D., & Wils P. Coupling of a targeting peptide to plasmid DNA by covalent triple helix formation. *FEBS Lett.* **1999** 453(1-2) 41-45.

(21) Tanimoto M., Kamiya H., Minakawa N., Matsuda A., & Harashima H. No enhancement of nuclear entry by direct conjugation of a nuclear localization signal peptide to linearized DNA. *Bioconjug. Chem.* **2003** 14(6) 1197-1202.

(22) van der Aa M., Koning G., van der Gugten J. *et al.* Covalent attachment of an NLS-peptide to linear dna does not enhance transfection efficiency of cationic polymer based gene delivery systems. *J. Control Release* **2005** 101(1-3) 395-397.

(23) Chan C.K., Hubner S., Hu W., & Jans D.A. Mutual exclusivity of DNA binding and nuclear localization signal recognition by the yeast transcription factor GAL4: implications for nonviral DNA delivery. *Gene Ther.* **1998** 5(9) 1204-1212.

(24) Vaysse L., Harbottle R., Bigger B., Bergau A., Tolmachov O., & Coutelle C. Development of a self-assembling nuclear targeting vector system based on the tetracycline repressor protein. *J. Biol. Chem.* **2004** 279(7) 5555-5564.

(25) Branden L.J., Mohamed A.J., & Smith C.I. A peptide nucleic acid-nuclear localization signal fusion that mediates nuclear transport of DNA. *Nat. Biotechnol.* **1999** 17(8) 784-787.

(26) Branden L.J., Christensson B., & Smith C.I. In vivo nuclear delivery of oligonucleotides via hybridizing bifunctional peptides. *Gene Ther.* **2001** 8(1) 84-87.

(27) Bremner K.H., Seymour L.W., Logan A., & Read M.L. Factors influencing the ability of nuclear localization sequence peptides to enhance nonviral gene delivery. *Bioconjug. Chem.* **2004** 15(1) 152-161.

(28) Ludtke J.J., Zhang G., Sebestyen M.G., & Wolff J.A. A nuclear localization signal can enhance both the nuclear transport and expression of 1 kb DNA. *J. Cell Sci.* **1999** 112(Pt 12) 2033-2041.

(29) Chan C.K. & Jans D.A. Enhancement of polylysine-mediated transferrinfection by nuclear localization sequences: polylysine does not function as a nuclear localization sequence. *Hum. Gene Ther.* **1999** 10(10) 1695-1702.

(30) Chan C.K., Senden T., & Jans D.A. Supramolecular structure and nuclear targeting efficiency determine the enhancement of transfection by modified polylysines. *Gene Ther.* **2000** 7(19) 1690-1697.

(31) Carlisle R.C., Bettinger T., Ogris M., Hale S., Mautner V., & Seymour L.W. Adenovirus hexon protein enhances nuclear delivery and increases transgene expression of polyethylenimine/plasmid DNA vectors. *Mol. Ther.* **2001** 4(5) 473-483.

(32) Hagstrom J.E., Sebestyen M.G., Budker V., Ludtke J.J., Fritz J.D., & Wolff J.A. Complexes of non-cationic liposomes and histone H1 mediate efficient transfection of DNA without encapsulation. *Biochim. Biophys. Acta* **1996** 1284(1) 47-55.

(33) Aronsohn A.I. & Hughes J.A. Nuclear localization signal peptides enhance cationic liposome-mediated gene therapy. *J. Drug Target* **1998** 5(3) 163-169.

(34) Murray K.D., Etheridge C.J., Shah S.I. *et al.* Enhanced cationic liposome-mediated transfection using the DNA-binding peptide mu (mu) from the adenovirus core. *Gene Ther.* **2001** 8(6) 453-460.

(35) Keller M., Harbottle R.P., Perouzel E. *et al.* Nuclear localisation sequence templated nonviral gene delivery vectors: investigation of intracellular trafficking events of LMD and LD vector systems. *Chembiochem.* **2003** 4(4) 286-298.

(36) Preuss M., Tecle M., Shah I., Matthews D.A., & Miller A.D. Comparison between the interactions of adenovirus-derived peptides with plasmid DNA and their role in gene delivery mediated by liposome-peptide-DNA virus-like nanoparticles. *Org. Biomol. Chem.* **2003** 1(14) 2430-2438.

(37) Wiseman J.W., Scott E.S., Shaw P.A., & Colledge W.H. Enhancement of gene delivery to human airway epithelial cells in vitro using a peptide from the polyoma virus protein VP1. *J. Gene Med.* **2005** 7(6) 759-770.

(38) Akuta T., Eguchi A., Okuyama H. *et al.* Enhancement of phage-mediated gene transfer by nuclear localization signal. *Biochem. Biophys. Res. Commun.* **2002** 297(4) 779-786.

(39) Ribbeck K. & Gorlich D. The permeability barrier of nuclear pore complexes appears to operate via hydrophobic exclusion. *EMBO J.* **2002** 21(11) 2664-2671.

(40) Ribbeck K. & Gorlich D. The permeability barrier of nuclear pore complexes appears to operate via hydrophobic exclusion. *EMBO J.* **2002** 21(11) 2664-2671.

(41) Fayazpour F., Lucas B., varez-Lorenzo C., Sanders N.N., Demeester J., & De Smedt S.C. Physicochemical and transfection properties of cationic Hydroxyethylcellulose/DNA nanoparticles. *Biomacromolecules.* **2006** 7(10) 2856-2862.

(42) Sanders N.N., Van Rompaey E., De Smedt S.C., & Demeester J. Structural alterations of gene complexes by cystic fibrosis sputum. *Am. J. Respir. Crit Care Med.* **2001** 164(3) 486-493.

(43) Ribbeck K. & Gorlich D. The permeability barrier of nuclear pore complexes appears to operate via hydrophobic exclusion. *EMBO J.* **2002** 21(11) 2664-2671.

(44) Galy V., Mattaj I.W., & Askjaer P. Caenorhabditis elegans nucleoporins Nup93 and Nup205 determine the limit of nuclear pore complex size exclusion in vivo. *Mol. Biol. Cell* **2003** 14(12) 5104-5115.

(45) Ribbeck K. & Gorlich D. The permeability barrier of nuclear pore complexes appears to operate via hydrophobic exclusion. *EMBO J.* **2002** 21(11) 2664-2671.

(46) Lukacs G.L., Haggie P., Seksek O., Lechardeur D., Freedman N., & Verkman A.S. Size-dependent DNA mobility in cytoplasm and nucleus. *J Biol. Chem.* **2000** 275(3) 1625-1629.

(47) Schwille P. Fluorescence correlation spectroscopy and its potential for intracellular applications. *Cell Biochem Biophys* **2001** 34(3) 383-408.

(48) Ribbeck K. & Gorlich D. The permeability barrier of nuclear pore complexes appears to operate via hydrophobic exclusion. *EMBO J.* **2002** 21(11) 2664-2671.

(49) Weyermann J., Lochmann D., & Zimmer A. A practical note on the use of cytotoxicity assays. *Int. J Pharm.* **2005** 288(2) 369-376.

(50) Boussif O., Lezoualc'h F., Zanta M.A. *et al.* A versatile vector for gene and oligonucleotide transfer into cells in culture and in vivo: polyethylenimine. *Proc. Natl. Acad. Sci. U. S. A* **1995** 92(16) 7297-7301.

(51) Grosse S., Thevenot G., Monsigny M., & Fajac I. Which mechanism for nuclear import of plasmid DNA complexed with polyethylenimine derivatives? *J Gene Med.* **2006** 8(7) 845-851.

(52) Koltover I., Salditt T., Radler J.O., & Safinya C.R. An inverted hexagonal phase of cationic liposome-DNA complexes related to DNA release and delivery. *Science* **1998** 281(5373) 78-81.

(53) Wolff J.A. & Budker V. The mechanism of naked DNA uptake and expression. *Adv. Genet.* **2005** 543-20.

(54) Davis H.L., Schleef M., Moritz P., Mancini M., Schorr J., & Whalen R.G. Comparison of plasmid DNA preparation methods for direct gene transfer and genetic immunization. *Biotechniques* **1996** 21(1) 92-99.

(55) Romero N.B., Benveniste O., Payan C. *et al.* Current protocol of a research phase I clinical trial of full-length dystrophin plasmid DNA in Duchenne/Becker muscular dystrophies. Part II: clinical protocol. *Neuromuscul. Disord.* **2002** 12 Suppl 1S45-S48.

(56) Tsurumi Y., Takeshita S., Chen D. *et al.* Direct intramuscular gene transfer of naked DNA encoding vascular endothelial growth factor augments collateral development and tissue perfusion. *Circulation* **1996** 94(12) 3281-3290.

(57) Symes J.F. Gene therapy for ischemic heart disease: therapeutic potential. *Am. J. Cardiovasc. Drugs* **2001** 1(3) 159-166.

(58) Yamamoto K., Kitayoshi T., Nishimura S., Chatani F., & Watanabe T. Absence of interactive effects of trans-1,2-cyclohexanediol, a major metabolite of the side-chain of candesartan cilexetil, on digoxin-induced arrhythmias in dogs. *J Pharmacol. Sci.* **2003** 92(4) 387-399.

(59) Mills G.A. & Walker V. Urinary excretion of cyclohexanediol, a metabolite of the solvent cyclohexanone, by infants in a special care unit. *Clin. Chem.* **1990** 36(6) 870-874.

Summary & General Conclusions

Summary & General Conclusions

SUMMARY

Genetic-based diseases are mainly caused by the absence of essential or the presence of malfunctioning proteins and can consequently be treated by gene therapy. In case of e.g. cystic fibrosis, the genetic disorder can be treated by introduction of the corrected Cystic Fibrosis Transmembrane Regulato) (CFTR) protein. Cancer and viral infections e.g. can be treated by suppression of oncogenic and vital viral proteins, respectively. Introduction of a specific protein can be obtained by using plasmid DNA (pDNA) that encodes this protein. Suppression of a specific protein can be achieved by introducing short interfering RNA (siRNA) molecules that induce sequence-specific messenger RNA (mRNA) degradation and subsequent protein expression knock down. To be successful, these synthetic nucleic acids should reach the cytoplasm (in case of siRNA) or the nucleus (in case of pDNA) of the target cells. Additionally, the nucleic acids should remain intact as their integrity is necessary to maintain their biological activity. Consequently, advanced delivery systems, either viral or non-viral, are needed and are the main focus of current gene therapy research.

As summarized in **Chapter 1**, different nucleic acid delivery systems are available. Although the viral systems have shown to be the most effective ones, their clinical use is limited mainly due to safety issues. Non-viral delivery systems are a safe(r) alternative but unfortunately they often lack high delivery efficiency, caused by the extra- and intracellular hurdles they need to take before reaching their intracellular target region. First, they suffer from rapid clearance from the blood after intravenous administration and often have difficulties to escape the bloodstream at the right place. Additionally, once the target cell is reached, both the extracellular matrix and the plasmamembrane limit the cellular uptake of the nucleic acids. Furthermore, even when taken up by the cell, both endosomal and cytoplasmic nucleic acid degradation have detrimental effects on the delivery efficiency. Once in the cytoplasm, the siRNA has reached its intracellular target region, while pDNA has one last, but difficult hurdle to take, namely nuclear import. The primary aim of this thesis was to improve the non-viral intracellular nucleic acid delivery by addressing different barriers: cellular uptake, endosomal release and nuclear import.

When a non-viral nucleic acid containing nanoparticle reaches the cell membrane, it is mostly taken up through endocytic processes such as clathrin-dependent or -independent endocytosis or macropinocytosis. Upon endocytosis, most particles end-up in vesicles that are processed from early to late endosomes with lysosomes as their final destination. The harsh environment of the lysosomes, with low pH and destructive enzymes, will cause inactivation and degradation of most particles together with their cargo. In this thesis, we tried to solve this problem either by avoiding endosomal uptake (**Chapter 2 and 3**) or by inducing endosomal escape (**Chapter 5**).

To circumvent endosomal degradation, it has been proposed to bypass the endosomal pathway by using cell penetrating peptides (CPPs), such as the HIV-1 Tat peptide, which rapidly translocate cargoes across the cell membrane. The HIV-1 Tat peptide consists of a short stretch of basic amino acids responsible for the translocation across cellular membranes called the protein transduction domain (PTD). The ability of the Tat peptide to transport cargoes across cell membranes could bring significant advantages to the cellular delivery of nucleic acids by non-viral carriers. Therefore, in **Chapter 2**, we attached this peptide to the lipoplex (LPX) surface and subsequently analyzed both transfection efficiency and cellular entry mechanism of these Tat-modified LPXs. Although the Tat peptide could slightly enhance the gene transfer of 30 mol% DOTAP containing LPXs, this was clearly not the case for the 50 mol% DOTAP containing LPXs. In contrast to what we aimed for, i.e. non-endocytic internalization of the Tat-LPXs, we found that the uptake mechanism of Tat-modified LPXs appeared to be energy dependent. By using endocytosis inhibitors, we demonstrated that both Tat-modified and unmodified LPXs were mainly taken up via cholesterol-dependent clathrin-mediated endocytosis, a pathway previously postulated to be responsible for the cellular uptake of cationic LPXs.

As an alternative approach to avoid endosomal degradation, the use of ultrasound has been proposed. It is believed that ultrasound, especially when combined with gas-filled microbubbles, induces small transient pores in the cell membrane, allowing entrance of large molecules directly into the cell cytoplasm. In **Chapter 3** we made use of LPXs supplemented with a poly(ethylene glycol) (PEG) containing lipid for the delivery of siRNA molecules to the cytoplasm of target cells. Although the PEG group is necessary to avoid rapid clearance from the blood after intravenous administration, the presence of PEG has a dramatic adverse effect on the delivery efficiency of the LPXs, probably through both reduced cellular uptake and decreased endosomal release. Therefore, we tried to load the PEGylated siRNA containing LPXs (PEG-siPlexes) onto the surface of ultrasound responsive microbubbles and studied their cellular distribution and gene silencing efficiency after ultrasound radiation. First, we showed that exposure of the PEG-siPlex loaded microbubbles to ultrasound resulted in a massive release of PEG-siPlexes with similar size, surface charge and complexation capacity as before binding to the microbubbles. Moreover, PEG-siPlexes loaded on microbubbles

were able to rapidly enter the target cells after exposure to ultrasound and to induce a pronounced gene silencing, in contrast to free PEG-siPlexes. Interestingly, in the absence of ultrasound these PEG-siPlex loaded microbubbles did not cause any gene silencing, allowing both space and time controlled gene silencing. Apparently, ultrasound combined with PEG-siPlexes bound to the microbubble surface is a promising approach for the *in vivo* delivery of siRNA.

As non-viral nucleic acid containing nanoparticles are mainly taken up by endocytic processes, several research groups have tried to quantitatively assess the contribution of each endocytic pathway in the uptake of non-viral gene delivery vehicles and to correlate these results with transfection efficiency. These studies are often performed through the use of endocytosis inhibitors, i.e. chemicals that are easy to apply and are presumed to specifically inhibit certain endocytic pathways. However, while studying the endocytic process involved in Tat-LPX uptake described in Chapter 2, we encountered several problems and decided to have a closer look at these inhibitors. In **Chapter 4** we clearly showed that unravelling of the uptake pathway of nanoparticles is not always as straightforward as one would think based on current literature. First, we clearly demonstrated that several of the tested inhibitors exhibit cell type dependent cytotoxic effects. Additionally, most inhibitors exhibited only limited inhibitor efficiency and very few inhibitors were shown to be specific for a certain endocytic pathway. Finally, we also noticed that most inhibitors dramatically change cellular morphology. Therefore, one must be aware of possible side effects when using these endocytosis inhibitors, as this can often lead to contradictory results. Moreover, one should also realize that different pathways may be operating simultaneously or may take over if one pathway is blocked. Subsequently, inhibiting one route, may lead to an increased uptake via an alternative route. Additionally, the existence of unknown endocytic processes or even worse, the induction of non-natural pathways due to the cellular manipulations, cannot be excluded. Based on our results, we can state that performing the correct control experiments to test the efficacy of these inhibitors is of extreme importance for obtaining reliable conclusions. And even when all control experiments are performed, using a combined approach, e.g. combining inhibition experiments with co-localization studies, is in any case the preferred strategy to study the endocytic uptake of delivery vehicles.

As most particles are taken up by endocytic processes, this often leads to endosomal degradation of the nucleic acids, unless the carrier is able to induce endosomal release. In **Chapter 5** we made use of non-toxic, biodegradable 1,4-butanediol (PbAE1) or 1,6-hexanediol (PbAE2) diacrylate-based polymers, called poly(β-amino esters), to deliver siRNA molecules to the cytoplasm of both hepatoma cells and primary hepatocytes. Both polymers were able to induce significant gene silencing, although based on confocal images the PbAE:siRNA complexes clearly end up inside the endo- and lysosomes. We found that the duration of gene silencing in the hepatoma cells was

maintained for at least 5 days after siRNA delivery in case of PbAE2, the polymer with the slowest degradation kinetics. In contrast, after 5 days gene expression had completely recovered in case of PbAE1. These observations, combined with the time-dependent cellular distribution of PbAE1 and PbAE2 complexes, suggest that the slowly degrading PbAE2 causes a sustained endosomal release of siRNA during a much longer period than PbAE1. This supports the hypothesis that the endosomal release mechanism of PbAE:siRNA complexes is based on an increase of osmotic pressure in the endosomal vesicles after polymer hydrolysis, as PbAEs are fully biodegradable through hydrolysis of their backbone esters to yield small molecular weight products.

In case of siRNA the cytoplasm is the final destination, but pDNA should cross a final barrier, the nuclear envelope (NE), before arriving at its intracellular target region. Two attempts to improve the nuclear transport of pDNA are described in this thesis: complexation of the pDNA with a nuclear localization signal (NLS) peptide (**Chapter 6**) and disruption of the nuclear barrier through interference with the hydrophobic interactions inside the nuclear pore complexes (NPCs) (**Chapter 7**).

The HIV-1 Tat protein contains a short amino acid stretch highly enriched in basic residues and responsible for NLS activity. In **Chapter 6** we prepared non-toxic, electrostatic Tat/pDNA complexes to enhance nuclear uptake of pDNA. In contrast to what we hoped for, cytoplasmic microinjection of Tat/pDNA complexes did not result in nuclear import of the labeled pDNA. Similarly, the transfection efficiency was barely increased when the pDNA was electrostatically complexed with the Tat peptide. In agreement with these results, the Tat/pDNA complexes were not able to interact with the nuclear import machinery, although the Tat peptide itself did. Taken together, the results of this study indicate that electrostatic coupling of an NLS to pDNA does not induce nuclear uptake of pDNA. We demonstrated that the latter is probably due to masking of the NLS domain after electrostatic interaction between Tat and pDNA.

As attempts to improve nuclear transport of pDNA through the use of the Tat peptide did not yield the desired result, we focussed on an alternative approach. Considering the hydrophobic nature of the NPC channel, we evaluated in **Chapter 7** whether non-selective gating of nuclear pores by *trans*-cyclohexane-1,2-diol (TCHD), an amphipathic alcohol that reversibly collapses the permeability barrier of the NPCs, could facilitate nuclear entry of plasmid DNA. First, we examined the effect of TCHD on nuclear import of cytoplasmic microinjected 158 kDa TRITC-dextran. As soon as 10 sec after addition of TCHD to the cells, TRITC-dextran was detected in the nucleus. Additionally, we also detected nuclear influx of pDNA in the presence of TCHD, indicating that TCHD indeed could disrupt the nuclear barrier, opening up the possibility for pDNA to enter the nucleus. Subsequently, the effect of TCHD on the transfection efficiency of naked pDNA and non-viral DNA containing nanoparticles, such as polyplexes and LPXs was tested. Although no increase could be detected in

case of polyplexes, TCHD incubation clearly increased the gene expression of both naked pDNA and LPXs, varying from 2- to 66-fold. In conclusion, we demonstrated that the amphipathic alcohol TCHD has huge potential to enhance gene transfer, especially of naked DNA.

GENERAL CONCLUSIONS

In conclusion, the primary aim of this thesis was to improve intracellular nucleic acid delivery by addressing different barriers encountered by non-viral delivery systems. Dependent on the approach we used, we succeeded in doing so. Avoiding endosomal uptake by attachment of the Tat peptide to the LPX surface appeared to be unsuccessful, while we were able to enhance the transfection efficiency by coupling our LPXs to a microbubble surface and subsequent ultrasound irradiation. We also succeeded in inducing an endosomal release of siRNA in both hepatoma cells and primary hepatocytes by using biodegradable poly(β-amino esters) (PbAEs), as these polymers were able to induce significant gene silencing. Moreover, PbAEs with slower degradation kinetics were able to cause a more prolonged gene silencing. Finally, enhancing nuclear import of pDNA was not possible by electrostatic NLS/pDNA complexes, but addition of TCHD proved to be a more successful approach.

Samenvatting & Algemene Besluiten

Samenvatting & Algemene Besluiten

SAMENVATTING

Genetische aandoeningen worden hoofdzakelijk veroorzaakt door de afwezigheid van essentiële of aanwezigheid van slecht functionerende eiwitten. Bijgevolg zijn deze aandoeningen het ideale doelwit voor gentherapie. Bij taaislijmziekte bijvoorbeeld kan de genetische afwijking behandeld worden door toevoeging van het gecorrigeerde 'cystic fibrosis transmembrane conductance regulator' (CFTR-) eiwit. Sommige kankers en virale infecties daarentegen kunnen behandeld worden door specifieke onderdrukking van respectievelijk kankerverwekkende of voor het virus levensnoodzakelijke eiwitten. Om het gewenste eiwit toe te voegen kan gebruik gemaakt worden van plasmide DNA (pDNA) dat codeert voor dit eiwit. De onderdrukking van de expressie van een specifiek eiwit kan verkregen worden door 'short interfering' RNA (siRNA-) moleculen aan de doelwitcellen toe te dienen. SiRNA-moleculen veroorzaken immers een sequentiespecifieke afbraak van boodschapper RNA (mRNA) en bijgevolg ook onderdrukking van de expressie van het overeenkomstige eiwit. Beide synthetische nucleïnezuren kunnen maar tot therapeutische successen leiden indien ze tot in het cytoplasma (in geval van siRNA) of tot in de kern (in geval van pDNA) van de doelwitcellen geraken. Bovendien moeten de nucleïnezuren intact hun doelwit bereiken, aangezien dit noodzakelijk is voor het behoud van hun biologische activiteit. Geavanceerde afgiftesystemen, viraal of niet-viraal, zijn dan ook noodzakelijk en vormen één van de belangrijkste onderzoeksonderwerpen binnen gentherapie.

Zoals samengevat in **Hoofdstuk 1** zijn er verschillende afgiftesystemen voor nucleïnezuren beschikbaar. Hoewel de virale dragers overtuigend het meest efficiënt zijn, wordt hun klinische toepasbaarheid beperkt door de mogelijke veiligheidsproblemen. Niet-virale dragers vormen een veilig(er) alternatief, maar helaas hebben deze dragers vaak slechts een beperkte afgifte efficiëntie door de vele hindernissen die ze moeten overwinnen vooraleer ze hun intracellulaire doelwitregio kunnen bereiken. Ten eerste worden ze snel verwijderd uit het bloed na intraveneuze toediening en zelden verlaten ze de bloedbaan op de juiste plaats. En indien ze er in slagen de doelwitcellen te bereiken, beperken zowel de extracellulaire matrix als de plasmamembraan de cellulaire opname van

de nucleïnezuren. Eenmaal opgenomen door de doelwitcellen worden ze blootgesteld aan endosomale en cytoplasmatische nucleasen die een desastreus effect hebben op de afgifte-efficiëntie. Het cytoplasma is de intracellulaire doelwitregio voor de siRNA-moleculen, maar pDNA moet nog een laatste en moeilijke hindernis nemen, namelijk de nucleaire membraan. Het hoofddoel van deze onderzoeksscriptie bestond erin om de efficiëntie van niet-virale intracellulaire nucleïnezuurafgifte te verhogen door de volgende hindernissen aan te pakken: cellulaire opname, endosomale vrijgave en nucleaire import.

Wanneer een niet-viraal nucleïnezuurbevattend nanopartikel de celmembraan bereikt, wordt het meestal opgenomen via endocytotische processen zoals clathrine-gemedieerde of -onafhankelijke endocytose of macropinocytose. Na endocytotische opname komen de meeste partikels terecht in intracellulaire vesikels die achtereenvolgens evolueren tot vroege en late endosomen met lysosomen als eindbestemming. De vernietigende omgeving van de lysosomen, met lage pH en afbraakenzymen, zorgt voor inactivatie en afbraak van de meeste partikels samen met hun cargo. In deze doctoraatsscriptie werd geprobeerd dit probleem aan te pakken enerzijds door de endosomale opname te omzeilen (**Hoofdstuk 2 en 3**) en anderzijds door de endosomale vrijstelling te stimuleren (**Hoofdstuk 5**).

Eén mogelijke strategie om endosomale afbraak te voorkomen, is het omzeilen van de endosomale opname door gebruik te maken van ‘cell penetrating peptides’ (CPPs) zoals het HIV-1 Tat-peptide. Het HIV-1 Tat-peptide bestaat uit een korte reeks van basische aminozuren die verantwoordelijk is voor de translocatie doorheen cellulaire membranen. Dit domein wordt het ‘protein transduction domain’ (PTD) genoemd. De mogelijkheid van het Tat-peptide om cargo’s integraal doorheen membranen te loodsen zou de afgifte-efficiëntie van niet-virale dragers significant kunnen verbeteren. In **Hoofdstuk 2** werd dit peptide dan ook aan het lipoplex (LPX) oppervlak gekoppeld, waarna zowel de transfectie-efficiëntie als de cellulaire opname van deze Tat-gemodificeerde LPX’en werden bestudeerd. Hoewel het Tat-peptide zorgde voor een lichte verhoging van de gentransfer in het geval van de 30 mol% DOTAP bevattende LPX’en, was dit duidelijk niet het geval voor de 50 mol% DOTAP bevattende LPX’en. In tegenstelling tot wat de bedoeling was, namelijk een endocytose-onafhankelijke opname, bleek de opname van de Tat-gemodificeerde LPX’en temperatuursafhankelijk te zijn. Gebruik van endocytose-inhibitoren toonde aan dat zowel de Tat-gemodificeerde als niet-gemodificeerde LPX’en hoofdzakelijk opgenomen werden via een cholesterol-afhankelijke clathrine-gemedieerde endocytose, een opnamemechanisme dat eerder reeds beschreven werd voor de cellulaire opname van kationische LPX’en.

Als alternatieve strategie om endosomale afbraak te vermijden werd in de literatuur het gebruik van ultrasone golven reeds voorgesteld. Algemeen wordt aangenomen dat ultrasone golven,

zeker in combinatie met microscopische gasbellen, in staat is om tijdelijke poriën in de celmembraan te induceren, waardoor grote moleculen in staat zijn om het cytoplasma te bereiken. In **Hoofdstuk 3** werden siRNA-liposoomcomplexen aangemaakt die poly(ethyleen glycol) (PEG-) gemodificeerde lipiden bevatten. Deze PEG-groep is noodzakelijk om een snelle verwijdering uit het bloed te voorkomen na intraveneuze toediening. De aanwezigheid van deze PEG-groep leidt echter tot een verminderde cellulaire opname en endosomale vrijstelling, wat een desastreus effect heeft op de transfectie efficiëntie van de LPX'en. Om dit probleem aan te pakken werd geprobeerd om deze gePEGyleerde siRNA bevattende LPX'en (PEG-siPlexen) op het oppervlak van microscopische gasbellen te binden en vervolgens hun cellulaire lokalisatie en onderdrukkingsefficiëntie te bestuderen na behandeling met ultrasone golven. Ten eerste konden we aantonen dat bestraling van PEG-siPlex geladen microscopische gasbellen met ultrasone golven resulteerde in een massale vrijstelling van PEG-siPlexen met dezelfde grootte, oppervlaktelading en complexatiecapaciteit als vóór binding met de microscopische gasbellen. Daarnaast bleken de PEG-siPlexen geladen op het oppervlak van microscopische gasbellen snel de doelwitcellen binnen te dringen na bestraling met ultrasone golven en, in tegenstelling tot de vrije PEG-siPlexen, een goede onderdrukking van het doelwitgen te veroorzaken. Bovendien werd geen onderdrukking van het doelwitgen gedetecteerd in de afwezigheid van ultrasone golven, wat zowel een plaats- als tijdsgecontroleerde genonderdrukking toelaat. Uit deze resultaten kunnen we concluderen dat ultrasone golven, gecombineerd met PEG-siPlex gebonden microscopische gasbellen, een veelbelovende strategie is voor de *in vivo* afgifte van siRNA.

Aangezien niet-virale nucleïnezuurbevattende nanopartikels hoofdzakelijk opgenomen worden via endocytotische processen, proberen verschillende groepen het aandeel van de verschillende opnamewegen in de cellulaire opname van een specifieke drager te bepalen en te correleren met de uiteindelijke transfectie-efficiëntie. Om dit te bestuderen wordt vaak gebruik gemaakt van endocytose-inhibitoren, dit zijn chemische componenten die gemakkelijk zijn in gebruik en die specifiek bepaalde endocytotische opnamewegen kunnen inhiberen. Bij het bestuderen van de opname van Tat-LPX'en in Hoofdstuk 2 werden echter verschillende problemen vastgesteld waardoor beslist werd het gebruik van deze inhibitoren in detail te bekijken. **Hoofdstuk 4** toont duidelijk aan dat het bestuderen van de opname van nanopartikels niet zo evident is als in de literatuur vaak beweerd wordt. Ten eerste stelden we duidelijk vast dan verscheidene van de geteste inhibitoren een celafhankelijke cytotoxiciteit vertoonden. Bovendien vertoonden de meeste inhibitoren slechts een beperkte efficiëntie en bleken ze vaak niet specifiek te zijn voor één opnameweg. Tenslotte werd ook aangetoond dat verschillende inhibitoren naast de inhibitie van endocytotische processen ook ernstige neveneffecten hebben op de cellulaire morfologie. Indien men dus gebruik wil maken van deze inhibitoren is het belangrijk om hiermee rekening te houden

om zodoende tegenstrijdige resultaten te vermijden. Daarnaast moet men ook stilstaan bij het feit dat meerdere endocytotische opnamewegen tegelijkertijd een rol kunnen spelen of het zelfs van elkaar kunnen overnemen indien een bepaalde opnameweg geblokkeerd wordt. Daardoor kan de inhibitie van de ene opnameweg resulteren in een verhoogde opname via een alternatieve opnameweg. Daarnaast is het niet uitgesloten dat nog niet alle endocytotische opnamewegen gekend zijn of zelfs nog erger, dat de uitgevoerde manipulaties resulteren in het induceren van onnatuurlijke opnamewegen. Op basis van onze resultaten kunnen we besluiten dat het extreem belangrijk is de correcte controle-experimenten uit te voeren om te bepalen hoe efficiënt en specifiek de gebruikte endocytose inhibitoren zijn, zodat betrouwbare resultaten verkregen worden. En zelfs indien alle noodzakelijke controle- experimenten uitgevoerd worden, is het absoluut raadzaam om voor de studie van de opnameweg van een bepaalde drager, een gecombineerde strategie te gebruiken waarbij inhibitorstudies gecombineerd worden met bijvoorbeeld colokalisatie-experimenten.

Aangezien de meeste nucleïnezuurbevattende nanopartikels opgenomen worden via endocytotische processen leidt dit vaak tot endosomale afbraak van de nucleïnezuren, tenzij de drager in staat is om endosomale vrijstelling te induceren. In **Hoofdstuk 5** werd gebruik gemaakt van niet-toxische, biodegradeerbare poly(β-amino ester) polymeren (1,4-butaandiol (PbAE1) en 1,6-hexaandiol (PbAE2) diacrylaat-gebaseerd) voor de afgifte van siRNA in het cytoplasma van doelwitcellen. Beide polymeren resulteerden in een significante genonderdrukking ondanks het feit dat ze volgens confocale beelden uitsluitend in de endo- en lysosomen gelokaliseerd waren. PbAE2, het traagst degraderende polymeer, bleek in staat om de eiwit productie gedurende ten minste 5 dagen te onderdrukken. Bij PbAE1 daarentegen was de eiwitexpressie na deze periode volledig hersteld. Deze waarnemingen, gecombineerd met de tijdsafhankelijke cellulaire distributie van beide polymeer:siRNA complexen, suggereren dat het traag degraderende PbAE2 polymeer in staat is om een meer continue endosomale vrijstelling te bewerkstelligen gedurende een veel langere periode dan PbAE1. Dit ondersteunt de hypothese dat het endosomale vrijstellingsmechanisme van de PbAE:siRNA complexen gebaseerd is op een toename in osmotische druk binnenin de endosomale vesikels na hydrolyse van de PbAEs. Door hydrolyse van de esters in de polymeer ruggengraat degraderen deze polymeren immers tot eindproducten met een laag moleculair gewicht.

In geval van siRNA is het cytoplasma de intracellulaire eindbestemming, maar pDNA moet nog een laatste barrière overbruggen voordat het zijn intracellulaire doelwitregio bereikt heeft, namelijk de nucleaire membraan. Twee strategieën om het nucleair transport van pDNA te verbeteren worden in deze onderzoeksscriptie beschreven: complexatie van het pDNA met een nucleair lokalisatiesignaal (NLS-) bevattend peptide (**Hoofdstuk 6**) en verstoring van de nucleaire

barrière door te interferen met de hydrofobe interacties binnenin de nucleaire poriëncomplexen (NPC's) (**Hoofdstuk 7**).

Het HIV-1 Tat-eiwit bevat een korte aminozuur reeks met hoofdzakelijk basische residuen en verantwoordelijk is voor de NLS-activiteit. Om de nucleaire opname van pDNA te verhogen werden in **Hoofdstuk 6** niet-toxische, elektrostatische NLS/pDNA-complexen aangemaakt. In tegenstelling tot wat verhoopt werd, resulteerde cytoplasmatische micro-injectie van deze complexen niet in nucleair import van het pDNA. Ook de transfectie- efficiëntie werd nauwelijks verhoogd na elektrostatische complexatie van het pDNA met het Tat-peptide. Het feit dat de Tat/pDNA-complexen, in tegenstelling tot het Tat-peptide zelf, niet in staat waren om te binden met de nucleaire importmachinerie is hiermee in overeenstemming. Samenvattend kan gesteld worden dat elektrostatische koppeling van een NLS met pDNA niet noodzakelijk resulteert in een verhoogde nucleaire opname en dat dit hoogstwaarschijnlijk veroorzaakt wordt doordat het functionele NLS-domein gemaskeerd wordt na elektrostatische interactie met pDNA.

Aangezien het gebruik van het Tat-peptide niet resulteerde in de verhoopte verhoging van nucleair pDNA transport, werd een alternatieve strategie uitgetest. Op basis van de hydrofobe eigenschappen van het NPC kanaal werd in **Hoofdstuk 7** nagegaan of het niet-selectief openen van de nucleaire poriën door middel van *trans*-cyclohexaan-1,2-diol (TCHD), een amfifiel alcohol dat in staat is om reversibel de permeabiliteit van de NPC's te verstoren, resulteerde in een toename van pDNA transport doorheen de NPC's. Eerst werd het effect van TCHD op de nucleaire import van cytoplasmatisch geïnjecteerd 158 kDa TRITC-dextraan nagegaan. Tien seconden na toevoeging van TCHD aan deze cellen kon het TRITC-dextraan reeds in de kern gedetecteerd worden. Op een gelijkaardige manier kon ook nucleaire influx van pDNA in de aanwezigheid van TCHD gedetecteerd worden. Deze data bewijzen dat TCHD inderdaad in staat is de NPC's te openen en vervolgens macromoleculen en pDNA de mogelijkheid biedt om de kern binnen te dringen. Tenslotte werd ook het effect van TCHD nagegaan op de transfectie-efficiëntie van naakt pDNA en niet-virale nanopartikels zoals polyplexen en LPX'en. Hoewel geen verhoging in transfectie- efficiëntie kon bekomen worden bij polyplexen, had TCHD wel een positief effect op zowel naakte pDNA-transfectie als bij gebruik van LPX'en, variërend van een 2- tot 66-voudige toename. Hiermee werd aangetoond dat het amfifiele alcohol TCHD grote mogelijkheden biedt voor het verhogen van niet-virale gentherapie, vooral in het geval van naakte gentransfer.

ALGEMENE BESLUITEN

Deze doctoraatsscriptie had tot doel de intracellulaire afgifte van nucleïnezuren te verhogen door in te grijpen ter hoogte van de verschillende hindernissen die niet-virale afgiftesystemen moeten overwinnen. Afhankelijk van de gekozen strategie zijn we daar in geslaagd. Het omzeilen van endosomale afbraak door aanhechting van het Tat-peptide op het LPX oppervlak bleek niet succesvol, terwijl koppeling van de LPX'en op het oppervlak van microscopische gasbellen gecombineerd met ultrasone golven wel resulteerde in een extreme verhoging van de transfectie-efficiëntie. We slaagden er ook in om endosomale vrijstelling van siRNA te induceren in zowel hepatomacellen als primaire hepatocyten door gebruik te maken van PbAE's, aangezien in beide gevallen significante genonderdrukking verkregen werd. Bovendien resulteerde het traagst afbreekbare polymeer in de langstdurende genonderdrukking. Tenslotte kon de nucleaire import van pDNA niet verhoogd worden door elektrostatische binding met een NLS-peptide, terwijl toevoeging van TCHD wel een succesvolle aanpak bleek te zijn.

Curriculum Vitae

Curriculum Vitae

PERSONALIA

Name	Vandenbroucke
Surname	Roosmarijn Els Jeanne Regina Stella
Nationality	Belgian
Place and date of birth	Izegem, 08/07/1979
Marital status	married, daughter (Lore, °08/05/2006)
Private address	Hogenhovestraat 7
	B-8700 Aarsele (Tielt)
Telephone	+32-479-26.80.56
	+32-51-68.75.70
Professional address	Lab. of General Biochemistry & Physical Pharmacy
	Faculty of Pharmaceutical Sciences
	Ghent University
	Harelbekestraat 72
	B-9000 Ghent
Telephone	+32-9-264.80.74
Fax	+32-9-264.81.89
E-mail	Roosmarijn.Vandenbroucke@UGent.be
URL	http://www.biofys.UGent.be

LANGUAGES

Dutch	mother tongue
English	fluent
French	good

DEGREES

July, 1999 KULAK - **Bachelor in Science**, **Biology**

July, 2001 Ghent University - **Master in Science**, **Biotechnology** with great distinction

Master thesis: "*Analyse van de E-cadherine-gemedieerde differentiële gen expressie in humane borstkankercellen met behulp van de techniek 'Molecular Indexing' "* (Promotor: Prof. dr. F. Van Roy; Co-promotor: dr. Geert Berx; Supervisor: dr. K. Strumane)

ADDITIONAL CERTIFICATES

Molecular Oncology

Laboratory Animal Science part I and II

Several courses to obtain the degree of "Geaggregeerde in de biologie":

- Onderwijs en maatschappij
- Pedagogische componenten van het leraarschap
- Educatieve interactie en communicatie
- Maatschappelijke & wetenschapsfilosofische analyse van de vakinhouden

CONFERENCE PROCEEDINGS

Vandenbroucke R, Lucas B, Demeester J, De Smedt S and Sanders, N. Nuclear accumulation of plasmid DNA can be enhanced by non-selective gating of the nuclear pore. Human Gene Therapy. 2007 October 1, 18(10): 973-973. **(IF_{2006} = 4.514)**

Vandenbroucke R, Lentacker I, Demeester J, De Smedt S and Sanders N. Loading of PEGylated siRNA lipoplexes on microbubbles restores their siRNA delivery capacity in the presence of ultrasound. Human Gene Therapy. 2007 October 1, 18(10): 1046-1046. **(IF_{2006} = 4.514)**

Vandenbroucke R, De Geest B, Demeester J, De Smedt S and Sanders, N. Prolonged gene silencing in hepatoma cells and primary hepatocytes after siRNA delivery with biodegradable poly(β-amino ester)s. Human Gene Therapy. 2007 October 1, 18(10): 1056-1056. **(IF_{2006} = 4.514)**

PEER REVIEWED PUBLICATIONS

De Geest BG, **Vandenbroucke RE**, Guenther AM, Sukhorukov GB, Hennink WE, Sanders NN, Demeester J and De Smedt SC. Intracellularly degradable polyelectrolyte microcapsules. Advanced Materials. 2006 18 (8): 1005+ apr 18. **(IF_{2006} = 7.896)**

Lentacker I, De Geest BG, **Vandenbroucke RE**, Peeters L, Demeester J, De Smedt SC and Sanders NN. Ultrasound-responsive polymer-coated microbubbles that bind and protect DNA. Langmuir. 2006 Aug 15;22(17):7273-8. **(IF_{2006} = 3.902)**

Strumane K, Bonnomet A, Stove C, **Vandenbroucke R**, Nawrocki-Raby B, Bruyneel E, Mareel M, Birembaut P, Berx G and van Roy F. E-Cadherin Regulates Human Nanos1, which Interacts with p120ctn and Induces Tumor Cell Migration and Invasion. Cancer Research. 2006 Oct 15;66(20):10007-15. **(IF_{2006} = 7.656)**

von Gersdorff K, Sanders NN, **Vandenbroucke R**, De Smedt SC, Wagner E and Ogris M. The Internalization Route Resulting in Successful Gene Expression Depends on both Cell Line and Polyethylenimine Polyplex Type. Molecular Therapy. 2006 Nov;14(5):745-53. **(IF_{2006} = 5.841)**

Vandenbroucke RE, De Smedt SC, Demeester J and Sanders NN. Cellular entry pathway and gene transfer capacity of TAT-modified lipoplexes. Biochimica et Biophysica Acta – Biomembranes. 2007 Mar;1768(3):571-9. **(IF_{2006} = 3.587)**

Braeckmans K, Remaut K, **Vandenbroucke RE**, Lucas B, De Smedt SC and Demeester J. Line FRAP with the confocal laser scanning microscope for diffusion measurements in small regions of 3-D samples. Biophysical Journal. 2007 Mar 15;92(6):2172-83. **(IF_{2006} = 4.757)**

Vandenbroucke RE, Lucas B, De Smedt SC, Demeester J and Sanders NN. Nuclear accumulation of plasmid DNA can be enhanced by non-selective gating of the nuclear pore. Nucleic Acids Research. 2007;35(12):e86. **(IF_{2006} = 6.317)**

Vandenbroucke RE. GTRV Summer school: Oligonucleotide-based strategies to control gene expression: delivery issues. IDrugs. 2007 10(11):778-781. **(IF_{2006} = 1.429)**

Vandenbroucke RE, Lentacker I, Demeester J, De Smedt S and Sanders NN. Ultrasound assisted siRNA release using PEG-siPlex loaded microbubbles. Journal of Controlled Release. 2008 Mar 20;126(3):265-73. **(IF_{2006} = 4.012)**

Raemdonck K, Van Thienen TG, **Vandenbroucke RE**, Sanders NN, Demeester J and De Smedt SC. Dextran Microgels for Time-Controlled Delivery of siRNA. Advanced Functional Materials. *In press.* **(IF_{2006} = 6.779)**

Vandenbroucke RE, De Geest BG, Bonné S, Vinken M, Van Haecke T, Wagner E, De Smedt SC, Demeester J and Sanders NN. Delivery of siRNA to hepatoma cells and primary hepatocytes using biodegradable poly(β-amino ester)s. Journal of Gene Medecine. *In revision.* **(IF_{2006} = 3.916)**

Vandenbroucke RE, Vercauteren D, Demeester J, Jones AT, De Smedt SC, Braeckmans K, Sanders NN. Pitfalls in the use of inhibitors to study endocytic uptake of gene carriers. *Submitted.*

Raemdonck K, **Vandenbroucke RE**, Sanders NN and De Smedt SC. Maintaining the silence: reflections on long-term RNAi. *Submitted.*

Nailis H, **Vandenbroucke RE**, Tilleman K, Deforce D, Nelis H and Coenye T. *ALS1* and *ALS3* gene expression and the role of Als1p and Als3p during *in vitro Candida albicans* biofilm formation. *Submitted.*

Fayazpour F, Lucas B, **Vandenbroucke RE,** Derveaux S, Tavernier J, Lievens S, Demeester J and De Smedt SC. Evaluation of digitally encoded layer-by-layer coated microparticles as cell carriers. *Submitted.*

Peeters L, Lentacker I, **Vandenbroucke RE**, Lucas B, Demeester J, Sanders NN and De Smedt SC. Can ultrasound solve the transport barrier of the neural retina? *Submitted*.

Lentacker I, Wang N, **Vandenbroucke RE**, Vercauteren D, Demeester J, De Smedt SC and Sanders NN. Shooting lipoplexes through the cell membrane with ultrasound responsive lipoplex loaded microbubbles. *In preparation*.

Lentacker I, **Vandenbroucke RE**, Lucas B, Demeester J, De Smedt SC and Sanders NN. New strategies for nucleic acid delivery to conquer cellular and nuclear membranes. *In preparation*.

Vandenbroucke RE, Demeester J, De Smedt SC and Sanders NN. Opening the gateway to the nucleus. *In preparation.*

CONFERENCES WITHOUT LECTURE OR POSTER PRESENTATION

May 23rd, 2003 – Spring Meeting of the Belgian-Dutch Biopharmaceutical Society – Utrecht University, The Netherlands

April 7th-9th, 2004 – 8th European Symposium on Controlled Drug Delivery – Noordwijk aan Zee, The Netherlands

CONFERENCES WITH POSTER PRESENTATION (presenting author)

September 24th - October 4th, 2003 – EMBO Practical Course and Minisymposium - EMBL Heidelberg, Germany
"Enhancement of nuclear uptake of therapeutic genes and macromolecules by using HIV-1 TAT peptide" – **Vandenbroucke RE**, Sanders NN, Demeester J and De Smedt SC

October 9th-12th, 2004 – Congress on Peptide-Membrane Interactions – Namen, Belgium
"Enhancement of cellular and nuclear uptake of macromolecules, therapeutic genes and lipoplexes by using NLS and PTD containing viral peptides" – **Vandenbroucke RE**, De Smedt SC, Demeester J and Sanders NN

June 1st-5th, 2005 – ASGT 8th Annual Meeting, St. Louis, MO, USA
"Enhancement of Cellular and Nuclear Uptake of Macromolecules, Therapeutic Genes and Lipoplexes by Using NLS and PTD Containing Viral Peptides" – **Vandenbroucke RE**, De Smedt SC, Demeester J and Sanders NN

August 25th-26th, 2005 – Pepvec2005 Montpellier "Mechanism of carrier-mediated intracellular delivery of therapeutics" – Montpellier, France
"Enhancement of Cellular and Nuclear Uptake of Macromolecules, Therapeutic Genes and Lipoplexes by Using NLS and PTD Containing Viral Peptides" – **Vandenbroucke RE**, De Smedt SC, Demeester J and Sanders NN

April 10th-13th, 2007 – Summer School on therapeutic ultrasound – Cargese, Corse
"Loading of siRNA lipoplexes on microbubbles can overcome the low transfection efficiency of highly PEGylated siRNA lipoplexes" – Lentacker I, **Vandenbroucke RE**, De Smedt SC, Demeester J and Sanders NN

April, 20th-21st, 2007 – Pre-Satellite Meeting of the 3rd Pharmaceutical Sciences World Congress (PSWC 2007) – Amsterdam, The Netherlands
"Loading of siRNA lipoplexes on microbubbles can overcome the low transfection efficiency of highly PEGylated siRNA lipoplexes" – **Vandenbroucke RE**, Lentacker I, De Smedt SC, Demeester J and Sanders NN

May 29th - June 3rd, 2007 – ASGT 10th Annual Meeting - Seattle, USA
"Nuclear accumulation of plasmid DNA can be enhanced by non-selective gating of the nuclear pore" – **Vandenbroucke RE**, Lucas B, Demeester J, De Smedt SC and Sanders NN

June 24th-27th, 2007 – 7th International Symposium on Frontiers in Biomedical Polymers – Ghent, Belgium
"Delivery of siRNA to hepatocytes using biodegradable poly(β-amino esters)" – **Vandenbroucke RE**, De Geest BG, De Smedt SC, Demeester J and Sanders NN

October 27th-30th, 2007 – ESGCT 15th Annual Meeting – Rotterdam, The Netherlands
"Loading of siRNA lipoplexes on microbubbles can overcome the low transfection efficiency of highly PEGylated siRNA lipoplexes" – **Vandenbroucke RE**, Lentacker I, Demeester J, De Smedt SC and Sanders NN
"Delivery of siRNA to hepatocytes using biodegradable poly(ß-amino esters)" – **Vandenbroucke RE**, De Geest B., Demeester J, De Smedt SC and Sanders NN

May 28th - June 1st, 2008 – ASGT 11th Annual Meeting - Boston, USA
"Evaluation of digitally encoded layer-by-layer coated microparticles as cell carriers" – Fayazpour F, Lucas B, **Vandenbroucke RE**, Derveaux S, Demeester J and De Smedt SC
"Pitfalls in the use of inhibitors to study endocytic uptake of gene carriers" – Vercauteren D, **Vandenbroucke RE**, Demeester J, De Smedt SC, Braeckmans K and Sanders NN.

CONFERENCES WITH LECTURE (presenting author)

November 28th, 2003 – Autumn Meeting of the Belgian-Dutch Biopharmaceutical Society – Groningen University, The Netherlands
"Enhancement of nuclear uptake of therapeutic genes and macromolecules by using NLS and PTD containing viral peptides" – **Vandenbroucke RE**, Sanders NN, Demeester J and De Smedt SC

September 4th-9th, 2004 – The Wilhelm Bernard Workshop, 18th International Workshop on the Cell Nucleus - Pavia, Iltaly
"Enhancement of nuclear uptake of therapeutic genes and macromolecules by using NLS and PTD containing viral peptides" – **Vandenbroucke RE**, Sanders NN, Demeester J and De Smedt SC

June 1st-5th, 2005 – ASGT 8th Annual Meeting - St. Louis, USA
"Studies on the intracellular release of genetic drugs from pharmaceutical carriers" – Lucas B, **Vandenbroucke RE**, Remaut K, De Smedt SC and Demeester J

December 2nd, 2005 – Autumn Meeting of the Belgian-Dutch Biopharmaceutical Society – Utrecht University, The Netherlands
"Layer-by-Layer Technology for Biomedical Applications" – De Geest BG, **Vandenbroucke RE**, Sanders NN, Demeester J and De Smedt SC

November 27th, 2006 – Autumn Meeting of the Belgian-Dutch Biopharmaceutical Society – Leiden University, The Netherlands
"Delivery of siRNA to hepatocytes using biodegradable poly(β-amino esters)" – **Vandenbroucke RE**, De Geest BG, De Smedt SC, Demeester J and Sanders NN

May 29th - June 3rd, 2007 – ASGT 10th Annual Meeting - Seattle, USA
"Delivery of siRNA to hepatocytes using biodegradable poly(β-amino esters)" – **Vandenbroucke RE**, De Geest BG, De Smedt SC, Demeester J and Sanders NN

September 6th-8th, 2007 – GTRV Summer School – La Grande Motte, France
"Loading of siRNA lipoplexes on microbubbles can overcome the low transfection efficiency of highly PEGylated siRNA lipoplexes" – **Vandenbroucke RE**, Lentacker I, De Smedt SC, Demeester J and Sanders NN

October 27th-30th, 2007 – ESGCT 15th Annual Meeting – Rotterdam, The Netherlands
"Nuclear accumulation of plasmid DNA can be enhanced by non-selective gating of the nuclear pore" – **Vandenbroucke RE**, Lucas B, Demeester J, De Smedt SC and Sanders NN

November 14th, 2007 – 2nd Cell Signaling and Bioluminescence Seminar – Brussels, Belgium
"Non-viral nucleic acid delivery: battle against the major drawbacks" – **Vandenbroucke RE**, Lentacker I, De Geest B, Lucas B, Demeester J, De Smedt SC and Sanders NN

November 27th, 2007 – Material Challenges for Biomedical Applications Symposium – Ghent, Belgium
"Lipoplex loaded microbubbles for gene delivery" – Lentacker I, **Vandenbroucke RE**, Demeester J, De Smedt SC and Sanders NN

December 7th, 2007 – FWO Minisymposium on Nuclear Import – Ghent, Belgium
"Nuclear accumulation of plasmid DNA can be enhanced by non-selective gating of the nuclear pore" – **Vandenbroucke RE**, Lucas B, Demeester J, De Smedt SC and Sanders NN

April 2nd-4th, 2008 – 10th European Symposium on Controlled Drug Delivery (ESCDD)– Noordwijk aan Zee, The Netherlands
"New strategies for DNA and siRNA delivery" – Sanders NN, **Vandenbroucke RE**, Lentacker I, Lucas B, Demeester J and De Smedt SC

June 9th-11th, 2008 – The 19th Helsinki Drug Research 2008 – Helsinki, Finland
"Opportunities for digitally encoded microcarriers in pharmacy and cell based assays" – Fayazpour F, Lucas B, Huyghebaert N, Braeckmans K, Derveaux S, **Vandenbroucke RE**, Remon JP, Demeester J, Vervaet C and De Smedt SC

RESEARCH VISITS

January 22nd - February 6th, 2004 – Corbett Lab, Emory University, Atlanta, Georgia, United States – "Importin α and β purification and GST pull down assays"

August 5th-7th, 2005 – Prof. Pepperkok, EMBL Heidelberg, Germany – "Microinjection experiments and CLSM"